Sneha Gautam
Roshini Praveen Kumar
Cyril Samuel *Editors*

Aerosol Optical Depth and Precipitation

Measuring Particle Concentration, Health Risks and Environmental Impacts

Springer

Aerosol Optical Depth and Precipitation

Sneha Gautam • Roshini Praveen Kumar
Cyril Samuel

Editors

Aerosol Optical Depth and Precipitation

Measuring Particle Concentration, Health Risks and Environmental Impacts

Editors
Sneha Gautam
Division of Civil Engineering
Karunya Institute of Technology
and Sciences
Coimbatore, Tamil Nadu, India

Roshini Praveen Kumar
Division of Civil Engineering
Karunya Institute of Technology
and Sciences
Coimbatore, Tamil Nadu, India

Water Institute, A Centre of Excellence
Karunya Institute of Technology
and Sciences
Coimbatore, Tamil Nadu, India

Cyril Samuel
Division of Civil Engineering
Karunya Institute of Technology
and Sciences
Coimbatore, Tamil Nadu, India

Contents

Unraveling the Complex Relationships Between Aerosol Optical Depth and Temperature: A Review

Ruchi Dangayach and Ashutosh Kumar Pandey

1 Introduction

Increased urbanization, industrialization, and population growth are the primary causes of escalating air pollution due to higher vehicular emissions, fossil fuel usage in industries, and increased demand for goods and agricultural practices leading to increased concentration of air pollutants in the atmosphere which is a significant contributing factor to the phenomenon of global warming and subsequent climate change. The ramifications of global warming and climate change encompass a wide array of severe consequences, including more frequent and intense extreme weather events, rising sea levels, melting glaciers, disruptions to ecosystems, and adverse impacts on human health and agriculture. The release of aerosols from anthropogenic causes is another crucial factor contributing to changes in the Earth's atmosphere and climate. Aerosols comprise small solid and liquid particles in the atmosphere, including windblown dust, sea salts, volcanic ash, wildfire smoke, and industrial pollution. These aerosols can have varied effects, depending on their size, type, and location. They may either cool or warm the Earth's surface, and they can influence cloud formation by either assisting or hindering it (NASA, n.d.-a). Aerosols direct effect can be quantified via aerosol optical depth (AOD) (Mielonen et al., 2016). Aerosol optical depth measures aerosols distributed within a column of air from the Earth's surface to the top of the atmosphere. It is closely related to particulate matter ($PM_{2.5}$ and PM_{10}), nitrogen dioxide (NO_2), sulfur dioxide (SO_2), and ozone (O_3) (Chu et al., 2003; Li et al., 2016). The ambient air's pollutant concentration is contingent upon both the emission quantity and the atmosphere's ability to assimilate or disperse these pollutants (WHO, 2010). Given the daily variability of meteorological factors like temperature and air pollutant concentrations, it becomes

R. Dangayach · A. K. Pandey (✉)
School of Earth Sciences, Banasthali Vidyapith, Tonk, Rajasthan, India
e-mail: ashutoshkumarpandey@banasthali.in

crucial to examine their correlation within the planetary boundary layer. This is of particular importance as the atmosphere plays a pivotal role in transporting air pollutants away from the emission sources. According to Lee et al. (2006), episodes of photochemical pollution involve the combination of diverse meteorological influences and chemical reactions leading to the presence of air pollutants such as O_3, NO_2 and PM_{10}. These pollutants pose significant health risks, particularly during heatwaves, as highlighted in studies by Analitis et al. (2014), Fouillet et al. (2006), and Johnson et al. (2004). The heightened levels of these pollutants during heatwaves not only cause discomfort and stress for vulnerable individuals due to elevated temperatures but can also result in mortality as observed in Analitis et al.'s (2014) research. The relationship between aerosols and temperature is a complex and multifaceted one. Aerosols can have both cooling and warming effects on the Earth's climate, depending on their properties and interactions with solar radiation and clouds and the overall net effect of aerosols on climate depends on their cooling and warming properties. However, it's important to note that aerosols effects on climate are regional in nature.

Comprehending the role of aerosols in the Earth's climate system holds paramount importance in enhancing our ability to forecast and address the ramifications of climate change. To achieve this understanding, researchers employ climate models to simulate the intricate interactions among aerosols, clouds, and radiation, thereby gaining valuable insights into their collective impact on the planet's temperature and climate patterns.

2   Material and Methods

In this chapter, a comprehensive literature search was conducted to identify studies on the relationship between aerosol optical depth (AOD) and temperature. Extensive search of scientific databases was conducted using relevant keywords related to AOD, temperature, cloud condensation nuclei, climate, and meteorological parameters. The search also included scientific journals, conference proceedings, relevant chapters, and technical reports from various organizations. Synthesizing the extracted data revealed emerging themes, variations in research methodologies, and noteworthy findings across the literature. Relevant figures from selected literature were included to illustrate the relationship discussed.

3   Results and Discussion

3.1   Aerosol Optical Depth (AOD)

Aerosols are extremely small liquid droplets and solid particles that remain suspended in the air for prolonged periods due to their lightweight nature. Particulate matter (PM) in our atmosphere can also be referred to as an aerosol because it is

suspended within the gases in the air. The particles are also referred to as aerosol particles and come in various sizes, for example, $PM_{2.5}$ and $PM_{10.}$ Major sources of aerosols include urban/industrial emissions, smoke from biomass burning, and secondary formation from gaseous aerosol precursors such as sea salt and dust (World Meteorological Organization, 2022). These aerosol particles influence the earth's climate. Aerosol particles play a multifaceted role in our climate, encompassing both direct and indirect effects. The direct effects are directly linked to the properties and actions of the aerosol particles themselves. On the other hand, the indirect effects are associated with how aerosol particles help in the formation of clouds (CAICE, 2020). The direct aerosol effect is based on the ability of particulate matter to absorb or scatter sunlight. Aerosol particles, along with the clouds they form, reflect around 25% of the sun's radiation back into space. As a result, less solar radiation reaches the Earth's surface, leading to a cooling effect on the climate (Fig. 1a). Indirect aerosol effects are associated with the influence of aerosols on clouds. For cloud droplets to form, two essential components are required in the atmosphere: water vapor and aerosol particles. The role of aerosol particles in this process is to provide a surface for the water vapor to condense upon when it cools, transitioning into the liquid phase and forming cloud droplets (Fig. 1b). As a result, aerosol particles serve as cloud condensation nuclei (CCN), essentially providing a "starting point" for cloud formation.

The properties and amount of CNN influence cloud formation in two significant ways:

(a) Twomey Effect is a phenomenon, where there is an increase in the concentration of aerosol particles (CCN) leading to a greater number of cloud droplets. This occurs because the additional aerosol particles provide more surface for water vapor to condense and form cloud droplets, resulting in clouds with a higher number of smaller droplets. This effect can have implications for cloud properties, such as brightness and persistence, and can impact climate and weather patterns.

(b) Albrecht Effect: In clouds that form in the presence of many CCN, the water droplets are smaller and more lightweight. Therefore, they are less likely to fall out of the cloud as rain. In clouds that form from few CCN, the water droplets are bigger and heavier, so they are more likely to cause rain.
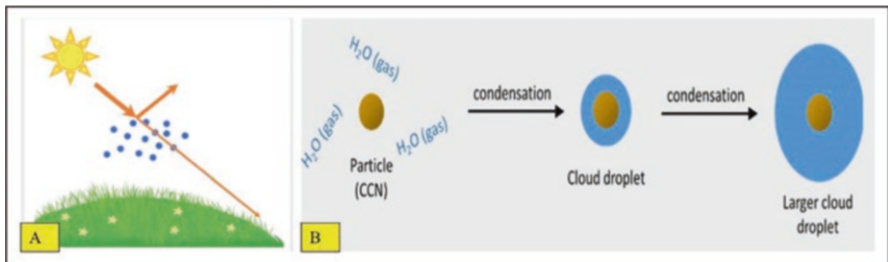
Fig. 1 Effect of Aerosol. (**a**) Direct aerosol effect. (**b**) Indirect aerosol effect (Cloud formation) (CAICE, 2020)

3.1.1 Measurement and Estimation of AOD

AOD is an important parameter in atmospheric science and climatology, and there are several methods to measure AOD. Some common ones are:

(a) Sun Photometer: is the most widely used method to measure AOD. It involves measuring the intensity of solar radiation at different wavelengths using a sun photometer. The sun photometer observes the Sun's direct or diffuse radiation as it passes through the Earth's atmosphere. By comparing the measured solar radiation at different wavelengths with theoretical values (assuming a clean atmosphere with no aerosols), researchers can determine AOD (Fig. 2a). For example, Aerosol Robotic Network (AERONET). AERONET is also known to collect data on sky brightness, which can be used to infer information about aerosol size distribution, refractive index, and SSA (Single Scattering Albedo). When not in use, a sun photometer faces downwards but once when it is active, it aligns itself with the sun and begins to collect data. Data obtained from AERONET are more accurate than data derived from Earth-orbiting satellites. AERONET is useful in the validation of global-scale satellite datasets and various other applications. By comparing data, the accuracy of the satellites can be determined and rectify any systematic inaccuracies. However, AERONET coverage is point-based and sparse, especially in regions with low population such as the Sahara Desert or the Arctic. Maritime Aerosol Network (MAN) is another type of ground-based photometer that is both user-friendly and portable. Microtops that contribute to MAN are mainly used to fill gaps in data over oceans (NASA, n.d.-d).

(b) Satellite Remote Sensing: To overcome the incapabilities of the sun photometer, various satellites were launched to measure AOD across a range of spatial and temporal resolutions, from high to low (Payra et al., 2023). Satellites equipped with remote sensing instruments can also measure AOD on a global scale. Instruments like Moderate Resolution Imaging Spectroradiometer (MODIS) Aqua and Terra, Advanced Very High-Resolution Radiometers (AVHRR), SeaWiFS, and VIIRS have been used to retrieve AOD data (Fig. 2b). These sensors are all broad-swath passive multispectral imaging radiometers and can be considered to be the first approximation of cameras in space. The Deep Blue Algorithm is used to calculate the AOD and Angstrom exponent over land by utilizing data from the mentioned satellite instruments. Through the utilization of measurements at various wavelengths, which exhibit varying contrast between surface and atmospheric characteristics, Deep Blue estimates AOD. At 412 nm referred to as the 'deep blue band', aerosol signals tend to be bright and surface features dark (NASA, n.d.-d).

(c) LiDAR (Light Detection and Ranging): LiDAR is an active remote sensing technique that uses laser light to measure the scattering and extinction of aerosols in the atmosphere. It provides vertical profiles of aerosol properties including AOD (Fig. 2c). The CALIOP (Cloud Aerosol Lidar with Orthogonal
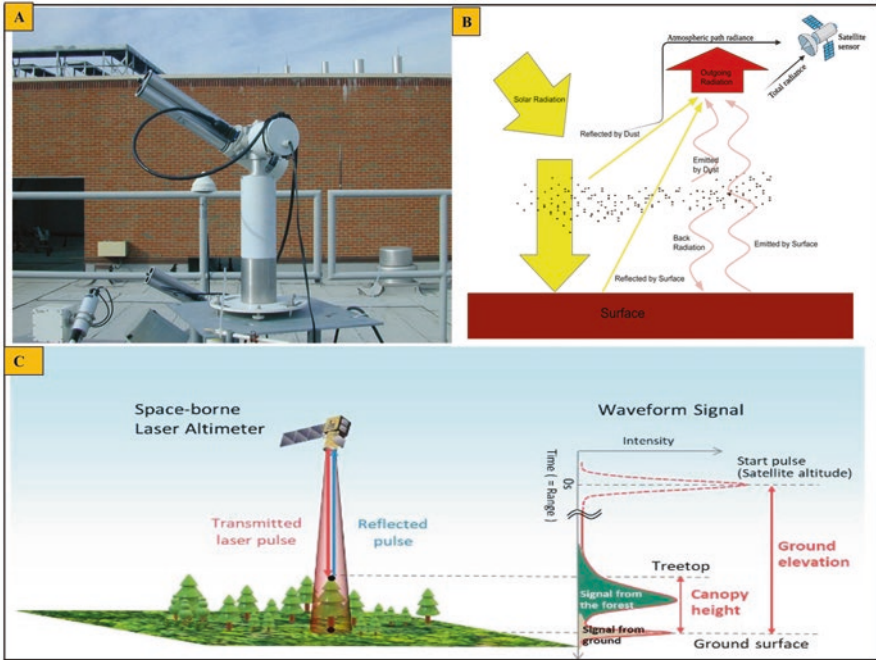
Fig. 2 Measurement of AOD. (Image credit: NASA, 2008). (**a**) Sun Photometer. (**b**) Atmospheric radiative process. (Modified. Image credit: NASA, 2020). (**c**) Spaceborne lidar schematic image. (Image credit: JAXA)

Polarization) onboard the CALIPSO satellite measured vertical profiles of aerosols and clouds since 2006 over the globe (Winker et al., 2010).

The main satellite platforms and sensors for global aerosol observations are Landsat (MSS), GOES (VISSR), Apollo- Soyuz (SAM), AEM-B (SAGE), NOAA (AVHRR), ERBS (SAGE-2), UARS (HALOE), SPOT-3 (POAM-2), SSD (LITE), ERS-2 (ATSR-2, GOME), ADEOS (POLDER-1), Earth Probe (TOMS), Orb View- 2 (SeaWiFS), TRMM (VIRS), SPOT-4 (POAM-3), Terra (MODIS, MISR), Meteor-3M (SAGE-3), PROBA (CHRIS), Odin (OSIRIS), Aqua (MODIS), ENVISAT (AATSR, MERIS, SCIAMACHY), ADEOS-2 (POLDER-2, ILAS-2, GLI), MSG-1 (SEVIRI), ICEsat (GLAS), Aura (OMI), PARASOL (POLDER-3), CALIPSO (CALIOP), MetOp-A(GOME-2), FY-3 (MERSI), HJ-1A/1B (CCD, IRS), COMS (GOCI), Suomi-NPP (VIIRS), MetOp-B (GOME-2), Himawari-8 (AHI), GF-4 (PMS), FY-4 (AGRI), TG-2 (MAI), TanSat (CAPI), Himawari-9 (AHI), Sentinel 5p (Tropomi), GCOM-C (SGLI), GF-5 (DPC), MetOp-C (GOME-2), GK-2B (GOCI-II), GFDM (SMAC), HJ-2 (PSAC) (Zhang et al., 2021).

(d) In-Situ measurement: can be deployed on the ground or on aircraft to directly measure aerosol properties, including AOD. Instruments such as nephelometers

and photometers can be used to measure the scattering and absorption of light by aerosols.

(e) Sun Photodiodes: are compact instruments that can measure AOD in real time. They measure AOD by quantifying the attenuation of sunlight at specific wavelength as it travels through the atmosphere and is scattered and absorbed by aerosol particles. The amount of scattering and absorption depends on the aerosol concentration, size, and composition. They are less accurate than sun photometers but are useful for quick measurements in the field.

It is important to note that measuring AOD can be influenced by factors such as cloud cover, surface reflection, and instrument calibration. Hence, careful data processing and calibration are essential to obtain accurate AOD values. Additionally, AOD measurements are often combined with other meteorological data and atmospheric models to better understand aerosol distribution and their impact on climate and air quality.

3.1.2   Factors That Influence AOD Variability

AOD variability is affected by a multitude of natural and anthropogenic factors that influence the concentration, spatial distribution, and properties of aerosols in the atmosphere. These factors include natural sources (volcanic eruptions, dust storms, sea spray, and biogenic emissions from vegetation), anthropogenic sources (vehicular exhaust, industrial emissions, power plants, construction activities, and combustion of fossil fuels), seasonal and regional variations (fluctuations in meteorological conditions such as weather patterns, temperature inversion, atmospheric stability, wind speed and direction), urbanization, topography, cloud cover, long-range transport, land use changes, climate change, and wildfires and biomass burning (de Leeuw et al., 2023; Che et al., 2019; Gui et al., 2019; Yoon et al., 2013; Floutsi et al., 2016; Arkian & Nicholson, 2018; Mehta & Khushboo, 2022). AOD, being a complex parameter, results from the intricate interplay of these diverse factors. Consequently, researchers employ advanced models and satellite observations to comprehend and quantify the contributions of individual sources of AOD variability, along with its implications for climate, air quality, and human health.

3.2   Temperature

Temperature is defined as the degree of hotness or coldness of an object and is usually measured in degrees- Fahrenheit or degrees- Celsius (National Geographic). The term 'atmospheric temperature' refers to the temperature of the Earth's atmosphere at various layers. Several factors (solar energy, humidity, and altitude) contribute to the fluctuation of temperatures, either elevating them to new levels or causing them to descend to lower levels. The Earth's distinct temperature plays a

pivotal role in sustaining life on our planet, and each layer has a different atmospheric temperature. Five distinct layers have been identified using thermal characteristics, chemical composition, movement, and density (NOAA, 2023). The five basic layers are:

(a) Troposphere: extending from the Earth's surface to approximately 18–20 km high at the equator, 9 km at 50°N and 50°S, and just 6 km high at the poles. As the altitude increases in this layer, the density of gases decreases, resulting in thinner air. Consequently, the temperature in the troposphere also decreases with height. As one ascends to higher altitudes, the average temperature, which is around 17 °C near the surface, drops to approximately −51 °C at the tropopause. All weather-related phenomena occur in this layer.

(b) Stratosphere: extends from 6 to 20 km above the Earth's surface to 50 km and holds 19% of the atmosphere's gases but very little water vapor. Heat is produced in the process of formation of ozone resulting in temperature increase. The temperature goes up to −15 °C at the top of the stratosphere. The transition boundary that separates the stratosphere from the mesosphere is stratopause.

(c) Mesosphere: extends from 50 km above the Earth's surface to 85 km. The temperature increases in this region. The gases in this region are thick enough to slow down meteors.

(d) Thermosphere: extends from 85 km above the Earth's surface to 600 km. Incoming high-energy UV and X-ray radiation from the sun begins to be absorbed by the molecules in this layer and causes a large temperature increase. The temperature can reach as high as 2000 °C near the top.

(e) Exosphere: the outermost layer of the atmosphere. It extends up to 10,000 km. In this layer, atoms and molecules escape into space and satellites orbit the Earth. Figure 3 shows the basic layers of atmosphere and their temperature profile. Table 1 lists the factors that influence climate (those that affect temperature).

3.3   Relationship Between AOD and Temperature

The relationship between AOD and temperature can be complex and depends on various factors and is an important parameter for studying air quality and climate change. In some cases, an inverse relationship is observed i.e., higher temperatures often lead to increased vertical mixing in the atmosphere, which can disperse aerosols and reduce their concentration, resulting in lower AOD values. Conversely, cooler temperatures may lead to more stable atmospheric conditions, allowing aerosols to accumulate resulting in increased AOD. In specific situations, a direct relationship is observed between AOD and temperature. For instance, periods of intense wildfires or biomass burning can lead to high temperatures producing more aerosols thus, increasing AOD. The relationship can vary depending on the region and season. In some areas, the influence of other factors like topography, vegetation, and
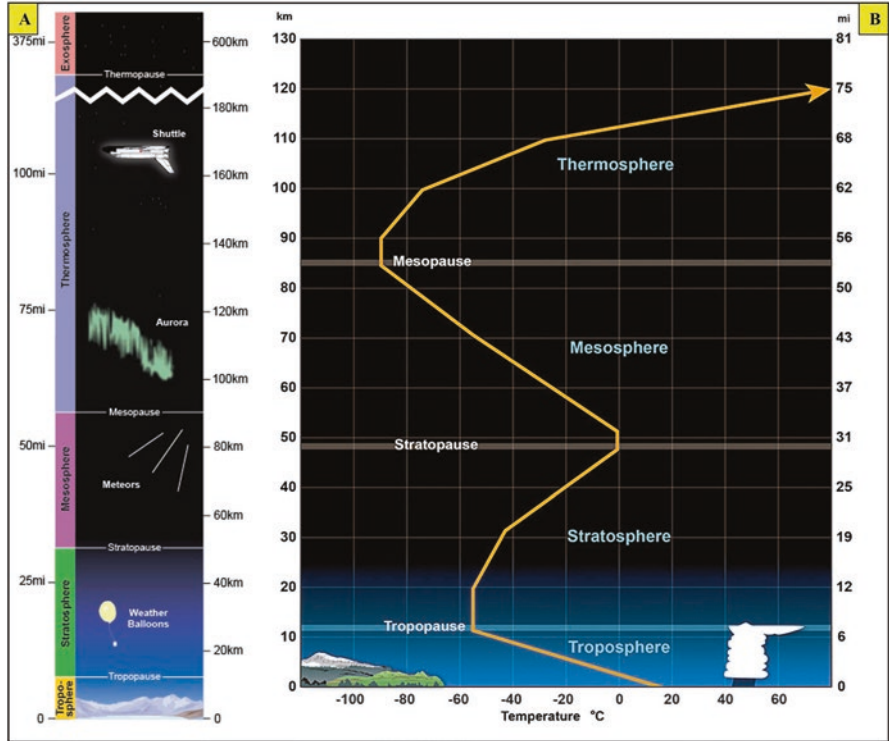
Fig. 3 Layers of atmosphere. (**a**) Basic layers of Atmosphere. (**b**) Average temperature profile of atmosphere. (Image credit: NOAA, 2023)

Table 1 Factors that affect temperature

Temperature	
Factor	Influence
Latitude	As latitude increases, the average yearly temperature decreases.
Nearness to centers of large landmasses	Locations near the center of large landmasses tend to have wide ranges in temperature, both between day and night and seasonally.
Nearness to large bodies of water	Has a moderate effect on the temperatures of coastal areas, producing low ranges in temperature, both between day and night and seasonally.
Location relative to large mountain ranges	Windward sides are cooled, while leeward sides are warmed.
Elevation	As elevation increases, the average yearly temperature decreases.
Ocean currents	Tend to warm temperatures of eastern coastal areas and cool temperatures of western coastal areas.

Source: NOAA

local sources of aerosols can dominate over temperature's direct impact on AOD and with the ongoing climate change, the relationship may be subject to shifts. Changes in the atmospheric patterns, increased frequency of wildfires and alterations in the sources and composition of aerosols can all contribute to complex interactions. Aerosol-cloud interactions, or "indirect effects", remain one of the most challenging yet crucial factors in climate prediction (Stevens & Feingold, 2009; Boucher et al., 2013). For stratocumulus, the effect of increased CCN leading to cloud brightening can be modulated by changes in precipitation and subsequent changes to cloud water amounts through entrainment processes (e.g., Ackerman et al., 2004).

Several researchers have conducted surveys on relationships between aerosol optical depth and temperature globally and some of them are listed in Table 2.

3.4 Aerosol-Induced Temperature Changes

Radiative forcing denotes the perturbation in the planet's energy balance due to external drivers, quantified as the instantaneous change in the net radiative flux at the tropopause. This measure captures the difference between the incoming solar irradiance absorbed by the Earth and the outgoing longwave radiation emitted by the planet (Fig. 4). Positive radiative forcing signifies an augmented energy input, potentially leading to climate warming, whereas negative radiative forcing signifies a diminished energy input, possibly inducing cooling. The metric is expressed in watts per square meter (W/m^2) and is used to assess the relative impact of different agents on climate change such as greenhouse gases, aerosols, land use modifications, solar variability, and stratospheric ozone alterations.

Prior to the industrial era, radiative forcing maintained a state of intricate equilibrium, leading to a relatively stable mean global temperature on Earth. This prompted researchers to compute radiative forcing with reference to a designated "baseline" year that predates the inception of global industrialization. Illustratively, the Intergovernmental Panel on Climate Change uses 1750 as a baseline year. In relation to this reference point, radiative forcing provides a direct assessment of how contemporary human actions have altered the global climate. Predominantly, the most substantial alteration involves the introduction of greenhouse gases into the atmosphere, which hinder the dissipation of heat from the Earth. However, additional modifications have also occurred. For example, deforestation has led to an increased exposure of the Earth's surface to sunlight. When this exposed surface is darker than the original forested area, the planet absorbs a greater amount of solar radiation. Conversely, in regions with lighter surfaces, such as the Arctic, a greater portion of sunlight is reflected back to space. The concept of radiative forcing facilitates a comprehensive comprehension of the assorted elements steering climate change dynamics and enables a comparative appraisal of their respective impacts on the planetary temperature regimes.

Table 2 Comparative study of literature

S.No.	Author	Findings
1	Roy (2008)	Concluded that the general trends in aerosol optical depths (AODs) display elevated levels of concentration across the densely inhabited and extensively industrialized Gangetic basin for both seasons. In both the summer and winter seasons, there was a primarily negative correlation between AOD and temperature. This implies that higher AOD levels were associated with lower temperatures in northeastern India and along the west coast near Mumbai. In contrast, the interior northwestern region of the subcontinent, extending toward Kashmir, saw a positive impact during the summer months. During the winter season, the correlation was largely negative, whereas it ranged from neutral to positive in the summer monsoon season. These disparities in responses could be ascribed to the influence of overcast skies and substantial precipitation during the summer monsoon period. These conditions led to the entrapment of longwave radiation within the Earth's atmosphere, resulting in elevated minimum temperatures. Conversely, the predominantly clear skies during the winter season led to a negative influence by aerosols on surface temperatures.
2	Chen et al. (2009)	Reported correlation between annual mean AOD and decrease in air temperature with a correlation coefficient of -0.33 at 95% confidence level in the Sinchuan Basin, China.
3.	Hu et al. (2011)	Concluded that there's a strong connection between AOT and really hot or cold weather on land. In some places, this connection changes over time. In China, especially in the eastern part, the links between AOT and extreme temperatures are strong. This is especially true on the eastern side of the line at $110°$ E. The areas where the connection is strongest are along the southern coast of China, the Loess Plateau, and the Sichuan Basin. The connection is even stronger in the North China Plain and the middle to lower parts of the Changjiang River.
4.	Gunaseelan et al. (2013)	The reported AOD above in Madurai is undergoing changes that align with temperature fluctuations. This clearly indicates an increase in temperature, leading to the upward movement of aerosols. This, in turn, impacts the distribution of aerosol sizes and leads to a greater amount of AOD.
5.	Gunaseelan et al. (2014)	Studied the effect of AOD on rainfall with reference to meteorology over metro cities in India and concluded that during the drought year (2009) a negative correlation was observed between AOD and temperature in Chennai, whereas in the years 2008 and 2010, a positive correlation was reported which may be due to the extremes in temperature and drought frequency causing atmospheric circulation changes in the city. However, in Delhi, a negative correlation was observed in the year 2010. In the case of Mumbai, a negative correlation was observed in all three years.
6.	Tariq and Ul-Haq (2019)	Investigated the aerosol optical depth angstrom exponent and their relationships with meteorological parameters over Lahore in Pakistan and concluded a positive correlation between AOD and temperature.
7.	Lin et al. (2019)	Reported statistically significant and positive correlations between AOD and temperature at North China Plain and Sichuan Basin. This could happen because the impact of transport of aerosols, such as organics, may be more influential than the effect of photochemical reactions in other regions.

Table 2 (continued)

S.No.	Author	Findings
8.	Jung et al. (2019)	The reported inverse relationship between AOD and air temperature during the KORUS-AQ campaign.
9.	Sarthi et al. (2019)	Reported high degree of correlation exists between AOD and a difference in T_{max} and T_{min} from January to June-July over the Gangetic plain, India.
10.	Zaman et al. (2021)	Reported elevated AOD levels (>0.70) during the pre-monsoon period in both northern and southern regions of Bangladesh. The escalation during the summer is attributed to elevated temperatures and robust wind velocities, resulting in the generation of substantial quantities of wind-driven dust particles (Alam et al., 2010).
11.	Gautam et al. (2022)	Concluded positive correlation between AOD and temperature at Amity University ($R^2 = 0.23$), 0.43 ARM College ($R^2 = 0.43$), and Karunya University ($R^2 = 0.13$). However, at Gandhi College and Singhad Institute, negative correlation was reported ($R^2 = 0.07$), which may be attributed to thermal inversion and frequent occurrence of atmospherically elevated haze, which may not be correlated to surface concentrations due to heterogeneity in the vertical profile or the fine mode fraction, as well as another factor that could cause AOD overestimation (Pena & Araya, 2019; Amarillo et al., 2021).
12.	Rani and Kumar (2022)	Concluded positive relation between AOD and air temperature in Northern India.
13.	Zeydan et al. (2023)	Reported positive correlations between AOD retrievals and temperature over Eastern Anatolia region, while negative correlations were reported in Marmara, Aegean, Mediterranean, and the Black Sea Region

3.5 Implications for Climate Change

Aerosol optical depth (AOD) and temperature are two crucial factors in the complex interplay of Earth's climate system. AOD quantifies the extent to which aerosols attenuate or alter the passage of sunlight through the atmosphere. Temperature, on the other hand, is a fundamental climate variable that is influenced by various natural and anthropogenic factors. The relationship between aerosol optical depth and temperature has significant implications for climate change dynamics. The implications of aerosol optical depth (AOD) and temperature on climate, particularly in relation to reflective aerosols and black carbon, are multifaceted and can significantly impact the Earth's climate system.

Reflective Aerosols: Reflective aerosols, such as sulfate aerosols, have a cooling effect on the climate due to their ability to scatter sunlight (NASA, n.d.-b). Some implications of reflective aerosols on climate are:

(a) Short-Term Cooling: Reflective aerosols scatter sunlight, reducing the amount of solar energy that reaches the Earth's surface. This results in localized cooling effects in regions with higher concentrations of these aerosols (Zhang, 2020). In the short term, reflective aerosols can offset some of the warming caused by greenhouse gases.
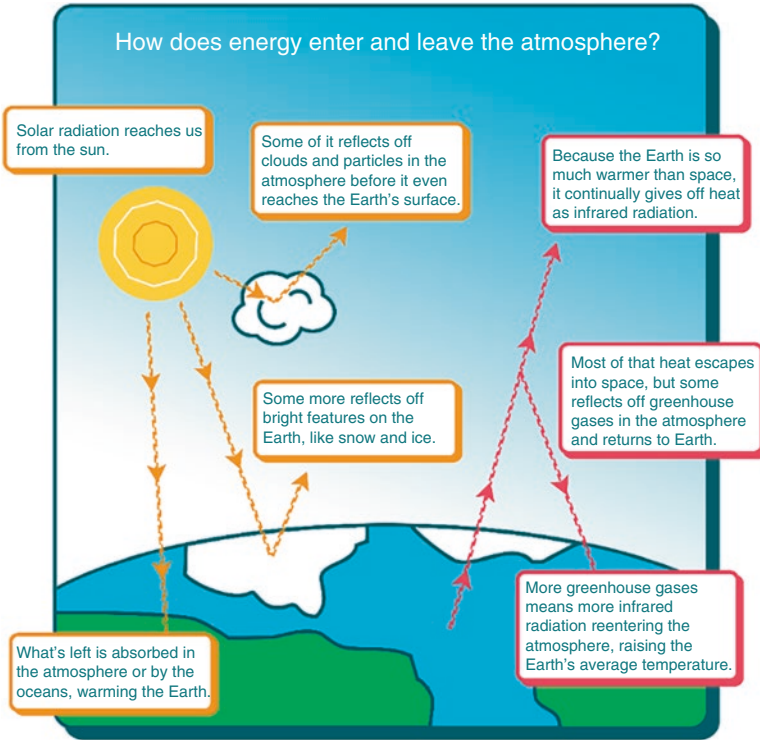
Fig. 4 Radiative forcing. (Image credit: Chandler (2020))

(b) Masking Warming: The cooling effect of reflective aerosols can mask a portion of the temperature increase attributed to greenhouse gases. This masking effect can make it challenging to accurately attribute temperature changes solely to greenhouse gas emissions.

(c) Regional Climate Patterns: Reflective aerosols can alter regional climate patterns by influencing temperature gradients, wind patterns, and precipitation distribution. This can lead to changes in weather patterns and precipitation amounts, affecting ecosystems and agriculture. Reflective aerosols, which reflect sunlight back into space, have diverse impacts on regional climate patterns tied to geographical locations. In tropical regions, they can induce cooling, potentially affecting monsoons and rainfall dynamics. Arctic regions might experience reduced ice melt due to decreased sunlight absorption, impacting polar climate and sea levels. Reflective aerosols in urban areas could alleviate the urban heat island effect, reshaping local weather patterns and circulation. In deserts, they may temper extreme heat and influence dust storms and atmospheric stability. Coastal zones could witness modified sea surface temperatures, affecting ocean currents and cyclone intensity. Such aerosols might also trigger shifts in global circulation patterns by altering jet streams, thus reshuf-

fling weather tracks and precipitation distribution. It's crucial to note that deploying these aerosols intentionally, though with potential benefits, raises complex scientific, ethical, and environmental questions that continue to be researched and debated.

(d) Aerosol-Cloud Interactions: Reflective aerosols can influence cloud formation by acting as cloud condensation nuclei (NASA, n.d.-c). This can lead to changes in cloud properties, which, in turn, affect the Earth's energy balance and climate.

Black Carbon: Black carbon, or soot, is a component of particulate matter emitted from incomplete combustion processes. Unlike reflective aerosols, black carbon absorbs sunlight, leading to warming effects. Some implications of black carbon on climate:

(a) Warming Effect: Black carbon absorbs sunlight, converting it into heat energy. This leads to warming of the atmosphere and surrounding air (CCAC). The presence of black carbon contributes to atmospheric heating and can impact local and regional temperature patterns. Black carbon, a type of aerosol resulting from incomplete combustion of fossil fuels and biomass, exerts significant regional climate impacts contingent on geographical locations. In the Arctic, where black carbon settles on snow and ice, it accelerates their melting by reducing surface reflectivity. Urban areas experience localized warming due to black carbon's heat-absorbing properties, intensifying heat island effects. In South Asia, its presence contributes to atmospheric warming, potentially altering the monsoon patterns and precipitation. Additionally, black carbon's ability to absorb sunlight and influence cloud formation can lead to complex regional climate responses.

(b) Impact on Snow and Ice: When black carbon is deposited on snow and ice surfaces, it reduces their reflectivity (albedo) (Beres et al., 2020). This accelerates snow and ice melt, contributing to the warming of regions with frozen surfaces. Black carbon can darken the snow/ice surface, affect the energy balance, and further lead to acceleration of the melting of cryosphere (Kang et al., 2020).

(c) Atmospheric Instability: The heating effect of black carbon can alter atmospheric stability, influencing weather patterns, circulation, and precipitation distribution (Cho, 2016).

The interplay of Reflective Aerosols and Black Carbon: The interplay between reflective aerosols and black carbon further complicates the climate system:

(a) Contrasting Effects: Reflective aerosols have a cooling effect, while black carbon has a warming effect. The simultaneous presence of both types of aerosols can lead to complex interactions and regional variations in temperature.

(b) Region-Specific Impact: The combined impact of reflective aerosols and black carbon can vary based on geographic location, emission sources, and atmospheric conditions. This variability adds intricacy to predicting climate responses.

(c) Feedback Loops: The presence of reflective aerosols can influence black carbon deposition patterns, altering its warming effects on snow and ice. These feedback loops can amplify or dampen the overall climate impact.

(d) Policy Implications: Effective climate mitigation policies must consider the diverse impacts of both aerosol types. Reductions in reflective aerosols could lead to rapid temperature increases if not coupled with strategies to address greenhouse gas emissions.

The implications of aerosol optical depth and temperature on climate, especially concerning reflective aerosols and black carbon, illustrate the complexity of Earth's climate system. Reflective aerosols can temporarily mitigate warming, while black carbon contributes to atmospheric heating and affects snow and ice melt. Understanding and accurately modeling the interactions between these aerosol types are crucial for predicting climate change outcomes and designing effective mitigation strategies that address both aerosols and greenhouse gases in the context of climate change.

3.6 Role of Aerosols on Human Health

Aerosols are small or liquid particles suspended in the air and can have both natural (wind-blown desert dust and sea salt) and anthropogenic (associated with combustion by-products) sources. In addition to their role in climate, aerosols are also of interest due to their capacity to reduce visibility, contribute to acid rain, and potentially impact human health. According to WHO (2022), the combined effects of ambient air pollution and household air pollution are associated with 6.7 million premature deaths annually. The effects on health caused by aerosols encompass both short-term acute symptoms such as asthma and bronchitis and long-term chronic irritation and inflammation of the respiratory tract which can potentially lead to cancer (Cross et al., 2001). Aerosols can damage lung tissue and lead to lung cancer. Aerosols containing allergenic particles such as pollen, mold spores, and pet dander can trigger allergenic reactions in susceptible individuals. These reactions may manifest as respiratory symptoms, skin irritations, and other discomforts. Communities living in regions with high levels of air pollution and aerosols, experience greater risk. These health disparities can disproportionately affect vulnerable populations, including children, the elderly, and those with pre-existing health conditions. Efforts to mitigate the health impacts of aerosols include implementing air quality regulations, promoting cleaner energy sources, improving industrial emissions control, and encouraging sustainable transportation practices.

4   Conclusions

In conclusion, the intricate relationship between aerosol optical depth and temperature is a multifaceted interplay influenced by a range of factors, each with its own distinct significance. Radiative forcing, driven by the interaction of aerosols with solar radiation, holds a pivotal role in shaping temperature trends. The geographical location amplifies these effects, showcasing regional variations in aerosol loading, atmospheric conditions, and resultant temperature changes. Reflective aerosols, characterized by their ability to reflect sunlight, have a cooling effect on temperature, impacting different regions diversely. On the other hand, black carbon, derived from combustion processes, contributes to localized warming due to its heat-absorbing properties. This dynamic interplay extends to rainfall patterns, as aerosols influence cloud properties and precipitation formation. Acknowledging these complexities is vital for understanding and addressing the broader implications of aerosol impacts on climate. As our understanding evolves, it is imperative to continue refining models and research methodologies to unravel the intricate relationships between aerosols, temperature, and rainfall, enabling more accurate predictions and informed decisions regarding climate mitigation and adaptation strategies.

References

Ackerman, A. S., Kirkpatrick, M. P., Stevens, D. E., & Toon, O. B. (2004). The impact of humidity above stratiform clouds on indirect aerosol climate forcing. *Nature, 432*, 1014–1017.

Alam, K., Iqbal, M. J., Blaschke, T., Qureshi, S., & Khan, G. (2010). Monitoring spatio-temporal variations in aerosols and aerosol-cloud interactions over Pakistan using MODIS data. *Advances in Space Research, 46*, 1162–1176. https://doi.org/10.1016/j.asr.2010.06.025

Amarillo, A., Carreras, H., Krisna, T., Mignola, M., Busso, I. T., & Wendisch, M. (2021). Exploratory analysis of carbonaceous PM2.5 species in urban environments: Relationships with meteorological variables and satellite data. *Atmospheric Environment, 245*, 117987.

Analitis, A., Michelozzi, P., D'Ippoliti, D., de Donato, F., Menne, B., Matthies, F., Atkinson, R. W., Iñiguez, C., Basagaña, X., Schneider, A., Lefranc, A., Paldy, A., Bisanti, L., & Katsouyanni, K. (2014). Effects of heat waves on mortality: Effect modification and confounding by air pollutants. *Epidemiology, 25*(1), 15–22.

Arkian, F., & Nicholson, S. E. (2018). Long-term variations of aerosol optical depth and aerosol radiative forcing over Iran based on satellite and AERONET data. *Environmental Monitoring and Assessment, 190*, 1–15.

Beres, N. D., Lapuerta, M., Cereceda-Balic, F., & Moosmuller, H. (2020). Snow surface albedo sensitivity to black carbon: Radiative transfer modelling. *Atmosphere, 11*, 1077. https://doi.org/10.3390/atmos11101077

Boucher, O., Randall, D., Artaxo, P., Bretherton, C., Feingold, G., Forster, P., Kerminen, V.-M., Kondo, Y., Liao, H., Lohmann, U., Rasch, P., Satheesh, S. K., Sherwood, S., Stevens, B., & Zhang, X. Y. (2013). Clouds and aerosols. In T. F. Stocker, D. Qin, G.-K. Plattner, M. Tignor, S. K. Allen, J. Boschung, A. Nauels, Y. Xia, V. Bex, & P. M. Midgley (Eds.), *Climate change 2013:The physical science basis, contribution of Working Group Ito the fifth assessment report of the Intergovernmental Panelon climate change*. Cambridge University Press. Available at: http://www.climatechange2013.org/images/uploads/WGIAR5_WGI12Doc2b_FinalDraft_Chapter07.pdf

CAICE. (2020). *Our science- introduction to aerosols*. Retrieved from: https://caice.ucsd.edu/introduction-to-aerosols/#what-is-an-aerosol

CCAC. *Black carbon*. Retrieved from: https://ccacoalition.org/short-lived-climate-pollutants/black-carbon

Chandler, D. (2020). Explained: Radiative forcing. *Climate Portal-MIT*. Retrieved from: https://climate.mit.edu/explainers/radiative-forcing#:~:text=Radiative%20forcing%20is%20what%20happens,infrared%20radiation%20exiting%20as%20heat

Che, H., Gui, K., Xia, X., Wangm, Y., Holben, B. N., Goloub, P., Cuevas-Agullo, E., Wang, H., Zheng, Y., & Zhao, H. (2019). Large contribution of meteorological factors to inter-decadal changes in regional aerosol optical depth. *Atmospheric Chemistry and Physics, 19*, 10497–10523.

Chen, L. X., Zhang, B., & Zhu, W. Q. (2009). Variation of atmospheric aerosol optical depth and its relationship with climate change in China east of 100˚E over the last 50 years. *Theoretical and Applied Climatology, 96*, 191–199. https://doi.org/10.1007/s00704-008-0023-7

Cho, R. (2016). The damaging effects of black carbon. *State of the planet.* Retrieved from: https://news.climate.columbia.edu/2016/03/22/the-damaging-effects-of-black-carbon

Chu, D. A., Kaufman, Y. J., Zibordi, G., Mao, J. T., Li, C. C., & Holben, B. N. (2003). Global monitoring of air pollution over land from the earth observing system-terra moderate resolution imaging spectroadiometer (MODIS). *Ecotoxicology and Environmental Safety, 108*, 46–61. https://doi.org/10.1029/2002JD003179

Cross, R., Anderson, A., Davidson, K., Cipriani, J., Stewart de V., & Hamlett, A. (2001). *Climate, aerosols and human health*. Retrieved from: https://icp.giss.nasa.gov/research/ppa/2001/2001_cross_etal.pdf

de Leeuw, G., Kang, H., Fan, C., Zhenqiang, L., Fang, C., & Zhang, Y. (2023). Meteorological and anthropogenic contributions to changes in aerosol optical depth (AOD) over China during the last decade. *Atmospheric Environment, 301*, 119676. https://doi.org/10.1016/j.atmosenv.2023.119676

Flousti, A. A., Korras-Carraca, M. B., Matsoukas, C., Hatzianastassiou, N., & Biskos, G. (2016). Climatology and trends in aerosol optical depth over the Mediterranean basin during the last 12 years (2002-2014) based on Collection 006 MODIS- Aqua data. *Science of Total Environment, 551*, 292–303.

Fouillet, A., Rey, G., Laurent, F., Pavillon, G., Bellec, S., Guihenneuc-Jouyaux, C., Clavel, J., Jougla, E., & Hémon, D. (2006). Excess mortality related to the August 2003 heat wave in France. *International Archives of Occupational and Environmental Health, 80*(1), 16–24.

Gautam, S., Elizabeth, J., Gautam, A. S., Singh, K., & Abhilash, P. (2022). Impact assessment of aerosol optical depth on rainfall in Indian rural areas. *Aerosol Science and Engineering, 6*, 186–196.

Gui, K., Che, H., Wang, Y., Wang, H., Zhang, L., Zhao, H., Zheng, Y., Sun, T., & Zhang, X. (2019). Satellite-derived PM2.5 concentration trends over Eastern China from 1998 to 2016: Relationships to emissions and meteorological parameters. *Environmental Pollution, 247*, 1125–1133.

Gunaseelan, I., Bhaskar, V., & Muthuchelian, K. (2013). The impact of aerosol optical depth impacts on rainfall in two different monsoon periods over Madurai, India. *Aerosol and Air Quality Research, 13*, 1608–1618. https://doi.org/10.4209/aaqr.2012.07.0197

Gunaseelan, I., Bhaskar, B. V., & Muthuchelian, K. (2014). The effect of aerosol optical depth on rainfall with reference to meteorology over metro cities in India. *Environmental Science and Pollution Research, 21*, 8188–8197. https://doi.org/10.1007/s11356-014-2711-4

Hu, T., Sun, Z., & Li, Z. (2011). Features of aerosol optical depth and its relation to extreme temperatures in China during 1980–2001. *Acta Oceanologica Sinica, 30*(2), 33–45. https://doi.org/10.1007/s13131-011-0103-x

Johnson, H., Kovats, S., McGregor, G., Stedman, J., Gibbs, M., Walton, H., & Cook, L. (2004). The impact of the 2003 heat wave on mortality and hospital admissions in England. *Epidemiology, 15*(4), S126.

Jung, J., Souri, A. H., Wong, D. C., Lee, A., Jeon, W., Kim, J., & Choi, Y. (2019). The impact of the direct effect of aerosols on meteorology and air quality using aerosol optical depth assimilation during the KORUS-AQ campaign. *JGR Atmospheres, 124*(14), 8303–8319. https://doi.org/10.1029/2019JD030641

Kang, S., Zhang, Y., Qian, Y., & Wang, H. (2020). A review of black carbon in snow and ice and its impact on the cryosphere. *Earth-Science Reviews, 210*, 103346. https://doi.org/10.1016/j.earscirev.2020.103346

Lee, J. D., Lewis, A. C., Monks, P. S., Jacob, M., Hamilton, J. F., Hopkins, J. R., Watson, N. M., Saxton, J. E., Ennis, C., Carpenter, L. J., Carslaw, N., Fleming, Z., Bandy, B. J., Oram, D. E., Penkett, S. A., Slemr, J., Norton, E., Rickard, A. R., Whalley, L. K., Heard, D. E., Bloss, W. J., Gravestock, T., Smith, S. C., Stanton, J., Pilling, M. J., & Jenkin, M. E. (2006). Ozone photochemistry and elevated isoprene during the UK heatwave of August 2003. *Atmospheric Environment, 40*(39), 7598–7613.

Li, R., Li, J. W., Liu, Z. J., Hua, J. J., Wang, Y., & Wang, W. Y. (2016). Satellite observational study on correlations among aerosol optical depth, NO2 and SO2 over China. *Chinese Science Bulletin, 61*, 2524–2535.

Lin, C. A., Chen, Y. C., Liu, C. Y., Chen, W. T., Seinfield, J. H., & Chou, C. C. K. (2019). Satellite-derived correlation of SO2, NO2 and aerosol optical depth with meteorological conditions over East Asia from 2005 to 2015. *Remote Sensing, 11*, 1738. https://doi.org/10.3390/rs11151738

Mehta, M., & Khushboo, R. (2022). Recent decadal aerosol trends over oceanic regions surrounding Indian landmass. *Aerosol Science and Engineering, 6*, 448–455.

Mielonen, T., Hienola, A., Kuhn, T., Merikanto, J., Lipponen, A., Bergman, T., Korhonen, H., Kolmonen, P., Sogacheva, L., Ghent, D., Arola, A., de Leeuw, G., Kokkola, H. (2016). Temperature dependence of aerosol optical depth over south-eastern US. *Atmospheric Chemistry and Physics* Discuss [preprint]. https://doi.org/10.5194/acp-2016-625.

NASA. (2008). *AERONET mission follow up: Finding an instrument's place under sun*. Retrieved from: https://www.nasa.gov/centers/langley/science/aeronet.html

NASA. (2020). *Radiative transfer*. Retrieved from: https://www.nasa.gov/content/radiative-transfer.

NASA. (n.d.-a). *Aerosol optical depth*. Retrieved from: https://earthobservatory.nasa.gov/global-maps/MODAL2_M_AER_OD.

NASA. (n.d.-b). *Aerosols and incoming sunlight (direct effects)*. Retrieved from: https://earthobservatory.nasa.gov/feactures/Aerosols/page3..php

NASA. (n.d.-c). *Aerosols and their importance*. Retrieved from: https://earth.gsfc.nasa.gov/climate/data/deep-blue/aerosols

NASA. (n.d.-d). *Climate and radiation. How aerosols are measured: The science of deep blue*. Retrieved from: https://earth.gsfc.nasa.gov/climate/data/deep-blue/science#:~:text=Aerosol%20Robotic%20Network%20(AERONET)%20is,in%20an%20aerosol-free%20atmosphere

National Geographic. *Temperature*. Retrieved from: https://education.nationalgeographic.org/resource/temperature/

NOAA. (2023). *Layers of the Atmosphere*. Retrieved from: https://noaa.gov/jetstream/atmosphere/layer-of-atmosphere#:~:test=As%20the%20density%20of%20the'˚C)%20at%20the%20tropopause

NOAA. *Teaching activity: Factors that affect climate*. Retrieved from: https://gml.noaa.gov/education/lesson_plans/Factors%20that%20Affect%20Climate.pdf

Payra, S., Sharma, A., Mishra, M. K., & Verma, S. (2023). Performance evaluation of MODIS and VIIRS satellite AOD products over the Indian subcontinent. *Frontiers in Environmental Science, 11*. https://doi.org/10.3389/fenvs.2023.1158641

Pena, M. A., & Araya, P. (2019). Hacia el modelado de material particulado fino en Santiago, Chile, mediante im`agenes MODIS. *Revista Geográfica de Chile Terra Australis, 55*(1), 74–81.

Rani, S., & Kumar, R. (2022). Spatial distribution of aerosol optical depth over India during COVID-19 lockdown phase-1. *Spatial Information Research, 30*, 417–426. https://doi.org/10.1007/s41324-022-00442-9

Roy, S. S. (2008). Impact of aerosol optical depth on seasonal temperatures in India: A spatio-temporal analysis. *International Journal of Remote Sensing, 29*(3), 727–740. https://doi.org/10.1080/01431160701352121

Sarthi, P. P., Kumar, S., Barat, A., Kumar, P., Sinha, A. K., & Varsha, G. (2019). Linkage of aerosol optical depth with rainfall and circulation parameters over the Eastern Gangetic Plains of India. *Journal of Earth System Science, 128*. https://doi.org/10.1007/s12040-019-1204-8

Stevens, B., & Feingold, G. (2009). Untangling aerosol effects on clouds and precipitation in a buffered system. *Nature, 461*, 607–613. https://doi.org/10.1038/nature08281

Tariq, S., & Ul-Haq, Z. (2019). Investigating the aerosol optical depth angstrom exponent and their relationships between with meteorological parameters over Lahore in Pakistan. *Proceedings of the National Academy of Sciences, India Section A: Physical Sciences, 90*, 861–867. https://doi.org/10.1077/s40010-018-0575-6

WHO. (2010). *WHO guidelines for indoor air quality: Selected pollutants*.

WHO. (2022). *Household air pollution*. Retrieved from https://who.int/news-room/fact-sheets/detail/household-air-pollution-and-health

Winker, D. M., Pelon, J., Coakley, J. A., Jr., Ackerman, S. A., Charlson, R. J., Colarco, P. R., Flamant, P., Fu, Q., Hoff, R. M., & Kittaka, C. (2010). The CALIPSO mission: A global 3D view of aerosols and clouds. *Bulletin of the American Meteorological Society, 91*, 1211–1229.

World Meteorological Organization. (2022). *Aerosols*. Retrieved from: https://public.wmo.int/en/our-mandate/focus-areas/environment/aerosols

Yoon, J., Burrows, J., Vountas, M., Hoyningen-Huene, W., Chang, D., Ritcher, A., & Hilboll, A. (2013). Changes in atmospheric aerosol loading retrieved from space based measurements during the past decade. *Atmospheric Chemistry and Physics Discussion, 13*, 26001–26041.

Zaman, S. U., Pavel, M. R. S., Joy, K. S., Jeba, F., Islam, M. S., Paul, S., Bari, M. A., & Salam, A. (2021). Spatial and temporal variation of aerosol optical depths over six major cities in Bangladesh. *Atmospheric Research, 262*, 105803. https://doi.org/10.1016/j.atmosres.2021.105803

Zeydan, O., Tariq, S., Qayyum, F., Mehmood, U., & Ul-Haq, Z. (2023). Investigationg the long-term trends in aerosol optical depth and its association with meteorological parameters and enhanced vegetation index over Turkey. *Environmental Science and Pollution Research, 30*, 20337–20356. https://doi.org/10.1007/s11356-022-23553-0

Zhang, B. (2020). The effect of aerosols to climate change and society. *Journal of Geoscience and Environment Protection, 8*(8). https://doi.org/10.4236/gep.2020.88006

Zhang, Y., Li, Z., Bai, K., Wei, Y., Xie, Y., Zhang, Y., & Li, D. (2021). Satellite remote sensing of atmospheric particulate matter mass concentration: Advances, challenges and perspective. *Fundamental Research, 1*(3), 240–258. https://doi.org/10.1046/j.fmre.2021.04.007

Impact Assessments of Aerosol Optical Depth and Lightning on Thunderstorm Over the Region of Uttarakhand, India

Alok Sagar Gautam, Sanjeev Kumar, Karan Singh, Shyam Narayan Nautiyal, and Sneha Gautam

1   Introduction

In the most recent decade in Uttarakhand, one of the subjects that has been the focus of active investigation is lightning due to its potentially devastating effects. Lightning is largely determined by the prevailing weather and environmental circumstances, as well as how these factors interact with the terrain of the area in which it forms. The occurrence of lightning is determined by a number of different climatic elements, including precipitation, aerosol optical depth (AOD), cloud base height, and convection (Kumar, 2018). Petersen and Rutledge (1998) have observed a high correlation between rainfall and lightning. However, the strength of correlation is found to be highly dependent on the local convective regime. Previous research, conducted by Zipser and Lutz in 1994, establishes a clear contrast between the reliance of Precipitation and Lightning on vertical velocity. Williams (2005) demonstrated that only a slight upward movement of an air parcel is required for precipitation, whereas a far deeper and more intense movement is required for lightning to take place. Lightning can only occur when the peak updraft speed is between 10 and 12 m/s as demonstrated by Zipser and Lutz (1994). In the months leading up to the monsoon and during the actual rainy season (monsoon), researchers Manohar, Kandalgaonkar, and Tinmaker (1999) found that there were extremely good positive connections

A. S. Gautam (✉) · S. Kumar · K. Singh
Department of Physics, Hemvati Nandan Bahuguna Garhwal University,
Srinagar Garhwal, Uttarakhand, India

S. N. Nautiyal
Department of Chemistry, SRT Campus, Hemvati Nandan Bahuguna Garhwal University,
Srinagar Garhwal, Uttarakhand, India

S. Gautam
Division of Civil Engineering, Karunya Institute of Technology and Sciences, Coimbatore,
Tamil Nadu, India

between days with seasonal rainfall and days with thunderstorms across the Indian region. Recent research indicates that convection and the presence of aerosols are the primary factors that have a significant impact on the amount of rainfall and lightning (Jnanesh et al., 2022). The greater the concentration of aerosol particles, the greater the quantity of smaller cloud droplets that will be produced. A reduction in the amount of precipitation that falls as a result of cloud droplet coalescence is caused by a rise in the amount of cloud droplets that are of a smaller size (Zhao et al., 2020). According to Williams and Satori (2004) and Williams and Stanfill (2002), increased aerosol concentration enhances liquid water content in mixed-phase regions, crucial for cloud electrification. Lightning and the yearly average number of cloud condensation nuclei were discovered to have a very good link with one another (Venevsky, 2014). There is a positive relationship between aerosols and the cloud droplet effective radius (Yuan & Qie 2008). Yuan & Qie (2008) concluded that this relation is the cause of the three-dimensional effect, humidity effect (aerosol swelling), the effect of partially cloudy and partially conditions brought on by atmospheric dynamics, as well as the effect of surface influence brought on by surface influence (Lal et al., 2018). The convective available potential energy (CAPE) is a measurement of the capacity of a portion of air to float (buoyancy of a parcel of air). CAPE is regarded to be a required condition necessary for the formation of thunderstorms because it is primarily influenced by the temperature of the air near the surface (Kumar, 2018). If the rising of a buoyant portion of air results in continuing to heights that are higher than the freezing level. Consensus suggests that the occurrence of graupels and ice crystals within the mixed phase region stands as the pivotal determinant in the likelihood of a thunderstorm generating significant electrification and lightning (Krehbiel, 1986). According to Gadgil and Srinivasan (1990), OLR, or Outgoing Longwave Radiation, can be used as a stand-in for deep convection. Principal component analysis (PCA) is a powerful tool for understanding the inter-relationship between lightning activities and meteorological parameters (Kamar, 2018). Researchers have investigated the connection between lightning and precipitation and very few studies are conducted in the state of Uttarakhand (Gautam et al., 2022a, 2023). The main objectives of our study were (a) to understand the spatial variation of lightning activities, (b) influence of aerosols, (c) contribution of deep convection activities, (d) role of surface temperature, and CAPE over Uttarakhand.

2 Material and Methods

2.1 Site Description

Uttarakhand is located on the southern slope of the Himalayan located in the Western Himalayas region and spread between 28°43′ N to 31°27′ N (longitude) and 77°34′ E to 81°02′ E (latitude) (Gaur et al., 2021; Bargali et al., 2022). Graphically, it is divided into three zones, as Himalaya, the Shiwalik, and the Terai

region with the two administrative divisions (a) Kumaon and (b) Garhwal. Uttarakhand shares its border with Nepal, China, and neighboring state states such as Uttar Pradesh, Himachal Pradesh, and Haryana (Bargali et al., 2022). Uttarakhand has a total area of 53,566 km^2 of which 93% is mountainous and 64% is covered by forest. Most of the northern part of the state is covered by high Himalayan peaks and glaciers (Rao et al., 2012; Negi, 1991). Uttarakhand has a population of 10,086,292 (Census, 2011). The hilly areas experience a temperate climate whereas the climate is tropical in the plain areas. The average annual rainfall of the state is 1550 mm and temperatures range from sub-zero to 43 °C (FSI, 2017). The Uttarakhand experiences intense lightning activities in the foothills of Himalayas and it is just located South-eastern direction of lightning hotspots (Tinmaker et al., 2021). The presence of deep valleys in the mountains provides additional opportunities for orographic lifting, and it is responsible for the vertical development of clouds for lightning activities (Gautam et al., 2022a). Figure 1 demonstrates the study location with an elevation map and lightning activities in the year 2022. The red spot shows the lightning flashes. Most of the lightning flashes have been observed in the mid-altitude regions of Uttarakhand (Fig. 1). Dehradun, Tehri, Pauri, Uttarkashi, Bageshwar, and Pithoragarh districts of Uttarakhand have been shown the maximum lightning activities in the year 2022.

2.2 Data and Methodology

The daily aerosol optical depth data at 550 nm was extracted from the Moderate Resolution Imaging Spectroradiometer (MODIS) mounted on Terra satellite in the spatial resolution of 1° × 1° (Chauhan & Singh, 2021; Singh & Chauhan, 2020;
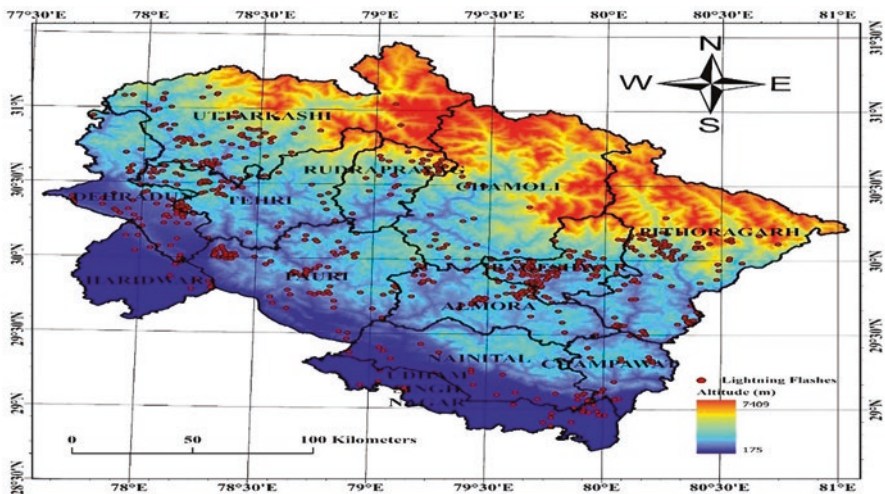
Fig. 1 Elevation map of Uttarakhand with lightning events during the study period in 2022. The red spot represents lightning activities

Zheng et al., 2017; Gautam et al., 2022a). The AOD data can be easily accessed from Giovanni portal of NASA from the website (https://giovanni.gsfc.nasa.gov/giovanni/). The lightning flash count data was extracted from the National Aeronautics and Space Administration (NASA)'s Search Earth data center (https://search.earthdata.nasa.gov/) and lightning activities were observed by the onboard Lightning Imaging Sensor (LIS) International Space Station (ISS) in the near real-time resolution 2 minutes and 4–8 km spatial resolution (Kumar, 2018; Gautam et al., 2022a, b). Convective Available Potential Energy, Temperature, and total precipitation data were downloaded from the Climate Data Store (https://cds.climate.copernicus.eu/) generated by the ERA5 platform. Outgoing Longwave Radiation data was extracted from the National Oceanic and Atmospheric Administration (NOAA) Physical Sciences Laboratory (PSL) (https://psl.noaa.gov/data/gridded/data.olrcdr.interp.html) in the 2.5° × 2.5° resolution (Kumar, 2018; Gautam et al., 2022a, b). More details of data are also provided in Table 1.

2.3 Principal Component Analysis

The principal component analysis is a statistical method, which is used to reduce the large number of variables into meaningful few variables called principal components, which have complete information. The PCA starts the computation of standardization by subtracting mean values from the data points for each variable. Now covariance is computed to understand the mutual variation of variables from mean values. Mathematically covariance can be computed using following mathematical equations:

$$Cov(x,y) = \frac{\sum_{i=1}^{n}(x_i - \bar{x})(y_i - \bar{y})}{(n-1)}$$

Where x and y are two dimensions and n be the total number of data points. We have used 6 parameters and 12 months in the study. The covariance matrix ($i = 12, j = 12$) is computed by using following formula.

$$C^{mn} = \left(c_{i,j}, c_{i,j,} = Cov\left(\dim_i, \dim_j\right)\right)$$

Where C^{mn} is covariance matrix and Dim_i & dim_j are the dimension of x and y. Eigen values and Eigen vector are computed by the computation of covariance matrix. The eigen vector whose eigen values are high as compared to others is considered a principal component. All these steps can be performed by using factoextra/FactoMineR packages in the Rstudio software (Version 2023.3.0.0). The PCA has been used as a potential to study the variability and interrelationship between the lightning, aerosol, and metrological parameters (Kumar, 2018).

Table 1 Satellite-derived atmospheric variables data description

Sr. No.	Variable Name	Data Source	Spatial Resolution	Temporal Resolution	Platform	References
1.	Aerosol Optical Depth (550 nm)	MODIS- Terra	1° × 1°	Daily	Obtained from NASA Giovanni portal (https://giovanni.gsfc.nasa.gov/giovanni/)	Chauhan and Singh (2021), Singh and Chauhan (2020), Zheng et al. (2017), Gautam et al. (2022a)
2.	Lightning Data	ISS LIS	4–8 km	Near Real Time (NRT): 2 minutes	Obtained from GHRC or Search Earth data center (https://search.earthdata.nasa.gov/)	Kumar (2018), Gautam et al. (2022a, b)
3.	Convective Available Potential Energy (J/kg)	ERA5Reanalysis	0.25° × 0.25°	Hourly	Obtained from Climate Data Store (https://cds.climate.copernicus.eu/)	Kumar (2018), Gautam et al. (2022a, b)
4.	Temperature (°C)	ERA5Reanalysis	0.25° × 0.25°	Hourly	Obtained from Climate Data Store (https://cds.climate.copernicus.eu/)	Kumar (2018), Gautam et al. (2022a, b)
5.	Total Precipitation (mm)	ERA5Reanalysis	0.25° × 0.25°	Hourly	Obtained from Climate Data Store (https://cds.climate.copernicus.eu/)	Kumar (2018), Gautam et al. (2022a, b)
6.	Outgoing Longwave Radiation (W/m²)	NCAR archives	2.5° × 2.5°	Daily	NOAA Physical Sciences Laboratory (PSL) (https://psl.noaa.gov/data/gridded/data.olrcdr.interp.html)	Kumar (2018), Gautam et al. (2022a, b)

3   Results and Discussion

3.1   Daily Variation of Flash Count and Parameters

The daily variations of AOD, flash count, CAPE, surface temperature, total precipitation, and OLR are clearly described in Fig. 2a–f. Daily AOD values were relatively low in January (0.02) and February (0.04). However, starting in Mar, there was a notable upward trend, with values ranging from 0.1 to 0.61, reaching a peak of 0.83. May saw a significant increase, with 26 days recording high AOD values (>0.9), indicating the transport of aerosols from polluted regions and deserts (Gautam et al., 2021). A decreasing trend in AOD values was observed, attributed to the summer monsoon's wet scavenging of aerosol particles (Bhattacharya et al., 2022), causing AOD to drop to 0.04. However, a subsequent increasing trend was reported, possibly linked to biomass-burning activities in nearby regions, particularly transported from Punjab, Haryana, and western Uttar Pradesh, as depicted in Fig. 2a. Figure 2b illustrates daily lightning activity patterns for the year 2022. Lightning activity remains relatively low during the winter monsoon, with counts not exceeding 6. In contrast, during the pre-monsoon period (March, April, and
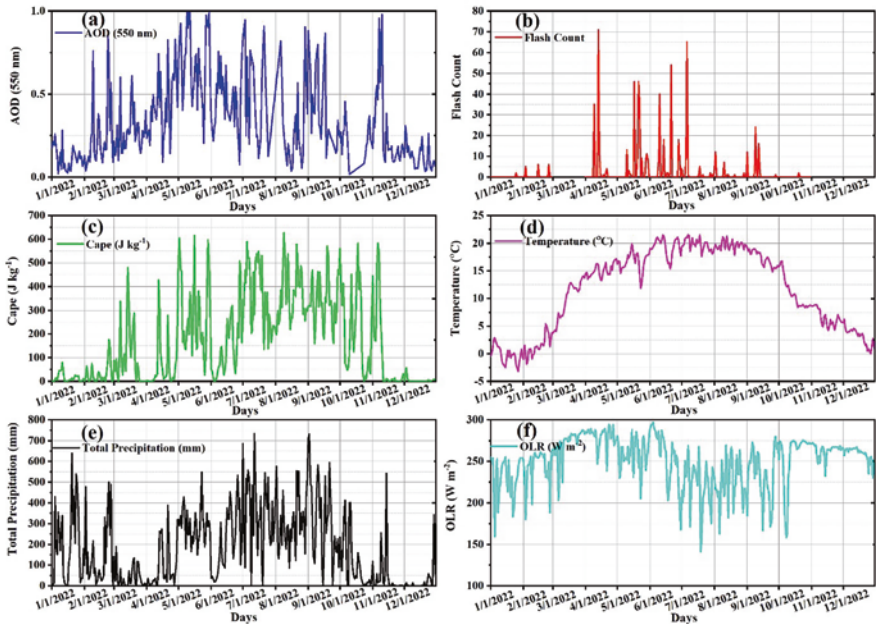
Fig. 2 Daily fluctuations of Aerosol Optical Depth (AOD) (**a), Flash Count (b), Convective Available Potential Energy (CAPE) (c), Temperature (d), Total Precipitation (e), and Outgoing Longwave Radiation (OLR) (f) are clearly illustrated for the year 2022**

May), lightning activity is notably dominant. The highest lightning flash counts of 71, 46, 46, and 26 occurred on April 13th, May 17th, May 17th, and May 17th, 2022, respectively. The increased lightning counts during the pre-monsoon period can be attributed to the heating of the Earth's surface. Additionally, deep convection activities resulted in high flash counts, reaching up to 65 in June, July, and September. To support our lightning observations, we have plotted CAPE data for a detailed analysis (Fig. 2c). CAPE exhibits noticeable variations, with values gradually increasing from January and peaking at 480.23 J/kg in March. Another increase is observed from April to May, with the highest value reaching 621.03 J/kg. Conversely, CAPE decreases after August, continuing through December. Low CAPE values in January, February, November, and December indicate reduced lightning activity due to the absence of the necessary buoyancy for thundercloud development (Kumar, 2018). The most significant temperature drop (-3.2 °C) occurred on January 27, 2022. Subsequently, temperatures exhibited an upward trend until May and Jun. However, a substantial temperature decrease followed due to heavy rainfall (547.23 mm on May 23, 2022). Following this rainy episode, as moisture persisted and rainfall continued, temperatures began to decline, as shown in Fig. 2d. During the winter monsoon period (Fig. 2e), we recorded daily high total rainfall, reaching up to 638.45 mm, 538.18 mm, 428.70 mm, and 432.24 mm. To assess deep convection, we employed OLR data, where low values (e.g., 160.12 w/m^2, 188.82 w/m^2, 210.35 w/m^2, 205.23 w/m^2, 141.10 w/m^2, 170.2 w/m^2, 173.2 w/m^2, and 167 w/m^2) in January, February, May, July, August, September, and October suggested the presence of clouds in the atmosphere. These conditions were associated with reduced rainfall and lightning activities (Kumar, 2018). In contrast, relatively peak OLR values (e.g., 287.7 w/m^2, 294 w/m^2, 297 w/m^2, 280.25 w/m^2, 275.02 w/m^2, 272.3 w/m^2, and 267.3 w/m^2) correspond to clear days in March, April, June, October, November, and December during the study (Fig. 2f). Sudeepkumar et al. (2022) employed these OLR datasets to classify rays as clear, partially cloudy, or cloudy.

3.2 Monthly Variation

In Fig. 3a–f, the monthly variation of AOD from January to May 2022 shows a steady increase, primarily attributed to aerosol emissions from the Thar Desert and arid regions. However, post-May 2022 (Fig. 3a), a notable decline in AOD is observed, indicative of aerosol removal processes within the atmosphere (Tesfaye et al., 2011; Babu et al., 2013). Lightning activity in Uttarakhand is most prominent during May, with notable events occurring in March, April, June, July, August, and September. These monthly trends align well with lightning patterns in the broader Indian monsoon zone (Fig. 3b). However, it is worth noting that the peak flash rate, at 0.065 flashes/km^2/day, is considerably lower compared to our location, which records a significantly higher rate of 6.5 flashes/km^2/day in May (Kumar, 2018).
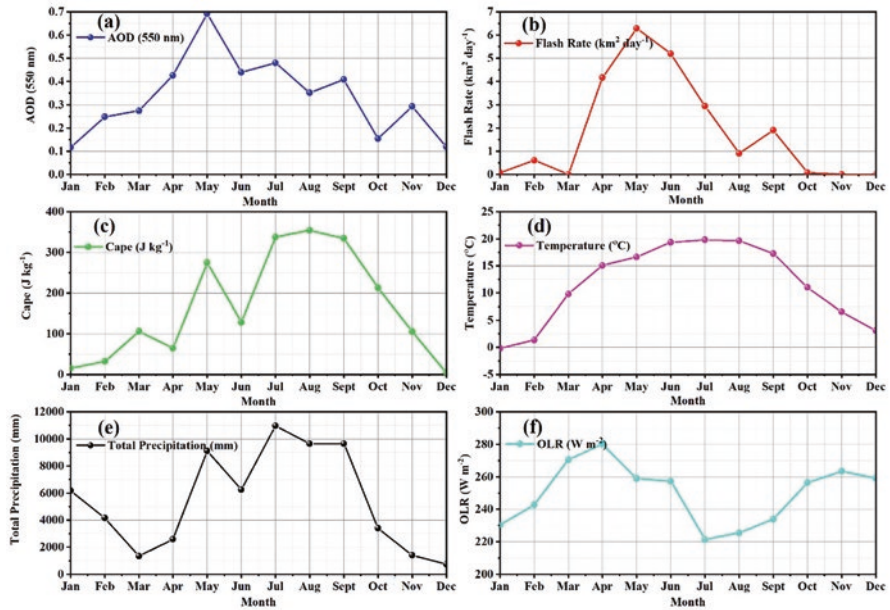
Fig. 3 Monthly fluctuations of Aerosol Optical Depth (AOD) (**a), Flash Count (b), Convective Available Potential Energy (CAPE) (c), Temperature (d), Total Precipitation (e), and Outgoing Longwave Radiation (OLR) (f) are clearly illustrated for the year 2022**

The CAPE values exhibit a progressive increase from January, reaching peaks in May (274.34), July (337.24), and Aug (354.23). This escalation can be attributed to rising surface temperatures. However, as the Earth's surface cools, a subsequent decline in lightning activity is observed (Fig. 3c). Stable weather conditions in June, coupled with slightly reduced rainfall in Uttarakhand (Fig. 3b–e), result in a decrease in CAPE values, further contributing to the drop-in lightning activities during that month. The low OLR values observed in June and July signify cloud presence, contributing to intense rainfall activities in Uttarakhand, with recorded levels of 10975.79 mm and 9640.69 mm, respectively. Kumar (2018) also reported a similar correlation between rainfall and OLR in July within the broader Indian monsoon zones, noting that approximately 65% of CAPE variability does not correlate with changes in flash rates. Around 22% of CAPE variability in the Himalayan foothills is associated with higher flash rates, likely influenced by diurnal mountain breeze, solar heating, orography, and monsoon convective systems (Ramesh Kumar & Kamra, 2012). In the wet northeast, a striking 86% of lightning incidents occur below 500 m elevation and decline sharply with higher elevation. Conversely, in the arid northwest, 49% of lightning occurrences are below 500 m elevation, gradually diminishing with increased elevation (Oulkar et al., 2019).

Table 2 Seasonal statistics of all variables during the study period 2022 over Uttarakhand

Season	AOD (550 nm)	Flash Rate (km²/day)	CAPE (J/kg)	Temperature (°C)	Total Precipitation (mm)	OLR (W/m²)
Winter	0.18	0.34	23.64	0.58	10335.52	236.5605
Pre-Monsoon	0.46	3.49	148.44	13.84	13044.13	269.8724
Monsoon	0.42	2.73	288.79	19.01	36513.20	234.5175
Post-Monsoon	0.22	0.03	159.18	8.78	4804.50	259.8769

3.3 Seasonal Variation

Seasonal statistics for various parameters, including AOD, flash rate, CAPE, temperature, total precipitation, and OLR, are discussed in Table 2. AOD dominance is observed during the pre-monsoon and monsoon seasons, attributed to aerosol transport and dust from neighboring countries such as Afghanistan, the Middle East, and Africa, as noted by Gautam et al. (2021). Lightning activity peaks during the premonsoon and monsoon seasons due to elevated land surface temperatures and CAPE, supporting the development of thunderclouds in Uttarakhand. Lower OLR values during the monsoon season indicate heightened convection activities, leading to thunderstorm formation and intense rainfall, in accordance with studies by Ghanekar et al. (2003) and Kumar (2018).

Furthermore, a decline in lightning activity is attributed to the cooling of the Earth's surface. The consistent trend in AOD and flash rate variations suggests the involvement of aerosol particles in lightning events. Under clean conditions (AOD < 1.0), there is a notable positive correlation between lightning frequency and aerosol optical depth (AOD), with a significant correlation coefficient ($r = 0.64$). This phenomenon is associated with aerosol microphysical effects, as documented by Shi et al. (2020).

3.4 Spatial Variation of Lightning Activities Over Uttarakhand

Limited lightning activity is observed during the summer monsoon in the Himalayan foothills and the northwestern region of Uttarakhand. In April, lightning events primarily concentrate in the northwestern districts, with a few occurrences in the northeastern district. May and June witnessed lightning activity throughout Uttarakhand, particularly in the mid-altitude areas. However, during July, August, and September, lightning events are concentrated in the southeastern part of Uttarakhand (Fig. 4). These patterns are predominantly influenced by the hot summer conditions and monsoon convection in the western region. Similar spatial variations have been reported by Gautam et al. (2022a) and Gautam et al. (2023).

Fig. 4 Monthly lightning events activity over Uttarakhand for the study period 2022

3.5 Principal Component Analysis

Variables, including flash count, AOD, temperature, CAPE, total precipitation, and OLR, are represented as eigenvectors, while PC1 and PC2 scores are depicted on the x and y axes. The angle (<90°) between eigenvectors indicates strong correlations. Notably, we observe a robust relationship between flash count, CAPE, and

Fig. 5 Principal component analysis for all variables during the study period 2022

temperature, attributed to air buoyancy due to land surface heating during the pre-monsoon and monsoon periods as shown in (Fig. 5). Additionally, there is a significant correlation between flash count and AOD, underscoring the contribution of aerosol particles to lightning events. OLR exhibits a negative correlation with flash count, CAPE, temperature, AOD, and total precipitation, aligning with findings in the Indian monsoon zone (Kumar, 2018).

4 Conclusions

Our 2022 study in Uttarakhand yields key findings of significant relationships between meteorological variables and lightning, emphasizing aerosol influence. These insights inform mitigation and preparedness strategies. AOD increases from January to May due to aerosol influx from the Thar Desert and arid regions. Post-May, AOD declines due to aerosol removal. May exhibits the highest lightning activity, with notable events in March, April, June, July, August, and September. While it aligns with monsoon zone lightning patterns (Fig. 3b), peak flash rates (0.065 flashes/km²/day) are lower than reported May values (6.5 flashes/km²/day) elsewhere (Kumar, 2018). CAPE values rise from January, peaking in May, July, and August, driven by increased surface temperatures. Earth's surface cooling leads to reduced lightning activity, particularly in June. Lower OLR values in June and July indicate cloud presence, resulting in substantial Uttarakhand rainfall (10975.79 mm and 9640.69 mm). A similar pattern was reported in July in the Indian monsoon zone (Kumar, 2018). About 65% of CAPE variability isn't linked

to flash rate changes. Roughly 22% of CAPE variability is associated with higher flash rates in Himalayan foothills, likely due to factors like solar heating, orography, and monsoon convective systems. Lightning occurrences differ by elevation, with 86% in the wet NE region below 500 m elevation, sharply declining with higher elevation. Conversely, in the dry NW region, 49% occur below 500 m elevation, gradually decreasing with increased elevation. Table 1 summarizes seasonal data, indicating AOD dominance in pre-monsoon and monsoon, higher lightning activity, lower OLR values, and AOD's positive correlation with lightning frequency under clean conditions. In the spatial variation, the lightning activity in Uttarakhand exhibits distinct seasonal variations, with the least activity in summer foothills and the highest in the southeastern region from July to September, largely influenced by summer and monsoon convection. Based on PCA, a strong link exists between flash count, CAPE, and temperature, driven by land surface heating during pre-monsoon and monsoon seasons. Flash count correlates significantly with AOD, indicating aerosol impact on lightning. OLR negatively correlates with flash count in monsoon zone.

References

Babu, S. S., Manoj, M. R., Moorthy, K. K., Gogoi, M. M., Nair, V. S., Kompalli, S. K., et al. (2013). Trends in aerosol optical depth over Indian region: Potential causes and impact indicators. *Journal of Geophysical Research: Atmospheres, 118*(20), 11–794. https://doi.org/10.1002/2013JD020507

Bargali, H., Kumar, A., & Singh, P. (2022). Plant studies in Uttarakhand, Western Himalaya: A comprehensive review. *Trees, Forests and People*, 100203. https://doi.org/10.1016/j.tfp.2022.100203

Bhattacharya, A., Venkataraman, C., Sarkar, T., Sharma, A. K., Sharma, A., Anand, S., et al. (2022). An analysis of the aerosol lifecycle over India: COALESCE intercomparison of three general circulation models. *Journal of Geophysical Research: Atmospheres, 127*(14), e2022JD036457. https://doi.org/10.1029/2022JD036457

Census. (2011). *Uttarakhand population census 2011, Uttarakhand religion, literacy, sex ratio - Census India*. https://www.censusindia.co.in//states/uttarakhand

Chauhan, A., & Singh, R. P. (2021). Effect of lockdown on HCHO and trace gases over India during March 2020. *Aerosol and Air Quality Research, 21*, 200445. https://doi.org/10.4209/AAQR.2020.07.0445

FSI. (2017). *India state of forest report 2017*. Forest Survey of India, Ministry of Environment, Forest and Climate Change. Government of India, Dehradun.

Gadgil, S, & Srinivasan, J. (1990). Low Frequency Variation of Tropical Convergence Zones. *Meteorol Atmos Physical 44: 119–132*. https://doi.org/10.1007/BF01026814

Gaur, A., Kumar, S., Vandita, S., Kumar, S., Singh, K., & Gautam, A. S. (2021). A case study of forest fires in Uttarakhand and adjoining areas in India. *Journal of Science and Technological Researches, 3*, 62. https://doi.org/10.51514/JSTR.3.3.2021.62-70

Gautam, A. S., Nainwal, H. C., Negi, R. S., Kumar, S., & Singh, K. (2021). Study of the aerosol parameters and radiative forcing during COVID-19 pandemic over Srinagar Garhwal, Uttarakhand. In *Environmental resilience and transformation in times of COVID-19: Climate change effects on environmental functionality* (pp. 163–172). https://doi.org/10.1016/B978-0-323-85512-9.00028-0

Gautam, A. S., Joshi, A., Chandra, S., Dumka, U. C., Siingh, D., & Singh, R. P. (2022a). Relationship between lightning and aerosol optical depth over the Uttarakhand region in India: Thermodynamic perspective. *Urban Science, 6*(4), 70. https://doi.org/10.3390/urbansci6040070

Gautam, A. S., Singh, K. P., Sharma, M., Gautam, S., Joshi, A., & Kumar, S. (2022b). Classification of different sky conditions based on solar radiation extinction and the variability of aerosol optical depth, Angstrom exponent, fine particles over Tehri Garhwal, Uttarakhand, India. *Mapan-Journal of Metrology Society of India, 38*(1), 21–36. https://doi.org/10.1007/s12647-022-00533-w

Gautam, A., Singh, V., Gautam, A. S., Kumar, P. R., Soni, P. S., Singh, R., & Singh, S. P. (2023). Lightning development over the distinct climate regions of Uttarakhand, India. *Indian Journal of Science and Technology, 16*(9), 632–639. https://doi.org/10.17485/IJST/v16i9.1886

Ghanekar, S. P., Puranik, P. V., & Bhide, U. V. (2003). Forecasting the onset of monsoon over Kerala using the peak in pre-monsoon convective activity over south peninsular India. *Mausam, 54*(3), 645–652. https://doi.org/10.54302/MAUSAM.V54I3.1555

Jnanesh, S. P., Lal, D. M., Gopalakrishnan, V., Ghude, S. D., Pawar, S. D., Tiwari, S., & Srivastava, M. K. (2022). Lightning characteristics over humid regions and arid regions and their association with aerosols over Northern India. *Pure and Applied Geophysics, 179*(4), 1403–1419. https://doi.org/10.1007/s00024-022-02981-6

Krehbiel, P. (1986). The Electrical Structure of Thunderstorms, in the Earth's Electrical Environment, 90–113. Washington, D.C.: Nat'l. Academy Press.

Kumar, P. (2018). Lightning, rainfall, AOD, and convection variabilities in the monsoon zone of India. *International Journal of Remote Sensing, 39*(3), 727–740. https://doi.org/10.1080/01431161.2017.1392636

Lal, D. M., Ghude, S. D., Mahakur, M., Waghmare, R. T. & Chate, D. M. (2018). Relationship between aerosol and lightning over Indo-Gangetic Plain (IGP), India. *Climate Dynamics, 50(483), 3865–3884.*

Manohar, G. K., Kandalgaonkar, S. S. & Tinmake, M. I. R. (1999). Tinmaker, Thunder- storm activity over India and the Indian southwest monsoon, *Journal of Geophysical Research, 104, 4169–4188.*

Negi, S. S. (1991). *Himalayan rivers, lakes, and glaciers*. Indus Pub. Co.

Oulkar, S., Siingh, D., Saha, U., & Kamra, A. K. (2019). Distribution of lightning in relation to topography and vegetation cover over the dry and moist regions in the Himalayas. *Journal of Earth System Science, 128*(7), 1–17. https://doi.org/10.1007/S12040-019-1203-9/METRICS

Petersen, W. A., & S. A. Rutledge (1998). On the relationship between cloud-toground lightning and convective rainfall, *J. Geophys. Res., 103, 14,025–14,040.*

Ramesh Kumar, P., & Kamra, A. K. (2012). The spatiotemporal variability of lightning activity in the Himalayan foothills. *Journal of Geophysical Research: Atmospheres, 117*(D24), 24201. https://doi.org/10.1029/2012JD018246

Rao, K. R. M., Kant, Y., Gahlaut, N., & Roy, P. S. (2012). Assessment of quality of life in Uttarakhand, India using geospatial techniques. *Geocarto International, 27*(4), 315–328. https://doi.org/10.1080/10106049.2011.627470

Shi, Z., Wang, H., Tan, Y., et al. (2020). Influence of aerosols on lightning activities in central eastern parts of China. *Wiley Online Library, 21*(2). https://doi.org/10.1002/asl.957

Singh, R. P., & Chauhan, A. (2020). Impact of lockdown on air quality in India during COVID-19 pandemic. *Air Quality, Atmosphere and Health, 13*, 921–928. https://doi.org/10.1007/S11869-020-00863-1/FIGURES/5

Sudeepkumar, B. L., Babu, C. A., & Varikoden, H. (2022). Variations in monsoon boundary layer structure with respect to cloudiness over the west coast of India. *Meteorology and Atmospheric Physics, 134*, 1–13. https://doi.org/10.1007/s00703-021-00839-5

Tesfaye, M., Sivakumar, V., Botai, J., & Mengistu Tsidu, G. (2011). Aerosol climatology over South Africa based on 10 years of Multiangle Imaging Spectroradiometer (MISR) data. *Journal of Geophysical Research: Atmospheres, 116*(D20). https://doi.org/10.1029/2011JD016023

Tinmaker, M. I. R., Jena, C. K., Ghude, S. D., Dwivedi, A. K., Islam, S., Kulkarni, S. H., et al. (2021). Relationship of lightning with different weather parameters during transition period of dry to wet season over Indian region. *Journal of Atmospheric and Solar-Terrestrial Physics, 220*, 105673. https://doi.org/10.1016/j.jastp.2021.105673

Venevsky, S. (2014). Importance of aerosols for annual lightning production at global scale, *Atmospheric Chemistry and Physics Discussions, 14, 4303–4325.* https://doi.org/10.5194/acpd-14-4303-2014

Williams, E. R. (2005). Lightning and climate: A review, *Atmospheric Research, 76, 1–4, 272–287.* https://doi.org/10.1016/j.atmosres.2004.11.014

Williams, E. R., & Sátori G. (2004). Lightning, thermodynamic and hydrological comparison of the two tropical continental chimneys, *Journal of Atmospheric and Solar-Terrestrial Physics, 66, 1213–1231.* https://doi.org/10.1016/j.jastp.2004.05.015

Williams, E., & Stanfill, S. (2002). The physical origin of the land–ocean contrast in lightning activity. *Comptes Rendus Physique, 3(10), 1277–1292.* https://doi.org/10.1016/s1631-0705(02)01407-x

Yuan, T., & Qie, X. (2008). Study on lightning activity and precipitation characteristics before and after the onset of the south China sea summer monsoon. *Journal of Geophysical Research, 113(D14), D14101.*

Zhao, P., Li, Z., Xiao, H., Fang, W., Zheng, Y., Cribb, M. C., Jin, X., & Zhou, Y. (2020). Distinct aerosol effects on cloud-to-ground lightning in the plateau and basin regions of Sichuan, Southwest China. *Atmospheric Chemistry and Physics, 20*(21), 13379–13397. https://doi.org/10.5194/acp-20-13379-2020

Zheng, S., Singh, R. P., Wu, Y., & Wu, C. (2017). A comparison of trace gases and particulate matter over Beijing (China) and Delhi (India). *Water, Air, and Soil Pollution, 228*, 1–15. https://doi.org/10.1007/S11270-017-3360-2/TABLES/4

Zipser, E. J., & Lutz, K. R. (1994). The vertical profile of radar reflectivity of convective cells: A strong indicator of storm intensity and lightning probability?, *Monthly Weather Review, 122, 1751–1759.*

Aerosol Variability and Its Impact on Cloud-Precipitation Interaction in Urban Areas of Maharashtra, India

Asha B. Chelani, Rahul V. Vyawahare, and Sneha Gautam

1 Introduction

The intricate interplay between aerosols, cloud dynamics, and precipitation has garnered significant attention in scientific literature (Balakrishnaiah et al., 2012; Manoj et al., 2013; Kant et al., 2019a, 2021; Panda & Kant, 2021). This research area has gained newfound importance in recent years, driven by the surge in anthropogenic aerosol emissions. Both modeling and observational studies have compellingly demonstrated that regions with elevated aerosol concentrations experience substantial alterations in cloud characteristics (Jones & Christopher, 2010). These aerosols serve as cloud condensation nuclei (CCN), directly influencing atmospheric radiative balance and causing shifts in cloud properties such as cloud cover, optical characteristics, and cloud particle size (Twomey, 1977; McFiggans et al., 2006; Freud et al., 2008).

One notable consequence of increased aerosol concentrations is the reduction in cloud radius, a phenomenon referred to as the first indirect effect (Twomey, 1977). Additionally, elevated aerosols induce changes in liquid water content, cloud thickness, and particulate size within clouds, leading to decreased precipitation efficiency but extended cloud lifespans, termed the second indirect effect (Albrecht, 1989).

A. B. Chelani (✉) · R. V. Vyawahare
Air Pollution Control Division, CSIR-National Environmental Engineering Research Institute (CSIR-NEERI), Nagpur, India
e-mail: ap_lalwani@neeri.res.in

S. Gautam
Division of Civil Engineering, Karunya Institute of Technology and Sciences, Coimbatore, Tamil Nadu, India

Water Institute, A Centre of Excellence, Karunya Institute of Technology and Sciences, Coimbatore, Tamil Nadu, India

The influence of aerosols on cloud-precipitation interactions has been studied extensively in various urban areas, yielding mixed results. Some investigations in heavily aerosol-polluted regions have reported decreased precipitation (Huang et al., 2009; Camponogara et al., 2014; Kant et al., 2019b; Leena et al., 2021; Berhane & Bu, 2021), while others have observed an increase in precipitation alongside aerosol concentrations (Kant et al., 2019c; Choudhury et al., 2020; Kant et al., 2021; Gautam et al., 2021; Nandini et al., 2022; Jasmine et al., 2022). Certain studies have suggested that the influence of aerosols on precipitation varies with atmospheric stability and environmental conditions (Tao et al., 2007; Koren et al., 2010; Kant et al., 2019b). These diverse findings underscore the significance of local anthropogenic emissions and the necessity to consider multiple parameters simultaneously, as individual parameter studies may not yield conclusive outcomes. It is evident that the aerosol-cloud-precipitation interaction cannot be generalized globally and requires region-specific investigations.

In the Indian context, much of the research has centered on aerosol interactions with clouds and precipitation over the Indo-Gangetic Plain (Kumar, 2013, 2014; Choudhury et al., 2020; Sarkar et al., 2022), with a few studies focusing on coastal regions (Kaskaoutis et al., 2009; Balakrishnaiah et al., 2012; Ramachandran & Kedia, 2013; Jasmine et al., 2022; Sharma et al., 2023; Tiwari et al., 2023). These studies have indicated that high aerosol loadings predominantly consist of mineral dust and light-absorbing black carbon, which can enhance rainfall (Ramachandran & Kedia, 2013). In contrast, studies in inland regions of Central India are relatively scarce (Shaeb et al., 2014), highlighting the importance of investigating aerosol-cloud-precipitation interactions in these areas.

To address this gap, we have selected six non-attainment cities in India for our study: Aurangabad, Chandrapur, Nashik, Nagpur, Solapur, and Pune. These cities have been designated as non-attainment areas by India's National Clean Air Programme (NCAP) due to consistently elevated levels of particulate matter exceeding national standards since 2015. For comparative purposes, we include Delhi, one of the most polluted cities on the Indo-Gangetic Plain. Our analysis utilizes data on Aerosol Optical Depth (AOD) and cloud properties, including Cloud Optical Thickness (COT), Cloud Top Temperature (CTT), Cloud Top Pressure (CTP), Cloud Fraction (CF), Cloud Effective Radius (CER), and Angstrom Exponent (AE) from the Moderate Resolution Imaging Spectroradiometer (MODIS) satellite sensor, as well as precipitation data from the Tropical Rainfall Measuring Mission (TRMM) satellite's precipitation radar, spanning the years 2010 to 2019. This comprehensive approach aims to provide valuable insights into the intricate aerosol-cloud-precipitation interactions specific to these inland urban regions of India.

2 Study Area

The study encompasses a diverse range of urban cities, each characterized by distinct climatic conditions and environmental influences:

Aurangabad (19°54′4″N 75°21′9″E): Situated in the central part of Maharashtra, Aurangabad enjoys a climate influenced by its proximity to the Western Ghats. Summers feature daytime temperatures ranging from 20 to 35 °C, while the monsoon season brings moderate to heavy rainfall. The winters are mild and pleasant, with temperatures spanning 10–28 °C. The city's population was recorded at 1,175,116 in the 2011 Census of India.

Chandrapur (19°58′13″N 79°18′12″E): Located near Nagpur, Chandrapur shares similar climatic conditions characterized by extreme summers and winters. With a population of 320,379 as per the 2011 Census of India, Chandrapur experiences scorching heat and heatwaves during May, typical of a tropical climate. The presence of coal-based power plants in proximity contributes to high air pollution levels.

Delhi (28°36′36″N 77°13′48″E): Positioned in the northern part of India, Delhi's climate is influenced by its inland location and distance from the ocean. The city, with a population of 16,753,235 according to the 2011 Census of India, grapples with temperature extremes and poor air quality, particularly during the winter months. Delhi faces significant air pollution issues, including smog formation due to adverse meteorological conditions and stubble burning in nearby states. Summers are hot with frequent heatwaves.

Nashik (19°59′50″N and 73°47′24″E): Nestled in the Deccan Plateau near the Western Ghats and surrounded by hills, Nashik boasts a pleasant climate. A population of 1,486,053 was recorded in the 2011 Census of India. Summers range from 25 °C to 40 °C, with the hottest months being April and May. The onset of the monsoon in July and its conclusion in September brings significant precipitation. Nashik is renowned for its grape crops.

Nagpur (21°8′48″N 79°5′19″E): Another inland city, Nagpur, has a population of 2,405,665 according to the 2011 Census of India. The city experiences dry and hot summers, with extremely high temperatures, reaching approximately 46 °C in May. Nagpur receives moderate to heavy rainfall during the monsoon season.

Solapur (17°39′36″N and 75°54′23″E): Situated in a semi-arid region, Solapur has a population of 951,118 as per the 2011 Census of India. The city's climate is characterized by its semi-arid geographical location and distance from major water bodies. Summers are extremely hot and dry, with daytime temperatures often exceeding 40 °C and sometimes reaching 45 °C or higher. The city experiences moderate rainfall during this period, with mild and comfortable winters.

Pune (18°31′13″N and 73°51′24″E): Pune's climate, influenced by its location in the Deccan Plateau, proximity to the Western Ghats, and high altitude, differs from the hotter cities of Nagpur, Chandrapur, and Delhi. Summers in Pune are relatively mild, with daytime temperatures ranging from 25 to 35 °C. The monsoon season brings moderate to heavy rainfall, while winters are characterized by pleasant weather. Pune's population was recorded at 3,124,458 in the 2011 Census of India.

These urban centers offer a diverse set of environmental conditions, including varying levels of pollution, temperature extremes, and precipitation patterns, providing a valuable backdrop for the study of aerosol-cloud-precipitation interactions. Figure 1 shows the location of selected cities in India.

Fig. 1 Location of selected cities

3 AOD, Precipitation, and Cloud Properties—Data Used

The Moderate Resolution Imaging Spectroradiometer (MODIS) is a crucial instrument mounted on both the Terra and Aqua polar-orbiting satellites, capturing data during the morning (at approximately 10:30 AM) and afternoon (around 1:30 PM). This instrument provides valuable information on various atmospheric parameters, including Aerosol Optical Depth (AOD), Angstrom Exponent (AE), and cloud properties such as Cloud Optical Thickness (COT), Cloud Fraction (CF), Cloud Top

Table 1 Aerosol, cloud, and precipitation data products (Platnick et al., 2003)

Variable	Data product	Unit
AOD	MOD08_D3_6_1_AOD_550_Dark_Target_Deep_Blue_Combined_Mean MYD08_D3_6_1_AOD_550_Dark_Target_Deep_Blue_Combined_Mean	–
CER	MOD08_D3_6_1_Cloud_Effective_Radius_Liquid_Mean MYD08_D3_6_1_Cloud_Effective_Radius_Liquid_Mean	micron
CF	MOD08_D3_6_1_Cloud_Fraction_Mean MYD08_D3_6_1_Cloud_Fraction_Mean	–
COT	MOD08_D3_6_1_Cloud_Optical_Thickness_Combined_Mean MYD08_D3_6_1_Cloud_Optical_Thickness_Combined_Mean	–
CTP	MOD08_D3_6_1_Cloud_Top_Pressure_Mean MYD08_D3_6_1_Cloud_Top_Pressure_Mean	hPa
CTT	MOD08_D3_6_1_Cloud_Top_Temperature_Mean MYD08_D3_6_1_Cloud_Top_Temperature_Mean	^{o}K
AE	MOD08_D3_6_1_Deep_Blue_Angstrom_Exponent_Land_Mean MYD08_D3_6_1_Deep_Blue_Angstrom_Exponent_Land_Mean	–
PRCP	TRMM_3B42_Daily_7_precipitation	mm/d

MOD and MYD denote the Terra and Aqua satellites, respectively

Pressure (CTP), Cloud Top Temperature (CTT), and Cloud Effective Radius Liquid (CER) (Jantarach et al., 2012). For this study, we accessed MODIS Level 3 data products, as listed in Table 1, encompassing these diverse variables at a spatial resolution of $1° \times 1°$.

The data, spanning from 2010 to 2019, was retrieved from NASA's official website (https://giovanni.gsfc.nasa.gov/). This platform not only offers access to the data but also provides comprehensive insights into the algorithms employed for the retrieval of aerosol and cloud properties (Platnick et al., 2003). To enhance data completeness and robustness, information from both the Terra and Aqua satellites was combined through averaging, mitigating the impact of observed missing values, and expanding the dataset. Additionally, daily precipitation (PRCP) data, vital for our analysis, was sourced from TRMM (Tropical Rainfall Measuring Mission) rainfall data, accessible via NASA's Giovanni interface (http://giovanni.gsfc.nasa.gov/giovanni/). This precipitation data, spanning the years 2010 to 2019, offers a higher spatial resolution of $0.25° \times 0.25°$. It's worth noting that TRMM measurements are rigorously validated through an extensive ground validation program, ensuring the reliability and accuracy of the precipitation data (Rosenfeld, 2000).

4   Results and Discussion

Before delving into the assessment of interactions among Aerosol Optical Depth (AOD) and other variables, a thorough data-cleaning process was undertaken. The percentage of missing values in the AOD data product during the study period was determined for each city and satellite. Specifically, the percentages were found to be

34% and 36% for Aurangabad, 33% and 34% for Chandrapur, 15% and 18% for Delhi, 35% and 37% for Nagpur, 32% and 34% for Nashik, 39% and 43% for Solapur, and 38% and 41% for Pune, respectively for the Terra and Aqua satellites.

To ensure data quality, only samples with valid AOD values were retained for subsequent analysis. This led to a dataset comprising 801, 820, 981, 791, 835, 746, and 763 samples for Aurangabad, Chandrapur, Delhi, Nashik, Nagpur, Solapur, and Pune, respectively, spanning the years from 2010 to 2019.

The investigation then turned to analyzing the monthly variations in AOD and precipitation (PRCP) to assess the impact of rainfall on AOD levels. In India, the summer monsoon typically spans from June to September (Ramachandran & Kedia, 2013). The monthly variation plot in Fig. 2a revealed elevated AOD levels (>0.5) during the monsoon months, from mid-June to August. Additionally, the winter months of November to January exhibited high AOD values. As expected, Delhi displayed consistently higher AOD levels compared to other cities, which exhibited
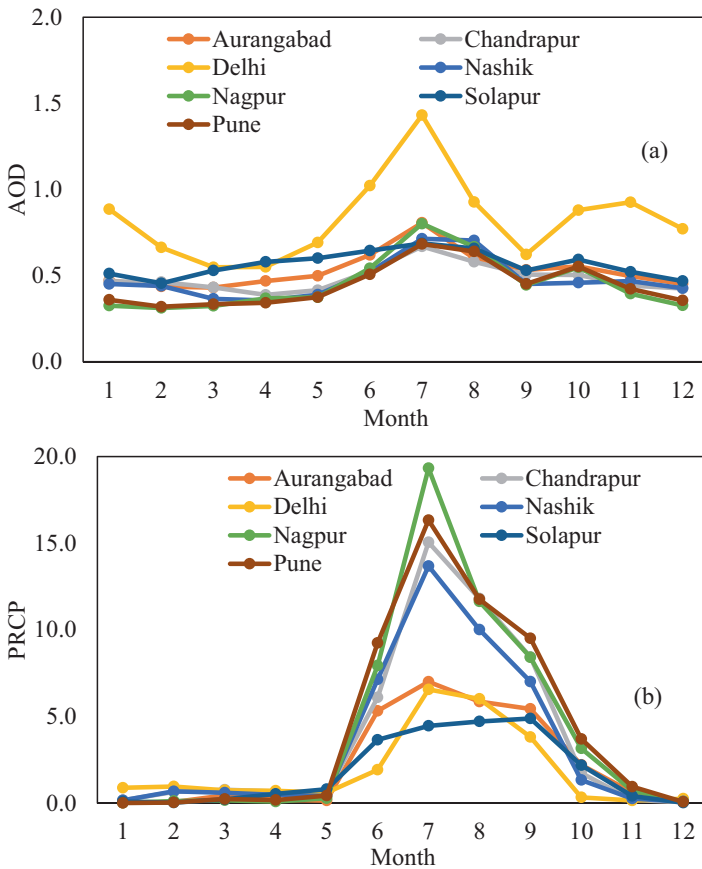
Fig. 2 Monthly variations in (**a**) AOD and (**b**) PRCP in different cities

similar seasonal trends. The Indian summer monsoon, characterized by significant geographical and temporal variability, is influenced by complex land-sea-atmosphere interactions (Ramachandran & Kedia, 2013). The increased AOD during monsoon months can be attributed to elevated humidity levels, promoting the hygroscopic growth of water-soluble aerosols and hindering their wet removal.

PRCP, as depicted in Fig. 2b, was predominantly observed from mid-June to the end of September. The annual average plot in Fig. 3a highlighted that AOD levels were notably higher in Delhi, while other cities exhibited relatively consistent AOD levels with no significant trends. PRCP remained temporally steady throughout the study period, as shown in Fig. 3b.

To further investigate changes in aerosol and cloud properties, the data was categorized into "rain" and "no-rain" samples. Table 2 presents the averages and standard deviations (1σ) for all selected variables. Notably, AOD levels were relatively consistent across all cities throughout the study period, except for Delhi, where
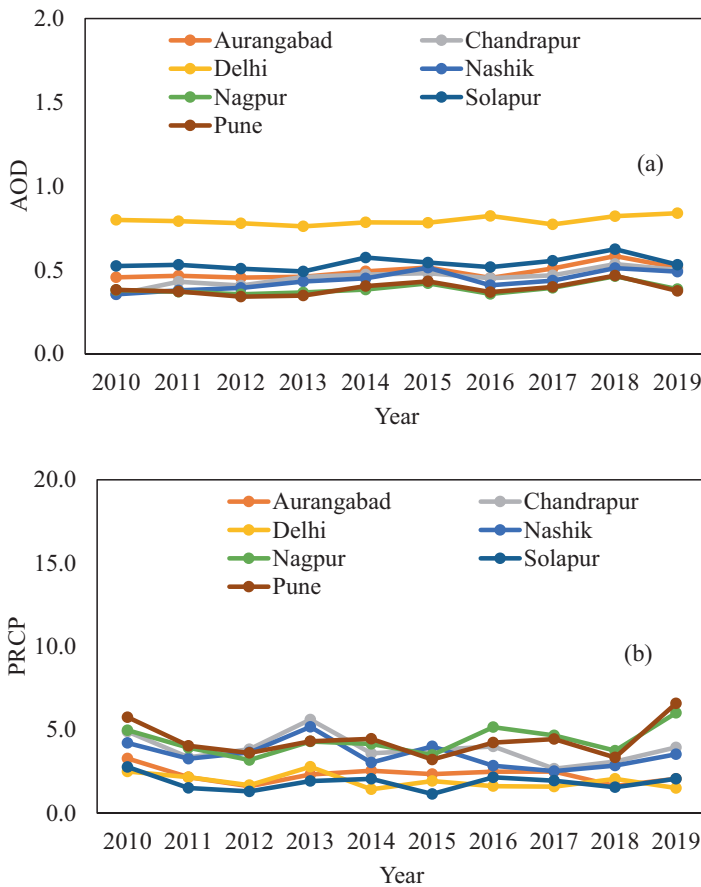
Fig. 3 Annual variations in (**a**) AOD and (**b**) PRCP in different cities

Table 2 AOD, cloud properties, and precipitation (average ± 1 σ) during rain and no-rain

City	AOD	CER	CF	COT	CTP	CTT	AE	PRCP
Rain								
Aurangabad	0.6 ± 0.2	15.9 ± 3.3	0.9 ± 0.2	14.8 ± 10.1	350.9 ± 159.4	250.3 ± 27.1	1.3 ± 0.5	12.3 ± 16.1
Chandrapur	0.6 ± 0.3	15.9 ± 3.6	0.9 ± 0.2	16.7 ± 15.6	339.5 ± 165.5	246.4 ± 28.6	1.3 ± 0.5	14.3 ± 22.7
Delhi	0.9 ± 0.5	16.2 ± 4.0	0.8 ± 0.3	15.3 ± 14.3	479.1 ± 210.0	258.4 ± 28.5	1.3 ± 0.6	9.9 ± 14.4
Nashik	0.6 ± 0.3	15.8 ± 3.6	0.9 ± 0.2	17.7 ± 13.8	340.3 ± 156.9	248.2 ± 27.2	1.5 ± 0.4	14.0 ± 19.6
Nagpur	0.6 ± 0.3	16.7 ± 3.4	0.9 ± 0.2	21.3 ± 13.9	360.1 ± 165.1	249.9 ± 26.7	1.3 ± 0.5	24.6 ± 31.6
Solapur	0.7 ± 0.3	16.1 ± 3.7	0.9 ± 0.2	12.5 ± 10.5	349.1 ± 161.9	249.9 ± 28.6	1.1 ± 0.5	10.1 ± 13.8
Pune	0.6 ± 0.3	17.0 ± 3.8	0.9 ± 0.2	20.5 ± 12.9	360.4 ± 161.9	250.8 ± 26.4	1.1 ± 0.6	24.7 ± 31.8
No Rain								
Aurangabad	0.5 ± 0.2	14.4 ± 4.4	0.3 ± 0.4	9.3 ± 8.6	606.6 ± 213.7	270.3 ± 28.7	1.4 ± 0.4	0.0 ± 0.0
Chandrapur	0.4 ± 0.3	15.2 ± 4.7	0.3 ± 0.4	8.4 ± 9.6	657.5 ± 241.7	275.6 ± 28.1	1.4 ± 0.4	0.02 ± 0.8
Delhi	0.8 ± 0.4	15.9 ± 5.2	0.4 ± 0.3	6.1 ± 6.8	738.7 ± 204.1	282.4 ± 22.6	1.4 ± 0.5	0.0 ± 0.0
Nashik	0.4 ± 0.3	14.4 ± 4.6	0.3 ± 0.4	10.7 ± 11.8	658.6 ± 229.1	276.2 ± 25.7	1.5 ± 0.3	0.0 ± 0.0
Nagpur	0.4 ± 0.2	14.8 ± 4.3	0.3 ± 0.4	11.6 ± 10.4	667.6 ± 223.8	274.7 ± 27.3	1.2 ± 0.5	0.0 ± 0.0
Solapur	0.5 ± 0.2	14.9 ± 4.5	0.4 ± 0.4	8.8 ± 9.4	585.3 ± 213.3	265.5 ± 30.0	1.1 ± 0.4	0.0 ± 0.0
Pune	0.4 ± 0.2	15.4 ± 4.3	0.4 ± 0.4	11.1 ± 9.9	665.7 ± 221.5	274.3 ± 27.8	1.1 ± 0.5	0.0 ± 0.0

AOD was substantially higher. Except Cloud Optical Thickness (COT) and Cloud Top Pressure (CTP), the variables Cloud Fraction (CF), Angstrom Exponent (AE), Cloud Effective Radius (CER), and Cloud Top Temperature (CTT) exhibited remarkable similarity across all locations.

Comparing these parameters between "no-rain" and "rain" periods, as detailed in Table 2, it was evident that AOD, CF, and COT were higher during rainy periods than during non-rainy periods. In contrast, CTT and CTP were observed to be higher during the no-rain periods. Notably, the difference was statistically significant for CF, COT, CTT, and CTP at a 95% confidence level, while it was not statistically significant for AOD. This suggests that atmospheric conditions play a crucial role in governing aerosol dynamics, while cloud properties such as CF, COT, CTT, and CTP are predominantly influenced by precipitation in the region.

For subsequent analysis, the focus was placed on samples with available rain data, excluding those categorized as "No rain" from further investigation.

4.1   Aerosol Mode

Discerning the type of aerosol based on its origin presents a formidable challenge, but several researchers have endeavored to tackle this by leveraging variations in Aerosol Optical Depth (AOD) across different wavelengths (Kaskaoutis et al., 2009; Pathak et al., 2012). While ground measurements of AOD have been the primary data source in most studies, a few have ventured into utilizing satellite data for this purpose (Rezaei et al., 2023).

The Ångström Exponent (AE) serves as a crucial metric, quantifying the changes in AOD concerning various wavelengths of light. AE is recognized as a representative indicator of AOD particle size. Specifically, high AE values (AE > 1.0) are indicative of smaller aerosol particles, whereas low AE values (AE < 0.75) are typically associated with coarse-mode particles. AE values within the range of 0.75–1.0 suggest a complex aerosol mode (Wang et al., 2014; Lin et al., 2021). Furthermore, according to NASA's guidance (https://earth.gsfc.nasa.gov/climate/data/deep-blue/science), values below 1 imply an optical prevalence of coarse particles (e.g., dust, ash, sea spray), while values exceeding 1 suggest the predominance of fine particles (e.g., smoke, industrial pollution).

In our analysis, AE > 1 was observed across all the cities listed in Table 2, indicating the dominance of fine particulate matter in the study areas. To further differentiate particle modes for each sample, we followed the approach outlined by Wang et al. (2014). Figure 4 illustrates the percentage occurrence of particle modes for the selected cities, revealing the fine-to-coarse mode ratios as 4.4, 5.1, 3.8, 15.3, 4.9, 2.3, and 2.4 for Aurangabad, Chandrapur, Delhi, Nashik, Nagpur, Solapur, and Pune, respectively. These ratios underscore the prevalence of fine aerosols across all locations, a trend driven by anthropogenic activities emitting fine-mode aerosols.

The remaining percentages represent complicated aerosols, though they are not explicitly depicted in the plot. Turning to the probability of rainy days, as depicted
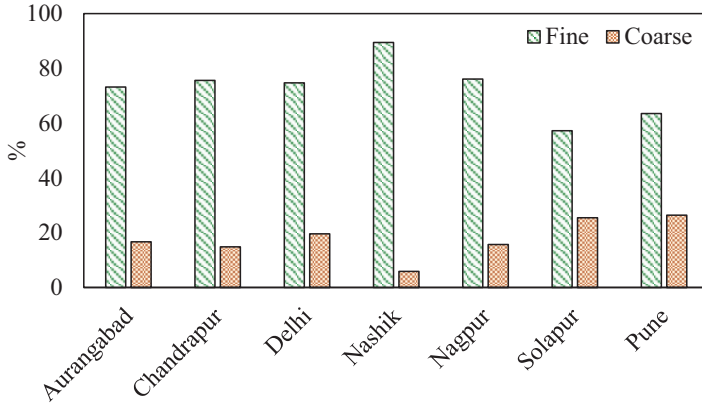
Fig. 4 Percentage of fine and coarse mode AOD in different cities
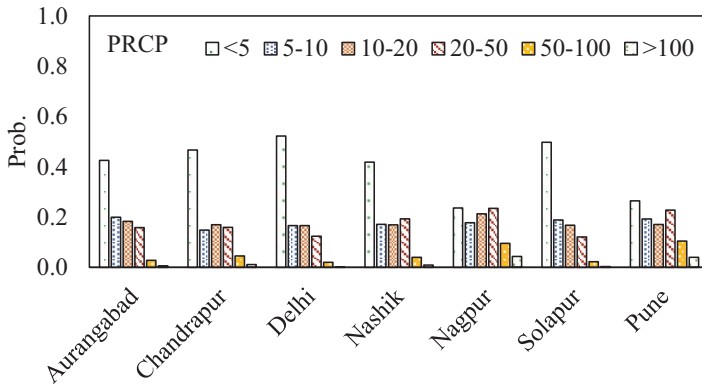
Fig. 5 Percentage distribution of PRCP in different cities

in Fig. 5, Chandrapur recorded the highest precipitation occurrence with 992 days, followed by Nashik (882 days), Delhi (710 days), Aurangabad (677 days), Solapur (663 days), Pune (650 days), and Nagpur (648 days) over the course of the 10-year study period.

To gain deeper insights into the prevalence of AOD values during precipitation days, we examined the frequency distribution, as illustrated in Fig. 6. AOD predominantly fell within the 0.5–1 range, followed by 0.1–0.5. Higher AOD values exceeding 1 were less frequent in all cities, except Delhi, which exhibited a higher number of AOD values exceeding 1.5. Given Delhi's status as the most polluted city, these higher values are expected. Solapur and Aurangabad reported the highest AOD values within the 0.5–1 range, followed by Nagpur, Pune, Delhi, Chandrapur, and Nashik.

Moreover, we conducted a comprehensive analysis of the correlation between AOD and cloud properties, along with precipitation, for both fine and coarse aerosol
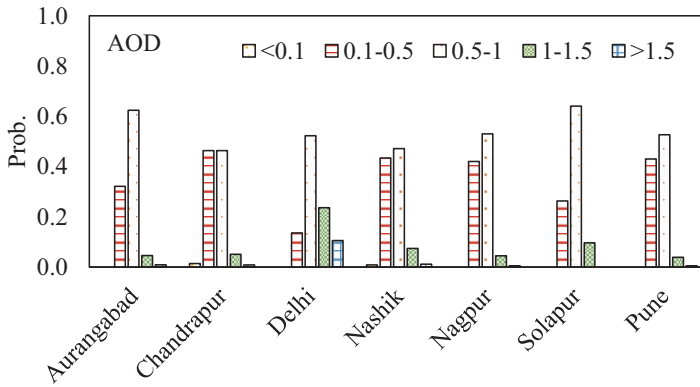
Fig. 6 Percentage distribution of AOD values in 7 cities

Table 3 Correlation of AOD with cloud properties and precipitation

City	CER	CF	COT	CTP	CTT	AE	PRCP
Aurangabad	0.03	0.15*	0.04	−0.11*	−0.21*	−0.04	−0.08
Chandrapur	0.07	0.24*	−0.11*	−0.08	−0.11*	0.19*	0.05
Delhi	0.03	0.41*	0.11*	−0.11*	−0.11*	0.06	0.15*
Nashik	0.17*	0.39*	−0.02	−0.04	−0.12*	0.27*	0.14*
Nagpur	0.06	0.28*	−0.06	−0.11*	−0.09	0.14*	0.04
Solapur	−0.04	0.04	0.04	−0.06	−0.16*	0.15*	−0.04
Pune	0.20*	0.36*	−0.16*	−0.22*	−0.25*	−0.01	0.08

*Significant at 5% confidence level, + significant at 1% confidence level

modes. Table 3 presents Pearson's correlation coefficients for AOD with cloud properties and precipitation, with statistical significance at a 5% confidence level. Additionally, Table 4 presents Pearson's correlation coefficients for precipitation with cloud properties. These correlation analyses are instrumental in unraveling the intricate relationships between aerosols, clouds, and precipitation in the study regions.

4.2 Correlation of AOD and PRCP with Cloud Properties

4.2.1 Cloud Fraction

Cloud fraction (CF) denotes the proportion of the sky obscured by clouds. In our analysis, a significant and positive correlation between Aerosol Optical Depth (AOD) and cloud fraction was observed in Aurangabad, Chandrapur, Delhi, Nashik, Nagpur, and Pune. Notably, precipitation also exhibited a substantial and positive correlation with cloud fraction in these cities. It is imperative to emphasize that

Table 4 Correlation of precipitation with cloud properties

City	CER	CF	COT	CTP	CTT	AE
Aurangabad	0.17[*]	0.18[*]	0.18[*]	−0.26[*]	−0.23[*]	0.12[*]
Chandrapur	0.20[*]	0.23[*]	0.37[*]	−0.29[*]	−0.32[*]	0.17[*]
Delhi	0.12[*]	0.32[*]	0.26[*]	−0.34[*]	−0.31[*]	0.16[*]
Nashik	0.22[*]	0.27[*]	0.23[*]	−0.31[*]	−0.32[*]	0.19[*]
Nagpur	0.05	0.23[*]	0.23[*]	−0.31[*]	−0.28[*]	−0.11[*]
Solapur	0.06	0.18[*]	0.02	−0.18[*]	−0.11[*]	0.11[*]
Pune	0.11[*]	0.24[*]	0.19[*]	−0.30[*]	−0.28[*]	−0.06

*Significant at 5% confidence level, [+] significant at 1% confidence level

these cities are characterized by elevated levels of dust particulate matter, in stark contrast to Solapur.

The noteworthy positive correlation between CF and AOD aligns with findings from other researchers studying regions burdened by high dust loads (Kumar, 2014; Kant et al., 2021). Furthermore, when examining fine and coarse mode aerosols separately, a positive correlation between AOD and CF persisted in these cities. The combination of a high dust burden and these cities' location within the hot tropical belt may underlie the observed positive correlation between AOD and CF.

This correlation analysis sheds light on the intricate relationships between aerosols, cloud cover, and precipitation in these urban areas, offering valuable insights into the complex interplay of atmospheric variables in regions characterized by elevated dust levels.

4.2.2 CTT

Cloud Top Temperature (CTT) displays a notable negative correlation with Aerosol Optical Depth (AOD) in the cities of Aurangabad, Chandrapur, Delhi, Nashik, Solapur, and Pune. Additionally, Cloud Top Pressure (CTP) exhibits a statistically significant negative correlation with AOD in Aurangabad, Delhi, Nagpur, and Pune. These observed correlations hold statistical significance at a 5% confidence level. Remarkably, similar findings have been documented in various regions by previous studies, including Rezaei et al. (2023) in Iran, Kant et al. (2019c) in the Indian region, Huang et al. (2020) in East China, and Nyasulu et al. (2022) in southeast Africa.

The observed negative correlation between CTT and AOD can be attributed to the capacity of increased aerosol levels to modulate humidity, subsequently influencing alterations in CTT (Sekiguchi et al., 2009). Furthermore, the possibility of aerosols contributing to cloud deepening has been proposed as an explanation for the negative relationship between CTT and AOD (Nyasulu et al., 2022). Furthermore, a significant negative correlation was observed between precipitation (PRCP) and both CTT and CTP. This correlation underscores the complex interplay between aerosols, cloud properties, and precipitation dynamics, emphasizing the multifaceted nature of atmospheric processes in these urban areas.

4.2.3 COT

Cloud Optical Thickness (COT) and Aerosol Optical Depth (AOD) exhibit significant correlations in Chandrapur, Delhi, and Pune. However, the nature of these correlations varies among these cities. In Chandrapur and Pune, a negative correlation is observed, while in Delhi, the correlation is positive. A negative correlation between aerosols and COT suggests a reduction in cloud reflectivity attributable to absorbing aerosols, which can lead to the vaporization of cloud droplets (Tiwari et al., 2023).

Additionally, COT displays a positive correlation with precipitation (PRCP) at all locations, except for Solapur. Notably, prior studies by Huang et al. (2020) and Nyasulu et al. (2022) have also reported a positive correlation between COT and AOD, particularly for lower AOD values. However, in our study, we observe a distinctive pattern: for higher AOD values (AOD > 0.5), the correlation between AOD and COT is consistently positive across all locations. For AOD values below 0.5, the correlation with COT is statistically significant and positive only at Nagpur and Solapur.

It's worth noting that the nature of the relationship between AOD and COT may depend on cloud-effective radius, as observed in the study by Kant et al. (2019a, b, c). These complex relationships underscore the multifaceted dynamics at play in the interactions between aerosols, cloud properties, and precipitation across different urban settings.

4.2.4 CER

Cloud Effective Radius (CER) serves as an indicator of the moisture content within clouds (Huang et al., 2009). As presented in Table 2, CER is consistently observed to exceed 14 microns in all the cities, surpassing the precipitation threshold for both land and ocean conditions (Srivastava et al., 2011; Rosenfeld, 2000). Notably, for warm clouds, larger cloud droplet radii are typically observed in clean oceanic atmospheres compared to polluted coastal or land regions (King et al., 2013; Tiwari et al., 2023).

The influence of high aerosol loading on CER is evident. Under stable atmospheric conditions devoid of vertical mixing, CER often exhibits a negative correlation with aerosol levels, commonly referred to as the first indirect effect. Conversely, it demonstrates a positive correlation with precipitation (PRCP), known as the second indirect effect. The correlation between CER and AOD is notably positive and statistically significant solely in Nashik and Pune. The presence of the second indirect effect is further highlighted by the positive correlation between PRCP and CER across all locations, except for Nagpur and Solapur, suggesting atmospheric instability with vertical mixing.

A higher AOD tends to result in an increased cloud radius, which in turn promotes precipitation (Cheng et al., 2016). However, when considering different AOD ranges, Table 5 reveals that the correlation of CER with AOD < 0.5 is negative and

Table 5 Correlation of AOD over different ranges with cloud properties and precipitation

City	CER	CF	COT	CTP	CTT	AE	PRCP
AOD < 0.5							
Aurangabad	−0.35*	−0.21*	0.09	−0.09	−0.16	−0.20*	−0.22*
Chandrapur	−0.05	−0.10	−0.03	−0.02	−0.06	−0.03	−0.05
Delhi	0.04	−0.23*	0.09	0.22*	0.10	−0.10	0.21*
Nashik	0.04	0.09	0.07	0.0	0.05	0.01	0.03
Nagpur	0.05	0.13	0.23*	−0.26*	−0.20*	0.11	0.01
Solapur	−0.20*	−0.24*	0.25*	−0.04	−0.09	−0.08	−0.25*
Pune	0.16+	0.10	−0.06	−0.10	−0.11	0.03	−0.08
AOD > 0.5							
Aurangabad	0.15*	0.16*	0.21*	−0.25*	−0.25*	0.08	−0.06
Chandrapur	0.18*	0.18*	0.37*	−0.27*	−0.30*	0.14*	−0.03
Delhi	0.12*	0.29*	0.24*	−0.32*	−0.30*	0.17*	0.12*
Nashik	0.19*	0.22*	0.23*	−0.29*	−0.29*	0.13*	0.06
Nagpur	0.03	0.18*	0.24*	−0.29*	−0.26*	−0.25*	0.03
Solapur	0.06	0.17*	0.03	−0.20*	−0.13*	0.08	0.08
Pune	0.09	0.20*	0.23*	−0.30*	−0.28*	−0.11*	0.20*

*Significant at 5% confidence level, + significant at 1% confidence level

significant only in Aurangabad, while it generally exhibits weak statistical significance within the AOD < 0.5 range. Conversely, a positive and significant correlation between CER and AOD is observed for AOD > 0.5 in Aurangabad, Chandrapur, Delhi, and Nashik.

Notably, the first indirect effect does not find robust support based on the correlation between CER and AOD within the study area. Nonetheless, it's worth mentioning that prior studies by Tang et al. (2014) and Huang et al. (2020) have reported a positive correlation coefficient between AOD and CER in locations with AOD exceeding 0.3. These nuanced findings highlight the intricacies of aerosol-cloud interactions and their impact on cloud properties and precipitation patterns across various urban contexts.

4.2.5 PRCP

Precipitation (PRCP) demonstrates significant correlations with Aerosol Optical Depth (AOD), with a positive correlation observed in Delhi and Nashik. However, for both AOD < 0.5 and AOD > 0.5, the correlations appear weak and lack statistical significance. Even when considering different aerosol modes, the correlation values remain statistically weak. Interestingly, PRCP exhibits statistically significant correlations with cloud properties in most cases, except for Cloud Effective Radius (CER) in Nagpur and Solapur. This correlation analysis suggests that the relationship between AOD and cloud properties and PRCP is not as pronounced as initially anticipated.

The observed weak correlations, although statistically significant, underscore that aerosol and cloud parameters are not solely reliant on one another. Rather, meteorological and atmospheric phenomena also play pivotal roles in governing the intricate interactions among aerosols, clouds, and precipitation. To gain a deeper understanding of these complex interactions, a more comprehensive approach is needed.

In response, a random forest model is introduced to predict PRCP using AOD and cloud properties as input variables, with PRCP serving as the response variable. This model is designed to elucidate the relative importance of aerosol and cloud properties in influencing precipitation patterns within the study area, offering a more nuanced perspective on the intricate dynamics at play in aerosol-cloud-precipitation interactions.

4.3   Random Forest Algorithm

The random forest algorithm, a supervised learning technique, has found applications in various fields, including air pollution assessment, as demonstrated by Kaminska (2018), Stafoggia et al. (2020), and Jiang et al. (2020). This algorithm, known for creating forests composed of decision trees using the "bagging method," offers reliable outcomes by training each decision tree on randomly selected features from the dataset. One of its most widely recognized applications is feature selection, a critical aspect of decision-making processes. A comprehensive description of the random forest algorithm can be found in Breiman (2001). In this study, the random forest module within the R package (R Core Development Team, 2021) is employed to extract the feature importance matrix.

To explore the complex interplay between aerosols, clouds, and precipitation, a random forest model is applied, employing PRCP as the response variable and AOD along with cloud properties such as Cloud Effective Radius (CER), Cloud Fraction (CF), Cloud Top Temperature (CTT), Cloud Top Pressure (CTP), and Cloud Optical Thickness (COT) as predictors. The model is trained using an 80:20 training-to-testing ratio and 10-fold cross-validation. The evaluation of the model's performance relies on metrics such as Root Mean Square Error (RMSE) and mean absolute percentage error (MAPE). As can be seen from Fig. 7a the MAPE values for Aurangabad, Chandrapur, Delhi, Nashik, Nagpur, Solapur, and Pune are 23%, 12%, 15.7%, 13.3%, 18.4%, 14.3%, and 21.2%, respectively, indicating reasonable model performance across all locations.

The feature importance assessment matrix, an inherent component of the random forest model, is presented in Fig. 7b. A high node purity, represented by % IncMSE (the percentage change in mean square error resulting from the inclusion of a variable in the model), signifies the greater importance of the variable in predicting PRCP. Notably, the three most critical variables in predicting PRCP are listed in Table 6 for each location, ranked by their importance. AOD and CF emerge as highly important variables, followed by COT and CTT in all cities except Delhi,
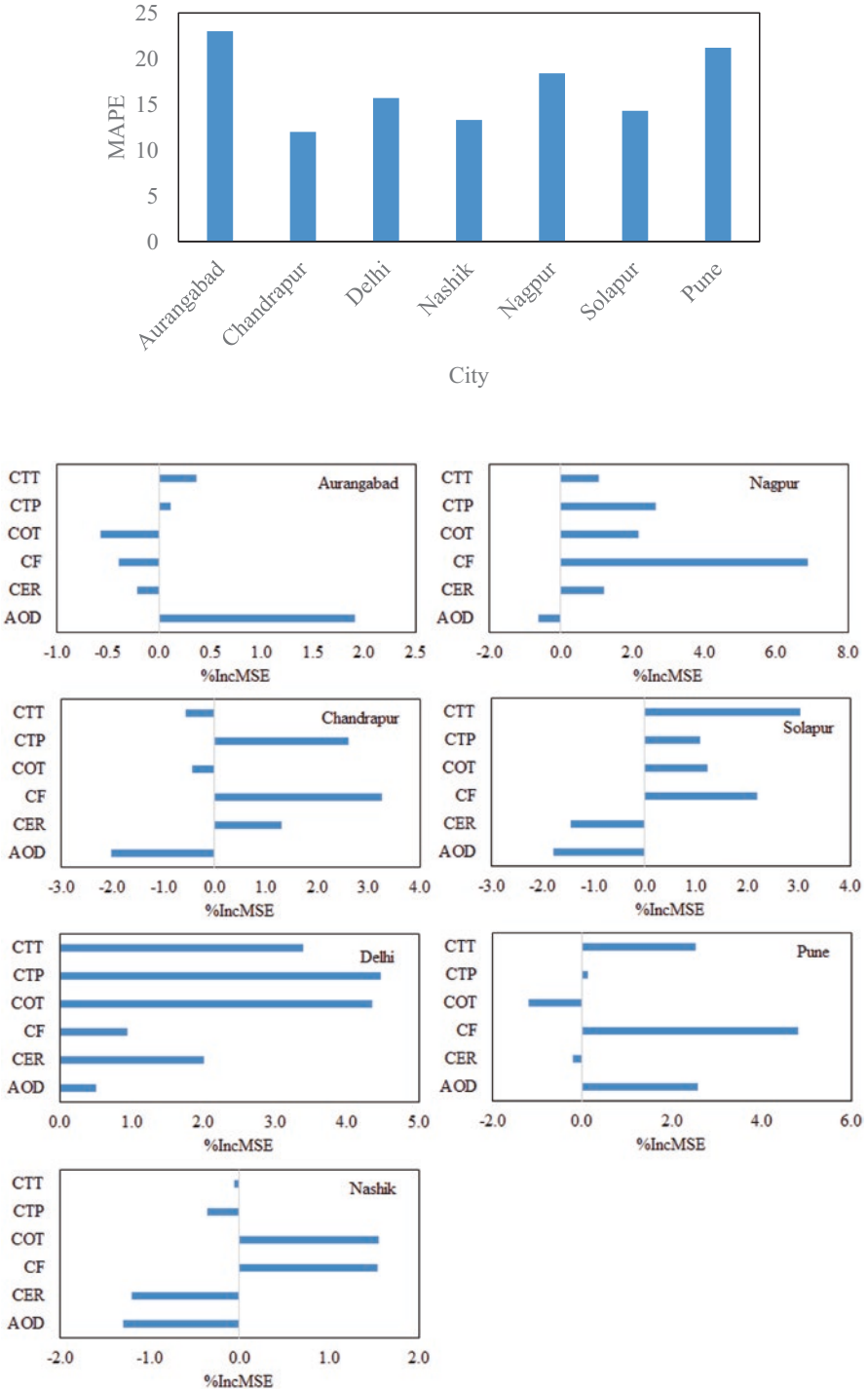
Fig. 7 (a) Mean absolute percentage error (MAPE) of Random Forest model in predicting PRCP over 7 cities. (b) Importance of predictor variables in predicting PRCP in 7 cities

Table 6 Importance ranking of first three variables in predicting PRCP

City	AOD	CF	COT	CTT	CTP	CER
Aurangabad	1	3	2			
Chandrapur	3	1			2	
Delhi			2	3	1	
Nashik	2	1	1			3
Nagpur		1	3		2	
Solapur	3	2		1		
Pune	2	1		3		

where CTP, CTT, and CTT play pivotal roles. Interestingly, meteorological factors take precedence in governing PRCP in the most heavily polluted city, Delhi, rather than AOD.

In summary, aerosol-cloud-precipitation interactions are intricate and exhibit spatiotemporal variability. Traditional correlation analysis alone may not provide a clear understanding of these relationships. The random forest model, by delineating the order of variable importance in predicting precipitation, offers valuable insights into the study of aerosol-cloud-precipitation interactions and serves as a means of validating correlation analysis results.

5   Conclusion

In conclusion, our study comprehensively evaluated aerosol-cloud-precipitation interactions across seven inland non-attainment cities characterized by high particulate matter levels. It was found that fine-mode aerosols, regardless of the predominant aerosol sources in each city, tended to dominate across all locations. Notably, higher Aerosol Optical Depth (AOD) values (>0.5) were observed during monsoon months, attributed to increased humidity, which led to the hygroscopic growth of water-soluble aerosols and hindered their wet removal. Delhi exhibited consistently higher AOD levels compared to the other cities in our study.

AOD levels were notably higher in Delhi, while other cities exhibited relatively consistent AOD levels with no significant trends. AE > 1 was observed across all the cities indicating the dominance of fine particulate matter in the study areas. The fine-to-coarse mode ratios were observed to be 4.4, 5.1, 3.8, 15.3, 4.9, 2.3, and 2.4 for Aurangabad, Chandrapur, Delhi, Nashik, Nagpur, Solapur, and Pune, respectively.

Furthermore, we observed that during both rainy and no-rain periods, AOD, Cloud Fraction (CF), and Cloud Optical Thickness (COT) tended to be higher during rainy periods, while Cloud Top Temperature (CTT) and Cloud Top Pressure (CTP) were more pronounced during no-rain periods. The statistical insignificance of these differences underscored the importance of atmospheric conditions in shaping aerosol behavior. Correlation analysis revealed several noteworthy associations,

including a significant positive correlation between AOD and cloud fraction and a negative correlation between

AOD and CTT in most cities. CTP was found to be negatively correlated with AOD in specific cities, including Aurangabad, Delhi, Nagpur, and Pune.

A significant and positive correlation between Aerosol Optical Depth (AOD) and cloud fraction was observed in Aurangabad, Chandrapur, Delhi, Nashik, Nagpur, and Pune. The combination of a high dust burden and these cities' location within the hot tropical belt may underlie the observed positive correlation between AOD and CF.

Moreover, we observed evidence of the second indirect effect through the correlation between Precipitation (PRCP) and Cloud Effective Radius (CER) in most locations, with the exception of Nagpur and Solapur, suggesting the influence of atmospheric instability and vertical mixing on precipitation patterns. To gain deeper insights into the governing variables of precipitation, we applied a random forest model, which highlighted the high importance of AOD and CF, followed by COT and CTT in predicting PRCP across most cities. Notably, meteorological factors emerged as the primary drivers of precipitation in Delhi, the city with the highest pollution levels, overshadowing the impact of AOD.

In summary, our study unveiled the complexity and spatiotemporal variability of aerosol-cloud-precipitation interactions in the study locations. Traditional correlation analysis alone proved insufficient to fully elucidate these relationships. The random forest model provided valuable insights by ranking the variables in terms of their importance in predicting precipitation, offering a complementary approach for the study of aerosol-cloud-precipitation interactions and validation of correlation analysis results.

References

Albrecht, B. A. (1989). Aerosols cloud microphysics and fractional cloudiness. *Science, 245*, 1227–1230.

Balakrishnaiah, G., Kumar, S., Reddy, B., Rama Gopal, K., Reddy, R. R., Reddy, L., Swamulu, C., Nazeer Ahammed, Y., Narasimhulu, K., KrishnaMoorthy, K., & Suresh Babu, S. (2012). Spatio-temporal variations in aerosoloptical and cloud parameters over Southern India retrieved from MODIS satellite data. *Atmospheric Environment, 47*, 435–445.

Berhane, S. A., & Bu, L. (2021). Aerosol—cloud interaction with summer precipitation over major cities in Eritrea. *Remote Sensing, 13*(4), 677.

Breiman, L. (2001). Random Forests. *Machine Learning, 45*, 5–32. https://doi.org/10.1023/A:1010933404324

Camponogara, G., Dias, M. A., & FSilva Carri'o, G. G. (2014). Relationship between Amazon biomass burning aerosols and rainfall over the La Plata Basin. *Atmospheric Chemistry and Physics, 14*, 4397–4407.

Census of India. (2011). https://censusindiagovin/censuswebsite/data/population-finder

Cheng, F., Zhang, J., He, J., Zha, Y., Li, Q., & Li, Y. (2016). Analysis of aerosol-cloud-precipitation interactions based on MODIS data. *Advances in Space Research*. https://doi.org/10.1016/jasr201608042

Choudhury, G., Tyagi, B., Vissa, N. K., Singh, J., Sarangi, C., Tripathi, S. N., & Tesche, M. (2020). Aerosol-enhanced high precipitation events near the Himalayan foothills. *Atmospheric Chemistry and Physics, 20*(23), 15389–15399.

Freud, E., Rosenfeld, D., Andreae, M., Costa, A., & Artaxo, P. (2008). Robust relations between CCN and the vertical evolution of cloud drop size distribution in deep convective clouds. *Atmospheric Chemistry and Physics, 8*, 1661–1675.

Gautam, S., Gautam, A. S., Singh, K., James, E. J., & Brema, J. (2021). Investigations on the relationship among lightning aerosol concentration and meteorological parameters with specific reference to the wet and hot humid tropical zone of the southern parts of India. *Environmental Technology & Innovation, 22*, 101414.

Huang, J., Zhang, C., & Prospero, J. M. (2009). African aerosol and large-scale precipitation variability over West Africa. *Environmental Research Letters, 4*(1), 015006.

Huang, J., Bu, L., Kumar, K. R., Khan, R., & Devi, N. L. (2020). Investigating the relationship between aerosol and cloud optical properties inferred from the MODIS sensor in recent decades over East China. *Atmospheric Environment, 239*, 117812.

Jantarach, T., Masiri, I., & Janjai, S. (2012). Comparison of MODIS aerosol optical depth retrievals with ground-based measurements in the tropics. *Procedia Engineering, 32*, 392–398.

Jasmine, M. K., Aloysius, M., Jayaprakash, R., Fathima, C. P., Prijith, S. S., & Mohan, M. (2022). Investigation on the role of aerosols on precipitation enhancement over Kerala during August 2018. *Atmospheric Environment, 279*, 119101.

Jiang, T. T., Chen, B., Nie, Z., Zhehao, R., Xu, B., & Tang, S. (2020). Estimation of hourly full-coverage PM_{25} concentrations at 1-km resolution in China using a two-stage random forest model. *Atmospheric Research*. https://doi.org/10.1016/jatmosres2020105146

Jones, T. A., & Christopher, S. A. (2010). Statistical properties of aerosol-cloud-precipitation interactions in South America. *Atmospheric Chemistry and Physics, 10*(5), 2287–2305.

Kaminska, J. A. (2018). The use of random forests in modelling short-term air pollution effects based on traffic and meteorological conditions: A case study in Wrocław. *Journal of Environmental Management, 217*, 164–174.

Kant, S., Panda, J., Pani, S. K., & Wang, P. K. (2019a). Long-term study of aerosol–cloud–precipitation interaction over the eastern part of India using satellite observations during pre-monsoon season. *Theoretical and Applied Climatology, 136*(1), 605–626.

Kant, S., Panda, J., & Gautam, R. (2019b). A seasonal analysis of aerosol-cloud-radiation interaction over Indian region during 2000–2017. *Atmospheric Environment, 201*, 212–222.

Kant, S., Panda, J., & Manoj, M. G. (2019c). A satellite observation-based analysis of aerosol-cloud-precipitation interaction during the February 2016 unseasonal heatwave episode over Indian region. *Aerosol and Air Quality Research, 19*(7), 1508–1525.

Kant, S., Panda, J., Rao, P., Sarangi, C., & Ghude, S. D. (2021). Study of aerosol-cloud-precipitation-meteorology interaction during a distinct weather event over the Indian region using WRF-Chem. *Atmospheric Research, 247*, 105144.

Kaskaoutis, D. G., Badarinath, K. V. S., Kharol, S., Sharma, A., & Kambezidis, H. D. (2009). Variations in the aerosol optical properties and types over the tropical urban site of Hyderabad India. *Journal of Geophysical Research, 114*(1–20), D22204.

King, M. D., Platnick, S., Menzel, W. P., Ackerman, S. A., & Hubanks, P. A. (2013). Spatial and temporal distribution of clouds observed by MODIS onboard the Terra and Aqua satellites. *IEEE Transactions on Geoscience and Remote Sensing, 51*(7), 3826–3852.

Koren, I., Remer, L. A., Altaratz, O., Martins, J. V., & Davidi, A. (2010). Aerosol-induced changes of convective cloud anvils produce strong climate warming. *Atmospheric Chemistry and Physics, 10*(10), 5001–5010.

Kumar, A. (2013). Variability of aerosol optical depth and cloud parameters over North Eastern regions of India retrieved from MODIS satellite data. *Journal of Atmospheric and Solar-Terrestrial Physics, 100–101*, 34–49.

Kumar, A. (2014). Long term (2003–2012) spatio-temporal MODIS (Terra/Aqua level 3) derived climatic variations of aerosol optical depth and cloud properties over a semi arid urban tropical region of Northern India. *Atmospheric Environment, 83*, 291–300.

Lin, J., Shen, X., Xing, J., Che, H., & Holben, B. N. (2021). Analysis of aerosol type and fine- and coarse-mode aerosol direct radiative forcing over regions in East and Southeast Asia based on AERONET Version 3 Data. *Aerosol Physics and Instrumentation, 21(7), 200503.*

Leena, P. P., Sravanthi, N., Anil Kumar, V., Pandithurai, G., & Panicker, A. S. (2021). Aerosol–cloud–rainfall properties inferred from satellite observations over different regions of the Indian subcontinent: variability trends and relationships during the summer monsoon. *Pure and Applied Geophysics, 178*, 4619–4631.

Manoj, M. G., Devara, P. C. S., Rao, Y. J., & Sonbawne, S. M. (2013). Lidar investigation of aerosol–cloud–precipitation interactions over a tropical monsoon environment: recharging of atmosphere. *Journal of Atmospheric and Solar - Terrestrial Physics, 93*, 80–86.

McFiggans, G., Artaxo, P., Baltensperger, U., Coe, H., Facchini, C., Feingold, G., Fuzzi, S., Gysel, M., Laaksonen, A., Lohmann, U., Mentel, T., Murphy, D., O'Dowd, C., & Snider, J. (2006). The effect of physical & chemical aerosol properties on warm cloud droplet activation. *Atmospheric Chemistry and Physics, 6*, 2593–2649.

Nandini, G., Vinoj, V., & Pandey, S. K. (2022). Arabian Sea aerosol-Indian summer monsoon rainfall relationship and its modulation by El-nino southern oscillation. npj Climate and Atmospheric. *Science, 5*(1), 25.

Nyasulu, M., Haque, M. M., Musonda, B., & Fang, C. (2022). The long-term spatial and temporal distribution of aerosol optical depth and its associated atmospheric circulation over Southeast Africa. *Environmental Science and Pollution Research, 29*(20), 30073–30089.

Panda, J., & Kant, S. (2021). Impact of urban and semi-urban aerosols on the cloud microphysical properties and precipitation. In *Air Pollution and Its Complications: From the Regional to the Global Scale* (pp. 25–36).

Pathak, B., Bhuyan, P. K., Gogoi, M., & Bhuyan, K. (2012). Seasonal heterogeneity in aerosol types over Dibrugarh-North-Eastern India. *Atmospheric Environment, 47*, 307–315.

Platnick, S., King, M. D., Ackerman, S. A., Menzel, W. P., Baum, B. A., Ri'edi, J. C., & Frey, R. A. (2003). The MODIS cloud products: algorithms and examples from Terra. *IEEE Transactions on Geoscience and Remote Sensing, 41*(2), 459–473.

R Core Development Team. (2021). R: A language and environment for statistical computing R Foundation for Statistical Computing Vienna Austria https://www.R-project.org/

Ramachandran, S., & Kedia, S. (2013). Aerosol-Precipitation Interactions over India: Review and Future Perspectives. *Advances in Meteorology*, Article ID 649156. https://doi.org/10.1155/2013/649156

Rezaei, M., Farajzadeh, M., & Kant, S. (2023). The observational evidence of association between types of aerosol mode-cloud-precipitation interaction over Iran. *Atmospheric Pollution Research, 14*, 101760.

Rosenfeld, D. (2000). Suppression of rain and snow by urban and industrial air pollution. *Science, 287*(5459), 1793–1796.

Sarkar, A., Panda, J., Kant, S., & Mukherjee, A. (2022). Influence of smoke aerosols on low level clouds over the Indian region during winter. *Atmospheric Research, 278*, 106358.

Sekiguchi, M., Nakajima, T., Suzuki, K., Kawamoto, K., Higurashi, A., Rosenfeld, D., Sano, I., & Mukai, S. (2009). A study of the direct and indirect effects of aerosols using global satellite data sets of aerosol and cloud parameters. *Journal of Geophysical Research, 108*, 4699.

Shaeb, K. H. B., Joshi, A. K., & Moharil, S. V. (2014). Aerosol optical properties and types over Nagpur Central India. *Sustainable Environment Research, 24*(1), 29.

Sharma, P., Ganguly, D., Sharma, A. K., Kant, S., & Mishra, S. (2023). Assessing the aerosols clouds and their relationship over the northern Bay of Bengal using a global climate model. *Earth and Space Science, 10*(2), e2022EA002706.

Srivastava, S., Ramachandran, S., Rajesh, T. A., & Kedia, S. (2011). Aerosol radiative forcing deduced from observations and models over an urban location and sensitivity to single scattering albedo. *Atmospheric Environment, 45*(34), 6163–6171.

Stafoggia, M., Johansson, C., Glantz, P., Renzi, M., Shtein, A., Hoogh, K. D., Kloog, I., Davoli, M., Michelozzi, P., & Bellander, T. (2020). A random forest approach to estimate daily particulate matter nitrogen dioxide and ozone at fine spatial resolution in Sweden. *Atmosphere, 11*, 239.

Tang, J., Wang, P., Mickley, L. J., Xia, X., Liao, H., Yue, X., & Xia, J. (2014). Positive relationship between liquid cloud droplet effective radius and aerosol optical depth over Eastern China from satellite data. *Atmospheric Environment, 84*, 244–253.

Tao, W.-K., Li, X., Khain, A., Matsui, T., Lang, S., & Simpson, J. (2007). The role of atmospheric aerosol concentration on deep convective precipitation: cloud-resolving model simulations. *Journal of Geophysical Research*, D24S18. https://doi.org/10.1029/2007JD008728112

Tiwari, S., Kumar, K., Singh, S., & Kumar, A. (2023). Current status of aerosol-cloud interactions and their impact over the Northern Indian Ocean: A comprehensive review. *Atmospheric Research, 283*, 106555.

Twomey, S. (1977). The influence of pollution on the shortwave albedo of clouds. *Journal of the Atmospheric Sciences, 34*(7), 1149–1152.

Wang, Z., Liu, D., Wang, Z., Wang, Y., Khatri, P., Zhou, J., Takamura, T., & Shi, G. J. (2014). Seasonal characteristics of aerosol optical properties at the SKYNET Hefei site (31.90°N, 117.17°E) from 2007 to 2013. *Journal of Geophysical Research, 119*, 6128–6139.

Comparative Health Risk Assessment of Black Carbon and Particulate Matter Emissions in East India During the COVID-19 First and Second Waves

Dilip Kumar Mahato and Balram Ambade

1 Introduction

Severe acute respiratory syndrome coronavirus 2 (SARS-CoV-2), commonly known as COVID-19, emerged at the end of 2019 and has had a profound global impact on the socio-ecological environment, particularly affecting large industries, businesses, and sustainable livestock (Waylen et al., 2019; Dumka et al., 2021; Balakrishnan et al., 2019; Kumar & Mishra, 2018; Pant et al., 2018; Guo et al., 2019). Recognizing its rapid spread and significance, the World Health Organization declared it a pandemic on January 30, 2020. With a population of approximately 139 million, India has been heavily affected, reporting 411,189 confirmed cases and 42,097 confirmed fatalities as of July 26, 2021, 08:00 IST, according to data from mohfw.gov.in. In response to this life-threatening epidemic, various measures have been implemented to mitigate the virus's spread, such as restrictions on overcrowding, enforcing social distancing, and promoting the consistent use of masks and hand sanitizers. The first confirmed case of COVID-19 in India was reported on January 27, 2020, in the state of Kerala (Andrews et al., 2020). During the First Wave of the pandemic, an estimated 15 million individuals were infected across India (Shil et al., 2021). Notably, India is one of the most affected countries by COVID-19, trailing only the USA according to a recent report by the WHO (https://covid19.who.int/region/amro/country/us). Although the number of COVID-19 cases appeared to decrease after the First Wave, there was a resurgence after February 11, 2021. India faced a challenging situation as daily cases surged, reaching nearly three times the previous peak value on April 19, 2021 (Ranjan et al., 2021). This emphasized the ongoing impact of the pandemic on the country and its population. Efforts to combat the

D. K. Mahato · B. Ambade (✉)

Department of Chemistry, National Institute of Technology, Jamshedpur, Jharkhand, India
e-mail: bambade.chem@nitjsr.ac.in

virus and its consequences continue as the world navigates through the complexities of the COVID-19 pandemic.

Until now, India has been affected by COVID-19 in two waves: the first (*April to May 2020*) and second (*April–June 2021*). The First Wave had a devasting impact on the whole country, either monetarily or in terms of human lives. From March 24th through May 31st, 2020 (Pathakoti et al., 2020; Singh & Chauhan, 2020), India was placed under complete lockdown in four different stages and then the unlocking procedure began with some restrictions. Furthermore, the Second Wave was somewhat more effective due to the lack of awareness of the COVID-19 guidelines. This Second Wave was anticipated to arrive in several Indian states in early March, imposing partial lockdowns.

Along with nationwide, COVID cases also arrived in a flash in Jamshedpur, an industrial city in Eastern India, the lockdown was imposed from April 22, 2021, along with relief in essential services. Both the wave of COVID-19 has a major mark on the ecosystem and the atmospheric environment. The atmospheric particulate matter gradually falls during pandemics due to decline in public activities. In the major cities, the major emission of $PM_{2.5}$ and Black Carbon is due to transportation (USEPA, 2014). Some of the satellite measurements revealed that the fall of public activity and vehicular movement could be the primary reason for reduction of airborne particulate matter in the atmosphere and most of the anthropogenic activities that happened from transportation and industrial activities have considerable reductions during the pandemic time (Feng et al., 2020; Huang et al., 2021). The pollution level of the atmosphere has shown a sharp decrease due to the lesser consumption of fossil fuels. There was a sharp fall in the concentration of Black Carbon and $PM_{2.5}$ which was the temporal variation during the lockdown over the entire World and India (Huang et al., 2021). Moreover, several publications (Ambade & Kurwadkar, 2021; Das et al., 2020; Dasgupta & Srikanth, 2020; Dhaka et al., 2020; Fu et al., 2020; Goel et al., 2021; Jia & Evangeliou, 2021; Kumari & Toshniwal, 2020; Nigam et al., 2021) from peer researchers indicated the radical improvement of air quality due to the reduction in the aerosol particle during lockdowns. The overall reducing BC in the megacity Hangzhou, China was 44% from 2.30 to 1.29 µg m^{-3} (Xu et al., 2020), separating two areas as urban area reduced to 1.33 µg m^{-3} (55%) and urban industrial area reduced to 1.84 µg m^{-3} (57%). In Dehradun, India, a significant reduction in EBC mass concentration levels was examined in the range from 2.12 to 2.74 µg m^{-3} (Pandey & Negi, 2022). Furthermore, Jain and Sharma (2020) highlighted the substantial drop of $PM_{2.5}$ concentration in the megacities in India at 41% (66–39 µg m^{-3}) through pre-lockdown to lockdown periods. In the Second Wave, the level of pollutant concentration in NCT (Delhi) had declined to nearly 4–16% as compared to the pre-lockdown period but greater compared to First Wave due to moderate restrictions. The $PM_{2.5}$ concentration was observed to be 82.8 µg m^{-3} (March 24 to April 30, 2019), 42.9 µg m^{-3} (March 24 to April 30, 2020), and 79.9 µg m^{-3} (April 7 to April 16, 2021) during the pre-lockdown, First Wave and Second Wave respectively (Saharan et al., 2022).

PM$_{2.5}$ and Black Carbon are the byproducts of partial combustion of fossil fuel and biomass burning suspended in the atmosphere for a longer time. According to the study, BC has an annual lifetime of 4–14 days (Cape et al., 2012). BC is the finest particle present in PM$_{2.5}$, which is major subgroup of particulate matter. PM$_{2.5}$ is an airborne particulate matter whose size diameter is equal to or less than 2.5 μm. The production of Black Carbon has resulted from the combustion in the presence of oxygen and temperature (Panicker et al., 2018). BC has a strong tendency to absorb solar radiation and becomes the second major cause of Global Warming after CO$_2$ (Ramanathan & Carmichael, 2008). In terms of Indian perspective like building activity, garbage burning also includes extra activity toward atmospheric pollution (Banerjee et al., 2015; Rana et al., 2019).

The artificially inflexible of BC is due to the aromatic structure, along with the property of surface absorption and reaction with different organic compounds that make it protected in the environment. These properties make the BC chemically and thermodynamically stable, which increases its lifetime in the atmosphere (Shrestha et al., 2010). The measurement of Black Carbon concentration indicates the level of pollution in the atmosphere (Huang et al., 2021; Bond et al., 2013; Ding et al., 2016; Qin & Xie, 2012; Shen et al., 2010; Wang et al., 2011, 2014; Zhao et al., 2020). According to the CPCB (Central pollution control board), most of the mean yearly PM$_{2.5}$ and PM$_{10}$ concentration have been registered as high atmospheric aerosol in the cities that comes under Indo-Gangetic Plains (IGP) (CPCB site, http://www.cpcb.nic.in). Airborne particulate matter has an adverse impact on human health, the atmosphere, and solar radiation. Exposure to human health can cause premature death, cardiovascular attack, respiratory problems, neuro-related diseases and many others (Kim et al., 2015; Schraufnagel et al., 2019). According to recent study, it has been noticed that long-term exposure to PM$_{2.5}$ has caused millions of deaths in India (Health Effects Institute, 2019).

In the present study, Sakchi and Gamharia are the most urbanized and Industrialized areas of Urban Agglomerates of Jamshedpur, these are some of the main hubs of anthropogenic activities in East India. In the urban area, the consumption of fossil fuels is a major source of air pollution. It has been reported that Black Carbon was the major pollutant in the world's aerosol borderline which could increase the haze in the atmosphere (Ding et al., 2016; Zhao et al., 2020; Geng et al., 2013; Huang et al., 2020; Wang et al., 2013). Haze pollution has a greater impact than fine aerosol particles on health related to respiratory tract diseases. It has been reported that PM$_{2.5}$ and BC concentration can accelerate the spreading of Sars-CoV-2 (Domingo & Rovira, 2020; Yao et al., 2020; Zhang et al., 2020; Zhu et al., 2020). So, it might be one of the factors responsible for the early entering of Second wave. However, it was more challenging to observe data during the lockdown period in First Wave. Despite that, we have done our monitoring. This study suggests the trend of air pollutants by comparing the two Waves of COVID19 so that Government of India can take necessary action regarding the increasing level of pollutants in the atmosphere.

2   Data Collection and Methodology

2.1   Description of Study Site

The area underneath the study is located in Sakchi (S1) (coordinates as 22.8048° N, 86.2028° E), and consider an urban area of East Singhbhum district and Gamharia (S2) (22.8151° N, 86.1029° E), a sub-urban industrial area of Saraikela Kharsawan district of the Indian state of Jharkhand. Both Sakchi and Gamharia are part of the Greater Jamshedpur Region. It is the 36th largest urban agglomeration and 72nd largest city in India.

According to the census of India in 2011, the population of urban agglomeration of Jamshedpur city was 1,339,438 (https://www.census2011.co.in/census/city/258-jamshedpur.html) and population density was around 6400 km^2. It is surrounded with large dense forest of dalma range and situated at a mean altitude of 159 m above sea level. Sakchi is one of the financial centers and oldest parts of the city, which is located in the center of Jamshedpur. Gamharia has a large industrial conglomerate that comes under the AIADA (Adityapur Industrial Area Development Authority). It is in the western part of the city. A major part of Jamshedpur comes under the Tata Group, that is TATA STEEL, TATA MOTORS, and many other subsidiaries of Tata group. Tata steel is second-largest steel producing company in India and captured one-fifth of area of the Jamshedpur city. Whereas Adityapur Industrial Area is the largest industrial belt in India, it is the industrial hub of the city that consists of small- and medium-scale industries and large-scale industries (Kumar et al., 2019).

The climate of the city is mostly tropical, hot, and humid. Since the COVID-19 cases arose at the start of March and lockdown was imposed from March 24 to May 31, 2020, samples taken were compared in the months of March, April, and May in the years 2020 and 2021. Due to the large industrial belt, both Sakchi and Gamharia have major emissions of atmospheric pollutants. As a result of being dense polluted region, the sharp fall of pollutants was noticeable during the pandemic. The movement of vehicles has been majorly immobile due to lockdown, which reduced transport emission of atmospheric pollutants. The ambient air samples were collected from two different sites, that is, S1 and S2 in Fig. 1. The total number collection of samples was 92 in these two sites during two waves of COVID-19. All samples of BC concentration were collected on everyday basis during First Wave (2020) and Second wave (2021). At the same time, the concentration of PM$_{2.5}$ was collected on weekly basis.
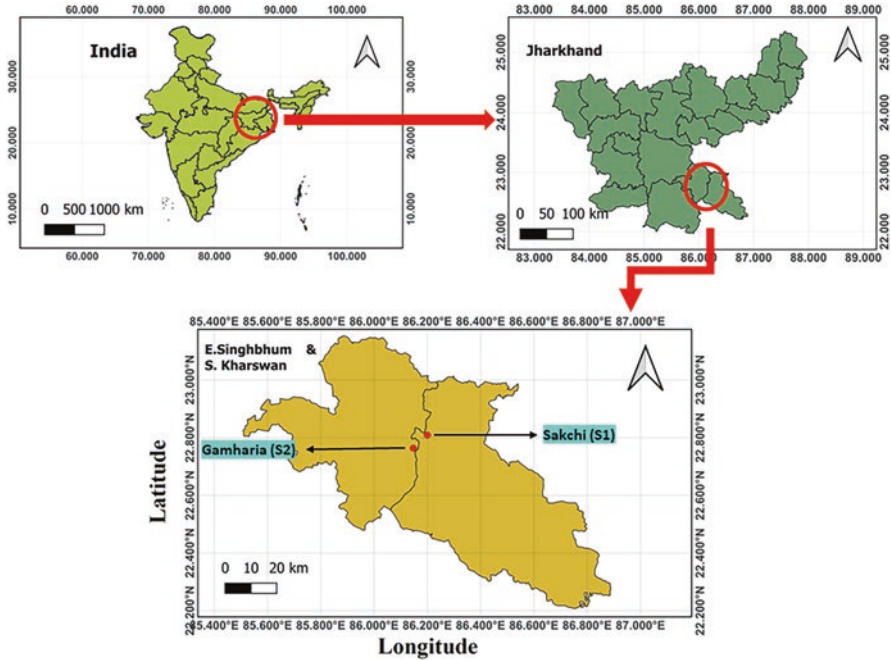
Fig. 1 Sampling sites Sakchi (S1) and Gamharia (S2)

2.2 Measurement of BC Mass Concentration

There are several reported methods for the measurement of BC mass concentration. We started monitoring from March to May during the First Wave and Second Wave of COVID-19. Constant real-time data collection of the aerosol BC mass concentrations was noted with the help of an Aethalometer (AE- 33 Magee Scientific, Berkeley, CA, USA). The instrument was operated at a constant flow rate of 2 L min^{-1} and sampling rate of one minute. The technique measures based on aerosol absorption coefficients mainly absorbs in seven different wavelengths that feature BC categorically in two sources biomass burning and fossil fuel combustion (Favez et al., 2010; Sciare et al., 2011; Sandradewi et al., 2008). The mass BC aerosol particle is shown as an instrument with the help of seven different wavelengths 370 nm (BC1), 470 nm (BC2), 525 nm (BC3), 590 nm (BC4), 660 nm (BC5), 880 nm (BC6), and 950 (BC7) nm. However, the maximum BC concentration is observed at 880 nm because at this wavelength BC is the principal absorber of light and others become negligible (Weingartner et al., 2003; Bodhaine, 1995).

2.3   PM$_{2.5}$ Measurements Method

For the measurement of PM$_{2.5}$ concentrations. The sample was collected in the mini volume sampler of Envirotech Model APM 550. The instrument works at a continuous flow rate of 16.5 L/m$^{3.}$ The sampler was set on the top of the building at sampling sites. During the sampling, 47 mm PTFE filter paper (Merck, List no-PM2547050) was utilized to collect particulate matter. The mass concentration of PM$_{2.5}$ was calculated by the gravimetric method. The filter paper was kept in a desiccator and weighted before the sampling. Then after the sampling, the filter paper was kept again in a desiccator for 24 hrs to remove the absorbed moisture during the sampling period. The weight of the particulates was determined by using a single pan-top loading digital weight balance (VWR, Model no: VWR1611-2263: with Weighing Chamber L × W × H: 162 × 171 × 225 mm). Foundation pollution was checked by utilizing functional spaces (unexposed filter paper) which were prepared simultaneously with field tests. The mass concentration of PM$_{2.5}$ was calculated by abiding by the National Ambient Air Quality Standard Procedure (NAAQS, 2019).

2.4   Backward Trajectory and Fire-Count Study

Backward trajectory analysis is the model for accessing the potential source of aerosol particles in atmosphere that provides a better insight view of pollutant-loaded particulate air parcel from one position to receptor position. It also determines the direction of airflow through which the possible source regions can be identified. 7 days isentropic back trajectory model was analyzed at 500 m above sea level in 3-D i.e., height, longitude, and latitude up to height of 3500 m with the help of Meteorological Data Explorer (METEX, http://db.cger.nies.go.jp/metex/trajectory.html) developed by Centre for Global Environmental Research (CGER), Japan and plotted by Igor software for First Wave and Second Wave of COVID19 from the month of March to May 2020 and March to May 2021. The backward trajectories based on our study have been conducted at different height up to 3500 m above sea level. The back trajectories explain the variations of aerosol that are combined with airborne species in the atmosphere. The backward trajectory analysis shows that the foremost concentration of particulate matter is found in Indo-Gangetic Plains (IGP) region. This might find concentrated due to the great Himalayan ranges, which restrict the pollutant-loaded air masses. Among these consecutive study periods, it was shown growth in air masses in the Second wave compared to the First Wave, which happened due to the nationwide lockdown in First Wave. However, there was partial lockdown in Second wave.

The fire-count data from NASA FIRMS were also included with back trajectories analysis (https://earthdata.nasa.gov/earth-observation-data/near-real-time/firms). The fire-count gives an idea about the active burning during the study time,

which might occur either naturally or anthropogenically. Several studies revealed that the fire-count happened due to the climatic change during COVID-19 (Mann et al., 2016; Krawchuk & Cumming, 2011).

2.5 Meteorological Parameters

The monthly meteorological parameter of the study area was collected from https://www.worldweatheronline.com. Data on meteorological variables of Ambient Temperature in °C, Wind Speed in km/h, Precipitation in mm, and Relative Humidity in % are noted, influencing the concentration of Black Carbon and $PM_{2.5}$. Analysis of meteorological data from the website (https://www.worldweatheronline.com) is shown in the current study. The maximum value of Temperature (Temp), Wind Speed (WS), Precipitation (Prep), and Relative Humidity (RH) was registered as 39.25 °C (dated: May 27, 2020), 28.13 km/h (dated: May 20, 2020), 8.38 mm (dated: April 17, 2020), and 63% (dated: May 27, 2020) respectively in the First Wave whereas, it was shown as 38.38 °C (dated: May 18, 2021), 31.88 km/h (dated: May 27, 2021), 4.78 mm (dated: May 18, 2021), and 85.75% (dated: May 18, 2021) respectively in the Second Wave. Daily mean values are calculated by averaging hourly data shown in Table 1. However, In the colder climate, the lower intensity of solar radiation along with the fog situations shows large concentrations of $PM_{2.5}$ and BC in the atmosphere. The visibility deprivation in the atmosphere during cold weather has been happening due to Mixed layer height (MLH). During the abruption of temperature, MLH results in atmospheric pollutants closer to the earth's surface.

The meteorological parameters variation during First Wave and Second Wave pandemic was graphically represented in Fig. 2a, b, respectively.

2.6 Health Risk Assessment

Exposure to Black Carbon by urbanite expansion of cities and suburbs increases the potential risks, which affect human healthiness. It enters the body by breathing to the local and regional emission sources. Past articles revealed that consuming BC in the body can cause heart diseases, lung cancer, respiratory infection, etc. (Van der Zee et al., 2016). The exact method for health risks assessment of BC has not been determined. However, health risks due to passive smoking are practically analogous with health effects due to exposure to BC (Van der Zee et al., 2016; Wu et al., 2018; Muller & Muller, 2013). In this study, we proposed to explain the health risks due to the consumption of BC to the residents of Jamshedpur. Subsequent to BC, Environmental Tobacco Smoke (ETS) does some damage by Passive Smoking Cigarettes. The receiver faces health threats similar to the effect of inhaling the same quantity of Passive Smoking Cigarettes (PSC). The similarity reflection of

Table 1 Meteorological parameter data which affect the $PM_{2.5}$ and BC concentration of First Wave and Second Wave during COVID-19

Parameters	First Wave			Second Wave		
	March	April	May	March	April	May
	Mean ± SD	Mean ± SD	Mean ± SD	Mean ± SD	Mean ± SD	Mean ± SD
Temp (°C)	29.13 ± 2.83	33.83 ± 3.12	34.57 ± 3.31	32.98 ± 1.75	35.57 ± 1.52	32.35 ± 3.11
W S (km/h)	7.26 ± 2.23	9.15 ± 2.48	13.23 ± 4.87	7.74 ± 3.01	10.56 ± 3.00	12.40 ± 5.90
Prep(mm)	0.23 ± 0.43	0.39 ± 1.5	0.12 ± 0.23	0.00 ± 0.00	0.00 ± 0.01	0.45 ± 0.87
R H (%)	38.06 ± 13.72	33.35 ± 14.09	42.83 ± 10.71	19.42 ± 5.78	28.00 ± 8.17	49.9 ± 13.77
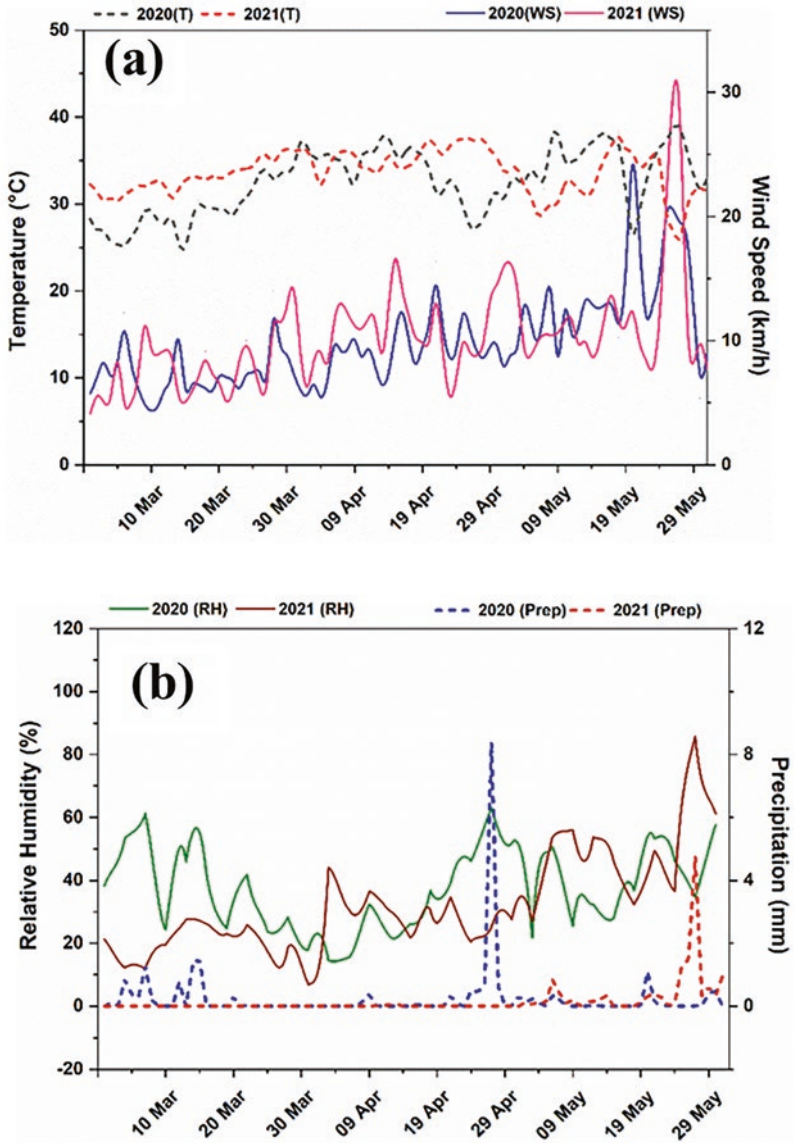
Fig. 2 The meteorological parameters during the First Wave (2020) and Second Wave (2021). (**a**) Represents Temperature vs. Wind Speed (WS) (**b**) Relative Humidity (RH) vs Precipitation respectively

health risk is because of the same inlet canal. The emission of BC and PSC in atmosphere usually radiates from common natural sources (Van der Zee et al., 2016). Now, we extend to estimate the health risks of Aerosol Black Carbon, which includes health consequences for adults and children. Four health outcomes are concerned to BC and ETS exposure (Wells, 1999; Oberg et al., 2010; WHO, 2014; Kelly & Fussell, 2015) i.e.,

(a) Low Birth Weight (LBW) stated for the infant weight below 2.5 kg after 37 weeks of birth
(b) Percentage lung function decrement in school-aged children (PLFD)
(c) Cardiovascular Mortality (CM) and
(d) Lung cancer (LC)

The health risk is estimated by Relative Risks (RR), which in fact depends on various health issues due to pollutants such as BC, $PM_{2.5}$, ETS, etc. Calculation of RR signifies the possibility of disease caused through air pollution (Van der Zee et al., 2016; Pani et al., 2019; Rothman et al., 2008; WHO, 2003). For a precise health outcome, the ratio R of the final relative risk coefficient denoted that the number of PSC is comparable to 1 µg m^{-3} increase in BC concentration for a certain health outcome i.e., R.

Therefore, R is written as:

$$R = \frac{\text{RRBC}}{\text{RRETS}} = \frac{\dfrac{\ln(\text{RRBC})}{\Delta C}}{\dfrac{\ln(\text{RRETS})}{\text{Na}}} \tag{1}$$

The equivalent amounts of PSC (N_{psc}) can be calculated by the following formula as:

$$N_{psc} = R \times \Delta BC = \frac{\text{RRBC}}{\text{RRETS}} \times \Delta BC = \frac{\dfrac{\ln(\text{RRBC})}{\Delta C}}{\dfrac{\ln(\text{RRETS})}{\text{Na}}} \times \Delta B \tag{2}$$

The calculation for RR_{BC} and RR_{ETS} has been taken from Pani et al. (2019) and Van der Zee et al. (2016).

Where,

RR_{BC} = the regression coefficient per 1 µgm^{-3} of BC
RR_{ETS} = the regression coefficient per cigarette
[ln(RR_{BC})/ΔC] = the resultant risks for change in ΔC
[ln(RR_{ETS})/number of assumed PSC] = the resultant risks of ETS exposure for the study number of PSC per day
RR_{BC} = relative risk of BC concentration with respect to health issue

RR_{ETS} = relative risk for ETS exposure

N_{psc} = the number of assumed PSC

ΔBC = changed in concentration of monitored and Background BC.

And,

$$\Delta BC = \left[\left(BC_{ob}\right) - \left(BC_{bac}\right)\right] \tag{3}$$

Where,

BC_{ob} = Observed BC

BC_{bac} = Background BC

The assumed number of Passive Smoke Cigarette (N_{psc}) is 9 in the case of PLFD which belongs to parental smoke whereas the N_{psc} is observed 7 for children having non-smoking parents for LBW, LC, and CM (van der Zee et al., 2016; Pani et al., 2019).

3 Results and Discussion

3.1 Temporal Variation of Black Carbon Concentrations

The mass concentrations of BC at two different sites are compared in Fig. 3. The mean value and standard deviation of the BC have been described in Table 2. The monthly averaged BC concentration at the S1 site was registered at around 35.5 ± 5.4 µgm⁻³, 21.8 ± 6.5 µgm⁻³, and 22.4 ± 4.7 µgm⁻³ whereas at S2 was recorded around 26.8 ± 2.5 µgm⁻³, 14.6 ± 2.44 µgm⁻³, and 25 ± 7.06 µgm⁻³ in the month of March, April, and May of the First Wave 2020 respectively. However, In the Second Wave 2021, the monthly averaged BC concentration at S1 was recorded around 31.99 ± 3.8 µgm⁻³, 33.8 ± 5.66 µgm⁻³, and 29 ± 4.94 µgm⁻³ and at S2 was noted around 32.26 ± 3 µgm⁻³, 36.72 ± 6 µgm⁻³, and 30.04 ± 6.5 µgm⁻³ in the respective month of March, April, and May. BC mass concentrations varied from 10 to 56.25 µgm⁻³ and 10 to 48.8 µgm⁻³ in the First Wave of two different sites S1 and S2 respectively, during the study period. However, In the Second wave, BC concentration varied from 23.56 to 67.65 µgm⁻³ and 23.25 to 70.8 µgm⁻³ in the respective sampling sites S1 and S2. From the data and observation, it was noticed that the gradual decrease in the concentration of BC with the reduction of human activities like industrial work, vehicular movement, public gathering, infrastructure work, etc. was suddenly shut down during the lockdown of the First Wave. BC mass concentration started reducing at the end of March due to close down as clearly depicted in Fig. 3a, b. However, some of the BC concentration was reported high during the initial time of lockdown. This is due to the long-term stability of BC in the atmosphere. Whereas, In the Second Wave, The BC concentration remains the same as on regular days due to the continuation of human activities. However, a little bit fall was shown due to
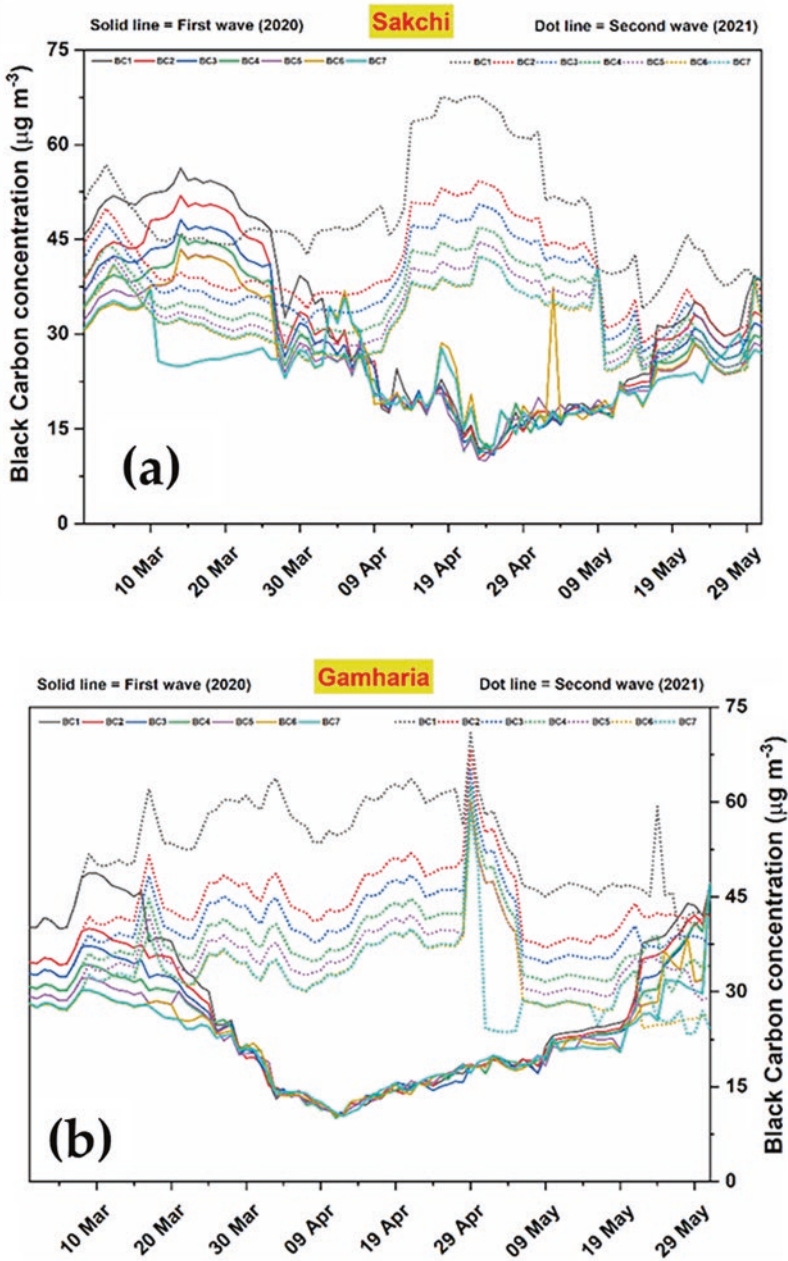
Fig. 3 Figure shows the variation in concentration of BC in the First Wave (2020) and Second Wave (2021) during COVID-19. (**a**) depicts the variation in Sakchi (S1) and (**b**) shows the variation in Gamharia (S2)

Table 2 Daily mean concentrations of BC in the middle of the two waves of COVID-19

BC ($\mu g\ m^{-3}$)	Month	BC1	BC2	BC3	BC4	BC5	BC6	BC7
		Mean ± SD	Mean ± SD	Mean ± SD	Mean ± SD	Mean ± SD	Mean ± SD	Mean ± SD
First Wave								
S1	March	49 ± 5.8	43.9 ± 6.4	41 ± 5.6	38.5 ± 5.4	36.3 ± 4.9	35.5 ± 5.4	28.6 ± 4.0
	April	20.8 ± 6.6	19.9 ± 6.2	19.7 ± 5.6	19.2 ± 5	19.1 ± 5.06	21.8 ± 6.5	21.4 ± 6.4
	May	26 ± 7.3	24.4 ± 6	23.2 ± 5.4	22.5 ± 4.5	22 ± 3.58	22.4 ± 4.7	21.7 ± 4.1
S2	March	37.5 ± 8.7	32.8 ± 6	31 ± 4.98	29.3 ± 3.7	27.9 ± 3.4	26.8 ± 2.5	26.4 ± 2.7
	April	14.3 ± 2.2	14.6 ± 2.1	14.3 ± 2.07	14.58 ± 2.45	14.64 ± 2.5	14.6 ± 2.44	14.7 ± 2.36
	May	28.3 ± 9.4	27.4 ± 8.7	26.4 ± 8.03	26.23 ± 7.8	25.04 ± 7.02	25 ± 7.06	24.01 ± 6.10
Second Wave								
S1	March	47.2 ± 3.6	40 ± 4.1	37.9 ± 4.1	35.2 ± 3.97	33.48 ± 3.88	31.99 ± 3.8	32 ± 3.79
	April	57.3 ± 8.9	45.45 ± 7	42.1 ± 6.5	38.5 ± 6.14	36 ± 5.88	33.8 ± 5.66	33.9 ± 5.59
	May	43 ± 6.27	35.8 ± 5.8	33.9 ± 5.6	31.8 ± 5.31	30.3 ± 5.12	29 ± 4.94	29.5 ± 5.2
S2	March	51.7 ± 6.9	42 ± 4.7	39.3 ± 4.2	36.30 ± 3.8	34.2 ± 3.4	32.26 ± 3	32.36 ± 3.06
	April	59.7 ± 3.7	48.1 ± 5.4	44.6 ± 5.4	41.2 ± 5.6	38.75 ± 5.5	36.72 ± 6	36.7 ± 5.7
	May	47.3 ± 4.7	41.9 ± 4.9	38.66 ± 4.8	35.47 ± 5.2	33.45 ± 5.1	30.04 ± 6.5	27.01 ± 2.6

the partial lockdown in the city. Several studies suggested that the BC and $PM_{2.5}$ concentration has a wide range in the Eastern and Northeastern parts of India (Nair et al., 2007; Lal et al., 2012). According to the GIOVANI NASA satellite, it was gathered because of the Indo-Gangetic Plains (IGP) region. The elaboration of the study is shown in Fig. 3a, b.

3.2   *Temporal Variation of PM$_{2.5}$ Concentrations*

The $PM_{2.5}$ concentrations range value is described in Table 3. The mass concentration of $PM_{2.5}$ at two sites, S1 and S2, are compared in Fig. 4a. The concentration of $PM_{2.5}$ at S1 was found to be approximately 128.25 ± 5.45 μgm^{-3}, 38.25 ± 10.57 μgm^{-3}, and 45.25 ± 3.03 μgm^{-3} in the respective study from the month of March to May 2020. At sampling site S2, the $PM_{2.5}$ concentration was approximately 120.75 ± 4.6 μgm^{-3}, 37.25 ± 6.87 μgm^{-3}, and 46.75 ± 7.9 μgm^{-3} in the respective study months. According to the NAAQs (National Ambient Air Quality Standards), the annual standard value for $PM_{2.5}$ is 40 μg/m^3 (NAAQS, 2019). However, this study observed beyond the standards. $PM_{2.5}$ was also dropped abruptly which followed the trends observed in BC during the First Wave of the pandemic, as shown in the graph plot in Fig. 4a. However, there was a negligible effect on the concentration of $PM_{2.5}$ compared to the normal days in the Second Wave. In contrast, some sudden dip in concentration was due to rainy days when fewer particles were suspended in the atmosphere. The sampling site S2 was more polluted than the S1 site as the industrial activities had restrictions despite a partial lockdown in Second Wave. The average mass concentration of $PM_{2.5}$ with standard deviation is plotted in the graph as shown in Fig. 4b. The mean percentage of BC in $PM_{2.5}$ concentration ranged from 27% to 39% during the study period, as shown in Table 4.

3.3   *Backward Trajectory and Fire-Count Analysis*

The seven-day back trajectories incorporated with fire-count data have been analyzed and plotted in Fig. 5a, b. In the present study, the backward trajectories were calculated during the First wave and Second wave of COVID-19 from March 1 to May 31 of the year 2020 and 2021. During the First Wave of the pandemic, the concentration of aerosol particles was found lowest due to the complete lockdown. On the other hand, the concentration of aerosol particles was found moderate due to partial lockdown during the second wave. Fire-count data were also used to access the active burning during the First and Second waves of pandemics. However, progressive industrial activities and vehicular movement were persisting with restricted norms. Air masses also contributed from countries like Afghanistan, Pakistan, and Iran in the West as well as Nepal in the North and Bangladesh in the Eastern part to the receptor site. The research study was done during summer season, the air masses were also influenced due to the IGP region. Due to the Himalaya Mountain range, it

Table 3 Monthly mean concentrations of $PM_{2.5}$ during the two waves of COVID-19

Month	PM₂.₅ (µg m⁻³)					
	S1			S2		
	March	April	May	March	April	May
	Mean ± SD	Mean ± SD	Mean ± SD	Mean ± SD	Mean ± SD	Mean ± SD
First Wave	128.25 ± 5.45	38.25 ± 10.57	45.25 ± 3.03	120.75 ± 4.6	37.25 ± 6.87	46.75 ± 7.9
Second Wave	126.75 ± 9.12	147.2 ± 12.3	136 ± 16.5	135 ± 10.6	151 ± 5.58	141.75 ± 10.23
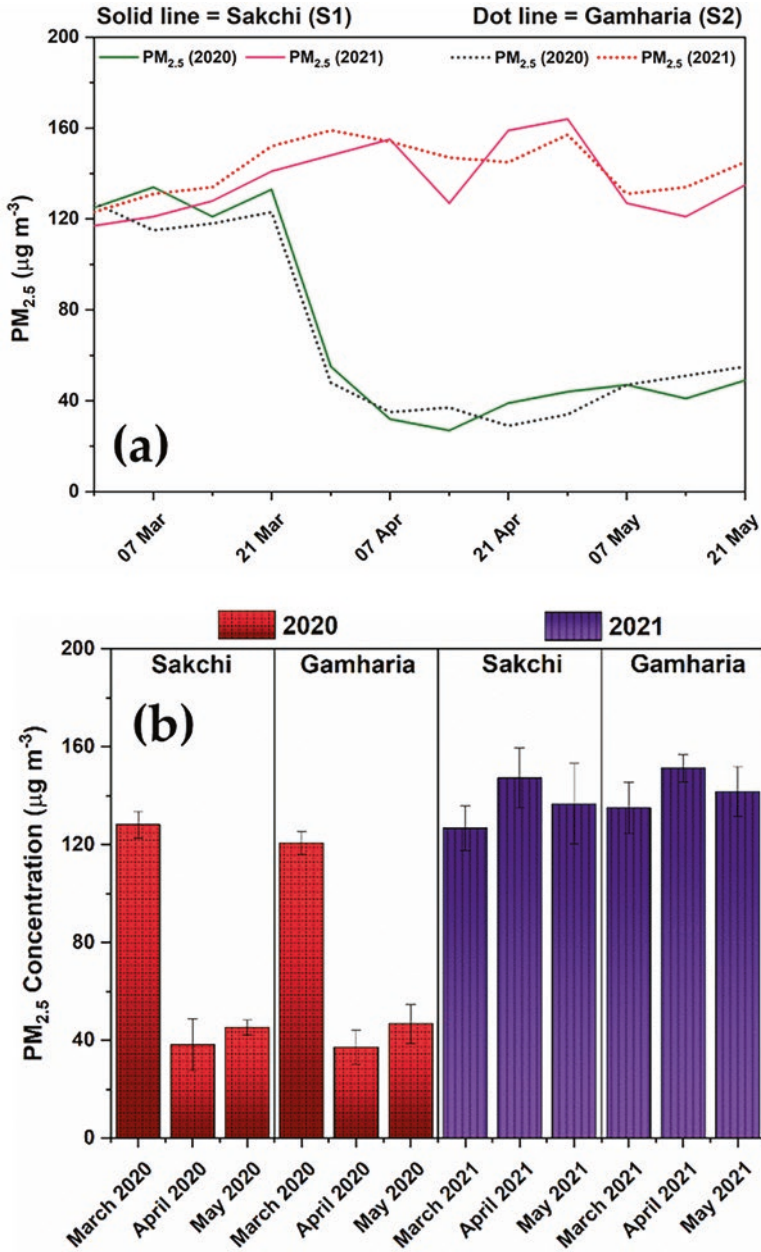
Fig. 4 (**a**) The comparison of PM$_{2.5}$ concentration in both location sites S1 and S2 in the First Wave and Second Wave of COVID-19 and (**b**) the average mass concentration with a standard deviation of PM$_{2.5}$ which compares two waves at Jamshedpur's sampling sites

Table 4 The mean and range of BC, PM$_{2.5}$ concentrations, and BC/PM$_{2.5}$ ratio %

	First Wave				Second Wave			
	S1		S2		S1		S2	
	Mean	Range	Mean	Range	Mean	Range	Mean	Range
Black Carbon ($\mu g\ m^{-3}$)	27.58	10–56	23.7	10–48.8	37	23.5–66.6	39.4	23.2–71
PM$_{2.5}$ ($\mu g\ m^{-3}$)	70.6	27–134	68.25	34–127	137	117–164	142.7	123–159
BC/PM$_{2.5,}$ (%)	39%		34.7%		27%		27.6%	

blocks the movement of aerosol. So, the maximum aerosol accumulated in IGP region. Some air masses were affected by the Bay of Bengal and other marine's particular matters. Some low-concentration result was observed due to the power of nearby clean marine air masses, which mixed with regional air masses. The incorporated fire-count data with backward trajectory was analyzed by Moderate Resolution Imaging Spectroradiometer (MODIS) with the help of the National Aeronautics and Space Administration (NASA) satellite to gain access to the active fire burning across India.

3.4   Health Risk Due to Exposure to BC in the Study Region

According to various studies and research conclusions, most of the health hazards of human cardiovascular disease and respiratory dysfunction have been registered due to long-term exposure to ambient air pollution (Van der Zee et al., 2016). Our study has reported the exposure risk of BC in two different sampling sites S1 and S2 of East India, during two waves of the COVID-19 pandemic. The assessment was done by assuming the daily consumption of observed monitored BC (BC$_{ob}$) concentration, i.e., equivalent to the daily average Background BC concentration (BC$_{bac}$) level. The average Background BC (BC$_{bac}$) was calculated as 1.25th percentile of overall observed BC set (Kondo et al., 2006; Rupakheti et al., 2017) i.e., 12.5 μgm^{-3}, and 23.6 μgm^{-3} for the respective First and Second wave of S1 and 10.6 μgm^{-3}, and 24.5 μgm^{-3} for the respective waves of S2. ΔBC (BC$_{ob}$ − BC$_{bac}$) was calculated as 14.1 & 7.99 μgm^{-3} for the respective waves at S1, whereas 11.6 & 8.4 μgm^{-3} at S2. The health risks were calculated with the help of the above formula mentioned in Eq. 2, which was expressed by van der Zee. The brief of the estimation was taken in terms of the assumed number of Passive Smoking Cigarettes (PSC). According to WHO, there was consumption of 14 cigarettes daily by smokers living in the USA and region of Northwestern Europe. Our calculation was determined on the assumption of van der Zee et al. (2016). The assessment may have some limitations. The assessment feature was estimated in an identical number of Passive Smoking Cigarette for an individual time as described in Table 5. Afterward from our study, the health risks due to BC exposure were observed at S1 at 25.3, 50.3, 45.4, and
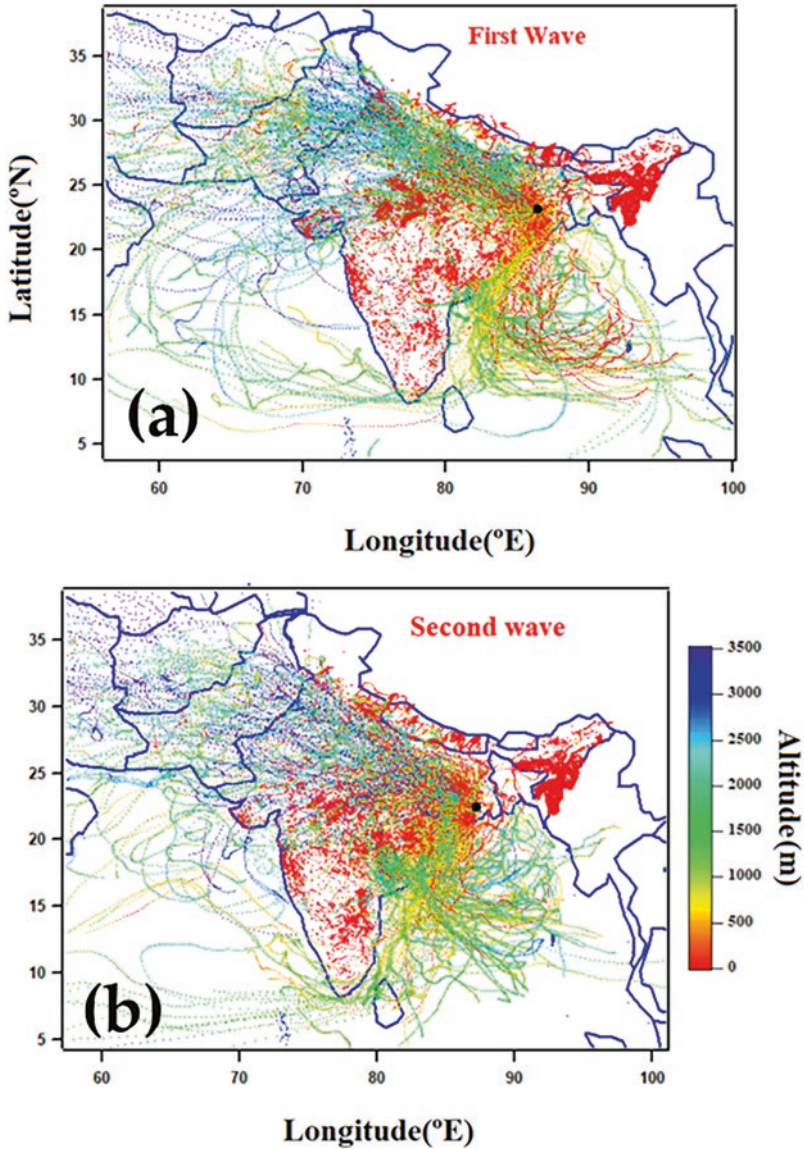
Fig. 5 Seven days back trajectories incorporated with fire-count analysis up to 3500 m altitude during First and Second Waves of COVID-19

103.7 and at the S2 site, at 20.8, 41.3, 37.3, and 85.1 number of PSC for CM, LC, LBW, and PLED respectively in the First Wave of COVID19 pandemic (2020). Whereas in the Second Wave of the COVID19 pandemic (2021), it was observed 14.4, 28.5, 25.7, and 58.7 at the S1 site and S2 sites 15, 29.9, 27, and 61.6 number of PSC for CM, LC, LBW, and PLED respectively. It was seen from the data that the

Table 5 Health risk estimation of BC concentration that evaluated from consumption of equivalent numbers of passively smoked cigarettes (PSC) per day with respect to different health outcomes

	First Wave		Second Wave (2021)	
	S1	S2	S1	S2
CM	25.3	20.8	14.4	15
LC	50.3	41.3	28.5	29.9
LBW	45.4	37.3	25.7	27
PLFD	103.7	85.1	58.7	61.6

health risk is greater in the First Wave compared to the Second wave. Despite being more strictly followed lockdown, the health risk level was seen as higher. This might be happened due to more concentration of ETS exposed in atmosphere before First Wave. Whereas, In the Second Wave, the Exposure of ETS collapsed due to the sharp fall from the First Wave. Exposure to BC contaminants in S1 was found equivalent to the Passive smoking cigarette, i.e., higher risk of PLFD (103.7 in First Wave of S1 and lower risk of CM (14.4 in the Second wave of S1) during Covid-19. The other health risk due to BC contamination or exposure to ETS reached higher values of 67.4, 31.8, 69.5, and 184.4 number of PSC for CM, LC, LBW, and PLFD respectively at the Tibetan Plateau (Wu et al., 2018). However, these health risk estimations are noticeable for further broad investigation with depth study. It should be a considerable threat to the health of local people residing nearby Jamshedpur city and the administration should take action to control the level of pollution.

4   Summary and Conclusions

Both the BC and $PM_{2.5}$ concentrations were higher in sampling site S2 during Second Wave, it might happen due to the large industrial activities. While Its concentration was higher in the S1 site during the First Wave due to complete lockdown, all human activities were restricted. During the First Wave, Emergency movement of vehicles like Ambulance, Police Patrolling, etc., and these hustle fustle was majorly noticed in the city center, i.e., at sampling site S1. During the study month of First Wave, the total average BC concentration was registered at 27.58 and 23.7 μgm^{-3} in S1 and S2 respectively. In the second wave, the total average BC concentration was registered at 37 and 39.4 μgm^{-3} in S1 and S2, respectively. The concentration changes of BC concentration have shown different results due to the different types of the study site. The total average concentration of $PM_{2.5}$ was measured at around 70.6 and 68.25 μgm^{-3} in the respective sites S1 and S2 during the study period of the First Wave. Whereas it was around 136.9 and 142.67 μgm^{-3} in S1 and S2 during the study period of Second wave. In both waves of COVID19, the observed concentrations of $PM_{2.5}$ were higher than the Annual NAAQ standards value of 40 $\mu g\ m^{-3}$ over the two study sites in those study months. The study period was started before the nationwide lockdown, which also passed the standard

Ambient Air Quality. This might exceed due to the presence of Particulate Matter in the atmosphere during the initial days of lockdown. The average percentage of BC in $PM_{2.5}$ concentration in these sampling sites ranged from 27% to 39% in both case studies. The concentration of BC and $PM_{2.5}$ was higher compared to other nearby cities due to being surrounded by dense forests, which causes forest fires. Backward trajectories were analyzed from a height of 500 m to 3500 m above sea level, incorporating the Fire-count data for air parcel movement to the receptor position. The health risks due to the exposure to BC were 20.8 to 103.7 Passive Smoking Cigarettes belonging to these study sites. These risks assessment may vary for different health consequences, i.e., CM, LC, LBW, and PLFD.

Author Contributions Balram Ambade: Conceptualization, write and analysis, Supervision and edit, Validation and review; Dilip Kumar Mahato: Conceptualization, software and methodology, Validation, review and edit.

Declarations Conflict of Interest All authors declare no conflict of interest. Ethical Approval All authors certify that they have no affiliation with or involvement in any organization or entity with any financial or nonfinancial interests in the subject matter or materials discussed in this manuscript.

Data Availability The data and materials generated and analyzed in this published article are available from the corresponding author upon reasonable request.

References

Ambade, B., & Kurwadkar, S. (2021). Emission reduction of black carbon and polycyclic aromatic hydrocarbons during COVID-19 pandemic lockdown. *Air Quality, Atmosphere & Health, 14*, 1081–1095.

Andrews, M. A., Areekal, B., Rajesh, K. R., Krishnan, J., Suryakala, R., Krishnan, B., Muraly, C. P., & Santhosh, P. V. (2020). First confirmed case of COVID-19 infection in India: A case report. *Indian Journal of Medical Research, 151*(5), 490–492.

Balakrishnan, K., Dey, S., Tarun, G., & Dhaliwal, R. S. (2019). The impact of air pollution on deaths, disease burden, and life expectancy across the states of India: The Global Burden of Disease Study 2017. *Lancet Planet Health, 3*, 26–39. https://doi.org/10.1016/S2542-5196(18)30261-4

Banerjee, T., Murari, V., Kumar, M., & Raju, M. P. (2015). Source apportionment of airborne particulates through receptor modelling: Indian scenario. *Atmospheric Research, 164–165*, 167–187.

Bodhaine, B. A. (1995). Aerosol absorption measurements at Barrow, Mauna Loa and the South Pole. *Journal of Geophysical Research, 100*(d5), 8967–8975. https://doi.org/10.1029/95jd00513

Bond, T. C., Doherty, S. J., Fahey, D. W., Forster, P. M., Berntsen, T., DeAngelo, B. J., et al. (2013). Bounding the role of black carbon in the climate system: A scientific assessment. *Journal of Geophysical Research: Atmospheres, 118*, 5380–5552.

Cape, J. N., Coyle, M., & Dumitrean, P. (2012). The atmospheric lifetime of black carbon. *Atmospheric Environment, 59*, 256–263.

Das, M., Das, A., Sarkar, R., Saha, S., & Mandal, A. (2020). Examining the impact of lockdown (due to COVID-19) on ambient aerosols (PM 2.5): A study on Indo-Gangetic Plain (IGP) cities, India. *Stochastic Environmental Research and Risk Assessment*, 0123456789. https://doi.org/10.1007/s00477-020-01905-x

Dasgupta, P., & Srikanth, K. (2020). Reduced air pollution during COVID-19: Learnings for sustainability from Indian cities. *Global Transitions, 2*, 271–282. https://doi.org/10.1016/j.glt.2020.10.002

Dhaka, S. K., Chetna, K., Panwar, V., Dimri, A. P., Singh, N., Patra, P. K., Matsumi, Y., Takigawa, M., Nakayama, T., Yamaji, K., Kajino, M., Misra, P., & Hayashida, S. (2020). PM2.5 diminution and haze events over Delhi during the COVID-19 lockdown period: An interplay between the baseline pollution and meteorology. *Scientifc Reports, 10*, 1–8. https://doi.org/10.1038/s41598-020-70179-8

Ding, A. J., Huang, X., Nie, W., Sun, J. N., Kerminen, V. M., Petäjä, T., et al. (2016). Enhanced haze pollution by black carbon in megacities in China. *Geophysical Research Letters, 43*(6), 2873–2879.

Domingo, J. L., & Rovira, J. (2020). Effects of air pollutants on the transmission and severity of respiratory viral infections. *Environmental Research, 187*, 109650.

Dumka, U. C., Kaskaoutis, D. G., Verma, S., Ningombam, S. S., Kumar, S., & Ghosh, S. (2021). Silver linings in the dark clouds of COVID-19: Improvement of air quality over India and Delhi metropolitan area from measurements and WRF-CHIMERE model simulations. *Atmospheric Pollution Research, 12*(2), 225–242.

Favez, O., El Haddad, I., Piot, C., Boreave, A., Abidi, E., Marchand, N., Jaffrezo, J. L., Besombes, J. L., Personnaz, M. B., Sciare, J., Wortham, H., George, C., & D'Anna, B. (2010). Inter-comparison of source apportionment models for the estimation of wood burning aerosols during wintertime in an Alpine city (Grenoble, France). *Atmospheric Chemistry and Physics, 10*(12), 5295–5314.

Feng, S., Jiang, F., Wang, H., Wang, H., Ju, W., & Shen, Y. (2020). NOx emission changes over China during the COVID-19 epidemic inferred from surface NO2 observations. *Geophysical Research Letters, 47*(19), 2020GL090080.

Fu, F., Purvis-Roberts, K. L., & Williams, B. (2020). Impact of the covid-19 pandemic lockdown on air pollution in 20 major cities around the world. *Atmosphere, 11*. https://doi.org/10.3390/atmos11111189

Geng, F., Hua, J., Mu, Z., Peng, L., Xu, X., Chen, R., & Kan, H. (2013). Differentiating the associations of black carbon and fine particle with daily mortality in a Chinese city. *Environmental Research, 120*, 27–32.

Goel, V., Hazarika, N., Kumar, M., Singh, V., Thamban, N. M., & Tripathi, S. N. (2021). Variations in Black Carbon concentration and sources during COVID-19 lockdown in Delhi. *Chemosphere, 270*, 129435. https://doi.org/10.1016/j.chemosphere.2020.129435

Guo, H., Kota, S. H., Shau, S. K., & Zhang, H. (2019). Contributions of local and regional sources to PM$_{2.5}$ and its health effects in North India. *Atmospheric Environment, 214*, 116867. https://doi.org/10.1016/j.atmosenv.2019.116867

Health Effects Institute. (2019). *State of global air 2019*. Special report.

Huang, X., Ding, A., Wang, Z., Ding, K., Gao, J., Chai, F., & Fu, C. (2020). Amplified transboundary transport of haze by aerosol-boundary layer interaction in China. *Nature Geoscience, 13*, 428–434.

Huang, X., Ding, A. J., Gao, J., Zheng, B., Zhou, D., & Qi, X. (2021). Enhanced secondary pollution offset reduction of primary emissions during COVID-19 lockdown in China. *National Science Review, 8(2)*, nwaa137.

Jain, S., & Sharma, T. (2020). Social and travel lockdown impact considering Coronavirus disease (COVID-19) on air quality in megacities of India: Present benefits, future challenges and way forward. 2020. *Aerosol and Air Quality Research, 20*, 1222–1236.

Jia, M., & Evangeliou, N. (2021). Black carbon emission reduction due to COVID-19 lockdown in China. *Geophysical Research Letters*, 1–10. https://doi.org/10.1029/2021GL093243

Kelly, F. J., & Fussell, J. C. (2015). Air pollution and public health: Emerging hazards and improved understanding of risk. *Environmental Geochemistry and Health, 37*, 631–649.

Kim, K. H., Kabir, E., & Kabir, S. (2015). A review on the human health impact of airborne particulate matter. *Environment International, 74*, 136–143.

Kondo, Y., Komazaki, Y., Miyazaki, Y., Moteki, N., Takegawa, N., Kodama, D., Deguchi, S., Nogami, M., Fukuda, M., & Miyakawa, T. (2006). Temporal variations of elemental carbon in Tokyo. *Journal of Geophysical Research: Atmospheres, 111*, D12205.

Krawchuk, M. A., & Cumming, S. G. (2011). Effects of biotic feedback and harvest management on boreal forest fire activity under climate change. *Ecological Applications, 21*(1), 122–136. https://doi.org/10.1890/09-2004.1

Kumar, A., & Mishra, R. K. (2018). Human health risk assessment of major air pollutants at transport corridors of Delhi, India. *Journal of Transport & Health, 10*(2018), 132–143. https://doi.org/10.1016/j.jth.2018.05.013

Kumar, A., Ambade, B., Sankar, T. K., Sethi, S. S., & Kurwadkar, S. (2019). *Source identification and health risk assessment of atmospheric PM2.5- bound polycyclic aromatic hydrocarbons in Jamshedpur, India*. Sustainable Cities and Society.

Kumari, P., & Toshniwal, D. (2020). Impact of lockdown on air quality over major cities across the globe during COVID19 pandemic. *Urban Climate, 34*, 100719. https://doi.org/10.1016/j.uclim.2020.100719

Lal, D. M., Ghude, S. D., Patil, S. D., Kulkarni, S. H., Jena, C., Tiwari, S., & Srivastava, M. K. (2012). Tropospheric ozone and aerosol long-term trends over the Indo-Gangetic Plain (IGP), India. *Atmospheric Research, 116*, 82–92.

Mann, M. L., Batllori, E., Moritz, M. A., Waller, E. C., Berck, P., Flint, A. L., Flint, L. E., & Dolfi, E. (2016). Incorporating anthropogenic influences into fire probability models: Effects of human activity and climate change on fire activity in California. *PLoS One, 11*(4), 0153589. https://doi.org/10.1371/journal.pone.0153589

Muller, R. A., & Muller, E. A. (2013). *Air pollution and cigarette equivalence* (p. 47). Berkeley Earth.

NAAQS (National Ambient Air Quality Standards). (2019). Ministry of Forest and Environment. Government of India, New Delhi.

Nair, V. S., Moorthy, K. K., Alappattu, D. P., Kunhikrishnan, P. K., George, S., Nair, P. R., Babu, S. S., Abish, B., Satheesh, S. K., Tripathi, S. N., Niranjan, K., Madhavan, B. L., Srikant, V., Dutt, C. B. S., Badarinath, K. V. S., & Reddy, R. R. (2007). Wintertime aerosol characteristics over the Indo-Gangetic Plain (IGP): Impacts of local boundary layer processes and long-range transport. *Journal of Geophysical Research, 112*, d13205. https://doi.org/10.1029/2006jd008099

Nigam, R., Pandya, K., Luis, A. J., Sengupta, R., & Kotha, M. (2021). Positive effects of COVID-19 lockdown on air quality of industrial cities (Ankleshwar and Vapi) of Western India. *Scientifc Reports, 11*, 1–12. https://doi.org/10.1038/s41598-021-83393-9

Oberg, M., Jaakkola, M. S., Prüss-Üstün, A., Schweizer, C., & Woodward, A. (2010). *Sec-ond hand smoke, assessing the environmental burden of disease at national and local levels* (Vol. 18). World Health Organization, Environmental Burden of Disease Series. http://www.who.int/quantifying_ehimpacts/publications/SHS.pdf

Pandey, C. P., & Negi, P. S. (2022). Characteristics of equivalent black carbon aerosols over Doon Valley in NW Indian Himalaya during COVID-19 lockdown 2020. *Environmental Monitoring and Assessment, 194*, 229 Vol.: (0123456789) 1 3. https://doi.org/10.1007/s10661-022-09879-9

Pani, S. K., Wang, S. H., Lin, N. H., Chantara, S., Lee, C. T., & Thepnuan, D. (2019). Black carbon over an urban atmosphere in northern peninsular Southeast Asia: Characteristics, source apportionment, and associated health risks. *Environmental Pollution, 259*, 113871.

Panicker, A. S., Aditi, R., Beig, G., Ali, K., & Solmon, F. (2018). Radiative forcing of carbonaceous aerosols over two urban environments in Northern India. *Aerosol and Air Quality Research, 18*, 884–894.

Pant, P., Lal, R. M., Guttikunda, S. K., Russell, A. G., Nagpure, A. S., Ramaswami, A., & Peltier, R. E. (2018). Monitoring particulate matter in India: Recent trends and future outlook. *Air Quality Atmosphere and Health, 12*, 45–58. https://doi.org/10.1007/s11869-018-0629-6

Pathakoti, M., Muppala, A., Hazra, S., Dangeti, M., Shekhar, R., Jella, S., Mullapudi, S. S., Andugulapati, P., & Vijayasundaram, U. (2020). An assessment of the impact of a nation-wide lockdown on air pollution — *A remote sensing perspective over India*. 1–16.

Qin, Y., & Xie, S. D. (2012). Spatial and temporal variation of anthropogenic black carbon emissions in China for the period 1980-2009. *Atmospheric Chemistry and Physics, 12*, 4825–4841.

Ramanathan, V., & Carmichael, G. (2008). Global and regional climate changes due to black carbon. *Nature Geoscience, 1*(4), 221–227.

Rana, A., Jia, S., & Sarkar, S. (2019). Black carbon aerosol in India: A comprehensive review of current status and future prospects. *Atmospheric Research, 218*, 207–230.

Ranjan, R., Sharma, A., & Verma, M. (2021). Characterization of the second wave of COVID-19 in India. 2021. *Current Science, 121*(1), 85–93.

Rothman, K. J., Greenland, S., & Lash, T. L. (2008.; Annals of Emergency Medicine, An International Journal). *Modern epidemiology* (p. 53–77). Wolters Kluwer/Lippincott Williams & Wilkins.

Rupakheti, D., Adhikary, B., Praveen, P. S., Rupakheti, M., Kang, S., Mahata, K. S., Naja, M., Zhang, Q., Panday, A. K., & Lawrence, M. G. (2017). Pre-monsoon air quality over Lumbini, a world heritage site along the Himalayan foothills. *Atmospheric Chemistry and Physics, 17*, 11041–11063.

Saharan, U. S., Kumar, R., Tripathy, P., Sateesh, M., Garg, J., Sharma, S. K., & Mandal, T. K. (2022). Drivers of air pollution variability during second wave of COVID-19 in Delhi, India. *Urban Climate, 41*, 101059.

Sandradewi, J., Prevot, A. S., Szidat, S., Perron, N., Alfarra, M. R., Lanz, V. A., Weingartner, E., & Baltensperger, U. (2008). Using aerosol light absorption measurements for the quantitative determination of wood burning and traffic emission contributions to particulate matter. *Environmental Science & Technology, 42*(9), 3316–3323.

Schraufnagel, D. E., Balmes, J. R., Cowl, C. T., De Matteis, S., Jung, S. H., Mortimer, K., Perez-Padilla, R., Rice, M. B., Riojas-Rodriguez, H., Sood, A., & Thurston, G. D. (2019). Air pollution and noncommunicable diseases: A review by the Forum of International Respiratory Societies' Environmental Committee, Part 2. *Air Pollution and Organ Systems Chest, 155*(2), 417–426.

Sciare, J., D'Argouges, O., Sarda-Esteve, R., Gaimoz, C., Dolgorouky, C., Bonnaire, N., Favez, O., Bonsang, B., & Gros, V. (2011). Large contribution of water-insoluble secondary organic aerosols in the region of Paris (France) during wintertime. *Journal of Geophysical Research: Atmospheres, 116*(22), D22203.

Shen, G., Yang, Y., Wang, W., Tao, S., Zhu, C., Min, Y., et al. (2010). Emission factors of particulate matter and elemental carbon for crop residues and coals burned in typical household stoves in China. *Environmental Science & Technology, 44*(18), 7157–7162.

Shil, P., Atre, N. M., Patil, A. A., Tandale, B. V., & Abraham, P. (2021). District-wise estimation of basic reproduction number (R0) for COVID-19 in India in the initial phase. *Spatial Information Research*. https://doi.org/10.1007/s41324-021-00412-7

Shrestha, G., Traina, J. S., & Swanston, W. C. (2010). Black carbon's properties and role in the environment: A comprehensive review. *Sustainability, 2*, 294–320.

Singh, R. P., & Chauhan, A. (2020). Impact of lockdown on air quality in India during COVID-19 pandemic. *Air Quality, Atmosphere & Health, 13*, 921–928. https://doi.org/10.1007/s11869-020-00863-1

USEPA. (2014). *National Emissions Inventory Report* [WWW Document]. https://gispub.epa.gov/neireport/2014/. Accessed 25 May 2020.

Van der Zee, S. C., Fischer, P. H., & Hoek, G. (2016). Air pollution in perspective: Health risks of air pollution expressed in equivalent numbers of passively smoked cigarettes. *Environmental Research, 148*, 475–483.

Wang, Z., Wang, T., Gao, R., Xue, L., Guo, J., Zhou, Y., et al. (2011). Source and variation of carbonaceous aerosols at Mount Tai, North China: Results from a semi-continuous instrument. *Atmospheric Environment, 45*(9), 1655–1667.

Wang, X., Chen, R., Meng, X., Geng, F., Wang, C., & Kan, H. (2013). Associations between fine particle, coarse particle, black carbon and hospital visits in a Chinese city. *The Science of the Total Environment, 458–460*, 1–6.

Wang, R., Tao, S., Balkanski, Y., Ciais, P., Boucher, O., Liu, J., et al. (2014). Exposure to ambient black carbon derived from a unique inventory and high-resolution model. *Proceedings of the National Academy of Sciences of the United States of America, 111*(7), 2459–2463.

Waylen, K. A., Blackstock, K. L., van Hulst, F. J., Damian, C., Horvath, F., Johnson, R. K., Kanka, R., Külvik, M., Macleod, C. J. A., Meissner, K., Oprina-Pavelescu, M. M., Pino, J., Primmer, E., Rîşnoveanu, G., Satalova, B., Silander, J., Spulerova, J., Suskevics, M., & Van Uytvanck, J. (2019). Policy-driven monitoring and evaluation: Does it support adaptive management of socio-ecological systems? *Science of the Total Environment, 662*, 373–384.

Weingartner, E., Saathoff, H., Schnaiter, M., Streit, N., Bitnar, B., & Baltensperger, U. (2003). Absorption of light by soot particles, determination of the absorption coefficient by means of aethalometers. *Journal of Aerosol Science, 34*, 1445–1463.

Wells, A. J. (1999). Deaths in the United States from passive smoking; ten-year update. *Environment International, 25*, 515–519.

WHO (World Health Organization). (2003). *Health aspects of air pollution with particulate matter, ozone and nitrogen dioxide*. http://www.euro.who.int/document/e79097.

WHO (World Health Organization). (2014). *Burden of disease from air pollution*. http://www.who.int/phe/health_topics/outdoorair/databases/FINAL_HAP_AAP_ BoD_24March2014.pdf, 02.02.16.

Wu, J., Lu, J., Min, X., & Zhang, Z. (2018). Distribution and health risks of aerosol black carbon in a representative city of the Qingha, Tibet plateau. *Environmental Science and Pollution Research, 25*(20), 19403–19412.

Xu, L., Zhang, J., Sun, X., Xu, S., Shan, M., & Yuan, Q. (2020). Variation in concentration and sources of black carbon in a megacity of China during the COVID-19 pandemic. *Geophysical Research Letters*, 47-2020GL090444. https://doi.org/10.1029/2020GL090444

Yao, Y., Pan, J. H., Liu, Z. X., Meng, X., Wang, W., Kan, H., & Wang, W. (2020). Temporal association between particulate matter pollution and case fatality rate of COVID-19 in Wuhan. *Environmental Research, 189*, 109941.

Zhang, R. Y., Li, Y. X., Zhang, A. L., Wang, Y., & Molina, M. J. (2020). Identifying airborne transmission as the dominant route for the spread of COVID-19. *Proceedings of the National Academy of Sciences of the United States of America, 117*(26), 202009637.

Zhao, D. L., Liu, D. T., Yu, C. J., Tian, P., Hu, D., Zhou, W., et al. (2020). Vertical evolution of black carbon characteristics and heating rate during a haze event in Beijing Winter. *Science of the Total Environment, 709*, 136251.

Zhu, Y. J., Xie, J. G., Huang, F. M., & Cao, L. Q. (2020). Association between short-term exposure to air pollution and COVID-19 infection: Evidence from China. *The Science of the Total Environment, 727*, 138704.

Source and Risk Assessment of Polychlorinated Biphenyls (PCBs) in Ambient Air and Its Human Health Implications

Thamaraikannan Mohankumar, Jawahar Salavath, Panjakumar Karunamoorthy, Dhananjayan Venugopal, Jayanthi Palaniyappan, Elango Duraisamy, and Ravichandran Beerappa

1 Introduction

Polychlorinated biphenyls (PCBs) include a group of synthetic aromatic chemical mixtures containing 2 benzene rings, connected to each other with varying numbers (1–10) of chlorine atoms, and are structurally related as 209 different compounds named 'congeners.' The structure and basic chemical formula for PCBs are given in Fig. 1. These compounds have been commercially used since 1929. Initially, it was used for a wide range of industrial applications as it served as an excellent heat exchange and electrical insulator liquid and for its flame-retardant properties. Later, its industrial applications widened at large as it was used in the manufacture of almost all commercial products such as plastics, adhesives, print materials, paints, electrical gadgets, etc., Recent studies across the globe have reported the presence of PCBs in ambient air and other environmental matrices (Sari et al., 2023; Dreyers & Minkos, 2023; Sau, 2023) Until 1960, it was widely used for such industrial applications across the world, till its toxic effects was observed in wildlife of Sweden (Ross, 2004). Further to this, PCBs were banned for use in 1979 by USEPA and are referred to as toxic contaminants in the environment and listed as one of the

T. Mohankumar
Industrial Hygiene & Toxicology Division, ICMR-Regional Occupational Health Centre (S), Bangalore, India

Department of Environmental Science, Periyar University, Salem, Tamil Nadu, India

J. Salavath · P. Karunamoorthy · D. Venugopal (✉) · R. Beerappa
Industrial Hygiene & Toxicology Division, ICMR-Regional Occupational Health Centre (S), Bangalore, India

J. Palaniyappan · E. Duraisamy
Department of Environmental Science, Periyar University, Salem, Tamil Nadu, India

Fig. 1 Structure and basic chemical formula for PCBs
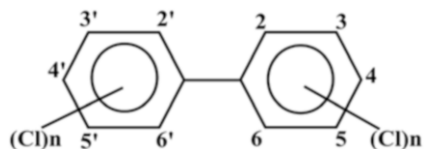
12 POPs in the Stockholm convention in 1972 and were prohibited for use between the 1980s and 1990s across the world.

Out of the existing 209 PCB congeners, almost 130 congeners are widely used for industrial applications and are released into the environment. Parmar and Qureshi (2023) reported that in India, industrial emissions are becoming important sources of PCBs and may become predominant in the coming years. The residues of these congeners were detected across various environmental matrices (Goel et al., 2016). PCBs have a high tendency to transport across wide regions through atmospheric air and accumulate and biomagnify in various ecosystems (Kumar et al., 2012).

PCBs in the environment gained scientific interest because of their persistence and the potential threats they pose to humans (Othman et al., 2022). Humans exposed to PCBs are reported to cause acute symptoms such as eye irritation, skin rashes, liver damage, immune system alterations, carcinogenic effects, chronic reproductive effects, etc., (Montano et al., 2022). Though PCBs were not produced in India, it has been reported that it is the prominent emitter of PCBs than the other countries such that PCB residues are found to exist in Himalayan regions through atmospheric drift and transport (Kang et al., 2009). Few other studies conducted in India and the Punjab Province of Pakistan indicate the presence of PCBs in ambient air (Syed et al., 2013; Goel et al., 2016). Under this context, the present chapter reviews its sources, its presence in various environmental matrices, exposure through ambient air, and its health implications.

1.1 History of PCB Use

In the year 1865, a new PCB-like chemical was discovered by a German Scientist Doebner as a byproduct of coal tar (Doebner, 1876). On exploring its potential use for industrial applications, it was then synthesized by the US in the year 1881 by Scmitz and Schultz. Due to its chemical structure (Fig. 1), it was commonly termed as chlorinated biphenyl. Its commercial production was started by Swan Chemical Company in the US in the year 1929 (www.epa.gov/pcbs/learn-about-polychlorinated-biphenyls). Further, the US emerged as the sole producer of PCBs commercially known as 'Araclors' which accounts for over 600,000 tons produced between 1930 and 1977. Besides, the European Union was reported to produce around 450,000 tons till 1984. Due to this extensive production, large quantities of PCBs were reported to get released into the environment to the extent that it was

detected in almost all the biotic and abiotic components (Risebrough & Brodine, 1971). In between, during 1960, Rachel Carson's Book, 'The Silent Spring' created an urge across the world to highlight residual remains and toxic effects of DDT and related Hydrocarbons post World War II, during which these compounds were used indiscriminately. Between 1950 and 1960, several concerns were raised across the globe that PCBs imposed a wide range of occupational health hazards on workers at PCB manufacturing units and also posed health risks to the common people who were inadvertently exposed to PCBs through using various types of electrical equipment and gadgets (Markovitz, 2018).

A considerable number of publications emerged highlighting the toxicity of chlorinated hydrocarbons well before the 1940s. Later in 1947, Robert Brown reported Aroclor compounds as 'objectionably toxic' and reported to cause severe dermatitis through occupational exposure (Brown, 1947). Later, a Swedish Chemist named, Sören Jensen determined PCBs as environmental contaminants (Jensen, 1966). Since then, several studies have reported the contaminant levels and its toxic effects in almost all the environmental matrices including biota of all habitats and humans. Concerning the toxic impacts on various compartments, several countries started banning its production and usage. Countries including Japan, Sweden, the USA, UK, etc., banned the production and use of PCBs in the years 1972, 1973, 1976, and 1981, respectively. Despite its ban and regulations and active research conducted over five decades, due to its persistent nature, PCBs still pose a threat to the environment and need a serious review of their existence and toxic effects.

1.2   Stockholm Convention on PCBs

The Stockholm Convention on POPs was convened in Sweden in the year 1972 and the member countries signed a multilateral agreement to stop the production, use, and unintentional release and exposure of 12 chlorinated hydrocarbons, of which the PCBs were a prominent one. The convention was adopted by many countries across the world and a PCB Elimination Network (PEN) was formed and came into force in May 2004. The purpose of Stockholm Convention in relevance to PCBs was to prohibit any new production and use of PCBs. The member nations of the convention are required to completely eliminate the use of PCBs in any form by 2025 and have to ensure sound strategies for PCB waste management by the year 2028 (https://chm.pops.int/Default.aspx?tabid=3016).

The member nations of the convention are bound by the Stockholm Convention legislations through appropriate enactment and have to devote considerable efforts to the stock and use of PCBs in their respective nations. As per the UNEP report, since the year 2000, about 200,000 t/y of PCBs have been eliminated globally, which accounts for 17 5 of the 2028 target (UNEP, 2021). However, the existing issues in the sound management of PCBs even after 30 years of its ban on production

emphasize the dearth need for its priority as an emerging pollutant to overcome its challenges. Despite this, the Stockholm Convention is an internationally proclaimed agreement that strives to eliminate PCBs across the globe.

PCBs have never been made in India but utilized them for industrial purposes. India is a signatory to the Stockholm Convention, which aims to cut down on and eventually get rid of harmful pollutants. The concentrations of polychlorinated biphenyls (PCBs) in air and soil were measured by several research teams from all over the world. Air statistics were available for the majority of regions, especially in Europe and Asia. The mean PCBs in air concentrations (pg/m^3) for background sites in Europe, North America, South America, Central America, Asia, and Australia were 70, 79, 66, 59, and 15, respectively. In comparison to air, soil data had better global coverage and were available from the majority of regions. At background sites, the average soil concentrations of PCB (pg/g dry weight) were 7500, 4300, 1400, 580, 390, and 280 for Europe, North America, South America, Asia, Africa, and Australia, respectively.

2 Sources and Distribution of PCBs

PCBs are widely used in industrial and commercial items, and their improper disposal has severely contaminated the environment. As of today, the following sources can still discharge PCBs into the environment (Othaman et al., 2022): (1) PCB-containing hazardous waste sites with poor maintenance; (2) combustion process of garbage incineration and open burning in landfills; (3) unintentional leaks and spills during chemical transportation; (4) spills or flames caused by PCB-containing capacitors, electrical transformers, or other goods; (5) inappropriate or illegal disposal of PCB wastes in landfills not equipped to manage hazardous waste (Wolska et al., 2014). Polychlorinated biphenyls (PCBs) continue to be a cause for worry due to their toxicity, persistence, long-range transport capabilities, and capacity to bio-accumulate in fatty tissues.

2.1 Industrial Sources of PCBs

Over the years, PCBs have been utilized extensively in several sectors. Both intentionally generated (IP-PCBs) and unintentionally produced (UP-PCBs) sources can release PCBs into the atmosphere. According to Liu et al. (2016), the latter are by-products of industrial processes. According to estimates, the top four sources of airborne PCBs in China are the petrochemical/plastic sector (6%), metallurgical industry (34%), and pigment/painting (34%). E-waste sources dominated (>50%) for typical Aroclor-PCBs (Zhao et al., 2019). They may escape during industrial

operations like smelting and cooking, as well as when coal, wood, crude oil, petrol, and diesel fuel are burned (Dumanoglu et al., 2017). In industrial locations, where PCBs are typically created accidentally, larger levels have been found in the atmosphere (Hu et al., 2014). PCBs in the atmosphere can exist as gaseous or particle phases. Due to their low vapor pressure, they can bond to particles and disperse as tiny particles. A silicone rubber manufacturing facility in Germany was found to be emitting considerable amounts of PCBs as gas, and this facility was recommended to implement mitigation measures (Othman et al., 2022; Hombrecher et al., 2021). Due to the rise in the use of newer chemicals and numerous carcinogens in the industrialized environment and due to economic expansion, the incidence of chronic illness and life diseases increased. Even in areas with no industrial activity and where they have never been used, PCBs in the air can travel great distances (Eckhardt et al., 2007). As a result, they are found everywhere. However, the concentrations may decrease as one gets further away from the emission source (Li et al., 2021).

2.2 Household Sources of PCBs

The regular use of food products such as fish, meats, dairy products, and chicken eggs are the main sources of PCBs that humans consume through diet (Othman et al., 2022). Salmon has recently been discovered to have the highest level of POPs, including PCBs, followed by canned tuna, beef steak, butter, and fried chicken. However, over the past 20 years, a drop in PCB concentration in food was observed, which indicates a gradual decline in dietary exposure. It is also important to note that because different human groups have diverse lifestyles, environments, and dietary patterns, they may have different exposure susceptibilities to PCBs.

Due to the temperature dependence of airborne PCBs' volatilization, this process may cause environmental reservoirs such as rivers, lakes, landfills, or contaminated building materials to release these chemicals into the environment (Zhang et al., 2021). The majority of the freshly revealed non-legacy PCBs are also present in airborne PCBs. Non-legacy PCBs can eventually build up in the bodies of exposed populations and are present in both indoor and outdoor areas. Worldwide air samples have been shown to include non-legacy PCBs, according to numerous studies. The most likely source of these pollutants is volatilization from regularly used paints (Anh et al., 2021). More than 50 non-legacy PCBs were found in household paint pigments in 2010 (Hu & Hornbuckle, 2010). Numerous researches have examined how indoor air quality affects PCB contamination. People spend a lot more time indoors than outside, and levels in indoor air may be many orders of magnitude higher than in outdoor air (Zhang et al., 2021). Numerous researches have examined how indoor air quality affects PCB contamination (Montano et al., 2022).

2.3   Current Status of PCBs Usage

Polychlorinated biphenyls (PCBs), are synthetic organic chemicals that were initially considered as a key industrial breakthrough for a variety of applications like in the production of heat exchangers, electrical machinery, and other components, but were later shown to be very dangerous, prompting calls for a ban or reduction in their use, in many countries have been prohibited due to environmental concerns. PCBs are persistent organic pollutants (POPs) that have been classified as Group 1 carcinogens or cancer-causing compounds by the International Agency for Research on Cancer (IARC).

Polychlorinated biphenyls (PCBs), a class of artificial or man-made organic chemicals that are considered harmful pollutants, will no longer be used in any form by the end of 2025, according to a notification made in this regard on April 6, 2016, by the Environment Ministry of India. The ministry banned PCBs under the Environment Protection Act, 1986. The Ministry of Environment has released the Regulation of Polychlorinated Biphenyls Order, 2016, which prohibits the import and manufacture of dangerous pollutant polychlorinated biphenyls in the country. Even PCB-containing devices will have to be phased out by December 2025. The notification stated, "The use of polychlorinated biphenyls containing equipment will be permitted until the earlier of December 31, 2025, or their certified lifetime, whichever is earlier," provided that they are properly maintained and there is no chance that polychlorinated biphenyls will leak or be released into the environment.

According to US EPA polychlorinated biphenyls (PCBs) come in a variety of toxicities and consistencies, ranging from thin, light-colored liquids to waxy solids that are yellow or black. PCBs were utilized in countless industrial and commercial applications because of their non-flammability, chemical stability, high boiling point, and electrical insulating qualities. PCBs are a member of the large class of synthetic organic compounds known as chlorinated hydrocarbons. PCBs were commercially manufactured in the United States from 1929 until manufactured were banned in 1979 by the Toxic Substances Control Act (TSCA). However, as stated in section 761.3 of Title 40 of the Code of Federal Regulations (CFR), EPA's regulations implementing TSCA for PCBs permit some unintentional production of PCBs to take place in prohibited manufacturing processes. Although PCBs are no longer commercially produced in the United States, they may still be present in items and materials manufactured before the 1979 PCB ban. Among the goods that might include PCBs are: Electrical equipment including voltage regulators and switches; heat transfer and hydraulic equipment; old electrical devices or appliances containing PCB capacitors; plasticizers in paints, plastics, and rubber products; pigments, dyes, and carbonless copy paper; and other industrial applications (US EPA, 2023).

PCBs are reported to occur in almost all matrices, whether natural or artificial. Due to its persistent nature, it tends to remain in the environment for longer periods of time. Its presence in various environmental compartments is attributed to its sources of contamination. Various sources of PCBs which can ultimately find their way to the environment are provided below.

3 Impact of PCBs on Various Ecosystems

3.1 Soil, Sediments, and Water

Numerous research studies have documented the presence of polychlorinated biphenyls (PCBs) in various environmental compartments, including water bodies, aquatic and marine sediments (as indicated by Dhananjayan et al., 2012), as well as in fish populations (Matson et al., 2022). PCBs, known for their persistence and strong affinity for suspended solids as highlighted in the works of Kodavanti and Loganathan (2019) and Storelli et al. (2009)), or even microplastics, tend to endure in aquatic ecosystems for extended periods. Their remarkable resistance to natural processes such as oxidation, reduction, exposure to acids, bases, and extreme temperature conditions is attributed to their hydrophobic nature, high chemical stability, and thermal resilience, as elucidated by Reddy et al. in 2019. Owing to these chemical attributes, persistent organic pollutants, like PCBs, exhibit a propensity to adsorb onto organic matter in the environment, displaying a preference for attaching to organic particles within aquatic environments, which ultimately leads to their deposition in sediments, as noted by Sari et al. in 2023.

Sediments serve as secondary reservoirs for PCBs within aquatic ecosystems, offering a valuable means to evaluate the concentrations and fate of these contaminants in the environment, as observed in the works of Irerhievwie et al. in 2020, Jafarabadi et al. in 2019. The sorption of PCBs onto sediments depends on both the specific properties of the PCB congeners and the characteristics of the sediments themselves, as discussed by Ngoubeyou et al. in 2022. PCB congeners with a higher degree of chlorination exhibit greater sorption capacities to sediments compared to their less chlorinated counterparts, as detailed by Jafarabadi et al. in 2019. Nevertheless, less chlorinated congeners may, at times, be detected in elevated concentrations within sediments due to their potential to be transported away from their primary emission sources, as demonstrated by Gao et al. in 2013 and Ngoubeyou et al. in 2022.

Owing to their distinctive attributes, polychlorinated biphenyls (PCBs) exhibit a strong affinity for soil, where they tend to exhibit remarkable persistence. Moreover, soil serves as a valuable barometer of pollution and environmental issues. The accumulation of PCBs in the soil can lead to potential contamination of vegetables and the food chain, as acknowledged by ATSDR in 2000. The proximity of soil to human habitation may also engender occupational exposure through various pathways, including ingestion, inhalation, and dermal contact, as well as individual exposure through the consumption of contaminated food. Elevated concentrations of these contaminants in soil raise significant health concerns for all exposed organisms. Consequently, a multitude of global studies have been conducted to assess the risks posed by PCBs in soil to both human and environmental well-being, as exemplified by Othman et al. in 2022.

3.2   Fishes, Birds, and Wildlife

Studies carried out since 1980 have revealed a considerable nationwide decline in PCB levels in freshwater fishes. Studies have reported that fishes from 97% of locations had PCB concentrations of 10 ppm or less, according to a 1986–1989 EPA national evaluation, while fishes from 74% of sites had concentrations of 1 ppm or less, according to Kuehl et al. (1994). However, fishes found close to some highly contaminated industrial areas have substantially greater levels of PCBs. Fish can metabolize some PCBs, but those that are not metabolized or eliminated end up in the fatty tissues of the fish. Bioaccumulation of PCBs is the end outcome. So, PCBs may also be ingested by humans who eat specific seafood. For these reasons, some waterways monitor fish for PCB levels. Species intake recommendations have been made by a number of states and federal regulatory organizations, especially for those species that are known to collect a number of toxins, including PCBs, mercury, and other persistent pollutants (Ross, 2004). By investigating the impacts of PCB exposure on an individual basis, it's possible to overlook the toxicological effects of PCBs on the entire ecosystem.

PCBs bioaccumulate in fish muscle, liver, and branchiate at high or low concentrations, with branchiate or liver concentrations being higher due to constant exposure to polluted water and high lipid levels (Klinčić et al., 2020). Effects of PCB bioaccumulation are influenced by the characteristics of the aquatic animals' systems, including their class or species, gender, age, weight, biomass, metabolism, morphology, physiology, longevity, development stage, mobility, type, and level of lipid-rich tissues, position in the food chain, feeding and living habits, body system condition (reproductive system), and health status. Environmental factors like habitat conditions, climate, water quality, source pollution concentration, and temporal weather conditions, as well as PCB characteristics like physicochemical properties, congener type, source, and affinity for lipids, also contribute to its bioaccumulation (Lambiase et al., 2021; Yaghmour et al., 2020; Olanca et al., 2014). The most important factors include lipid content, position in the food chain, level and length of exposure (Storelli et al., 2009). Animals that inhabit waters close to PCBs-using industrial sites are more likely to bioaccumulate congeners in higher quantities (Cui et al., 2018).

PCBs are widely distributed in the natural environment. As a consequence, PCBs get accumulated and biomagnified at the top of the food chain. Since birds are at the top of the aquatic and terrestrial ecosystem, PCBs from the contaminated food sources accumulate in the lipid tissues of birds. Several studies have monitored the PCB congeners in different tissues of birds (Dhananjayan et al., 2011; Dhananjayan 2012; Dhananjayan and Muralidhran 2013). In general, birds are considered good indicators of environmental contaminants and they can provide highly valuable data about the level of contamination in their habitat. The most selected samples for monitoring are feathers, blood, eggs, and tissues (Tong et al., 2022).

A study by Lindsay et al. (2013) compared ponds with and without the addition of turtles and found that turtles dramatically raised pH, conductivity, sediment

accumulation, leaf litter decomposition rates, and increased invertebrate biodiversity. The activities of the turtles accelerated the pond's biogeochemical cycling rates, creating a habitat that attracted more species and boosted biodiversity overall. Due to their mobility, turtles have the potential to transport PCBs from one location to another by swallowing contaminated foods and becoming prey in another area (Zhang et al., 2001). Abiotic, anthropogenic, and ecological interactions affect turtle populations, and persistent POP exposure may contribute to those variables directly or indirectly (Gibbons et al., 2000). Through trophic interactions, turtles can swallow PCBs that subsequently become accessible to embryos through maternal transfer, however, this can also result in higher external intake because PCBs have been found throughout the whole turtle lifespan. Consequently, turtles are an illustration of a creature that can be utilized as a bio-indicator to illustrate significant environmental effects across the ecosystem (Baker & Kjellerup, 2016).

4   Risk Assessment of PCBs in Ambient Air

Several studies have reported the occurrence of PCBs in the air (Othman et al., 2022). The industrialized portion of the waterway may be receiving silt that is PCB-rich from its tributaries, according to detailed homolog profiles.

4.1   *Studies Across the World*

The volatilization of PCB-containing items that are disposed of as trash in landfills is the main cause of PCBs in the atmosphere (Li et al., 2021; Zhu et al., 2022). The widespread usage of PCBs in commercial and manufacturing products as well as their improper disposal have seriously contaminated the environment. PCBs can still leak into the environment today from the sources listed, which are (i) inadequately managed sites for hazardous waste that have PCBs; (ii) improper or illegal dumping of the PCB wastes into landfills not intended for handling toxic waste; (iii) random accidental leaks or spills when the transportation of the hazardous chemical; (iv) fires or leaks from electrical transformers that are capacitors, or other products with PCBs; (v) waste combustion and open burning in landfills (US EPA, 2021). The various studies documented the presence of PCBs in ambient air (Table 1).

PCBs were primarily found in the gas phase and reached their highest concentrations during warm period of time most likely as a result of an increase in evaporation rates. This hypothesis was corroborated by the strong and considerable positive variation in temperature seen for various congeners Barbas et al. (2018). According to the study by Chakraborty et al. (2013), from December 2006 to February 2007 in seven major cities from the northern (New Delhi and Agra), eastern (Kolkata), western (Mumbai and Goa), and southern (Chennai and Bangalore) parts of India, the

Table 1 Total PCBs levels reported in ambient air samples across the world

Country	Total PCBs	Mean or Range (pg m⁻³)	References
Turkey	41	2259.63 ± 647.18	Sari et al. (2023)
Turkey	25	60–120	EkerSanli et al. (2023)
Eastern Siberia	6	41–128	Mamontova and Mamontova (2022)
Indonesia	62	29–220	Sudaryanto et al. (2023)
Turkey	50	945.9 ± 491.6	Sari et al. (2023)
Argentina	38	25	Miglioranza et al. (2021)
Eastern China	18	81 ± 46	Li et al. (2021)
Germany	6	300–1500	Hombrecher et al. (2021)
West Antarctica	19	1.5–29.7	Hao et al. (2019)
China	29	40–537	Xu et al. (2019)
Spain	–	437	Barbas et al. (2018)
India	32	254–432	Goel et al. (2016)
Turkey	35	349–94,363	Aydin et al. (2014)
China	–	7825–76,330	Chen et al. (2014)

atmospheric concentration of PCBs was measured on a daily basis by active air sampling. In the Indian atmosphere, the average concentration of 25 congener PCBs was 4460 pg/m⁻³. In Catalonia, Spain, they used the passive air sampler for the analysis of PCBs in the different seasons with a range of 24.85–27.2 pg/m³concentrations of the PCBs were observed in 2011 spring season (Vilavert et al., 2014). Similarly, Passive sampling was used to investigate the spatial and seasonal patterns of air PCBs in the industrial area of Aliaga; Iron-steel manufacturing, which consists of steel-making and ship-breaking operations, coal and wood burning, and evaporative emissions from technical PCB mixtures were identified as PCB sources. These sources contributed to 12 to 57%of the PCB concentrations in the atmospheric ambient air (Aydin et al., 2014).

Barbas et al. (2018) reported that the amount of PCB-related total toxicity gas and total suspended particulate matter form was greater; also they found the danger of inhalation using the hazardous levels of PCBs in ambient air. Moreover, their findings show that there is minimal cancer risk associated with inhaling PCBs at ambient levels in the study region. Likewise, the study conducted by Goel et al. (2016) low health risk estimates from inhalation within tolerable limits and lower amounts of PCBs than guideline values, indicating a minimal risk to adults from exposure to PCBs present in Kanpur's ambient air. In India, PCBs were never manufactured, and imports were prohibited in 1998 (UNIDO FSP India PCBs, 2009). Surprisingly, the distribution of PCB emissions globally reveals that India emits more PCBs than other nations, which may have an impact on PCB levels in the Himalayas (Kang et al., 2009). Passive air samples taken from urban, rural, and wetland sites along India's coastline (Zhang et al., 2008) revealed concentrations that were greater (216–1077 pg/m³) than those found in other Asian nations (5–340 pg/m³) but equivalent to those found in urban areas in Europe (20–1700 pg/

m^3). Total PCB levels in the air were 34 to 389 pg/m^3, which is substantially lower than the levels reported for India (Syed et al., 2013). It is noted that in both investigations conducted in India and Pakistan (Zhang et al., 2008; Syed et al., 2013), the highest PCBs concentrations were found at urban locations or sites close to urban centers.

PCB compounds in oil used in transformers and capacitors to boost dielectric strength are the most likely cause of this finding. According to Syed et al. (2013), PCBs are in equilibrium or are deposited into the atmosphere in urban and industrial regions of Punjab Province, Pakistan, although soils constitute a possible secondary source of PCBs in agricultural areas. In comparison to schools in rural areas, urban schools along a PCBs contaminated canal of Lake Michigan had much higher PCBs concentrations; in actuality, the concentration was greater in indoor areas. Also, there have been records of substantially lower air PCBs amounts in distant places (Marek et al., 2017). At 16 background sites in the Tibetan Plateau, monitoring of the geographical pattern and temporal trends of PCBs revealed values ranging from 0.10 to 3.90 g/m^3 (Wang et al., 2016).

In Denmark, the health authority considered prolonged exposure to air concentrations between 300 and 3000 ng/m^3 as risky to health and advised taking steps to minimize these. According to the Danish Health and Medicines Authority (2013), concentrations exceeding 3000 ng/m^3 are regarded as posing an elevated health risk, and quick action to reduce concentration is indicated. Meyer et al. (2013) have established that people living in buildings containing high PCB levels in building materials are acquiring the bulk of their overall PCBs burden through exposures in their homes, nearly 40 years after the Danish ban on the use of PCB in construction products. Blood levels for several congeners were 100 times greater than those seen in the reference group (Andersen et al., 2020).

While PCB levels are decreasing in developed regions like the United States and Europe, they are rising in many developing countries like China, South Africa, and India. The increased PCB levels in India cannot be explained by the current PCBs emission inventory. Electronic waste recycling facilities, ship-breaking operations, and open solid waste dumping grounds are some of the local or regional sources of PCB emissions in India. Exposure to atmospheric PCBs, particularly those that resemble dioxin, explains why it's essential to eliminate PCB release sources in India to safeguard both human health and the atmospheric environment (Chakraborty et al., 2013).

Both dietary and non-dietary exposure to PCBs was considered in the calculation of human exposure. The primary route of PCBs exposure, which typically accounts for 25–65% of all exposure, is through diet. Regarding non-dietary exposure, air inhalation makes up a greater share than dust intake and can occasionally approach 60 to 70% (Dai et al., 2016). Not all studies were carried out under precisely the same circumstances. Therefore, certain findings from active sampling and passive sampling may differ. Additionally, various instrument analytical techniques might also affect the outcomes. Therefore, uniform sampling and analytical techniques may help to produce results that are more dependable and comparable.

4.2   Estimation of PCBs in Ambient Air

The determination of the PCBs in the air samples has various methodologies. Figure 2 shows the metodology flowchart of PCBs analysis in ambient air. Polyurethane foam and quartz microfiber filter or glass microfiber filter paper Grade GF/A were used for gas phase and particle sampling, respectively. They were weighed and stored in a controlled temperature and humidity weighing chamber until sampling. PUFs were pre-cleaned by Soxhlet extraction with acetone and diethyl ether for 24 hours, wrapped in aluminum foil, and stored in polyethylene bags at −20 °C until deployment. The PUFs were pre-cleaned with a mixture of solvents and extracted with Soxhlet extraction and ultrasonic extraction method. All the extracted solvents were condensed using rotary evaporator and cleaned with column chromatography techniques. The final extracts were concentrated to 1 ml under a stream of N_2 after being solvent exchanged into hexane. Different studies reported various methods of PCBs analysis in air (Table 2 and Fig. 2).

A total of different mixtures of PCB congeners were identified and quantified using a Gas Chromatography Mass Detector (GC-MSD). A capillary column was used for the separation of PCBs. In constant-flow mode, helium was used as the carrier gas, and the oven temperature was set at varying temperature programs. The temperature of the injector was 2500 C. Every PCB congener's limit of detection (LOD) was calculated by multiplying the average of the blanks. The calculation did not take into account values below the limit of detection.

4.3   Risk Evaluation of PCBs

The presence of PCBs in the environment poses a risk to both human and animal health because they are recognized as probable human carcinogens and endocrine-disrupting compounds (Mwanza et al., 2021). A study carried out by Guzzella et al. (2005) reported total concentration of PCB 101, PCB 118, PCB153, and PCB 138 were about 0.18–2.33 ng/g dry wt in surface sediments from West Bengal's coastal estuary environment in northeast India. The sources of contamination have a direct connection to human activity, including industrial discharge, automotive exhausts, street runoff, slum sewage, and atmospheric transport. According to Huang et al. (2020), food safety issues are posed by international food trade due to the collateral movement of contaminants that are hazardous to human health. Consumption of fish and global trade in fish products exposes people to persistent organic pollutants like the polychlorinated biphenyl (PCB) congener PCB-153. However, there is a lack of knowledge regarding the anticipated daily intake and health risks to people.

Dermal contact, ingestion, and inhalation are the three main ways that people are exposed to PCBs in ambient air. Supplemental Guidance for Dermal Risk Assessment (Part E), Supplemental Guidance for Inhalation Risk Assessment (Part F), and The Human Health Evaluation Manual (Part A) were used to calculate the

Table 2 Various techniques used for analysis of PCBs in ambient air

Country	Extraction Method	Instrument	Column	Recoveries %	References
Russia	Soxhlet	GC-ECD	DB 5 (60 mm × 0.25 mm × 0.2 μm)	34–93	Mamontova and Mamontova (2022)
Denmark	Ultrasonication	GC-MS	DB XLB (30 mm × 0.25 mm × 0.25 μm)	79–95	Andersen et al. (2020)
Spain	Accelerated solvent extraction (ASE)	GC-HRMS	TG-Dioxin (60 mm × 0.25 mm × 0.2 μm)	60–120	Lopez et al. (2021)
China	Soxhlet	GC-MS/MS	CP Sil 8 (50 mm × 0.25 mm × 0.12 μm)	62–76	Zhao et al. (2019)
China	Soxhlet	GC-MS/MS	HP-5MS UI (15 mm × 0.25 mm × 0.25 μm)	92–111	Xu et al. (2019)
Spain	Soxhlet	GC-HRMS	DB 5MS (60 mm × 0.25 mm × 0.25 μm)	79–95	Barbas et al. (2018)
Turkey	Soxhlet	GC-MS	HP 5 MS (30 mm × 0.25 mm × 0.25 μm)	87–94	Cetin et al. (2017)
Turkey	Soxhlet	GC-MS	HP 5 MS (30 mm × 0.25 mm × 0.2 μm)	93–107	Ugranli et al. (2016)
Turkey	Soxhlet	GC-MS	HP 5 MS (30 mm × 0.25 mm × 0.25 μm)	86–93	Aydin et al. (2014)
Spain	Accelerated solvent extraction (ASE)	HRGC-HRMS	GC HP 5890	41–171	Vilvert et al. (2014)
India	Soxhlet	GC-MSD	CP Sil 8 (50 mm × 0.25 mm × 0.25 μm)	69–125	Chakraborty et al. (2013)
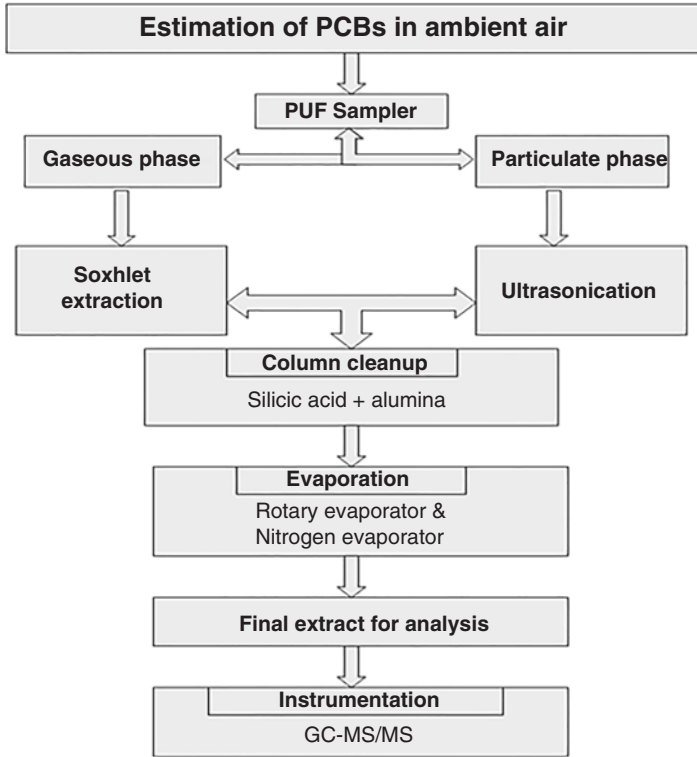
Fig. 2 Flow chart shows ambient air sampling and estimation of PCBs

exposure dose through each of the three pathways. The exposure dose was computed independently for each element and route and expressed as a daily intake. Below are three equations used to identify the pathways, these are chronic daily intake (CDI), concentration exposure to the PCBs (EC), and Dose for dermal absorption (DAD) (USEPA, 2009). Table 3 shows the values and description of each parameter.

$$\text{CDI}(\text{mg} / \text{kg}) = (\text{Cing} \times \text{EF} \times \text{ED} \times \text{IR} \times \text{CF}) / (\text{AT} \times \text{BW}) \tag{1}$$

$$\text{EC}(\mu g / \text{m}^3) = (\text{Cinh} \times \text{EF} \times \text{ED} \times \text{ET}) / \text{ATn} \tag{2}$$

$$\text{DAD}(\text{mg} / \text{kg}) = (\text{Cdermal} \times \text{ED} \times \text{EF} \times \text{CF} \times \text{AF} \times \text{SA} \times \text{ABS}) / (\text{BW} \times \text{AT}) \tag{3}$$

Risk characterization for both carcinogenic and non-carcinogenic risks can be assessed. The hazard quotient (HQ) was used to assess the non-carcinogenic risk of a single pollutant in an exposure route. To evaluate the total potential for non-carcinogenic consequences caused by many chemicals, the hazard index (HI),

which is the sum of HQ, was applied. If the HI is less than 1, the possibility risk of non-carcinogenic consequences is not significant and may occasionally be disregarded. On the other hand, an HI equal to or more than 1 denotes the possibility of non-carcinogenic effects, with a likelihood that tends to rise with increasing HI values (USEPA, 2001). The chance that a person would acquire any sort of cancer as a result of lifetime contact with carcinogenic hazards is known as a carcinogenic risk (CR).

The following equations were used to determine the HQ and Cancer risk posed by PCBs in ambient air by inhalation, ingestion, and dermal contact.

$$HQ = CDI / RFD = DAD / (RFD \times GIABS) = EC / (RFC \times 1000) \tag{4}$$

$$CR = CDI \times SF = DAD \times (SF / GIABS) = IUR \times EC \tag{5}$$

where GIABS stands for gastrointestinal absorption factor, SF stands for oral slope factor $((mg/kg/day)^{-1})$, and IUR stands for inhalation unit risk $(\mu g/m^3)^{-1})$. RFD stands for oral reference dosage (mg/kg/day), whereas RFC stands for inhalation reference concentration (mg/m^3) (USEPA, 2016). The SF, RFD, RFC GIABS, and IUR values for PCBs can be found in the regional screening level (RSL) summary tables given by the USEPA (Table 3). The PCBs concentration detected in biological and environmental studies will be compared with the guideline values prescribed by various statutory agencies for risk analysis (Table 4).

5 Human Health Implications

Numerous epidemiological investigations highlight the environmental and occupational exposure of PCBs at various occupations. The various health impacts were associated with exposure to PCBs (Fig. 3). Varying levels of adverse health outcomes were related to PCBs. The adverse health outcomes such as endocrine malfunctions, neuropsychological and neurobehavioral deficits, reproductive malfunctions, dementia, immune system dysfunctions, cardiovascular diseases, neurotoxicity, and cancer were reported due to PCBs exposure (Simhadri et al., 2020; Raffetti et al., 2017; Pessah et al., 2019; Bräuner et al., 2021; Montano et al., 2022).

5.1 *Neurotoxicity*

Several studies reported that exposure to PCBs increases the risk of neuropsychological disorders such as cognitive impairment, impaired psychomotor, and memory deficits (Pessah et al., 2019), risk of autism spectrum disorders (Panesar et al.,

Table 3 Risk assessment input parameters for PCBs

Parameters	Unit	Value
Concentration of PCBs (C)	pg/m³	PCBs concentration
Average lifetime (AT)	Days	70 years (carcinogens) 30 years (non-carcinogens) (Vilavert et al., 2014)
Average lifetime (ATn)	Hours	70 years × 24 hours (carcinogens) 30 years × 24 hours years (non-carcinogens)
Body weight (BW)	kilogram	70 (Vilavert et al., 2014)
Exposure duration (ED)	Year	30 (Vilavert et al., 2014)
Conversion factor (CF)	mg/day	1/1000000 (USEPA, 2001)
Exposure time (ET)	hours/day	24
Exposure frequency (EF)	days/year	350 (Vilavert et al., 2014)
Ingestion rate (IR)	mg/day	114 (Vilavert et al., 2014)
Inhalation rate (IR)	m³/day	20 (Vilavert et al., 2014)
Surface area (SA)	cm²	4050 (Vilavert et al., 2014)
Skin adherence factor (AF)	mg/ cm²/day	1 (Vilavert et al., 2014)
Absorption factor for dermal (ABS)	–	0.14 (ATSDR, 2023)
GIABS	–	1 (USEPA, 2021)
IUR	µg/m³	1.1E−03 (USEPA, 2009)
Slope factor	(mg/kg/day)⁻¹	3.9E+00 (USEPA, 2009)
Reference dose	mg/kg/day	2.3E−05 (USEPA, 2009)
Reference concentration	mg/m³	1.3E−03 (USEPA, 2009)

Table 4 Standards and guideline values for PCBs in Air

Agency	Standard/Guideline	PCBs concentration in Air (ng/m³)
Environmental Production Agency (US) for health guidelines (EPA, 2017)	Inhalation unit risk	10
Agency for Toxic Substances and Disease Registry for environmental guideline (ATSDR, 2005)	Cancer risk evaluation guide	10
EPA for environmental guidelines, (EPA, 2015)	Regional screening level	28 (low risk) 4.9 (high risk)
National Institute for Occupational Safety and Health, (NIOSH, 2016)	Recommended exposure limit (10 hrs/day, 40 hrs/week)	1000
Occupational Safety and Health Administration (OSHA, 1989)	Permissible exposure limit (8 hrs/day, 40/week)	10,00,000 for PCBs with 42% Chlorinated 5,00,000 for PCBs with 54% Chlorinated
Massachusetts Department of Environmental Production (US), (1990) Health guidelines	Threshold effects exposure limit (TEL) Allowable ambient limit (AAL)	3 (24 hrs) (TEL) 0.5 (annual) (AAL)

Annual guideline concentration (AGC) 2 ng/m³ (Aroclors 1248,1254,1260,1262,1268), 10 ng/m³ (Aroclors 1016,1221,1232,1242) (New work state Department of Environmental Conservation US, 2016)
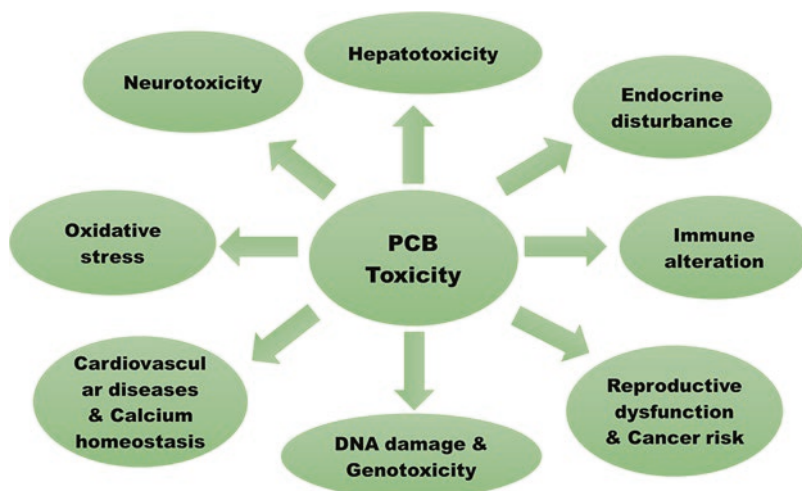
Fig. 3 Health impact of PCBs exposure

2020), and attention deficit hyperactivity disorder in children (De Cock et al., 2012). It was also observed that PCB 11 interferes with brain development (Sethi et al., 2017). An epidemiological study suggested that non-dioxin-like PCBs and low-chlorine PCBs are primarily accountable for neurotoxicity (Klocke et al., 2020). Dementia and Parkinson's diseases were reported among the exposed population in highly polluted cities (Raffetti et al., 2020).

5.2   Immune Suppression

Few epidemiological studies found that PCB exposure was associated with immune suppression and thymic atrophy (Park et al., 2008). The toxicity of PCBs involved in the inhibition of defense antioxidant enzymes such as superoxide dismutase (SOD- catalyzes the dismutation of superoxide anion to H_2O_2,), glutathione S-transferases (GSTs), catalase, glutathione reductase (catalyzes the reduction of glutathione disulfide (GSSG)), and glutathione peroxidase-1 (GPx-1) (Liu et al., 2009).

5.3   Endocrine Disturbance

The endocrine-disrupting nature of PCBs was well documented in various experiential studies including humans (Marushka et al., 2021). Population exposure to PCBs reported alteration in hormone levels, infertility (Patel et al., 2015), earlier onset of menopause, reduced pregnancy rate (Neblett et al., 2020), and altered menstrual

function (Grindler et al., 2015). Bioaccumulation of PCBs in males consequently disrupts the endocrine system, which has been associated with infertility, declined semen quality, and anogenital distance (Stukenborg et al., 2021).

5.4 Reproductive Dysfunctions

High-level exposure to PCBs influences sexual hormones, sperm quantity, sperm abnormalities (motility, morphology, and gametes), and sperm DNA integrity (Paul et al., 2017). A study found a significant correlation between increased serum PCB levels and lower testosterone among the American male population (Goncharov et al., 2009) and testicular cancer (Bräuner et al., 2021). Transfer of PCBs from mother to fetus via the placenta results in transgenerational effects (Mori et al., 2014; Gore et al., 2021). The prenatal exposure to PCBs affects the normal growth of newborns (Lignell et al., 2013), and reduces the intelligence quotient (IQ) (Stewart et al., 2008).

5.5 Hepatotoxic and Carcinogenic Effect

PCBs, furans, and dioxin cause hepato carcinogenesis through various mechanisms, including the development of oxidative stress, an increase in reactive oxygen species (ROS), induced mutations, and epigenomic changes in hepatic cells (Helal et al., 2022). Human biomonitoring cohort studies in capacitor manufacturing workers, exposed to Aroclors mixtures reported abnormal function of gall bladder (Donato et al., 2021). The highest levels of PCB burden were observed in various tissues of patients living adjacent to e-waste dumping sites, indicating a possible association between PCB exposure and the incidence of cancer (Zhao et al., 2009).

A cohort study from Germany found a significant negative association between liver enlargements with increased PCB concentration (Kaifie et al., 2019). A cohort study in the USA associated elevated levels of PCB congeners with liver toxicity among former workers involved in PCB production (Clair et al., 2018). A cohort study by Niehoff et al. (2020) reported highest concentration of PCBs (151, 170, 172,180,177 and 195) congeners in serum was linked to melanoma development and hepatic cancers (Niehoff et al., 2020). PCBs' possible carcinogenicity has been explored in epidemiological investigations. The risk of breast cancer was observed among occupationally exposed workers (Silver et al., 2009). A retrospective study investigated the increased incidence of cancer among capacitor manufacturing workers (Iwasaki et al., 2023).

5.6   Other Dysfunctions

PCB exposure was associated with diabetes (Marushka et al., 2021), cardiovascular diseases mainly hypertension (Raffetti et al., 2017). Some studies have shown PCBs alter the cellular homeostasis of calcium (Pessah et al., 2010). PCBs are associated with various diseases and affect multiple organs i.e. skin, immune system, and liver are also carcinogenic (Lauby-Secretan et al., 2013).

5.7   Genotoxic Effect and Oxidative Stress

Metabolic conversion of the parent PCB to hydroxylated and other metabolic progeny appears to play a dominant role, especially in genotoxicity (Robertson & Ludewig, 2011). Hyperactivation of antioxidant genes (Gsta2, Gsta2, Prdx1, Gfap, Amigo2) was found in response to oxidative stress due to PCB exposure. Astrocytes exposed to PCBs elicit an increase in reactive oxygen species (ROS) (Montano et al., 2021). An in-vitro study using peripheral lymphocytes exposed to PCB congener (PCB 52, PCB 77), showed DNA damage in lymphocytes (Montano et al., 2021).

6   Conclusion

Though PCBs were banned several years before, their occurrence in environmental matrices and their exposure to humans through ambient air is of high concern. The distribution and source of PCB pollution in ambient air across the globe still remain unclear. The occurrence of high PCB levels, notably in urban and industrial areas, might result from extensive PCB use and intensive human activity. Furthermore, PCB exposure in the indoor and outdoor environment may pose a serious health risk for humans through the inhalation of contaminated air or through the ingestion of dust. Under this preview, this review has highlighted several studies that exposed the presence of PCBs in the environment and their toxic health effects. Besides, international treaties and regulations such as the Stockholm Conventions play a crucial role in combating the detrimental effects of PCBs on humans and the environment. Despite of this an integrated approach and management strategies are to be devised internationally to combat the ill effects of PCB pollution.

References

Andersen, H. V., Gunnarsen, L., Knudsen, L. E., & Frederiksen, M. (2020). PCB in air, dust and surface wipes in 73 Danish homes. *International Journal of Hygiene and Environmental Health, 229*, 113429.

Anh, H. Q., Watanabe, I., Minh, T. B., & Takahashi, S. (2021). Unintentionally produced polychlorinated biphenyls in pigments: An updated review on their formation, emission sources, contamination status, and toxic effects. *Science of Total Environment, 755*, 142504.

ATSDR, Agency for Toxic Substances and Disease Registry). (2005). *Public health assessment guidance manual (2005 Update): Appendix F*, http://www.atsdr.cdc.gov/hac/phamanual/appf.html. Accessed 1 Oct 2017.

ATSDR, Agency for Toxic Substances and Disease Registry. (2023). *Exposure dose guidance for soil/sediment dermal absorption*. U.S. Department of Health and Human Services, Public Health Service.

ATSDR. Agency for Toxic Substances and Disease Registry. (2000). *Toxicological profile for polychlorinated biphenyls (update)*. US Department of Health and Human Services.

Aydin, Y. M., Kara, M., Dumanoglu, Y., Odabasi, M., & Elbir, T. (2014). Source apportionment of polycyclic aromatic hydrocarbons (PAHs) and polychlorinated biphenyls (PCBs) in ambient air of an industrial region in Turkey. *Atmospheric Environment, 97*, 271–285.

Baker, J. E., & Kjellerup, B. V. (2016). Toxicological effects of polychlorinated biphenyls (PCBs) on freshwater turtles in the United States. *Chemosphere, 154*, 148–154.

Barbas, B., De la Torre, A., Sanz, P., Navarro, I., Artíñano, B., & Martínez, M. A. (2018). Gas/particle partitioning and particle size distribution of PCDD/Fs and PCBs in urban ambient air. *Science of Total Environment, 624*, 170–179.

Bräuner, E. V., Lim, Y. H., Koch, T., Uldbjerg, C. S., Gregersen, L. S., Pedersen, M. K., Frederiksen, H., Petersen, J. H., Coull, B. A., Andersson, A. M., & Hickey, M. (2021). Endocrine disrupting chemicals and risk of testicular cancer: A systematic review and meta-analysis. *The Journal of Clinical Endocrinology and Metabolism, 106*(12), e4834–e4860.

Brown, R. M. (1947). The Toxicity of the "Arochlors". *Chemist-Analyst, 36*, 33.

Cetin, B., Ozturk, F., Keles, M., & Yurdakul, S. (2017). PAHs and PCBs in an Eastern Mediterranean megacity, Istanbul: Their spatial and temporal distributions, air-soil exchange and toxicological effects. *Environmental Pollution, 220*, 1322–1332.

Chakraborty, P., Zhang, G., Eckhardt, S., Li, J., Breivik, K., Lam, P. K., Tanabe, S., & Jones, K. C. (2013). Atmospheric polychlorinated biphenyls in Indian cities: Levels, emission sources and toxicity equivalents. *Environmental Pollution, 182*, 283–290.

Chen, S. J., Tian, M., Zheng, J., Zhu, Z. C., Luo, Y., Luo, X. J., & Mai, B. X. (2014). Elevated levels of polychlorinated biphenyls in plants, air, and soils at an e-waste site in Southern China and enantio selective biotransformation of chiral PCBs in plants. *Environmental Science & Technology, 48*(7), 3847–3855.

Clair, H. B., Pinkston, C. M., Rai, S. N., Pavuk, M., Dutton, N. D., Brock, G. N., Prough, R. A., Falkner, K. C., McClain, C. J., & Cave, M. C. (2018). Liver disease in a residential cohort with elevated polychlorinated biphenyl exposures. *Toxicological Sciences, 164*(1), 39–49.

Cui, L., Wang, S., Yang, X., Gao, L., Zheng, M., Wang, R., Qiao, L., & Xu, C. (2018). Fatty acids, polychlorinated dibenzo-p-dioxins and dibenzofurans, and dioxin-like polychlorinated biphenyls in paired muscle and skin from fish from the Bohai coast, China: Benefits and risks associated with fish consumption. *Science of Total Environment, 639*, 952–960.

Dai, Q., Min, X., & Weng, M. (2016). A review of polychlorinated biphenyls (PCBs) pollution in indoor air environment. *Journal of the Air & Waste Management Association (1995), 66*(10), 941–950.

Danish Health and Medicines Authority. (2013). *Health risks of PCB in the indoor climate in Denmark*. Copenhagen, Denmark, Located on. https://www.sst.dk/-/media/Udgivelser/2013/Health-risks-of-PCB-in-the-indoor-climate-in-Denmark.ashx?la=da&hash=D6F51261D8EC7EF95D081F23FCE9B03A1FD9F033101

De Cock, M., Maas, Y. G., & Van De Bor, M. (2012). Does perinatal exposure to endocrine disruptors induce autism spectrum and attention deficit hyperactivity disorders? Review. *Acta Paediatrica, 101*(8), 811–818.

Dhananjayan, V. (2012). Organochlorine pesticides and polychlorinated biphenyls in various tissues of waterbirds in Nalabana bird sanctuary, Chilika Lake, Orissa, India. *Bulletin of Environmental Contamination and Toxicology, 89*(1), 197–201.

Dhananjayan, V., & Muralidharan, S. (2013). Levels of polycyclic aromatic hydrocarbons, polychlorinated biphenyls, and organochlorine pesticides in various tissues of white-backed vulture in India. *BioMed Research International, 2013, 190353*, 1–9.

Dhananjayan, V., Muralidharan, S., & Jayanthi, P. (2011). Distribution of persistent organochlorine chemical residues in blood plasma of three species of vultures from India. *Environmental Monitoring and Assessment, 173*(1–4), 803–811.

Dhananjayan, V., Muralidharan, S., & Peter, V. R. (2012). Occurrence and distribution of polycyclic aromatic hydrocarbons in water and sediment collected along the Harbour Line, Mumbai, India. *International Journal of Oceanography, 403615*, 1–7.

Doebner, O. G. (1876). Constitution der Diphenyldisulfosäure und ihrerUmwandlungsprodukte. *Berichte der Deutschen Chemischen Gesellschaft, 9*(1), 129–131.

Donato, F., Moneda, M., Portolani, N., Rossini, A., Molfino, S., Ministrini, S., Contessi, G. B., Pesenti, S., De Palma, G., Gaia, A., & Zanardini, E. (2021). Polychlorinated biphenyls and risk of hepatocellular carcinoma in the population living in a highly polluted area in Italy. *Scientific Reports, 11*(1), 3064.

Dreyer, A., & Minkos, A. (2023). Polychlorinated biphenyls (PCB) and polychlorinated dibenzo-para-dioxins and dibenzofurans (PCDD/F) in ambient air and deposition in the German background. *Environmental Pollution, 316*(1), 120511.

Dumanoglu, Y., Gaga, E. O., Gungormus, E., Sofuoglu, S. C., & Odabasi, M. (2017). Spatial and seasonal variations, sources, air-soil exchange, and carcinogenic risk assessment for PAHs and PCBs in air and soil of Kutahya, Turkey, the province of thermal power plants. *Science of Total Environment, 580*, 920–935.

Eckhardt, S., Breivik, K., Manø, S., & Stohl, A. (2007). Record high peaks in PCB concentrations in the Arctic atmosphere due to long-range transport of biomass burning emissions. *Atmospheric Chemistry and Physics, 7*(17), 4527–4536.

EkerSanli, G., Erkul, S. N., & Tasdemir, Y. (2023). Spatio-temporal variations, fugacity fractions and air-soil exchanges of PCBs in industrial, urban and semi-rural sites. *Polycyclic Aromatic Compounds, 44*, 1–18.

Environmental Protection Agency (US). IRIS toxicological review of polychlorinated biphenyls (PCBS) (Scoping and problem formulation materials), Washington DC, https://cfpub.epa.gov/ncea/iris_drafts/recordisplay.cfm? deid¼309645 (2015, accessed 1 October 2017).

EPA, US Environmental Protection Agency (US). IRIS file for polychlorinated biphenyls (PCBs) CASRN 1336-36-3, https://cfpub.epa.gov/ncea/iris2/chemicalLanding.cfm?substance_nmbr¼4294. Accessed 1 Oct 2017. Environmental Protection Agency, Washington.

Gao, S., Chen, J., Shen, Z., Liu, H., & Chen, Y. (2013). Seasonal and spatial distributions and possible sources of polychlorinated biphenyls in surface sediments of Yangtze Estuary, China. *Chemosphere, 91*(6), 809–816.

Gibbons, J. W., Scott, D. E., Ryan, T. J., Buhlmann, K. A., Tuberville, T. D., Metts, B. S., Greene, J. L., Mills, T., Leiden, Y., Poppy, S., & Winne, C. T. (2000). The Global Decline of Reptiles, Déjà Vu Amphibians: Reptile species are declining on a global scale. Six significant threats to reptile populations are habitat loss and degradation, introduced invasive species, environmental pollution, disease, unsustainable use, and global climate change. *BioScience, 50*(8), 653–666.

Goel, A., Upadhyay, K., & Chakraborty, M. (2016). Investigation of levels in ambient air near sources of Polychlorinated Biphenyls (PCBs) in Kanpur, India, and risk assessment due to inhalation. *Environmental Monitoring and Assessment, 188*, 1–11.

Goncharov, A., Rej, R., Negoita, S., Schymura, M., Santiago-Rivera, A., & Morse, G. (2009). Akwesasne Task Force on the Environment; Carpenter, D.O. Lower serum testosterone

associated with elevated polychlorinated biphenyl concentrations in native American men. *Environmental Health Perspectives, 117*, 1454–1460.

Gore, A. C., Thompson, L. M., Bell, M., & Mennigen, J. A. (2021). Transgenerational effects of polychlorinated biphenyls: 2. Hypothalamic gene expression in rats. *Biology of Reproduction, 105*(3), 690–704.

Grindler, N. M., Allsworth, J. E., Macones, G. A., Kannan, K., Roehl, K. A., & Cooper, A. R. (2015). Persistent organic pollutants and early menopause in US women. *PLoS One, 10*(1), e0116057.

Guzzella, L., Roscioli, C., Vigano, L., Saha, M., Sarkar, S. K., & Bhattacharya, A. (2005). Evaluation of the concentration of HCH, DDT, HCB, PCB and PAH in the sediments along the lower stretch of Hugli estuary, West Bengal, northeast India. *Environment International, 31*(4), 523–534.

Hao, Y., Li, Y., Han, X., Wang, T., Yang, R., Wang, P., Xiao, K., Li, W., Lu, H., Fu, J., & Wang, Y. (2019). Air monitoring of polychlorinated biphenyls, polybrominateddiphenyl ethers and organochlorine pesticides in West Antarctica during 2011–2017: Concentrations, temporal trends and potential sources. *Environmental Pollution, 249*, 381–389.

Helal, M., Ghanem, S., & El-Sikaily, A. (2022). Impact of PCBs, furan and dioxin on hepato-carcinogenesis. In *Persistent Organic Pollutants (POPs)-monitoring, impact and treatment*. IntechOpen.

Hombrecher, K., Quass, U., Leisner, J., & Wichert, M. (2021). Significant release of unintentionally produced non-Aroclor polychlorinated biphenyl (PCB) congeners PCB 47, PCB 51 and PCB 68 from a silicone rubber production site in North Rhine-Westphalia, Germany. *Chemosphere, 285*, 131449.

Hu, D., & Hornbuckle, K. C. (2010). Inadvertent polychlorinated biphenyls in commercial paint pigments. *Environmental Science & Technology, 44*(8), 2822–2827.

Hu, J., Zheng, M., Liu, W., Nie, Z., Li, C., Liu, G., & Xiao, K. (2014). Characterization of polychlorinated dibenzo-p-dioxins and dibenzofurans, dioxin-like polychlorinated biphenyls, and polychlorinated naphthalenes in the environment surrounding secondary copper and aluminum metallurgical facilities in China. *Environmental Pollution, 193*, 6–12.

Huang, T., Ling, Z., Ma, J., Macdonald, R. W., Gao, H., Tao, S., Tian, C., Song, S., Jiang, W., Chen, L., & Chen, K. (2020). Human exposure to polychlorinated biphenyls embodied in global fish trade. *Nature Food, 1*(5), 292–300.

Irerhievwie, G. O., Iwegbue, C. M., Lari, B., Tesi, G. O., Nwajei, G. E., & Martincigh, B. S. (2020). Spatial characteristics, sources, and ecological and human health risks of polychlorinated biphenyls in sediments from some river systems in The Niger Delta, Nigeria. *Marine Pollution Bulletin, 160*, 111605.

Iwasaki, M., Itoh, H., Sawada, N., & Tsugane, S. (2023). Exposure to environmental chemicals and cancer risk: epidemiological evidence from Japanese studies. *Genes and Environment, 45*(1), 10.

Jafarabadi, A. R., Bakhtiari, A. R., Mitra, S., Maisano, M., Cappello, T., & Jadot, C. (2019). First polychlorinated biphenyls (PCBs) monitoring in seawater, surface sediments and marine fish communities of the Persian Gulf: Distribution, levels, congener profile and health risk assessment. *Environmental Pollution, 253*, 78–88.

Jensen, S. (1966). Report of a new chemical hazard. *New Scientist (1971), 32*, 612.

Kaifie, A., Schettgen, T., Gube, M., Ziegler, P., Kraus, T., & Esser, A. (2019). Functional and structural liver abnormalities in former PCB exposed workers–analyses from the HELPcB cohort. *Journal of Toxicology and Environmental Health, Part A, 82*(1), 52–61.

Kang, J. H., Choi, S. D., Park, H., Baek, S. Y., Hong, S., & Chang, Y. S. (2009). Atmospheric deposition of persistent organic pollutants to the East Rongbuk Glacier in the Himalayas. *Science of Total Environment, 408*(1), 57–63.

Klinčić, D., Romanić, S. H., Katalinić, M., Zandona, A., Čadež, T., Sarić, M. M., Šarić, T., & Aćimov, D. (2020). Persistent organic pollutants in tissues of farmed tuna from the Adriatic Sea. *Marine Pollution Bulletin, 158*, 111413.

Klocke, C., Sethi, S., & Lein, P. J. (2020). The developmental neurotoxicity of legacy vs. contemporary polychlorinated biphenyls (PCBs): similarities and differences. *Environmental Science and Pollution Research, 27*, 8885–8896.

Kodavanti, P. R. S., & Loganathan, B. G. (2019). Polychlorinated biphenyls, poly brominated biphenyls, and brominated flame retardants. In R. C. Gupta (Ed.), *Biomarkers in toxicology* (2nd ed., pp. 501–518). Academic Press.

Kuehl, D. W., Haebler, R., & Potter, C. (1994). Colpanar PCB and metal residues in dolphins from the US Atlantic coast including Atlantic bottlenose obtained during the 1987/88 mass mortality. *Chemosphere, 28*(6), 1245–1253.

Kumar, B., Verma, V. K., Singh, S. K., Kumar, S., & Sharma, C. S. (2012). Occurrence of congener specific polychlorinated biphenyls in soils from roadside agricultural fields. *Asian Journal of Plant Sciences, 2*(3), 299.

Lambiase, S., Serpe, F. P., Pilia, M., Fiorito, F., Iaccarino, D., Gallo, P., & Esposito, M. (2021). Polychlorinated organic pollutants (PCDD/Fs and DL-PCBs) in loggerhead (Caretta caretta) and green (Chelonia mydas) turtles from Central-Southern Tyrrhenian Sea. *Chemosphere, 263*, 128226.

Lauby-Secretan, B., Loomis, D., Grosse, Y., El Ghissassi, F., Bouvard, V., Benbrahim-Tallaa, L., Guha, N., Baan, R., Mattock, H., & Straif, K. (2013). Carcinogenicity of polychlorinated biphenyls and polybrominated biphenyls. *The Lancet Oncology, 14*(4), 287–288.

Li, M., Zhou, Y., Wang, G., Zhu, G., Zhou, X., Gong, H., Sun, J., Wang, L., & Liu, J. (2021). Evaluation of atmospheric sources of PCDD/Fs, PCBs and PBDEs around an MSWI plant using active and passive air samplers. *Chemosphere, 274*, 129685.

Lignell, S., Aune, M., Darnerud, P. O., Hanberg, A., Larsson, S. C., & Glynn, A. (2013). Prenatal exposure to polychlorinated biphenyls (PCBs) and poly brominated diphenyl ethers (PBDEs) may influence birth weight among infants in a Swedish cohort with background exposure: A cross-sectional study. *Journal of Environmental Health, 12*, 1–9.

Lindsay, M. K., Zhang, Y., Forstner, M. R., & Hahn, D. (2013). Effects of the freshwater turtle Trachemysscriptaelegans on ecosystem functioning: an approach in experimental ponds. *Amphibia-Reptilia, 34*(1), 75–84.

Liu, N., Rizzi, N., Boveri, L., & Priori, S. G. (2009). Ryanodine receptor and calsequestrin in arrhythmogenesis: What we have learnt from genetic diseases and transgenic mice. *Journal of Molecular and Cellular Cardiology, 46*(2), 149–159.

Liu, G., Zheng, M., Jiang, X., Jin, R., Zhao, Y., & Zhan, J. (2016). Insights into the emission reductions of multiple unintentional persistent organic pollutants from industrial activities. *Chemosphere, 144*, 420–424.

López, A., Coscollà, C., Hernández, C. S., Pardo, O., & Yusà, V. (2021). Dioxins and dioxin-like PCBs in the ambient air of the Valencian Region (Spain): Levels, human exposure, and risk assessment. *Chemosphere, 267*, 128902.

Mamontova, E. A., & Mamontov, A. A. (2022). Air Monitoring of polychlorinated biphenyls and organochlorine pesticides in Eastern Siberia: Levels, temporal trends, and risk assessment. *Atmosphere, 13*(12), 1971.

Marek, R. F., Thorne, P. S., Herkert, N. J., Awad, A. M., & Hornbuckle, K. C. (2017). Airborne PCBs and OH-PCBs inside and outside urban and rural US schools. *Environmental Science & Technology, 51*(14), 7853–7860.

Markowitz, G. (2018). From industrial toxins to worldwide pollutants: A brief history of polychlorinated biphenyls. *Public Health Reports, 133*(6), 721–725.

Marushka, L., Hu, X., Batal, M., Tikhonov, C., Sadik, T., Schwartz, H., Ing, A., Fediuk, K., & Chan, H. M. (2021). The relationship between dietary exposure to persistent organic pollutants from fish consumption and type 2 diabetes among First Nations in Canada. *Canadian Journal of Public Health, 112*(1), 168–182.

Massachusetts Department of Environmental Protection (US). The chemical health effects assessment methodology and the method to derive allowable ambient limits: volume I, Boston. http://www.mass.gov/eea/docs/dep/air/laws/chem-aal.pdf (1990, accessed 6 March 2017).

Matson, P. G., Stevenson, L. M., Efroymson, R. A., Jett, R. T., Jones, M. W., Peterson, M. J., & Mathews, T. J. (2022). Variation in natural attenuation rates of polychlorinated biphenyls (PCBs) in fish from streams and reservoirs in East Tennessee observed over a 35-year period. *Journal of Hazardous Materials, 438*, 129427.

Meyer, H. W., Frederiksen, M., Göen, T., Ebbehøj, N. E., Gunnarsen, L., Brauer, C., Kolarik, B., Müller, J., & Jacobsen, P. (2013). Plasma polychlorinated biphenyls in residents of 91 PCB-contaminated and 108 non-contaminated dwellings—an exposure study. *International Journal of Hygiene and Environmental Health, 216*(6), 755–762.

Miglioranza, K. S., Ondarza, P. M., Costa, P. G., de Azevedo, A., Gonzalez, M., Shimabukuro, V. M., Grondona, S. I., Mitton, F. M., Barra, R. O., Wania, F., & Fillmann, G. (2021). Spatial and temporal distribution of Persistent Organic Pollutants and current use pesticides in the atmosphere of Argentinean Patagonia. *Chemosphere, 266*, 129015.

Montano, L., Donato, F., Bianco, P. M., Lettieri, G., Guglielmino, A., Motta, O., Bonapace, I. M., & Piscopo, M. (2021). Semen quality as a potential susceptibility indicator to SARS-CoV-2 insults in polluted areas. *Environmental Science and Pollution Research, 28*(28), 37031–37040.

Montano, L., Pironti, C., Pinto, G., Ricciardi, M., Buono, A., Brogna, C., Venier, M., Piscopo, M., Amoresano, A., & Motta, O. (2022). Polychlorinated biphenyls (PCBs) in the environment: Occupational and exposure events, effects on human health and fertility. *Toxics, 10*(7), 365.

Mori, C., Nakamura, N., Todaka, E., Fujisaki, T., Matsuno, Y., Nakaoka, H., & Hanazato, M. (2014). Correlation between human maternal–fetal placental transfer and molecular weight of PCB and dioxin congeners/isomers. *Chemosphere, 114*, 262–267.

Mwanza, M. M., Ndunda, E. N., Bosire, G. O., Nyamori, V. O., & Martincigh, B. S. (2021). Advances in sample pretreatment and detection of PCBs in the environment. *Journal of Hazardous Materials, 4*, 100028.

National Institute for Occupational Safety and Health (US). (2016). *CDC – NIOSH pocket guide to chemical hazards – Chlorodiphenyl (54% chlorine)*, https://www.cdc.gov/niosh/npg/npgd0126.html. Accessed 1 Oct 2017.

Neblett, M. F., Curtis, S. W., Gerkowicz, S. A., Spencer, J. B., Terrell, M. L., Jiang, V. S., Marder, M. E., Barr, D. B., Marcus, M., & Smith, A. K. (2020). Examining reproductive health outcomes in females exposed to polychlorinated biphenyl and polybrominated biphenyl. *Scientific Reports, 10*(1), 3314.

Ngoubeyou, P. S. K., Wolkersdorfer, C., Ndibewu, P. P., & Augustyn, W. (2022). Toxicity of polychlorinated biphenyls in aquatic environments – A review. *Aquatic Toxicology, 251*, 106284.

Niehoff, N. M., Zabor, E. C., Satagopan, J., Widell, A., O'Brien, T. R., Zhang, M., Rothman, N., Grimsrud, T. K., Van Den Eeden, S. K., & Engel, L. S. (2020). Prediagnostic serum polychlorinated biphenyl concentrations and primary liver cancer: A case-control study nested within two prospective cohorts. *Environmental Research, 187*, 109690.

Occupational Safety and Health Standards, 29 C.F.R. Sect. 1910.1000 (1989).

Olanca, B., Cakirogullari, G. C., Ucar, Y., Kirisik, D., & Kilic, D. (2014). Polychlorinated dioxins, furans (PCDD/Fs), dioxin-like polychlorinated biphenyls (dl-PCBs) and indicator PCBs (ind-PCBs) in egg and egg products in Turkey. *Chemosphere, 94*, 13–19.

Othman, N., Ismail, Z., Selamat, M. I., Sheikh Abdul Kadir, S. H., & Shibraumalisi, N. A. (2022). A review of Polychlorinated Biphenyls (PCBs) pollution in the air: Where and how much are we exposed to? *International Journal of Environmental Research, 19*(21), 13923.

Panesar, H. K., Kennedy, C. L., KeilStietz, K. P., & Lein, P. J. (2020). Polychlorinated biphenyls (PCBs): Risk factors for autism spectrum disorder? *Toxics, 8*(3), 70.

Park, H. Y., Hertz-Picciotto, I., Petrik, J., Palkovicova, L., Kocan, A., & Trnovec, T. (2008). Prenatal PCB exposure and thymus size at birth in neonates in Eastern Slovakia. *Environmental Health Perspectives, 116*(1), 104–109.

Parmar, J., & Qureshi, A. (2023). Accounting of the use and emissions of Polychlorinated Biphenyl Compounds (PCBs) in India, 1951–2100. *Environmental Science & Technology, 57*(12), 4763–4774.

Patel, S., Zhou, C., Rattan, S., & Flaws, J. A. (2015). Effects of endocrine-disrupting chemicals on the ovary. *Biology of Reproduction, 93*(1), 20–21.

Paul, R., Moltó, J., Ortuño, N., Romero, A., Bezos, C., Aizpurua, J., & Gómez-Torres, M. J. (2017). Relationship between serum dioxin-like polychlorinated biphenyls and post-testicular maturation in human sperm. *Reproductive Toxicology, 73*, 312–321.

Pessah, I. N., Cherednichenko, G., & Lein, P. J. (2010). Minding the calcium store: Ryanodine receptor activation as a convergent mechanism of PCB toxicity. *Pharmacology & Therapeutics, 125*(2), 260–285.

Pessah, I. N., Lein, P. J., Seegal, R. F., & Sagiv, S. K. (2019). Neurotoxicity of polychlorinated biphenyls and related organohalogens. *Acta Neuropathologica, 138*(3), 363–387.

Raffetti, E., Speziani, F., Donato, F., Leonardi, L., Orizio, G., Scarcella, C., Apostoli, P., & Magoni, M. (2017). Temporal trends of polychlorinated biphenyls serum levels in subjects living in a highly polluted area from 2003 to 2015: A follow-up study. *International Journal of Hygiene and Environmental Health, 220*(2), 461–467.

Raffetti, E., Donato, F., De Palma, G., Leonardi, L., Sileo, C., & Magoni, M. (2020). Polychlorinated biphenyls (PCBs) and risk of dementia and Parkinson disease: A population-based cohort study in a North Italian highly polluted area. *Chemosphere, 261*, 127522.

Reddy, A. V. B., Moniruzzaman, M., & Aminabhavi, T. M. (2019). Polychlorinated biphenyls (PCBs) in the environment: Recent updates on sampling, pretreatment, cleanup technologies and their analysis. *Journal of Chemical Engineering, 358*, 1186–1207.

Risebrough, R., & Brodine, V. (1971). More letters in the wind. In S. Novick & D. Cottrell (Eds.), *Our world in peril: An environment review* (pp. 243–255). Fawcett.

Robertson, L. W., & Ludewig, G. (2011). Polychlorinated Biphenyl (PCB) carcinogenicity with special emphasis on airborne PCBs. *Gefahrstoffe, Reinhaltung der Luft= Air quality control/Herausgeber, BIA und KRdLim VDI und DIN, 71*(1–2), 25.

Ross, G. (2004). The public health implications of polychlorinated biphenyls (PCBs) in the environment. *Ecotoxicology and Environmental Safety, 59*(3), 275–291.

Sari, M. F., Esen, F., & Cetin, B. (2023). Concentration levels, spatial variations and exchanges of polychlorinated biphenyls (PCBs) in ambient air, surface water and sediment in Bursa, Türkiye. *Science of Total Environment, 880*, 163224.

Sau, K. (2023). Concentrations of PCDD/Fs and dl-PCBs in ambient air in Hanoi, Vietnam, between 2017 and 2021, and health risk assessments. *Environmental Science and Pollution Research, 30*, 98440–98451.

Sethi, S., Keil, K. P., Chen, H., Hayakawa, K., Li, X., Lin, Y., Lehmler, H. J., Puschner, B., & Lein, P. J. (2017). Detection of 3, 3′-dichlorobiphenyl in human maternal plasma and its effects on axonal and dendritic growth in primary rat neurons. *Toxicological Sciences, 158*(2), 401–411.

Silver, S. R., Whelan, E. A., Deddens, J. A., Steenland, N. K., Hopf, N. B., Waters, M. A., Ruder, A. M., Prince, M. M., Yong, L. C., Hein, M. J., & Ward, E. M. (2009). Occupational exposure to polychlorinated biphenyls and risk of breast cancer. *Environmental Health Perspectives, 117*(2), 276–282.

Simhadri, J. J., Loffredo, C. A., Trnovec, T., Murinova, L. P., Nunlee-Bland, G., Koppe, J. G., Schoeters, G., Jana, S. S., & Ghosh, S. (2020). Biomarkers of metabolic disorders and neurobehavioral diseases in a PCB-exposed population: what we learned and the implications for future research. *Environmental Research, 191*, 110211.

Stewart, P. W., Lonky, E., Reihman, J., Pagano, J., Gump, B. B., & Darvill, T. (2008). The relationship between prenatal PCB exposure and intelligence (IQ) in 9-year-old children. *Environmental Health Perspectives, 116*(10), 1416–1422.

Storelli, M. M., Losada, S., Marcotrigiano, G. O., Roosens, L., Barone, G., Neels, H., & Covaci, A. (2009). Polychlorinated biphenyl and organochlorinepesticide contamination signatures in deep-sea fish from the Mediterranean Sea. *Environmental Research, 109*(7), 851–856.

Stukenborg, J. B., Mitchell, R. T., & Söder, O. (2021). Endocrine disruptors and the male reproductive system. *Best Practice & Research. Clinical Endocrinology & Metabolism, 35*(5), 101567.

Sudaryanto, A., Ilyas, M., Wahyono, I. B., Aviantara, D. S., Takahashi, S., Isobe, T., Tanabe, S., & Kunisue, T. (2023). Spatial distribution of atmospheric polychlorinated biphenyls (PCBs) in Jakarta Great Area using passive air sampler. In *IOP Conference Series: Earth and Environmental Science* (Vol. 1201, No. 1, p. 012029). IOP Publishing.

Syed, J. H., Malik, R. N., Li, J., Zhang, G., & Jones, K. C. (2013). Levels, distribution and air–soil exchange fluxes of polychlorinated biphenyls (PCBs) in the environment of Punjab Province, Pakistan. *Ecotoxicology and Environmental Safety, 97*, 189–195.

Tong, Y., Zhao, X., Li, H., Pei, Y., Ma, P., & You, J. (2022). Using homing pigeons to monitor atmospheric organic pollutants in a city heavily involving in coal mining industry. *Chemosphere, 307*, 135679.

Ugranli, T., Gungormus, E., Kavcar, P., Demircioglu, E., Odabasi, M., Sofuoglu, S. C., Lammel, G., & Sofuoglu, A. (2016). POPs in a major conurbation in Turkey: Ambient air concentrations, seasonal variation, inhalation and dermal exposure, and associated carcinogenic risks. *Environmental Science and Pollution Research, 23*, 22500–22512.

UNEP. *Towards elimination of PCBs*. https://www.unep.org/explore-topics/chemicals-waste/what-we-do/persistent-organic-pollutants/toward-elimination-pcb. Accessed on 21 May 2021.

USEPA. (2001). *Risk assessment guidance for superfund: Volume III-Part A, process for conducting probabilistic risk assessment*; EPA 540-R-02-002; US Environmental Protection Agency: Washington, DC, USA.

USEPA. (2009). *Risk assessment guidance for superfund, Vol. I: human health evaluation manual* (F, supplemental guidance for inhalation risk assessment) EPA/540/R/070/002 Environmental Protection Agency, Washington.

USEPA. (2016). *Regional Screening Levels (RSLs)*. Available online: https://www.epa.gov/risk/regionalscreening-levels-rsls. Accessed on 11 March 2016.

USEPA. *Polychlorinated Biphenyls (PCBs)*. Available online: https://www.epa.gov/pcbs/learn-about-polychlorinatedbiphenyls-pcbs. Accessed on 18 Oct 2021.

USEPA. (2023). *Polychlorinated Biphenyls (PCBs)*. Available online: https://www.epa.gov/pcbs/learn-about-polychlorinated-biphenyls

USEPA, United States Environmental Protection Agency. (2021). *Regional Screening Levels (RSLs)*. United States of America, Washington, DC. Available at: https://www.epa.gov/risk/regional-screening-levels-rsls-generic-tables. Accessed Feb 2022.

Vilavert, L., Nadal, M., Schuhmacher, M., & Domingo, J. L. (2014). Seasonal surveillance of airborne PCDD/Fs, PCBs and PCNs using passive samplers to assess human health risks. *Science of Total Environment, 466*, 733–740.

Wang, X., Ren, J., Gong, P., Wang, C., Xue, Y., Yao, T., & Lohmann, R. (2016). Spatial distribution of the persistent organic pollutants across the Tibetan Plateau and its linkage with the climate systems: A 5-year air monitoring study. *Atmospheric Chemistry and Physics, 16*(11), 6901–6911.

Wolska, L., Mechlińska, A., Rogowska, J., & Namieśnik, J. (2014). Polychlorinated biphenyls (PCBs) in bottom sediments: Identification of sources. *Chemosphere, 111*, 151–156.

Xu, C., Niu, L., Zou, D., Zhu, S., & Liu, W. (2019). Congener-specific composition of polychlorinated biphenyls (PCBs) in soil-air partitioning and the associated health risks. *Science of Total Environment, 684*, 486–495.

Yaghmour, F., Samara, F., & Alam, I. (2020). Analysis of polychlorinated biphenyls, polycyclic aromatic hydrocarbons and organochlorine pesticides in the tissues of green sea turtles, Chelonia mydas,(Linnaeus, 1758) from the eastern coast of The United Arab Emirates. *Marine Pollution Bulletin, 160*, 111574.

Zhang, X., Naidu, A. S., Kelley, J. J., Jewett, S. C., Dasher, D., & Duffy, L. K. (2001). Baseline concentrations of total mercury and methyl mercury in salmon returning via the Bering Sea (1999–2000). *Marine Pollution Bulletin, 42*(10), 993–997.

Zhang, G., Chakraborty, P., Li, J., Sampathkumar, P., Balasubramanian, T., Kathiresan, K., Takahashi, S., Subramanian, A., Tanabe, S., & Jones, K. C. (2008). Passive atmospheric sampling of organochlorine pesticides, polychlorinated biphenyls, and polybrominateddiphenyl

ethers in urban, rural, and wetland sites along the coastal length of India. *Environmental Science & Technology, 42*(22), 8218–8223.

Zhang, D., Saktrakulkla, P., Tuttle, K., Marek, R. F., Lehmler, H. J., Wang, K., Hornbuckle, K. C., & Duffel, M. W. (2021). Detection and quantification of polychlorinated biphenyl sulfates in human serum. *Environmental Science & Technology, 55*(4), 2473–2481.

Zhao, G., Wang, Z., Zhou, H., & Zhao, Q. (2009). Burdens of PBBs, PBDEs, and PCBs in tissues of the cancer patients in the e-waste disassembly sites in Zhejiang, China. *Science of Total Environment, 407*(17), 4831–4837.

Zhao, S., Jones, K. C., Li, J., Sweetman, A. J., Liu, X., Xu, Y., Wang, Y., Lin, T., Mao, S., Li, K., & Tang, J. (2019). Evidence for major contributions of unintentionally produced PCBs in the air of China: Implications for the national source inventory. *Environmental Science & Technology, 54*(4), 2163–2171.

Zhu, M., Yuan, Y., Yin, H., Guo, Z., Wei, X., Qi, X., Li, H., & Dang, Z. (2022). Environmental contamination and human exposure of polychlorinated biphenyls (PCBs) in China: A review. *Science of Total Environment, 805*, 150270.

Air Pollution in the Southern Part of Iraq and Its Health Risks

Nader A. Salman, Maha K. Al-Mishrey, Hamid T. Al-Saad, and Ahmed Rushdi

1 Preface

Environmental pollution can be defined as an unacceptable change in the biological, chemical, or physical characteristics of the air, water, or land that can affect organisms and all life (Briggs, 2003; Spellman, 2017). When humans are exposed to air pollution, it can cause respiratory-related diseases and aggravate the conditions such as asthma and bronchitis (Kampa & Castanas, 2008; Manisalidis et al., 2020). The energy needs of the industries and domestic activities are met by burning fuels, which also emit poisonous wastes leading to air contamination. Sulfur dioxide (SO_2), Nitrogen dioxide (NO_2), volatile organic compounds (VOCs) and particulate matters ($PM_{2.5}$ and PM_{10}) are known to be the major air pollutants in Iraq (Al-Kasser, 2021; Al-Kasser & Alkam, 2018a, b). Degradation of air quality in Iraq cities is mainly due to emissions from vehicles on roads, power plants, and oil fields (Rabee, 2015; Kadhem et al., 2017). In the past few decades or so, there has been a tremendous rise in road transportation, an increase in the number of fuel-consuming vehicles, and the establishment of a large number of industries that have resulted in a drastic increase in the concentration of gaseous and particulate matter in the air (Shehabalden & Azeez, 2017). The increase in population growth and the accompanying increase in industrial development and transportation have a significant

N. A. Salman
Al-Manara College for Medical Sciences, Maysan, Iraq

M. K. Al-Mishrey
Department of Biology, College of Science, University of Basrah, Basra, Iraq

H. T. Al-Saad (✉)
College of Marine Sciences, University of Basrah, Basra, Iraq

A. Rushdi
ETAL, Corvallis, OR, USA

impact on the increased concentrations of pollutants in the surrounding air, which has a negative impact on human and environmental health (Suryati et al., 2019). Besides all the abovementioned human and developmental activities that cause the deterioration of the air quality in Iraq, the burning of solid wastes by uncontrolled methods releases large quantities of pollutants into the atmosphere (Sardar et al., 2013).

2   The Study Area

Air pollution is a significant public concern in southern Iraq, and it is currently the subject of extensive scientific research (e.g., Al-Asadi, 1998; Al-Mayahi, 2005; Al-Imarah et al., 2007; Al-Saad et al., 2010; Garabedian, 2010; Al-Hassen, 2011; Qassim, 2011; Douabul et al., 2013; Sultan et al., 2013; Karmalla et al., 2013; Abdullah & Hussien, 2014; and Al-Hassen, et al., 2015b). This area is rich in petroleum and many industrial and human activities, which are the main sources of gas emissions around it (Fig. 1). These emission sources contaminate the ambient air in Basra. According to the abovementioned studies, Basra has been recorded, in the last two decades, to emit high quantities of harmful gases, causing elevated levels of outdoor air pollution, and to reach the levels of health risk to the public. The previous studies, however, have focused on the gaseous pollutant concentrations and their implications on human health in the study area (Garabedian, 2010; Al-Hassen, 2011; Sultan et al., 2013; Al-Hassen et al., 2015a). Basrah has a hot desert climate, like the rest of the surrounding region, though it receives slightly more precipitation than inland locations due to its location near the coast. During the summer months, from June to August, Basra is consistently one of the hottest cities on the planet, with temperatures regularly exceeding 40 °C (104 °F) and approaching 45 °C (113 °F) in July. In winter, Basra experiences mild weather with average high temperatures around 20 °C (68 °F). On some winter nights, minimum temperatures are below 0 °C (32 °F). High humidity (sometimes exceeding 90%) is common due to the proximity to the marshy area and the Gulf (https://www.worlddata.info/).

Basrah is the main port in the southern part of Iraq; it suffers continuous environmental contamination, including air pollution introduced by dust and suspended particulates (Khattak, 1982). Suspended dust particles transported by wind are a common problem, almost year-round, in this part of the world (Abo Rizq et al., 2008), due to the toxic pollutants they carry, such as petroleum hydrocarbons and trace metals (Al-Mayahi, 2005). Al-Ali et al. (2001) have estimated the quantities of fallen dust in Basrah city in addition to the sources, distribution, and sizes of this dust, as well as its elemental structure.

Fig. 1 A map showing the southern part of Iraq. (Image source: https://www.google.com/url)

3 Sources of Air Pollution

3.1 Industrial Emissions

Industry is one of the largest sources of air pollutants, especially if they depend on fossil fuels, oil, and natural gas as the main source of energy. It releases large amounts of gases and particles that accumulate in the atmosphere, changing the composition of the air and leading to an imbalance of the surrounding ecosystems, which eventually causes harm to living system (Al-Hassen, 2011). According to the United Nations Environment Program (UNEP, 2013) toxic smoke from burning oil wells in southern Iraq and from oil-filled trenches and bomb-ignited fires in Baghdad

is the clearest evidence so far that the current conflict may further damage Iraq's already highly stressed environment.

The anthropogenic sources of gaseous emissions in the city of Basrah have stationary and mobile origins (Al-Hassen, 2011). The stationary sources include major industrial plants such as petrochemical complex, steel and iron plant, oil Refinery, fertilizer factory, gas liquefier plant, Hartha and Najebia thermal power stations, and minor industrial plants such as gas-fueled power stations, asphalt plants, gypsum factories, and gas flames. As well, there are many workshops, bake houses, restaurants, electrical generators, and incinerators. These sources, in total, emit from their smokestacks into the local atmosphere thousands of metric tons of gases every day (Karem et al., 2016). Recently, automobile exhausts have become the predominant mobile source of gaseous emissions, because of the large increase in traffic. Garabedian (2010) estimated that CO and NOx emissions released from automobile exhausts in the city are about 6370 and 956 kg/year, respectively. For example, the air pollution of industrial areas in Southern Iraq (i.e. Khor Al-Zubair industrial area) ranged from 10.11 to 35.63, 100.01 to 400.01, 0.21 to 3.12, 0.92 to 9.59, 1.12 to 5.28, 10.51 to 28.21, 9.21 to 20.52, and 0.11 to 1.25 ppm for CO, CO_2, NO_x, SO_x, H_2S, HCs, CH_4, and HCHO, respectively, whereas O_3 concentrations ranged from 0.01 to 0.24 ppb (Sultan et al., 2013).

3.2 Dust Pollutants

Dust refers to the mixture of airborne tiny particles that settle upon surfaces or are suspended in the air; most of this airborne mixture is organic and inorganic, such as hydrocarbons and trace metals (Ballard, 2001; Morawska & Salthammer, 2006). Particulate matter (PM) is the sum of all solid and liquid particles suspended in air, many of which are hazardous and cause a serious threat due to their quick and uncontrolled spread. Dust is also the carrier of trace metals in the atmosphere, from which they get into the soil. The main sources of trace metals in the atmosphere are fuel combustion and the electric power industry (Krolak, 2001). They can increase due to human activity and because of the dynamic nature of the atmosphere; they can be deposited in areas far from their initial sources. The higher levels of metals such as Cu in the environment are likely due to the leaching of metals from metal pipes that are used for several purposes (Singh & Mosely, 2003). Also, mineral dust, highly weathered and wind-eroded soils, and cultivated soils are the major sources for the concentration increase of trace metals in falling dust (Schutz & Rahn, 1982).

The high concentration of atmospheric dust in Fig. 2 signifies that the air is at a hazardous level. Al-Hassen (2011) pointed out that the amount of dust falling in the city was higher compared to the countryside and found that the amount of dust falling in the city of Basrah was 21.5 g/m^2 in 2009. Trace metals (Fe, Cu, Mn, and Ni) in settling dust were estimated in seven selected locations in Basrah; they were 9312.68 ppm (Fe) in Qurna, 350.17 ppm (Cu) in Al-Ma'aqil, 300.79 ppm (Mn) in Qurna, and 76.31 (Ni) in Al-Ma'aqil, while lower values were 2256.98 ppm (Fe) in

Fig. 2 An image showing the dust storms in southern Iraq. (Image source: https://ichef.bbci.co.uk/news/-1.jpg)

Al-Zubair, 0.25 ppm (Cu) in Safwan, 178.03 ppm (Mn) in Abu Al-Khaseeb, and ND (Ni) in Al-Fao (Garabedian, 2008). Cu, Fe, Mn, and Ni were highly correlated with each other, indicating they were from the same sources.

Hassan et al. (2017) examined the effects of climatic factors on the distribution and prevalence of some trace elements in samples of dust fallout from areas near the oil refinery in the Shaiba area in the province of Basrah. Both chromium (Cr) and lead (Pb) were major in all Shaiba area. Pb, Cr, and cadmium (Cd) contamination might be coming from other areas as well as locally due to its high prevalence in all locations. Nickel (Ni) appears locally polluted due to its high rates at only two sites in the refinery area. The highest amount of dust was recorded in autumn (20.51 g/m^2), followed by winter (15.85 g/m^2), Spring (14.93 g/m^2), and summer (11.15 g/m^2). The Pb concentrations have the highest mean (14.70 mg/m^3) in the winter, whereas Cr (7.91 mg/m^3) in the summer. There was no significant difference in concentration of Cd, Ni, and Pb among seasons, except, Cr.

4 Types of Air Pollutants

4.1 Gaseous Pollutants

The atmosphere is mostly polluted by gaseous emissions from both human and industrial activities, particularly in urban areas (Kampa & Castanas, 2008). The concentration of polluting gases in the air, including CO, CO_2, NO_x, SO_x, O_3, and

others, is closely linked to the surrounding sources of pollutants (Bahino et al., 2018). Recently, automobile exhausts have become the primary source of mobile gaseous emissions due to the significant increase in traffic. Studies conducted over the past decade in the region have indicated high levels of CO, NO_2, SO_2, and HCs concentrations. Al-Asadi et al. (2015) analyzed the concentrations of some air pollutants in Basrah City and found that the concentration of CO was 300 ppm. Al-Mayahi (2005) reported that CO concentrations range from 10 mg/L to 80 mg/L, while Al-Hassen (2011) determined that the average concentration is 27 mg/L. Al-Saad et al. (2010) reported that the SO_2 concentrations range from 10 mg/L to 15 mg/L. The average concentrations of CO_2 and NO_2 were 300 mg/L and 3 mg/L, respectively. Douabul et al. (2013) studied the gaseous pollutants in Basrah and showed that the concentration of CO ranged from 4.0 mg/L to 18.0 mg/L, with a mean concentration of 10.6 mg/L (Table 1). They reported that the concentrations of CO_2 ranged from 230.0 mg/L to 280.0 mg/L (mean = 262.1 mg/L), the SO_2 ranged from 0.4 mg/L to 0.9 mg/L (mean = 0.6 mg/L), and NO_2 ranged from 0.5 mg/L to 1.3 mg/L (mean = 0.9 mg/L). Moreover, the concentration of HCs gases ranged from 0.3 mg/L to 1.3 mg/L (mean = 0.8 mg/L). Al-Hassen et al. (2015a) studied the spatial distribution of the Concentrations of Air Pollutants in Basra Province (Table 1). They reported that the mean concentration of CO was 15.30 ppm, CO_2 was 235.61 ppm, NOx was 1.15 ppm, SO_x was 2.18 ppm, H_2S was 2.19 ppm, HCs was 14.01 ppm, CH_4 was 12.58 ppm and O_3 was 0.08 ppb. Most of these concentrations exceeded the maximum permissible limits for National Emission Standards in Iraq. Also, some of the recorded emission concentrations were higher in ambient air than those reported by Al-Hassen et al. (2015b) and were related to the effect of diffusion and dispersion on the ambient air pollutants.

The results of Karem et al. (2016) for the mean concentrations of gasses emitted from the West Qurna-2 oil field in Basra, showed that the highest concentration of CO, CO_2, NO_x, SO_x, H_2S, CH_4, and HCs) were 27.517, 312.475, 2.655, 3.15, 3.367, 14.597, and 14.060 ppm, respectively; and the lowest concentrations were 18.755, 270.4, 1.042, 2.227, 2.36, 11.765, and 11.240 ppm, respectively. The highest concentration of O_3 gas was 0.1 ppb and the lowest was 0.08 ppb. The values of the seasonal emitted gasses showed that the highest mean of the gasses (CO, CO_2, NO_x, SO_x, H_2S, CH_4, HCs, and O_3) concentrations were recorded in winter (23.946, 307.58, 1.898, 2.921, 3.131, 13.731, 13.508 ppm, and 0.104 ppb, respectively), while the lowest were in summer (22.389, 289.09, 1.49, 2.432, 2.457, 12.468, 12.076 ppm, and 0.084 ppb).

Table 1 Concentrations of some gaseous pollutants (ppm) in Basrah, Southern Iraq

CO	NOx	SOx	References
10.6	0.9	0.6	Douabul et al. (2013)
15.3	1.15	2.18	Al-Hassen et al. (2015a)
300	–	–	Al-Asadi et al. (2015)
10–80	–	–	Al-Mayahi (2005)
–	3.0	10–15	Al-Saad et al. (2010)

More recently, gaseous emissions were seasonally monitored at ten stations of the West Qurna-1 oil field in Basrah by Al-Saad et al. (2019). The results of the regional mean concentrations of the gases in their study showed that the highest concentrations of the gases CO, CO_2, NO_x, SO_x, H_2S, CH_4, and HCs) were 31.70, 390.17, 3.86, 4.28, 4.00, 16.96, and 16.76 ppm, respectively; whereas the lowest concentrations were 15.99, 202.62, 0.94, 2.01, 2.09, 7.32, and 3.29 ppm respectively. The highest mean concentration of O_3 gas was 0.32 ppb and the lowest was 0.01 ppb). The result of the seasonal gas emission showed that the highest mean concentrations of the gases CO, CO_2, NO_x, SO_x, H_2S, CH_4, and HCs were respectively 27.19, 323.06, 2.96, 3.82, 3.45, 14.24, and 13.66 ppm in winter; while the lowest were (21.59, 299.14, 2.58, 3.24, 2.95, 13.43, and 11.83 ppm recorded in summer. The highest seasonal mean concentration of the O_3 gas was 0.16 ppb measured in spring and the lowest was 0.097 ppb in summer (Al-Saad et al., 2019). The seasonal levels of these gasses, except O_3, were as follows: winter > spring > autumn> summer. Al-Sabbagh et al. (2023) showed that hydrocarbon gases were detected in the Basra Province with different concentrations except in Alnajebia and Shatt Al Basra power plants. The highest average of the hydrocarbon concentrations was recorded at Allhais at 995, 598.15, 418.7, 358.89, and 279.13 ppm for methane (CH_4), ethane (C_2H_6), propane (C_3H_8), butane (C_4H_{10}), and pentane (C_5H_{12}), respectively. The lowest average was measured at the Majnoon oil field for CH_4 = 395 ppm, C_2H_6 = 238.8 ppm, C_3H_8 = 167.16 ppm, C_4H_{10} = 142.2 ppm, and C_5H_{12} = 111.4 ppm. The distribution of these hydrocarbons in the air showed positive correlations with the average monthly wind speed.

4.2 Heavy Metals Pollutants

According to Duffus (2002), heavy metals are characterized by high stability with a density greater than 4.5 gm.cm^{-3} and high atomic numbers greater than 24 such as mercury, lead, cadmium, and others. Many of them are necessary for normal development in living systems in small quantities but then become toxic at high concentrations (Jeje & Oladepo, 2014). Similar to PAHs, heavy metal sources in southern Iraq include industrial activities, oil refineries, cement plants, brick industries, tire wear, brake linings, and road construction materials, road traffic, fuel combustion, power plants, and home and public generators (Al-Kasser, 2021).

According to Garabedian (2008), trace metals in falling dust such as Cu, Fe, Mn, and Ni were highly correlated with each other, as estimated in seven selected locations in Basrah. The study of Al-Saad et al. (2010) showed that the atmospheric dust in Basrah was relatively contaminated with trace elements. The trace element contamination in atmospheric dust at Basrah Governorate showed a considerable decrease from places of high activities to low activities (mechanical workshops to residential areas). Automobile and metal construction workshops, as well as construction wastes, could be responsible for the accumulation of trace elements in the atmospheric dust and particulate matter in Basrah. This region's ambient air had a

Table 2 Heavy metal levels in the air of some cities in Southern Iraq

Pb	Cr	Cd	Cu	Ni	Hg	Units	Sites	References
95.2	22.99	0.79	–	43.55	–	µg/m^3	Basrah	Ewaid et al. (2020)
3.19	0.33	0.06	5.25	–	–	µg/m^3	Diwaniyah	Al-Kasser and Alkam (2018a)
4.99	–	2.01	7.73	4.93	1.82	ppm	Maysan	Ajmi et al. (2018)

high content of trace elements, especially Fe and Mn. The atmospheric dust in Basrah is relatively contaminated with trace elements. The studies revealed that trace elements significantly varied among selected stations as well as during different months.

For comparison, the data of Table 2 showed the concentrations of some heavy metals in three different cities in the region. The level of air contamination in Basrah, apparently, is more than that in Maysan and Diwaniyah due to the vast industrial and oil production activities in Basrah. The concentrations of Pb, Cr, and Ni as recorded by Ewaid et al. (2020) in Basrah reached 95, 23, and 44 µg/m^3 respectively. They exceeded values recorded by Al-Kasser and Alkam (2018a) for the same metals in Diwaniyah city (Table 2).

Hassan et al. (2017) examined the impact of climatic factors on the distribution and prevalence of the trace elements Ni, Cd, Pb, and Cr in samples of dust near the oil refinery of the Shaibah area in Basrah and found that the air quality was within the normal ranges. They also noticed that the concentration of trace elements varied with the wind direction and temperature changes during the seasons of the year. Recently, Al-Gizzi et al. (2020) determined four heavy metal concentrations (Pb, Cr, Cd, and Ni) in emissions released from electric generators that used diesel or gasoline fuel in Basrah city, and their concentrations in leaves of six green plant species. Taher et al. (2023a) used the spider webs of Pholcidae to study air pollution, as they could accumulate and retain heavy metals such as Pb, Co, Ni, and Zn. The study found that the highest concentration of heavy metals recorded in all regions was Ni, followed by Zn and Pb, whereas the lowest concentration was Co.

4.3   Total Suspended Particles

Total suspended particulate (TSP) refers to the totality of small solid matter released, documented, and/or otherwise observed in the atmosphere. Total suspended particulates are considered to be a primary contributor to air pollution, smog formation, and environmental contamination. Suspended particles can be emitted from natural and anthropogenic sources, and they range from 0.001 to greater than 100 micrometers in size (Daher, 2013). Air quality tests in Iraq since 2008 have revealed hazardously high levels of fine particulate matter (Abo Rizq et al., 2008; Al-Hassen, 2011; Kssam, 2011). According to Hashim (2012), the average dust deposit in Iraq is about four times and half greater than the allowable limits. The results showed that the annual average of dust deposition during the year 2008 was 32.9 g/m^2/month,

Table 3 Total suspended particles (μg/m³) in the air of some southern Iraqi cities

TSP	City	References
510.2	Maysan	Ajmi et al. (2018)
1807.3	Al-Diwaniyah	Al-Kasser (2018)

whereas the World Health Organization (WHO) recommended less than 9 g/m²/month. Shehabalden and Azeez (2017) showed that air quality index (AQI) values for total suspended particles (TSP) in μg/m³ in Basra were high. As for other cities in the region, the data from Table 3 showed TSP values in Maysan and Al-Diwaniyah to be 510.2 and 1807.3 μg/m³ as recorded by Ajmi et al. (2018) and Al-Kasser (2018), respectively. Regarding the ratio of PM2.5 and PM10 in the total particulate matter (TPM), it has been noted that none of the above reviewed articles have measured such parameters.

4.4 Polycyclic Aromatic Hydrocarbons (PAH)

Polycyclic aromatic hydrocarbons, which originate from pyrolysis or incomplete combustion of fossil fuels and organic materials, are characterized by low vapor pressure and can adsorb suspended particles in the air (Srogi, 2007). The most important sources of their emission to the atmosphere in southern Iraq include oil refineries, power plants, home and public generators, transportation, petrol stations, and brick industry (Hassan et al., 2016; Al-Kasser, 2021). Douabul et al. (2013) and Al-Hassen et al. (2015b) have reported some data regarding the levels of polycyclic aromatic hydrocarbons (PAH) in Basrah city. The recorded levels varied widely between 1.3 and 31.2 ppm within two years, which indicates an ascending trend (Table 4). Taher et al. (2023b) found that the aromatic hydrocarbons PAH levels in the nets of Pholcidea spiders were accumulated from different sources, such as industrial or traffic activities at different locations. They are high-molecular weight compounds and can be effectively measured using spider webs.

5 Air Quality Index (AQI)

The AQI is an index for reporting daily air quality and tells how clean or polluted your air is and what associated health effects might be of concern. The AQI focuses on the health effects an individual may experience within a few hours or days after breathing polluted air. The Environmental Protection Agency (EPA) calculates the AQI for five major air pollutants regulated by the Clean Air Act, ground-level ozone, particle pollution (also known as particulate matter), carbon monoxide, sulfur dioxide, and nitrogen dioxide. For each of these pollutants, the EPA has established national air quality standards to protect public health. Ground-level ozone and

Table 4 Total suspended particles ($\mu g/m^3$) in the air of some southern Iraqi cities

PAH	Units	City	References
1.3	ppm	Basrah	Douabul et al. (2013)
31.2	ppm	Basra	Al-Hassen et al. (2015a, b)
5031.4	ng/m³	Al-Diwaniyah	Al-Kasser and Alkam (2018b)

airborne particles are the two pollutants that pose the greatest danger to human health in Basrah city.

Shehabalden and Azeez (2017) showed high annual and seasonal AQI values, where the winter record indicated the highest values, which were higher than the global limitations but still within the local restrictions. They have postulated that the AQI values for total suspended particles of TSP ($\mu g/m^3$) in Basra were more than 101, which is unhealthy for sensitive people. However, most concentrations of gases (CO, NO_x, and SO_2 in ppm) were within local limitation (AQI < 50) but higher than the world limitation of air pollution quality.

6 Health Hazards

Breathing clean air is one of the most important components of a healthy environment, and clean air is free of pollutants and toxic elements (Youssef et al., 2007). The accumulation of harmful substances in the atmosphere in different concentrations and ratios has negative effects on the environment and living organisms (Al-Hassan, 2014). A recent report by the Department of Health's Committee on the Medical Effects of Air Pollution estimates the number of deaths and hospital admissions due in part to poor air quality. The suggestion that up to 24,000 deaths a year are brought forward by air pollution should act as a spur to encourage creative approaches to air quality problems (Megainey, 1999). The health effects caused by air pollutants may range from subtle biochemical and physiological changes to difficulty breathing, wheezing, coughing, and aggravation of existing respiratory and cardiac conditions (REF). These effects cause increased medication use, doctor or emergency room visits, more hospital admissions, and even premature death. Specifically, health hazards in southern Iraq may be caused by the following sources:

6.1 Gaseous Pollutants

According to WHO (2000), diseases related to gaseous pollutant exposure include respiratory allergies and infections, weakness in lung function, asthma, cardiovascular diseases, nervous system disturbance, and an increase in the incidence of bacterial and viral diseases. Previous studies have indicated that high concentrations of CO, NO_2, SO_2, and HCs within the industrial area in Basra city are constantly

increasing and becoming hazardous to human health. The lack of management and control of the gaseous discharges and residues in urban and industrial areas has increased the possibility that the air quality has become worse (Douabul et al., 2013). Recently, the general quality of ambient air in Basra city has been decreasing because of an increase in the city's population and high traffic levels, as well as the expansion and establishment of several industrial plants, including petrochemical plants, oil refineries, burned natural gas flames, fertilizer plants, paper and pulp mills, power generation stations, and industrial workshops (Al-Saad et al., 2010). These have put the local population in direct daily contact with the different gaseous pollutants that are caused by daily urban activities, mostly by increasing the use of fossil fuel combustion from electrical generators and motor vehicles, as well as exposing the population to industrial activities.

6.2   Particulate Matter

According to Bodor et al. (2023), particulate matter (PM) is one of the most significant air pollutants and is a major environmental health problem. Therefore, long- and short-term exposure via inhalation, ingestion, and dermal absorption of particulate matter may cause a series of health issues, such as cardiopulmonary and lung cancer disease. Suspended particles, due to their toxic organic and inorganic contents, can affect human and environmental health (Tasic et al., 2006). These tiny particles, made up of many elements, including silica, sulfates, and heavy metals such as Pb, Cr, Cu, and Zn have raised greater concern than large particulate matter because these tiny particles can travel deep into the lungs, where they can cause more damage (Abo Rizq et al., 2008; Al-Hassen, 2011; Kssam, 2011). The aerodynamic diameter of PM's is in the range of 0.001 to 500 μm; therefore, PM, including the PM10 (coarse particulate) and PM2.5 (fine particulate), has wide-ranging deleterious effects on human health, especially PM2.5, which can enter via the respiratory system, and the accumulation over time can result in a variety of inflammatory responses (Moran-Zuloaga et al., 2021; Sharma et al., 2019).

The work of Shehabalden and Azeez (2017) contains important information about Basrah province and the pollution risk to the health of people. The health impact of the falling dust does not depend on the quantity, but on the quality of the contents (Al-Saad et al., 2010; Kssam, 2011). Sultan et al. (2013) concluded that the air quality is safe in the Khor Al-Zubair industrial area. Some gaseous pollutant concentrations, however, may be potentially hazardous to public health. Therefore, the need for more rigorous monitoring with repeated measures across seasons and spaces to reduce air pollution is necessary. Karmalla et al. (2013) concluded that about three-quarter of the surveyed areas in Basrah city and their inhabitants may have suffered from carbon monoxide, and this problem perhaps worsens accompanied by the anticipated rise in gaseous emissions released into the urban environment of the area.

6.3   Hydrocarbons

Health hazards associated with total hydrocarbons were mostly related to the proportion of petroleum hydrocarbon gases (PAHs) that were conceded to carcinogenic pollutants. In terms of daily HC intake, the range would normally span from less than 10 ng to more than 100 ng (Chlopek et al., 2016). In general, the average concentrations of HCs among the studied locations were high and fell within the hazard range for human and environmental health (Larsen & Larsen, 1996). Chlopek et al. (2016) have pointed out the health risks of polycyclic aromatic hydrocarbons to humans in terms of their carcinogenicity, ability to induce mutations, and endocrine disruptions, even at relatively low levels.

6.4   Heavy Metals

Heavy metals in the atmosphere can cause humans toxic and carcinogenic effects. They entered the body by inhalation, ingestion of particulate form, or absorption within the skin, leading to renal, neuro-, hepato- and immunotoxicity (Wan et al., 2016). The same authors postulated that they may cause congenital abnormalities, which may affect human behavior, and cause impairment in the functions of the brain and nervous system that may lead to attention impairment and autism disease.

7   Conclusions

The review of air pollution in Southern Iraq concluded that:

1. Gaseous pollutants such as CO, NOx, Sox, and PAH are increasing in the region, especially in Basrah, because of the burning of the accompanied gas from the nearby oil fields and refineries.
2. The other sources of air pollutants are fuel combustion, industry, transportation, and electric power generation stations.
3. There is an increase in the number of suspended particles in the air due to dust suspension by wind and dust storms.
4. An increase in the heavy metals concentration such as Pb, Cr, Cu, Cd, Ni, Co, and Hg results from oil industries and traffic activities.
5. Many pollutants exceeded the national and international standards criteria.
6. Air pollutants may be the cause of many diseases, such as cancer, respiratory, and cardiovascular diseases

References

Abdullah, A. S., & Hussien, H. H. (2014). Estimation of gaseous pollutants emitted from Al-Najybia Power Station in Basra. *Journal of Thi-Qar Science, 4*, 68–71.

Abo Rizq, H., Albaho, M., Christopher, A., & Thomas, B. (2008). Influence of Foliar dust deposition on Ficus Benjamina Variegata stomatal conductance. *European Journal of Scientific Research, 20*(3), 443–451.

Ajmi, R., Zeki, H., Ati, E., & Al-Newani, H. (2018). Monitoring of some heavy metals transboundary air pollution. *Journal of Engineering and Applied Science, 13*(23), 9862–9867.

Al-Ali, J. T. Kh., Hassan, AJ. Ch. And Al-Badran, B. N. A. (2001). Quantities of fallen dust at Basrah Governorate. Marine Mesopotamica, 16(2):261–272.

Al-Asadi, K. A. W. (1998). *The influence of climatic factors on the major industries in Basra and their reflections on the environmental pollution*. Ph.D. Thesis, College of Arts, University of Basra, 197. (In Arabic).

Al-Asadi, K. A., Alwaeli, A. A., & Kazem, H. A. (2015). Assessment of air pollution caused by oil investments in Basra Province-Iraq. *Journal of the National Academy of Sciences, 4*(1), 82–86.

Al-Gizzi, I. A., Al-Hejuje, M. M., & Nema, J. D. (2020). Concentration of some heavy metals emissions from electrical generators in air and green plants in Basrah City, Iraq. *Biological and Applied Environmental Research, 4*(2), 90–101.

Al-Hassan, S. I. (2014). *Introduction to ecology and its problems* (1st ed.). Dar Al Maaref for University Books.

Al-Hassen S. I. (2011). *Environmental pollution in Basra City*, Ph.D. thesis, College of Arts, University of Basra, p. 232.

Al-Hassen, S. I., Al-Qarroni, E. H., Qassim, M. H., Al-Saad, H. T., & Alhello, A. (2015a). An experimental study on the determination of air pollutant concentration released from selected outdoor gaseous, emission sources Basra city, southern Iraq. *Journal of International Academic Research for Multidisciplinary, 3*(1), 88–89. http://www.jiarm.com/FEB2015/paper19552. pdf

Al-Hassen, S. I., Sultan, A., Ateek, A., AL-Saad, H. T., Mahdi, A., & Alhello, A. (2015b). Spatial analysis on the concentrations of air pollutants in Basra Province (Southern Iraq). *Open Journal of Air Pollution, 4*, 139–148.

Al-Imarah, F. J. M., Al-Mohameed, R. S. J., & Ibraheem, S. I. (2007). Extent of atmospheric pollution by some industrial emissions released from petrochemicals and gas liquefier industries in Khor Al-Zubair. *Journal of Kerbala*. Special Issue on the Annual Environment of Meeting of Babylon University, 1–6.

Al-kasser, M. (2018). *Evaluation the level of some toxic pollutants in atmospheric total suspended particles in Al-Diwaniya City – Iraq*. Ph.D. thesis. Faculty ofScience, University of Al-Qadisiyah.

Al-Kasser, M. K. (2021). Air pollution in Iraq sources and effects. *IOP Conference Series: Earth and Environmental Science, 790*, 01201.

Al-Kasser, M., & Alkam, F. (2018a). Spatial and seasonal variation of atmospheric particulate matter heavy metals in Al-Diwaniyah City, Iraq. *Indian Journal of Natural Sciences, 8*(49), 24441–14498.

Al-Kasser, M., & Alkam, F. (2018b). Determination of atmospheric particulate matter polycyclic aromatic hydrocarbons (PAHs) in Al-Diwaniyah City, Iraq. *Advance Research Journal of Multidisciplinary Discoveries, 29*(1), 1–4.

Al-Mayahi, A. K. A. (2005). *Environmental analysis for parameters affecting in the quality of atmospheric pollutants for Basrah Governorate*. M. Sc. Thesis, Department of Geography, College of Education, Basrah University, Basrah Iraq, pp. 241.

Al-Saad, H. T., Al-Imarah, F. J. M., Hassan, W. F., Jasim, A. H., & Hassan, I. F. (2010). Determination of some trace elements in the fallen dust on Basra Governorate. *Basrah Journal of Science, 28*, 243–252. http://www.iasj.net/iasj?func=fulltext&aId=55085

Al-Saad, H. T., Kadhim, H. A., & Al-Hejuje, M. M. (2019). Air pollution assessment at West Qurna −1 oil felid at Basrah Governorate, southern Iraq. *Journal of Scientific and Engineering Research, 6*(7), 1–10.

Al-Sabbagh, M. R., Al-Muhyi, A. H., & Azeez, M. (2023). Methane and hydrocarbon emission rates from oil and gas production in the province of Basra, South of Iraq. In *Ninth national conference on the environment and natural resources (NCENR-2023). IOP Conf. Series: Earth and environmental science 1215* (p. 012019). IOP Publishing. https://doi.org/10.1088/1755-1315/1215/1/012019

Bahino, J., Yoboue, V., Galy-Lacaux, C., Adon, M., Akpo, A., Keita, S., Liousse, C., Gardrat, E., Chiron, C., Ossohou, M., Gnamien, S., & Djossou, J. (2018). A pilot studyof gaseous pollutants' measurement (NO2, SO2, NH3, HNO3 and O3) in Abidjan,Cote d'Ivoire: Contribution to an overview of gaseous pollution in African cities. *Atmospheric Chemistry and Physics, 18*, 5173–5198.

Ballard, M. (2001). *World trade center dust, Its potential to interact with artifacts & works of art*, http://aic.stanford.edu/health/wtc1.html

Bodor, K., Szép, R., Keresztesi, A., & Bodor, Z. (2023). Temporal evolution of PM2.5, PM10, and total suspended particles (TSP) in the Ciuc basin (Transylvania) with specific microclimate condition from 2010 to 2019. *Environmental Monitoring and Assessment, 195*(7), 798. https://doi.org/10.1007/s10661-023-11407-2

Briggs, D. (2003). Environmental pollution and the global burden of disease. *British Medical Bulletin, 68*(1), 1–24.

Chlopek, Z., Suchocka, K., Dudek, M., & Jakubowski, A. (2016). Hazards posed bypolycyclic aromatic hydrocarbons contained in the dusts emitted from motor vehiclebraking systems. *Archives of Environmental Protection, 42*(3), 3–10.

Daher, N. (2013). *Size-resolved Particulate Matter (PM) in urban areas: Toxico-chemical characteristics, sources, trends and health implications*. Ph.D. thesis. Faculty of The USC Graduate School, University of Southern California.

Douabul, A. A., Al-Maarofi, S. S., Al-Saad, H. T., & Al-Hassen, S. I. (2013). Gaseous pollutants in Basra City, Iraq. *Air, Soil and Water Research, 6*, 15–21. https://doi.org/10.4137/ASWR.S10835

Duffus, J. (2002). Heavy metals - a meaningless term. *Pure and Applied Chemistry, 74*(5), 793–807.

Ewaid, S. H., Abed, S. A., Abbas, A. J., & Al-Ansari, N. (2020). Estimation the virtual water content and the virtual water transfer for Iraqi wheat. *Journal of Physics: Conference Series, 1664.*, 1st international virtual conference on pure science 10th–11th June 2020, College of Science, University of Al-Qadisiyah, Iraq. https://doi.org/10.1088/1742-6596/1664/1/012143

Garabedian, S. A. (2008). Levels of some trace metals in falling dust at Basrah Governorate, Southern Iraq. *Marina Mesopotamica, 23*(2), 279–286.

Garabedian, S. A. K. (2010). *Study of the main pollutants of air caused by transportation in Basra*. Proceedings of the scientific conference of marine science center and the national specialized workshop on oceanography, 23–24 December 2008, pp. 125–136. (In Arabic).

Hashim, K. S. (2012). Studying of dust deposits quantity in Babylon Governorate/ Iraq during year 2008. *Journal of Babylon University/Engineering Sciences, 4*(20), 1062–1070.

Hassan, W. F., Hassan, I. F., Al-Khuzaie, D. K., et al. (2016). *Monitoring of air quality in Shaibah in Basra city/Iraq*. The first of international conference on Dust 2–4 March 2016, Shahid Chamran University, Ahvaz, Iran Paper No. 900.

Hassan, W. F., Hassan, I. F., Al-Khuzaie, D. K., Abdulnabi, Z. A., Khalaf, H. H., Kzaal, R. S., & Almansour, W. I. (2017). Monitoring of trace elements in dust fallout in Shaibah, Basrah city, Iraq. *Mesopotamia Environmental Journal, 4*(1), 35–41.

Jeje, J., & Oladepo, K. (2014). Assessment of heavy metals of boreholes and hand dug wells in Ife north local government area of Osun State, Nigeria. *International Journal of Science & Technology, 3*(4), 209–214.

Kadhem, J. A., Reza, K. S., & Ahmed, W. K. (2017). Alternative fuel use in Iraq: A way to reduce air pollution. *European Journal of Engineering and Technology Research, 2*(5), 20–30.

Kampa, M., & Castanas, E. (2008). Human health effects of air pollution. *Environmental Pollution, 151*(2), 362–367.

Karem, D. S., Hamzah, I., Kadhim, A., & Al-Saad, H. T. (2016). Study the air pollution in West Qurna-2 oil field Southern Iraq. *Journal of Pharmaceutical, Chemical and Biological Sciences, 4*(3), 416–430.

Karmalla, H. A., Al-Hassen, S. I., Adam, R. S., & Qassim, M. H. (2013). A cartographic representation to levels and impacts of carbon monoxide pollutant in Basra City, Southern Iraq. *Journal of Thi-Qar Science, 4*, 105–115. (In Arabic).

Khattak, M. N. (1982). Inorganic constituents in Dhahran atmospheric aerosols. *Journal of the Air Pollution Control Association, 32*(2), 176–176.

Królak, E. (2001). Heavy metal content in falling dusts, Soil and dandelion, *EJPAU, 4*(1), 1–12.

Kssam, M. H. (2011). *A geographic analysis for air pollution problem in AL- Zuber City and its healthy effects.* A Master thesis College of Arts University of Basra.

Larsen, J. C., & Larsen, P. B. (1996). Chemical carcinogens. In R. E. Hester & R. M. Harrison (Eds.), *Air pollution and health* (p. 44–52). RSC.

Manisalidis, I., Stavropoulou, E., Stavropoulos, A., & Bezirtzoglou, E. (2020). Environmental and health impacts of air pollution: A review. *Frontiers in Public Health, 8*, 14.

Megainey, C. (1999). Introduction to environmental protection. In W. H. Bassett (Ed.), *Clay's handbook of environmental health* (18th ed., pp. 684–703). E & FN Spon.

Moran-Zuloaga, D., Merchan-Merchan, W., Rodríguez-Caballero, E., Hernick, P., Cáceres, J., & Cornejo, M. H. (2021). Overview and seasonality of PM10 and PM2.5 in Guayaquil. Ecuador. *Aerosol Science and Engineering, 5*(4), 499–515. https://doi.org/10.1007/s41810-021-00117-2

Morawska, L., & Salthammer, T. (Eds.). (2006). *Indoor environment: Airborne particles and settled dust*. Wiley.

Qassim, M. H. (2011). *A geographic analysis for air pollution problem in Al-Zubayr City and its healthy effects*. M.A. Thesis, College of Arts, University of Basra, Basra, 180.

Rabee, A. M. (2015). Estimating the health risks associated with air pollution in Baghdad City, Iraq. *Environmental Monitoring and Assessment, 187*, 1–12.

Sardar, K., Ali, S., Hameed, S., Afzal, S., Fatima, S., Shakoor, M., Bharwana, S., & Tauqeer, H. (2013). Heavy metals contamination and what are the impacts on living organisms. *Greener Journal of Environmental Management and Public Safety, 2*(4), 172–179.

Schutz, L., & Rahn, K. (1982). Trace element concentrations in erodible soils. *Atmospheric Environment, 16*(1), 171–176.

Sharma, R., Kumar, R., Sharma, D. K., Son, L. H., Priyadarshini, I., Pham, B. T., et al. (2019). Inferring air pollution from air quality index by different geographical areas: Case study in India. *Air Quality, Atmosphere and Health, 12*(11), 1347–1357. https://doi.org/10.1007/s11869-019-00749-x

Shehabalden, S. H., & Azeez, N. M. (2017). Air quality index over Basra province, South of Iraq. *International Journal of Technologies: Research & Applications, 5*(2), 112–114.

Singh, & Mosely, L. M. (2003). Trace metal levels in drinking water on viti levui Fiji Islands. *Pacific Journal of Natural and Applied Sciences, 21*, 31–34.

Spellman, F. R. (2017). *The science of environmental pollution* (p. 425). CRC Press.

Srogi, K. (2007). Monitoring of environmental exposure to polycyclic aromatichydrocarbons: A review. *Environmental Chemistry Letters, 5*, 169–195.

Sultan, A. A., Al-Hassen, S. I., Ateeq, A. A., & Al-Saad, H. T. (2013). Ambient air quality in the industrial area of Khor Al-Zubayr, Southern Iraq. *Journal of Petroleum Research & Studies, 4*, 1–11. http://www.iasj.net/iasj?func=fulltext&aId=87876

Suryati, I., Khair, H., & Gusrianti, D. (2019). Distribution analysis of nitrogen dioxide (NO2) and ozone (O₃) in Medan city with Geographic Information System(GIS). *MATEC Web of Conferences, 276*, 6013. https://doi.org/10.1051/matecconf

Taher, H. Z., Azeez, N. M., & Najim, S. A. (2023a). Monitoring of the heavy metals by using pholcidae spider webs in Basrah Province. *The Seybold Report, 18. I0 6*, 1852–1859. https://doi.org/10.17605/OSF.IO/K9ZWS

Taher, H. Z., Azeez, N. M., & Najim, S. A. (2023b). Poly aromatic hydrocarbons accumulated on Pholcidea Spider Webs in Basra Province. Fifth international conference for agricultural and environment sciences. *IOP Conference Series: Earth and Environmental Science, 1158*(2023), 032006. IOP Publishing. https://doi.org/10.1088/1755-1315/1158/3/032006

Tasic, M., Rajsic, S., Novakovic, V., & Mijic, Z. (2006). Atmospheric aerosols and their influence on air quality in urban areas. *Physics, Chemistry and Technology, 4*(1), 83–91.

UNEP. (2013). *Desk study on the environment in Iraq*, First published in Switzerland in 2003 by the United Nations Environment Programme. ISBN 92–1–158628-3. http://www.unep.org

Wan, D., Han, Z., Yang, J., Yang, G., & Liu, X. (2016). Heavy metal pollution in settled dust associated with different urban functional areas in a heavily air-polluted city in North China. *International Journal of Environmental Research and Public Health, 13*, 1–13.

WHO (World Health Organization). (2000). *Air quality guidelines for Europe* (2nd ed.). WHO Regional Publications, European Series, No. 91.

Youssef, R. M., Ismail, K. A., & Bashir, F. (2007). Modeling by simulation to describe the spread of radioactive pollutants. *Journal of Surra Man Ra'a, 3*(8), 153–169.

Optical Characteristics and Radiative Effects of Anthropogenic and Natural Aerosols Over an Urban Area

Ihsan Flayyih Hasan AL-Jawhary

1 Introduction

The ability to forecast potential climatic changes with far-reaching ecological consequences relies on an in-depth examination of atmospheric aerosols, which are comprised of solid and liquid particles suspended in the atmosphere (Chen et al., 2014; Gui et al., 2017). Among the multitude of natural and human-induced factors, atmospheric aerosols arising from biomass burning, mineral dust, volcanic ashes, smoke, sea salt, and particulate matter take precedence. Aerosols play a pivotal role in the Earth's system (Brock et al., 2011), directly impacting global and regional climate changes (Qian et al., 2011; Levy et al., 2013), air quality (Gao et al., 2011), human health (Zhang et al., 2014; Lu et al., 2015; Mukherjee and Agrawal, 2017; Souza et al., 2019), the ecological balance of flora and fauna (Steiner, 1994), both through direct effects and indirect radiation forcing. Additionally, aerosols wield significant influence over cloud processes (Shang et al., 2014) and variations in visibility (Zhang et al., 2017a, b). These aerosols play a substantial role in altering the hydrologic cycle, greenhouse gas concentrations, and the distribution of the greenhouse effect, consequently shaping the physical and chemical processes occurring in the atmosphere.

Aerosol optical thickness (AOT), utilized to gauge the column loading of aerosols, serves as the most comprehensive variable for remotely assessing aerosol loading in the atmosphere. In recent times, it has become common practice to track the geographical and temporal distribution of aerosols, both on a global and local scale, through satellite remote sensing and ground-based data (Che et al., 2015; Filonchyk et al., 2018; Sarkar & Mishra, 2018). Monitoring aerosols at regional and global scales is facilitated by satellite instruments like the Moderate Resolution Imaging

I. F. H. AL-Jawhary (✉)
Department of Biology-College of Education for Pure Sciences, University of Thiqar, Thiqar, Iraq

Spectroradiometer (MODIS), offering extensive and continuous coverage of the study area.

Meteorological variables, including pressure (PRS), average temperature (TEM), relative humidity (RHU), precipitation (PREC), evaporation (EVP), wind speed (WSP), wind direction (WDI), sunshine duration (SSD), and the individual effects of various weather factors on particulate matter (PM) concentrations, are intricately linked with aerosols. Temperature, humidity, wind speed, and precipitation all exert significant influence on PM concentrations (Dawson et al., 2007, 2009; Deng et al., 2012; Jiménez-Guerrero et al., 2012; Yang et al., 2013; Wang & Yang, 2014). Given their central role in atmospheric processes and the substantial level of uncertainty associated with them, aerosols are a focal point of climate research. Aerosol particles scatter, reflect, and absorb incoming solar radiation, both directly (Chylek & Wong, 1995; Solomon et al., 2007) and indirectly (Charlson et al., 1992; Kim et al., 2014), contributing to the considerable uncertainties in contemporary climate prediction (Parry et al., 2007; Istomina et al., 2011; Alexandrov et al., 2016).

Numerous studies have delved into this domain, emphasizing aerosol emissions, optical-physical properties, and their climatic implications (Ramanathan & Ramana, 2005; Ramanathan et al., 2007; Srivastava et al., 2012; Lau, 2014; Soni, 2015; Paliwal et al., 2016), and their impacts on regional hydrology (Matt et al., 2018). These studies have identified an escalation in aerosols over the Himalayan region, particularly during the winter and post-monsoon seasons, attributed to substantial anthropogenic emissions from the combustion of fossil and renewable fuels (Acharya & Sreekesh, 2013). According to Ramanathan and Carmichael (2008), black carbon aerosols in the high Himalayas likely play a significant role in the melting of snow and glaciers through enhanced solar heating. Li et al. (2016) contend that the Himalayan region should be considered highly vulnerable. Owing to their profound influence on hydrological processes and the regional energy balance, affecting billions of people downstream, aerosol deposition and transport over the Himalayas are garnering increasing attention (Nepal et al., 2014).

2   Worldwide Distribution of Aerosols

Anticipated impacts of various aerosol types in specific regions depend on a range of factors. The composition of aerosols worldwide exhibits significant geographic and temporal variations. Advances in remote sensing from both aerial and ground-based platforms, along with in-situ observations, have significantly enhanced our knowledge of aerosol distribution across the globe. However, there remain substantial inquiries regarding the chemical composition of aerosols and the extent of human influence on Aerosol Optical Depth (AOD).

3   Rainfall in Rural Areas and the Effect of Aerosol Optical Depth

Cloud formation and life cycle are significantly influenced by aerosol. Numerous studies have explored anthropogenic aerosols' influence on clouds and their optical features (Gautam et al., 2022). The greatest method for estimating indirect air quality surveillance and management in megacities of developing nations like India, where many cities have elevated concentration levels of air pollutants with insufficient coverage of spatial and temporal monitoring, is using atmospheric remote sensing. One of the most significant water cycle components and factors that significantly affect global water availability is rainfall (Copernicus Climate Change Service (C3S) ERA5, 2017; Kalpana et al., 2020; Gautam et al., 2021a, b, c).

Numerous research (Ramanathan et al., 2001, 2005; Kalpana et al., 2020; Gautam et al., 2021a) revealed the potential influence of aerosol on cloud formation and related cycles. Numerous studies (Ackerman et al., 2000; Ramanathan et al., 2001; Kaufman et al., 2005; Chelani & Gautam, 2021) have shown fluctuations in optical characteristics because of the impact of aerosol produced by anthropogenic activities. The different chemical contents of aerosol are characterized by its anthropogenic and natural sources (Ranjan et al., 2007; Humbal et al., 2018, 2019; Chauhan & Singh, 2020, 2021; Gollakota et al., 2021; Bisht et al., 2021). As a result, it establishes how an aerosol's refractive index changes. Aerosol and monsoon-related issues have been significantly linked to the loading of atmospheric pollutants brought on by modernization and industrialization in the urban and rural atmosphere, particularly in Asian nations like India, China, Pakistan, Bangladesh, etc. (Gautam et al., 2021b; Chelani & Gautam, 2021, 2022).

However, the prolonged monsoon season is likely a factor in how sustainably Asian nations develop and how much freshwater they have available. Through the region's uneven distribution of monsoon rain, Lau et al. (2008) examined the reported significant loss of human life and property due to famine or severe drought. According to some studies, air aerosol might significantly limit seasonal mean solar radiation by 10%, highlighting global cooling effects (Ramanathan et al., 2001; Chung et al., 2005). Many scientists have noticed in recent years that variations in rainfall patterns in the Asian region are caused by aerosol radiative factors (Menon et al., 2002; Meehl et al., 2008). Understanding aerosol behavior and its potential effects on water resources and agriculture requires fundamental research that is gaining attention from both the scientific community and the public. According to the reported literature (Ramasubramanian et al., 1998; Gautam et al., 2021a, b, c), total incremental concentrations of air pollutants were predicted to remain the same in urban and rural Indian regions in the future. The study being presented is a brand-new effort to analyze how aerosol behavior has affected rainfall patterns over the past 7 years (2015–2021) in rural areas of the Indian region using satellite measurements.

Because they have a bearing on climatic forcing, atmospheric aerosols have drawn more and more meteorologists' attention in recent years (Gunaseelan et al.,

2014). The sources of these aerosols come from both natural and anthropogenic activities, which have an impact on the radiation budget of the Earth's atmosphere in two ways: directly by scattering and absorbing solar radiation, and indirectly by changing the microphysical characteristics of clouds to change their radiative properties (IPCC, 2007). The environment, air quality, visibility, and human health are all profoundly influenced by the direct and indirect effects of atmospheric aerosols and suspended particles. Recent years have seen a strong interest in evaluating both natural and human aerosols because of aerosol activities on climate (Ramachandran et al., 2012).

Recent research has demonstrated the importance of aerosols in modifying major climate phenomena like the Indian summer monsoon (Lau & Kim, 2006). The short lives of tropospheric aerosols cause distress on local and seasonal levels because of gravity settling and rain washout. Mineral dust, soot, and water droplets all significantly contaminate aerosols (McCartney, 1976). Over metropolitan regions, the total aerosol loading is significantly higher than in rural areas (Peterson, 1969). We were inspired to investigate the seasonal fluctuations of aerosol and rainfall interaction by the geographical and temporal variability in aerosol features linked to the increase in aerosol emissions over India in the last two decades (Streets et al., 2009).

4   Aerosol's Impact on Solar Radiation

Precipitation is influenced by atmospheric aerosols in three ways: directly, indirectly, and semi-directly (Rosenfeld et al., 2008; Tao et al., 2012; Fan et al., 2016). The scattering and absorption of incoming solar light by air aerosols is referred to as the direct effect (Fig. 1).

This effect lowers the quantity of radiation that can reach the Earth's surface, which cools the surface and affects the stability of the atmosphere (Rosenfeld et al., 2008; Liu et al., 2011; Fan et al., 2016; Chen et al., 2017). As a result, variations in precipitation are caused by altered evaporation processes and circulation patterns. Aerosols alter the microphysical characteristics of clouds, and consequently their radiative characteristics, through a process known as the indirect effect. Two distinct indirect effects exist. The first indirect effect is the decrease in cloud condensation nuclei (CCN) size brought on by an increase in aerosols while the liquid water content remains constant (Twomey, 1977). These tiny cloud droplets prevent precipitation from falling from shallow, transient clouds. The suppression of precipitation causes an increase in cloud longevity in the second indirect effect, which is a continuation of the first indirect effect. Extreme precipitation is possible due to the lifetime extension of clouds in convective systems (Andreae et al., 2004).

According to the semi-direct effect, absorbing aerosols heat the cloud in which they mix. The cloud coverage decreases because of the subsequent evaporation of the cloud droplets (Huang et al., 2006). As a result, the amount of solar radiation that reaches the atmosphere beneath the clouds (Cook & Highwood, 2004), will rise, raising the temperature there. This causes the atmosphere beneath the aerosol

Aerosol direct effect
Scattering and absorption
of solar radiation

Aerosol indirect effect
Decrease of cloud droplet size, increase of droplet number,
increased scattering of solar radiation, decrease of precipitation

Unperturbed cloud   Cloud with more aerosols
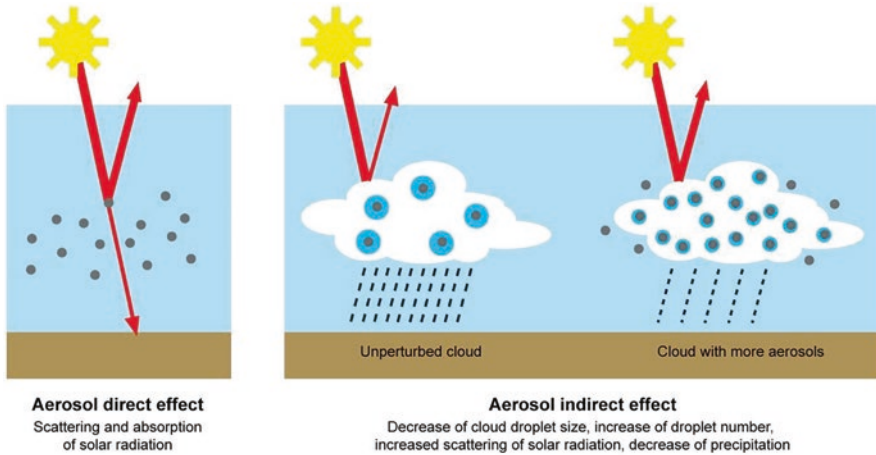
Fig. 1 Direct and indirect effect of aerosol on solar radiation. (https://www.meteoswiss.admin.ch/climate/climate-change/monitoring-the-atmosphere/aerosols-and-climate.html)

plume to become more stable, which may reduce surface evaporation and convection processes. There might be less rain today, though. Due to these considerations, the potential effects of aerosols on precipitation remain highly unknown.

Several earlier investigations investigated the impact of aerosols on precipitation. Based on observational data products, these studies have found either positive or negative relationships between aerosol proxies (such as Aerosol Optical Depth, or AOD) and precipitation intensity (Koren et al., 2012; Cheng et al., 2017). It is crucial to remember that the observed connection does not necessarily indicate causation and that exogenous factors could be to blame. These include the moist deposition of aerosols brought on by precipitation (Grandey et al., 2014; Gryspeerdt et al., 2014), and the hygroscopic development of aerosols brought on by the condensation of water vapor on the particles when the relative humidity (RH) increases (Hänel, 1976; Jones et al., 2010).

RH may influence how aerosols and precipitation interact, according to several studies (Khaan et al., 2005; Fan et al., 2007). Based on satellite-retrieved data, recent research also points to RH as one of the key drivers of the precipitation-AOD relationship (Jones et al., 2010; Altaratz et al., 2013).

In addition to having one of the most complex cloud-precipitation systems in the world with tangled meteorological scales and distinct geographic features, Southeast Asia is known to have significant temporal and geographical variations in AOD (Blake Cohen, 2014). Furthermore, due to the unique monsoonal seasons and changes in the Inter Tropical Convergence Zone, Southeast Asia also features a highly dynamic hydrological system (Zveryaev & Aleksandrova, 2004). A lot of aerosols are released into the atmosphere during the regular widespread biomass-burning episodes that occur in Southeast Asia (Taylor, 2010; Miettinen et al., 2013). Then, these aerosols are dispersed over the area, resulting in transboundary smoky haze. To understand if these aerosols influence precipitation across this area, however, is crucial.

5 Effect of Aerosol on Climate Change

According to Putaud et al. (2010), atmospheric aerosols are suspensions of liquid, solid, or mixed particles that have a highly varied chemical composition and size distribution. Their diversity is brought on by the variety of sources and production procedures (Fig. 2).

Primary aerosols are released directly into the atmosphere, while secondary aerosols are created in the atmosphere from precursor gases. Organic and inorganic components both makeup primary aerosols. Inorganic primary aerosols come from volcanic eruptions, mineral dust, and sea spray, and they are typically rather massive (greater than 1 m). The atmospheric lifespan of these coarse particles is typically barely a few days. Carbonaceous aerosols, which include both organic carbon (OC) and solid black carbon (BC), are produced through combustion processes, biomass burning, and the use of plant and microbial components. Aerosols' primary anthropogenic light-absorbing component is BC. Its primary sources are the burning of biomass, including wood, and fossil fuels like coal, oil, and gasoline. Aerosols with primary BC and OC content are typically smaller than 1 m.

By condensation of vapors on already-existing particles or by nucleation of new particles, secondary aerosol particles are created in the atmosphere from precursor gases. Cloud processing produces a sizable portion of the mass of secondary aerosols (Ervens et al., 2011). Secondary aerosols are tiny particles with lives of a few days to a few weeks. Their sizes range from a few nanometers to 1 m. Sulfate, nitrate, and ^{O}C are the three primary chemicals that make up secondary aerosols.
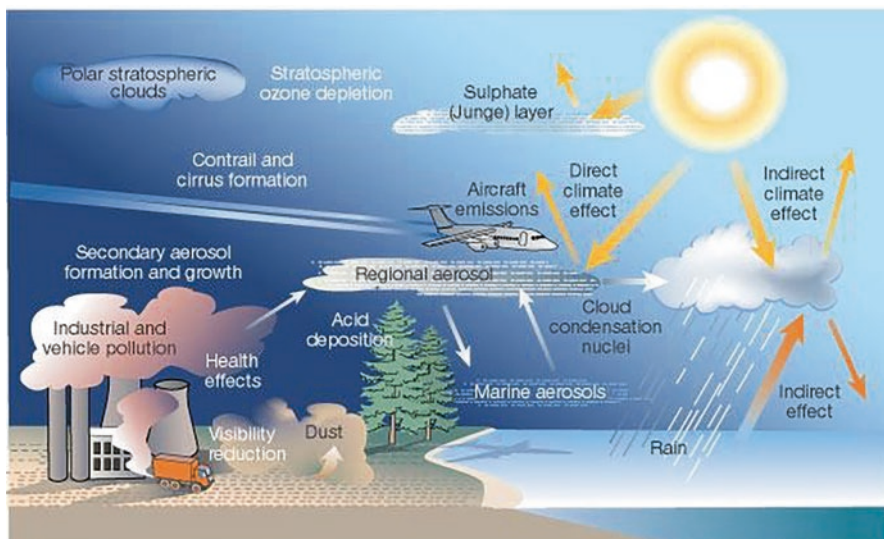
Fig. 2 Direct and indirect effects of aerosol on climate change. (https://www.iasparliament.com/current-affairs/aerosols)

The primary precursor gases are released through the burning of fossil fuels, but fires and biogenic volatile organic compound (VOC) emissions are also significant. Rarely, both at the surface and in the stratosphere, volcanic eruptions produce enormous quantities of primary and secondary aerosols (Boulon et al., 2011). Through coagulation, condensation, and chemical reactions, the size and chemical makeup of the particles change over time. The ability of particles to absorb water and grow depends on their chemical makeup, size, and surrounding relative humidity. Depending on their makeup, various particles have varied effects on the atmosphere, and it is difficult to quantify these effects because of the enormous variety of sources and size distributions. The climatic impact of aerosols is influenced by both particle growth and the mixing of various particle kinds.

Aerosols are microscopic floaters in the atmosphere. Both natural occurrences and human activity emit them. While some aerosols have a cooling effect, others warm the temperature. Image sources (Kirk, 2023). Various varieties of aerosol exist. Natural ones include things like volcanic gases, wildfire smoke, and salty sea spray. Aerosols produced by human activity can include soot or air pollution particles. Aerosols play a complicated function in climate science. Light-colored airborne particles will typically reflect incoming sunlight and result in cooling. Dark-colored particles absorb solar radiation, warming the atmosphere. Aerosols are a prominent topic in climate research because various particle kinds have various effects.

The layer of the atmosphere that starts at about 33,000 feet (10,000 meters) aloft is known as the stratosphere, and it is here that explosive volcanic eruptions can inject gases all the way up. Depending on how large and how high the plume is, sulfur dioxide gas emitted by volcanoes reacts with atmospheric water to generate small particles that can travel around the world and remain in the atmosphere for several years. These clear sulfate aerosols cool the atmosphere while blocking incoming light. A more recent example is the massive eruption of Mount Pinatubo in 1991. The eruption's sulfates caused the atmosphere to decrease by 0.7–0.9 °F (0.4–0.5 °C), making 1992 and 1993 the 35 years's two coldest years.

Sulfate particles and sulfur dioxide (SO_2) are released when fossil fuels are burned, and like volcanic aerosols, they can reflect sunlight and cool the atmosphere. Air pollution only lasts for 3–5 days since it does not reach as high in the atmosphere as volcanic aerosols do. However, since these aerosols are continuously created, they are always present. In an ironic turn of climate science, air pollution brought on by the combustion of fossil fuels slightly cools the Earth in contrast to the warming brought on by greenhouse gases. However, neither the environment nor human life benefits from air pollution. Every year, almost eight million people die prematurely due to air pollution brought on by fossil fuels. Inhaling the microscopic particles released during the burning of fossil fuels increases the risk of developing lung cancer, heart disease, respiratory infections, and asthma.

The COVID-19 epidemic illustrated what might occur if people cut back on aerosol pollution. In the spring of 2020, there was a significant decline in the usage of fossil fuels for industrial activities, power use, driving, and air travel. This resulted in cleaner and clearer air, which warmed some areas by up to 0.2–0.5 °F (0.1–0.3 °C).

However, it was also calculated that this decrease in air pollution saved 77,000 lives in China and 11,000 lives in Europe. Additionally, other cities saw bright skies and views for the first time in a long time.

Soot is formed of dark carbon particles produced by burning wood, other plant materials, or fossil fuels. The atmosphere warms as a result of these black particles absorbing sunlight. When soot settles on snow or ice, it accelerates melting because it darkens the surface. This results in more warming. The main causes of soot include wildfires, cooking fires, industrial processes, and diesel engines. The swift cooling of the atmosphere that would result from reducing soot emissions would also improve human health. Researchers are attempting to comprehend the interactions between aerosols and clouds better. Some human-made aerosols can alter the size or duration of water droplets within clouds. Clouds reflect more sunlight as water droplets get smaller. Overall, this causes the environment to cool. Like dust, some aerosols can affect how ice particles form in clouds that are cooler. Keep checking back for updates as the science advances because this is an area of current research.

The Earth would be significantly warmer than it now is if it weren't for aerosol pollution. According to the IPCC's 2021 report, aerosol air pollution has caused the world to be around 0.7 °F (0.4 °C) colder than it otherwise would be. In contrast, the warming caused by greenhouse gas emissions has increased by 2.7 °F (1.5 °C). This is an intriguing situation. It may appear strangely advantageous to combat climate change if air pollution were present. But that doesn't imply that air pollution is necessary to keep the planet a little bit cooler. There will be a steady decline in air pollution aerosols as people and economies switch to energy sources that generate fewer particle pollutants, which could have a short-term warming effect. It's doubtful that there will be much of a temperature increase because these changes will take place gradually over several decades.

6   Controlling the Distribution of Aerosol Particles in Troposphere

To calculate the direct and indirect radiative forcing caused by aerosol particles, global aerosol size distributions of mass, number, and chemical composition are required. The development of an observational network to map global aerosol distributions at the resolution required for climate models is not economically possible due to the short lives of particles in the troposphere and the resulting spatial (vertical and horizontal) and temporal variability. Aerosol characterization and process studies must be conducted in a variety of naturally occurring and anthropogenically disrupted environments that are globally representative due to the regional diversity in aerosol properties and the interactions between the different chemical components. Chemical transport models and estimations of radiative forcing both require natural emissions and the associated background aerosol. This is due to several

factors. First off, a considerable portion of the Earth's overall aerosol load can be attributed to the emissions of natural aerosols and their gaseous precursors (Chin et al., 1996).

Second, the mass and number distribution of the background aerosol can be altered by interactions between human-produced gaseous emissions (Sievering et al., 1995; Chuang et al., 1997) and the background aerosol. Third, the total aerosol dispersion and subsequent radiative effect are not always the sum of the separate background and anthropogenic components since the many aerosol components interact with one another. Fourth, to define radiative forcing, subtract the radiative effect from background aerosols from the radiative effect caused by aerosols. It is impossible to precisely calculate the direct and indirect forcing brought on by anthropogenically originated emissions without knowledge of the background aerosol characteristics.

Is the last chance to halt global warming, or just a grandiose illusion? Ingenious strategies to artificially chill the Earth are being developed by scientists. In a nutshell, here are three concepts. The most popular method involves dispersing microscopic sulfur dioxide droplets into the stratosphere, a layer of the atmosphere between 10 and 50 kilometers (6–30 miles) above the surface of the Earth. They can survive there for roughly a year while reflecting sunlight to chill the planet. The Pinatubo volcanic explosion in the Philippines in 1991 served as a demonstration of the theory. Because of how strong its blast was, it immediately sent 15 million tons of sulfur dioxide into the stratosphere. Over the next 2 years, the eruption caused the planet's temperature to drop by more than 0.5 °C. Additionally, research demonstrates that it is not technically challenging to repeat such an injection of sulfur dioxide into the stratosphere (Fig. 3).

Although it seems impossible, some scientists are looking into ways to chill the Earth by covering significant portions of the ocean with synthetic foam. This procedure is often referred to as "ocean foaming" or "microbubbles." (Tim, 2021) if other scientists have different opinions from Keith's, they can all agree on one thing: we need to reduce greenhouse gas emissions as soon as we can and figure out long-term adaptation strategies. Because it will not be possible to entirely stop global warming even with solar engineering. Oceans cover over 70% of the surface of the Earth. Due to its depth, the water is primarily black, which reflects relatively little light and absorbs a lot of heat. The surface heats up less quickly the lighter it is. The albedo effect is what is meant by this. Additionally, it might be used in the water.

"The idea of microbubbles in the ocean is making a foam to reflect away some portion of incoming solar radiation and to deploy it in strategic locations where you could possibly effectuate certain climate outcomes," Corey Gabriel, a climate scientist from the University of California San Diego, explains. Theoretically, this foam may reflect 10 times as much sunlight as surfaces of black water. This should be able to cool the Earth by 0.5 °C if there is enough foam. Some experts have proposed that specialized ships may be used to stir the foam. Or it might be set up in various oceanic regions by container ships throughout the world.

The method, however, remains largely unexplored and is far from being a viable solution. And the impact that huge amounts of sea foam could have on marine
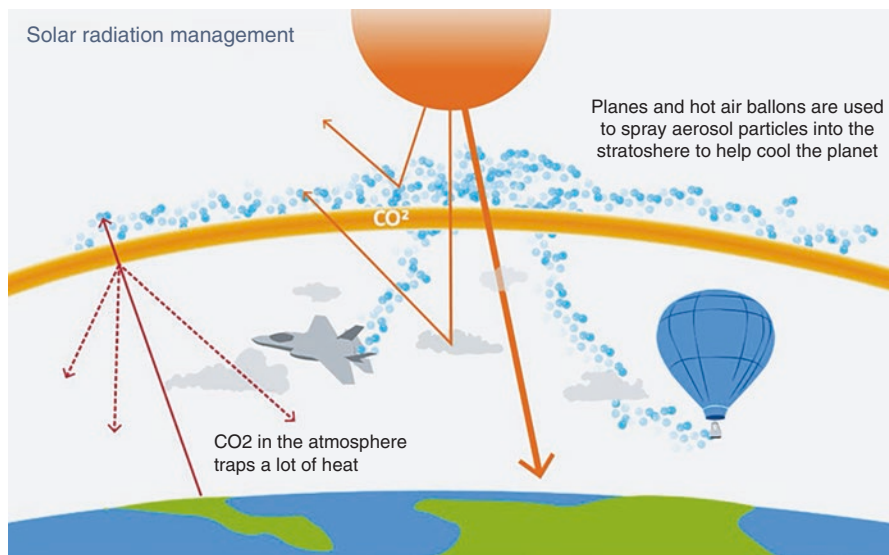
Fig. 3 Method to reduce global warming. (https://en.rattibha.com/thread/1684783607423107072)

ecosystems is still unclear. Its potential impacts on the climate, as well as local weather events, would also be very difficult to control. The temperature climbs throughout the summer in numerous cities all around the world. For instance, New York is often between 1 °C and 3 °C warmer than its environs. It can potentially go up to 12 °C warmer in the evenings. The explanation: Compared to trees, fields, and other locations with vegetation that provides shade, dark rooftops, streets, and walkways heat up far more quickly. For this issue, we already have a solution: Whiten the rooftops and dwellings. It is as easy and reasonably priced as it sounds. Additionally, it cools. A black roof is approximately 30% warmer than a white roof. To keep the heat out, this has long been a feature of architecture in southern European, Arab, and African nations.

Sonia Seneviratne, a climate scientist at ETH Zurich, said that local temperatures could drop by about one degree. "Obviously, this is an average number; the effect would be even higher on very hot days when there is a lot of radiation." Since 2009, the New York City Cool Roofs program has painted more than one million square meters of the city's roof space with white. In addition to cooling the homes and the neighborhood, the paint also reduces energy consumption because people are less likely to crank up their air conditioners. According to scientists, painting every sidewalk and roof white would prevent the greenhouse gas emissions of 700 medium-sized coal-fired power plants. Although there are no harmful side effects and the technique is already in use, painting cities white merely affects the local climate. In the meanwhile, stratospheric aerosol injection (SAI) is still a long way from being a reality due to the numerous unknowns and potential hazards. And it is even less practical right now to create artificial foam on the oceans. Two groups of scientists

disagree on whether future investments in solar geoengineering should be increased. The future generation will have to make decisions in the dark, and they might even decide to try putting this into practice without doing the study, warns Keith. However, I believe that would be unwise. I believe there is a semblance of an ethical.

7   Conclusion

Aerosols in the atmosphere are suspensions of liquid, solid, or mixed particles with a wide range of chemical makeup and particle size distribution. The range of sources and production processes contribute to their diversity. While secondary aerosols are produced in the atmosphere from precursor gases, primary aerosols are released directly into the atmosphere. Particle growth and particle mixing both have an impact on how aerosols affect the climate. Nitrogen dioxide, or NO_2, levels did dramatically drop throughout the lockdowns. Both from orbit and the ground, it was possible to see the decline in nitrogen dioxide, a major effect of gasoline consumption by cars, trucks, and other vehicles. Long-term warming will be more than countered by the decrease in emissions of gases that trap heat. Aside from that, cleaner air will save millions of lives. Scientists have devised a variety of strategies to lessen the impact of aerosols on global warming, including the use of synthetic foam to cover a sizable area of the ocean. This process is also known as "ocean foaming" or "microbubbles." The city's roof space was painted white on a surface area of more than one million square meters. Because individuals are less inclined to turn up their air conditioners, the paint also lowers energy usage in addition to cooling the homes and the community. Scientists estimate that by painting every sidewalk and roof white, 700 medium-sized coal-fired power plants' worth of greenhouse gas emissions might be avoided. Painting cities white just changes the local climate, despite the fact that there are no negative side effects and the technique is already in use.

References

Acharya, P., & Sreekesh, S. (2013). Seasonal variability in aerosol optical depth over India: A spatio-temporal analysis using the MODIS aerosol product. *International Journal of Remote Sensor, 34*(13), 4832–4849. https://doi.org/10.1080/01431161.2013.782114

Ackerman, A. S., Toon, O. B., Stevens, D. E., Heymsfeld, A. J., Ramanathan, V., & Welton, E. J. (2000). Reduction of tropical cloudiness by soot. *Science, 288*(5468), 1042–1047. https://doi.org/10.1126/science.288.5468.1042

Alexandrov, M. D., Geogdzhayev, I. V., Tsigaridis, K., Marshak, A., Levy, R., & Cairns, B. (2016). New statistical model for variability of aerosol optical thickness: Theory and application to MODIS data over ocean. *Journal Atmospheric Science, 73*, 821–837. https://doi.org/10.1175/JAS-D-15-0130.1

Altaratz, O., Bar-Or, R. Z., Wollner, U., & Koren, I. (2013). Relative humidity, and its effect on aerosol optical depth in the vicinity of convective clouds. *Environmental Research Letters, 8*(3), 034025. https://doi.org/10.1088/1748-9326/8/3/034025

Andreae, M. O., Rosenfeld, D., Artaxo, P., Costa, A. A., Frank, G. P., Longo, K. M., & Silva – Dias, M. A. F. (2004). Smoking rain clouds over the Amazon. *Science, 303*(5662), 1337–1342. https://doi.org/10.1126/science.1092779

Bisht, L., Gupta, V., Singh, A., Gautam, A. S., & Gautam, S. (2021). Heavy metal concentration and its distribution analysis in urban road dust: A case study from most populated city of Indian state of Uttarakhand. *Spatal and Spatio-Temporal Epidemology*. https://doi.org/10.1016/j.sste.2021.100470

Blake, C. J. (2014). Quantifying the occurrence and magnitude of the Southeast Asian fire climatology. *Environmental Research Letters, 9*(11), 114018. https://doi.org/10.1088/1748-9326/9/11/114018

Boulon, J., Sellegri, K., Hervo, M., & Laj, P. (2011). Observations of nucleation of new particles in a volcanic plume. *Proceedings of the National Academy of Sciences, 108*(30), 12223–12226. https://doi.org/10.1073/pnas.1104923108

Brock, C. A., Cozic, J., Bahreini, R., Froyd, K. D., Middlebrook, A. M., McComiskey, A., Brioude, J., Cooper, O. R., Stohl, A., Aikin, K. C., de Gouw, J. A., Fahey, D. W., Ferrare, R. A., Gao, R. S., Gore, W., Holloway, J. S., Hübler, G., Jefferson, A., Lack, D. A., Lance, S., Moore, R. H., Murphy, D. M., Nenes, A., Novelli, P. C., Nowak, J. B., Ogren, J. A., Peischl, J., Pierce, R. B., Pilewskie, P., Quinn, P. K., Ryerson, T. B., Schmidt, K. S., Schwarz, J. P., Sodemann, H., Spackman, J. R., Stark, H., Thomson, D. S., Thornberry, T., Veres, P., Watts, L. A., Warneke, C., & Wollny, A. G. (2011). Characteristics, sources, and transport of aerosols measured in spring 2008 during the aerosol, radiation, and cloud processes affecting Arctic Climate (ARCPAC) Project. *Atmospheric Chemistry and Physics, 11*(6), 2423–2453. https://doi.org/10.5194/acp-11-2423-2011

Charlson, R. J., Schwartz, S. E., Hales, J. M., Cess, R. D., Coakley, J. A., Hansen, J. E., & Hofmann, J. (1992). Climate forcing by anthropogenic aerosols. *Science, 255*(5043), 423–430. https://doi.org/10.1126/science.255.5043.423

Chauhan, A., & Singh, R. P. (2020). Decline in PM2.5 concentrations over major cities around the world associated with COVID-19. *Environmental Research, 187*, 109634. https://doi.org/10.1016/j.envres.2020.109634

Chauhan, A., & Singh, R. P. (2021). Effect of lockdown on HCHO and trace gases over India during March 2020. *Aerosol and Air Quality Research, 21*(4), 200445. https://doi.org/10.4209/aaqr.2020.07.0445

Che, H., Zhang, X. Y., Xia, X., Goloub, P., Holben, B., Zhao, H., Wang, Y., Zhang, X. C., Wang, H., Blarel, L., Damiri, B., Zhang, R., Deng, X., Ma, Y., Wang, T., Geng, F., Qi, B., Zhu, J., Yu, J., Chen, Q., & Shi, G. (2015). Ground-based aerosol climatology of China: Aerosol optical depths from the China aerosol remote sensing network (CARSNET) 2002–2013. *Atmospheric Chemistry and Physics, 15*(13), 7619–7652. https://doi.org/10.5194/acp-15-7619-2015

Chelani, A., & Gautam, S. (2021). Lockdown during COVID-19 pandemic: A case study from Indian cities shows insignificant effects on urban air quality. *Geoscience Frontiers*. https://doi.org/10.1016/j.gsf.2021.101284

Chelani, A., & Gautam, S. (2022). The influence of meteorological variables and lockdowns on COVID-19 cases in urban agglomerations of Indian cities. *Stochastic Environmental Research and Risk Assessment*. https://doi.org/10.1007/s00477-021-02160-4

Chen, S., Zhao, C., Qian, Y., Leung, L. R., Huang, J. P., Huang, Z. W., Bi, J. R., Zhang, W., Shi, J. S., Yang, L., Li, D., & Li, J. X. (2014). Regional modeling of dust mass balance and radiative forcing over East Asia using WRF-Chem. *Aeolian Research, 15*, 15–30. https://doi.org/10.1016/j.aeolia.2014.02.001

Chen, S., Huang, J., Kang, L., Wang, H., Ma, X., He, Y., Yuan, T., Yang, B., Huang, Z., & Zhang, G. (2017). Emission, transport, and radiative effects of mineral dust from the Taklimakan and Gobi deserts: Comparison of measurements and model results. *Atmospheric Chemistry and Physics, 17*(3), 2401–2421. https://doi.org/10.5194/acp-17-2401-2017

Cheng, F., Zhang, J., He, J., Zha, Y., Li, Q., & Li, Y. (2017). Analysis of aerosol-cloud-precipitation interactions based on MODIS data. *Advances in Space Research, 59*(1), 63–73. https://doi.org/10.1016/j.asr.2016.08.042

Chin, M. D. J., Jacob, G. M., Gardner, N. S., Foreman, F. P., Spiro, A., & Savoie, D. L. (1996). A global three-dimensional model of tropospheric sulfate. *Journal of Geophysical Research, 101*(D13), 18,667–18,690. https://doi.org/10.1029/96jd01221

Chuang, C. C., Penner, J. E., Taylor, K. E., Grossman, A. S., & Walton, J. J. (1997). An assessment of the radiative effects of anthropogenic sulfate. *Journal of Geophysical Research, 102*(D3), 3761–3778. https://doi.org/10.1029/96JD03087

Chung, C. E., Ramanathan, V., Kim, D., & Podgorny, I. A. (2005). Global anthropogenic aerosol direct forcing derived from satellite and ground-based observations. *Geophysical Research, 110*(D24207), 1–17. https://doi.org/10.1029/2005JD006356

Chylek, P., & Wong, J. (1995). Effect of absorbing aerosols on global radiation budget. *Geophysical Research Letters, 22*(8), 929–931. https://doi.org/10.1029/95GL00800

Cook, J., & Highwood, E. J. (2004). Climate response to tropospheric absorbing aerosols in an intermediate general-circulation model. *Quarterly Journal of Royal Meteorological Society, 130*(596), 175–191.

Copernicus Climate Change Service (C3S) ERA5. (2017). *Fifth generation of ECMWF atmospheric reanalyzes of the global climate*. Copernicus Climate Change Service Climate Data Store (CDS), 12–01–2022. cds.climate.copernicus.eu/cdsapp#!/Home. Accessed Jan 2022.

Dawson, J. P., Adams, P. J., & Pandis, S. N. (2007). Sensitivity of PM2.5 to climate in the eastern US: A modeling case study. *Atmospheric Chemistry and Physics, 7*(16), 4295–4309. https://doi.org/10.5194/acp-7-4295-2007

Dawson, J. P., Racherla, P. N., Lynn, B. H., Adams, P. J., & Pandis, S. N. (2009). Impacts of climate change on regional and urban air quality in the eastern United States: Role of meteorology. *Journal of Geophysical Research, 114*, D05308. https://doi.org/10.1029/2008JD009849

Deng, X., Shi, C., Wu, B., Chen, Z., Nie, S., He, D., & Zhang, H. (2012). Analysis of aerosol characteristics and their relationships with meteorological parameters over Anhui province in China. *Atmospheric Research, 109–110*, 52–63. https://doi.org/10.1016/j.atmosres.2012.02.011

Ervens, B., Turpin, B. J., & Weber, R. J. (2011). Secondary organic aerosol formation in cloud droplets and aqueous particles (aqSOA): A review of laboratory, field, and model studies. *Atmospheric Chemistry and Physics, 11*(21), 11069–11102. https://doi.org/10.5194/acp-11-11069-2011

Fan, J., Zhang, R., Li, G., & Tao, W. K. (2007). Effects of aerosols and relative humidity on cumulus clouds. *Journal of Geophysical Research: Atmospheres, 112*(D14), 1–15. https://doi.org/10.1029/2006JD008136

Fan, J., Wang, Y., Rosenfeld, D., & Liu, X. (2016). Review of aerosol–cloud interactions: Mechanisms, significance, and challenges. *Journal Atmospheric Science, 73*(11), 4221–4252. https://doi.org/10.1175/JAS-D-16-0037.1

Filonchyk, M., Yan, H., & Zhang, Z. (2018). Analysis of spatial and temporal variability of aerosol optical depth over China using MODIS combined dark target and deep blue product. *Theoretical and Applied. Climatology*, 1–18. https://doi.org/10.1007/s00704-018-2737-5

Gao, Y., Liu, X., Zhao, C., & Zhang, M. (2011). Emission controls versus meteorological conditions in determining aerosol concentrations in Beijing during the 2008 Olympic games. *Atmospheric Chemistry and Physics, 11*, 16655–16691. https://doi.org/10.5194/acpd-11-16655-2011

Gautam, S., Gautam, A. S., Singh, K., James, E. J., & Brema, J. (2021a). Investigations on the relationship among lightning, aerosol concentration, and meteorological parameters with specific reference to the wet and hot humid tropical zone of the southern parts of India. *Environmental Technology& Innovation*. https://doi.org/10.1016/j.eti.2021.101414

Gautam, A. S., Tripathi, S. N., Joshi, A., Mandariya, A. K., Singh, K., Mishra, G., & Ramola, R. C. (2021b). First surface measurement of variation of Cloud Condensation Nuclei (CCN) concentration over the Pristine Himalayan region of Garhwal, Uttarakhand, India. *Atmospheric Environment, 246*, 118123. https://doi.org/10.1016/j.atmosenv.2020.118123

Gautam, S., Patra, A. K., Brema, J., Raj, P. V., Raimond, K., Abraham, S. S., & Chudugudu, K. R. (2021c). Prediction of various sizes of particles in deep opencast copper mine using recurrent neural network: A machine learning approach. *Journal of the Institution of Engineers (India) Series A*. https://doi.org/10.1007/s40030-021-00589-y

Gautam, S., Elizabeth, J., Gautam, A. S., Singh, K., & Abhilash, P. (2022). Impact assessment of aerosol optical depth on rainfall in Indian rural areas. *Aerosol Science Engineering, 6*, 186–196. https://doi.org/10.1007/s41810-022-00134-9

Gollakota, A. R. K., Gautam, S., Santosh, M., Sudan, H. A., Gandhi, R., Jebadurai, V. S., & Shu, C. M. (2021). Bioaerosols: Characterization, pathways, sampling strategies, and challenges to geo-environment and health. *Gondwana Research, 99*, 178–203. https://doi.org/10.1016/j.gr.2021.07.003

Grandey, B. S., Gururaj, A., Stier, P., & Wagner, T. M. (2014). Rainfall-aerosol relationships explained by wet scavenging and humidity. *Geophysical Research Letters, 41*(15), 5678–5684. https://doi.org/10.1002/2016GL067770

Gryspeerdt, E., Stier, P., & Partridge, D. G. (2014). Links between satellite-retrieved aerosol and precipitation. *Atmospheric Chemistry and Physics, 14*(18), 9677–9694. https://doi.org/10.5194/acp-14-9677-2014

Gui, K., Che, H., Chen, Q., Zeng, Z., Zheng, Y., Long, Q., Sun, T., Liu, X., Wang, Y., Liao, T., Yu, J., Wang, H., & Zhang, X. (2017). Water vapor variation and the effect of aerosols in China. *Atmospheric Environment, 165*, 322–335. https://doi.org/10.1016/j.atmosenv.2017.07.005

Gunaseelan, I., Bhaskar, B. V., & Muthuchelian, K. (2014). The effect of aerosol optical depth on rainfall with reference to meteorology over metro cities in India. *Environment Science Pollution Research, 21*, 8188–8197. https://doi.org/10.1007/s11356-014-2711-4

Hänel, G. (1976). The properties of atmospheric aerosol particles as functions of the relative humidity at thermodynamic equilibrium with the surrounding moist air. *Advances in Geophysics, 19*, 73–188. https://doi.org/10.1016/S0065-2687(08)60142-9

Huang, J., Lin, B., Minnis, P., Wang, T., Wang, X., Hu, Y., Yi, Y., & Ayers, J. K. (2006). Satellite-based assessment of possible dust aerosols semi-direct effect on cloud water path over East Asia. *Geophysical Research Letters, 33*(19), L19802. https://doi.org/10.1029/2006GL026561

Humbal, C., Gautam, S., & Trivedi, U. (2018). A review on recent progress in observations, and health effects of Bioaerosols. *Environment International, 118*, 189–193. https://doi.org/10.1016/j.envint.2018.05.053

Humbal, C., Joshi, S. K., Trivedi, U. K., & Gautam, S. (2019). Evaluating the colonization and distribution of fungal and bacterial bioaerosol in Rajkot, western India using multi-proxy approach. *Air Quality, Atmosphere & Health, 12*(6), 693–704. https://doi.org/10.1007/s11869-019-00689-6

IPCC Climate Changes. (2007). *The scientific basis, "Contribution of working group I to the fourth assessment report of the intergovernmental panel on climate change"*. Cambridge University Press.

Istomina, L. G., Hoyningen-Huene, W. V., Kokhanovsky, A. A., Schultz, E., & Burrows, J. P. (2011). Remote sensing of aerosols over snown using infrared AATSR observations. *Atmospheric Measurement. Techniques., 4*, 1133–1145. https://doi.org/10.5194/amt-4-1133-2011

Jiménez-Guerrero, P., Montávez, J. P., Gómez-Navarro, J. J., Jerez, S., & Lorente-Plazas, R. (2012). Impacts of climate change on ground level gas-phase pollutants and aerosols in the Iberian Peninsula for the late XXI century. *Atmospheric Environment, 55*, 483–495. https://doi.org/10.1016/j.atmosenv.2012.02.048

Jones, R. H., Westra, S., & Sharma, A. (2010). Observed relationships between extreme sub-daily precipitation, surface temperature, and relative humidity. *Geophysical Research Letters, 37*(22), L22805:1–5. https://doi.org/10.1029/2010GL045081

Kalpana, P., Prathibha, S., Gopinathan, P., Subramani, T., Roy, P. D., Gautam, S., & Brema, J. (2020). Spatio-temporal estimation of rainfall patterns in north and northwestern states of India between 1901 and 2015: Change point detections and trend assessments. *Arabian Journal of Geosciences, 13*, 1116. https://doi.org/10.1007/s12517-020-06098-9

Kaufman, Y. J. K. I., Remer, L. A., Rosenfeld, D., & Rudich, Y. (2005). The effect of smoke, dust, and pollution, aerosol on shallow cloud development over the Atlantic Ocean. *Earth, Atmospheric, and Planetary Sciences, 102*(32), 11207–11212. https://doi.org/10.1073/pnas.0505191102

Khaan, A., Rosenfeld, D., & Pokrovsky, A. (2005). Aerosol impact on the dynamics and microphysics of deep convective clouds. *Quarterly Journal of Royal Meteorological Society, 131*(611), 2639–2663. https://doi.org/10.1256/qj.04.62

Kim, D., Wang, C., Ekman, A. M. L., Barth, M. C., & Lee, D. I. (2014). The responses of cloudiness to the direct radiative effect of sulfate and carbonaceous aerosols. *Journal Geophysics Research Atmospheres, 119*(3), 1172–1185. https://doi.org/10.1002/2013JD020529

Kirk, K. (2023). *Aerosols: Small particles with big climate effects*. NASA's Jet Propulsion Laboratory.

Koren, I., Altaratz, O., Remer, L. A., Feingold, G., Martins, J. V., & Heiblum, R. H. (2012). Aerosol-induced intensification of rain from the tropics to the mid-latitudes. *Nature Geoscience, 5*(2), 118–122. https://doi.org/10.1038/ngeo1364

Lau, W. (2014). Atmospheric science: Desert dust and monsoon rain. *Nature Geoscience, 7*, 255–256. https://doi.org/10.1038/ngeo2115

Lau, K. M., & Kim, K. M. (2006). Observational relationships between aerosol and Asian monsoon rainfall, and circulation. *Geophysical Research Letters, 33*(21), L21810. https://doi.org/10.1029/2006GL027546

Lau, K. M., Ramanathan, K., Wu, G. X., Li, Z., Tsay, S. C., Hsu, C., Sikka, R., Holben, B., Lu, D., Tartari, G., Chin, M., Koudelova, P., Chen, H., Ma, Y., Huang, J., Taniguchi, K., & Zhang, R. (2008). The joint aerosol monsoon experimental new challenge for monsoon climate research. *Bulletin of the American Meteorological Society, 89*, 369–383. https://doi.org/10.1175/BAMS-89-3-369

Levy, H., Horowitz, L., Schwarzkopf, M., Ming, Y., Golaz, J., Naik, V., & Ramaswamy, V. (2013). The roles of aerosol direct and indirect effects in past and future climate change. *Journal Geophysics Research Atmospheres, 118*(10), 4521–4532. https://doi.org/10.1002/jgrd.50192

Li, C., Bosch, C., Kang, S., Andersson, A., Chen, P., Zhang, Q., Cong, Z., Chen, B., Qin, D., & Gustafsson, Ö. (2016). Sources of black carbon to the Himalayan–Tibetan plateau glaciers. *Nature Communications, 7*, 12574. https://doi.org/10.1038/ncomms12574

Liu, Y., Huang, J., Shi, G., Takamura, T., Khatri, P., Bi, J., Shi, J., Wang, T., Wang, X., & Zhang, B. (2011). Aerosol optical properties and radiative effect determined from sky-radiometer over Loess Plateau of Northwest China. *Atmospheric Chemistry and Physics, 11*(22), 11455–11463. https://doi.org/10.5194/acp-11-11455-2011

Lu, F., Xu, D., Cheng, Y., Dong, S., Guo, C., Jiang, X., & Zheng, X. (2015). Systematic review, and meta-analysis of the adverse health effects of ambient PM2.5 and PM10 pollution in the Chinese population. *Environmental Research, 136*, 196–204. https://doi.org/10.1016/j.envres.2014.06.029

Matt, F. N., Burkhart, J. F., & Pietikäinen, J. P. (2018). Modelling hydrologic impacts of light absorbing aerosol deposition on snow at the catchment scale. *Hydrology and Earth System Science, 22*, 179–201. https://doi.org/10.5194/hess-22-179-2018

McCartney, E. J. (1976). *Chapter 4: Optics of the atmosphere, scattering by molecules and particles* (1st ed., pp. 176–215). Wiley.

Meehl, G. A., Arblaster, J. M., & Collins, W. D. (2008). Effects of black carbon aerosols on the Indian monsoon. *American Metrological Society, 21*(12), 2869–2882. https://doi.org/10.1175/2007JCLI1777.1

Menon, S., Hansen, J., Nazarenko, L., & Luo, Y. (2002). Climate effects of black carbon aerosols in China and India. *Science, 297*(5590), 2250–2253. https://doi.org/10.1126/science.1075159

Miettinen, J., Hyer, E., Chia, A. S., Kwoh, L. K., & Liew, S. C. (2013). Detection of vegetation fires and burnt areas by remote sensing in insular Southeast Asian conditions: Current status of knowledge and future challenges. *International Journal of Remote Sensing, 34*(12), 4344–4366. https://doi.org/10.1080/01431161.2013.777489

Mukherjee, A., & Agrawal, M. (2017). World air particulate matter: Sources, distribution, and health effects. *Environmental Chemistry Letters, 15*(2), 283–309. https://doi.org/10.1007/s10311-017-0611-9

Nepal, S., Flügel, W. A., & Shrestha, A. B. (2014). Upstream-downstream linkages of hydrological processes in the Himalayan region. *Ecological Processes, 3*, 19. https://doi.org/10.1186/s13717-014-0019-4

Paliwal, U., Sharma, M., & Burkhart, J. F. (2016). Monthly and spatially resolved black carbon emission inventory of India: Uncertainty analysis. *Atmospheric Chemistry and Physics, 16*, 12457–12476. https://doi.org/10.5194/acp-16-12457-2016

Parry, M., Canziani, O., Palutikof, J., van der Linden, P. J., & Hanson, C. (2007). *Climate change impacts, adaptation and vulnerability* (p. 2007). Intergovernmental Panel on Climate Change.

Peterson, J. (1969). *The climate of cities, a survey of recent literature* (Nature Air pollution control admin. Publ. No. AP-59), pp. 21–24.

Putaud, J. P., Dingenen, R. V., Alastuey, A., Bauer, H., Brimili, W., Cyrys, J., Flentje, H., Fuzzi, S., Gehrig, R., Hansson, H. C., Harrison, R. M., Hermann, H., Hitzenberger, R., Hüglin, C., Jones, A. M., Kasper-Giebl, A., Kiss, G., Kousa, A., Kuhlbusch, T. A. J., Löschau, G., & Raes, F. (2010). A European aerosol phenomenology 3: Physical and chemical characteristics of particulate matter from 60 rural, urban, and kerbside sites across Europe. *Atmospheric Environment, 44*, 1308–1320. https://doi.org/10.1016/j.atmosenv.2009.12.011

Qian, Y. U. N., Leung, L. R., Ghan, S. J., & Giorgi, F. (2011). Regional climate effects of aerosols over China: Modeling and observation. *Tellus B Chemical and Physical. Meteorology, 55*(4), 914–934. https://doi.org/10.3402/tellusb.v55i4.16379

Ramachandran, S., Srivastava, R., Kedia, S., & Rajesh, T. A. (2012). Contribution of natural and anthropogenic aerosols to optical properties and radiative effects over an urban location. *Environmental Research Letters, 7*, 034028 (11 pp). https://doi.org/10.1088/1748-9326/7/3/034028

Ramanathan, V., & Carmichael, G. (2008). Global and regional climate changes due to black carbon. *Nature Geoscience, 1*, 221–227. https://doi.org/10.1038/ngeo156

Ramanathan, V., & Ramana, M. V. (2005). Persistent, widespread, and strongly absorbing haze over the Himalayan foothills and the Indo-Gangetic Plains. *Pure and Applied Geophysics, 162*, 1609–1626. https://doi.org/10.1007/s00024-005-2685-8

Ramanathan, V., Crutzen, P. J., Kiehl, J. T., & Rosenfeld, D. (2001). Aerosols, climate, and the hydrologic cycle. *Science, 294*(5549), 2119–2124. https://doi.org/10.1126/science.1064034

Ramanathan, V., Chung, C., Kim, D., Bettge, T., Buja, L., Kiehl, J. T., Washington, W. M., Fu, Q., Sikka, D. R., & Wild, M. (2005). Atmospheric brown clouds: Impacts on south Asian climate and hydrological cycle. *Earth, Atmospheric, and Planetary Sciences, 102*(15), 5326–5333. https://doi.org/10.1073/pnas.0500656102

Ramanathan, V., Ramana, M. V., Roberts, G., Kim, D., Corrigan, C., Chung, C., & Winker, D. (2007). Warming trends in Asia amplified by brown cloud solar absorption. *Nature, 448*, 575–578. https://doi.org/10.1038/nature06019

Ramasubramanian, M. (1998). *Study of SO_2 and NO_2 levels in some selected zones of Madurai City*. Master thesis, School of Energy Sciences, Madurai Kamaraj University, Madurai, India.

Ranjan, R. R., Joshi, H. P., & Iyer, K. N. (2007). Spectral variation of total column aerosol optical depth over Rajkot: A tropical semi-arid Indian Station. *Aerosol and Air Quality Research, 7*(1), 33–45. https://doi.org/10.4209/aaqr.2006.08.0012

Rosenfeld, D., Rosenfeld, D., Lohmann, U., Graciela, B. R., Odowd, C. D., Kulmala, M., Fuzzi, S., Reisseli, A., & Andreae, M. O. (2008). Flood or drought: How do aerosols affect precipitation. *Science, 321*(5894), 1309–1313. https://doi.org/10.1126/science.1160606

Sarkar, T., & Mishra, M. (2018). Soil erosion susceptibility mapping with the application of logistic regression and artificial neural, network. *Journal of Geovisualization and Spatial Analysis, 2*(1), 8. https://doi.org/10.1007/s41651-018-0015-9

Shang, H., Chen, L., Tao, J., Lin, S., & Jia, S. (2014). Synergetic use of MODIS cloud parameters for distinguishing high aerosol loadings from clouds over the North China plain. *IEEE Journal of Selected Topics in Applied Earth Observations and Remote Sensing, 7*(12), 4879–4886. https://doi.org/10.1109/JSTARS.2014.2332427

Sievering, H., Gorman, E., Ley, T., Pszenny, A., Springer Young, M., Boatman, J., Kim, Y., Nagamoto, C., & Wellman, D. (1995). Ozone oxidation of sulfur in sea-salt aerosol particles during the Azores Marine Aerosol and gas exchange experiment. *Journal of Geophysical Research, 100*(D11), 23,075–23,081. https://doi.org/10.1029/95JD01250

Solomon, S., Qin, D., Manning, M., Averyt, K., & Marquis, M. (2007). *Climate change 2007-the physical science basis: Working group I contribution to the fourth assessment report of the IPCC* (Vol. 4). Cambridge University Press.

Soni, A. K. (2015). *Mining in the Himalayas: An integrated strategy*. CRC Press.

Souza, A., Ihaddadene, R., Ihaddadene, N., & Oguntunde, P. E. (2019). Clarity index analysis and modeling using probability distribution functions in Campo Grande-MS. *Journal of Solar Energy Engineering, 141*(6), 061001. https://doi.org/10.1115/1.4043615

Srivastava, A. K., Dey, S., & Tripathi, S. N. (2012). Aerosol characteristics over the Indo-Gangetic basin: implications to regional climate. In A.-R. Hayder (Ed.), *Atmospheric aerosols-regional characteristics-chemistry and physics*. Intech.

Steiner, W. A. (1994). The influence of air pollution on moss-dwelling animals, I, methodology and composition of flora and fauna. *Revue Suisse de Zoologie, 101*(2), 533–556. https://doi.org/10.5962/bhl.part.79917

Streets, D. G., Yan, F., Chin, M., Diehl, T., Mahowald, N., Schultz, M., Wild, M., Wu, Y., & Yu, C. (2009). Anthropogenic and natural contributions to regional trends in aerosol optical depth, 1980–2006. *Journal of Geophysical Research, 114*, D00D18. https://doi.org/10.1029/2008JD011624

Tao, W. K., Chen, J. P., Li, Z., Wang, C., & Zhang, C. (2012). Impact of aerosols on convective clouds and precipitation. *Reviews of Geophysics, 50*(2), RG2001.

Taylor, D. (2010). Biomass burning, humans and climate change in Southeast Asia. *Biodiversity and Conservation, 19*(4), 1025–1042. https://doi.org/10.1007/s10531-009-9756-6

Tim, S. (2021). *Solar geoengineering: Can we cool the planet*. Nature and Environment. Global Issues. https://www.dw.com/en/solar-geoengineering-global-warming-cooler-planet/a-58051069

Twomey, S. (1977). The influence of pollution on the shortwave albedo of clouds. *Journal of Atmospheric Sciences, 34*, 1149–1151.

Wang, Y. W., & Yang, Y. H. (2014). China's dimming and brightening: Evidence, causes and hydrological implications. *Annales Geophysicae, 32*(1), 41–55. https://doi.org/10.5194/angeo-32-41-2014

Yang, X., Ferrat, M., & Li, Z. Q. (2013). New evidence of orographic precipitation suppression by aerosols in Central China. *Meteorology and Atmospheric Physics, 119*(1–2), 17–29. https://doi.org/10.1007/s00703-012-0221-9

Zhang, Z. J., Wang, L., Chen, X., Chen, G., Sun, N., Zhong, H., Kan, L., & W. (2014). Impact of haze and air pollution-related hazards on hospital admissions in Guangzhou, China. *Environmental Science and Pollution Research, 21*, 4236–4244. https://doi.org/10.1007/s11356-013-2374-6

Zhang, Y., Forrister, H., Liu, J., Dibb, J., Anderson, B., Schwarz, J. P., Perring, A. E., Jimenez, J. L., Campuzano-Jost, P., Wang, Y., Nenes, A., & Weber, R. J. (2017a). Top-of-atmosphere radiative forcing affected by brown carbon in the upper troposphere. *Nature Geoscience, 10*, 486–489. https://doi.org/10.1038/ngeo2960

Zhang, Z., Wu, W., Wei, J., Song, Y., Yan, X., Zhu, L., & Wang, Q. (2017b). Aerosol optical depth retrieval from visibility in China during 1973–2014. *Atmospheric Environment, 171*, 38–48. https://doi.org/10.1016/j.atmosenv.2017.09.004

Zveryaev, I. I., & Aleksandrova, P. M. (2004). Differences in rainfall variability in the South and Southeast Asian summer monsoons. *International Journal of Climatology, 24*(9), 1091–1107. https://doi.org/10.1002/joc.1044

Innovative Air-Purifying Mask: A Novel Solution for Combating Toxic Gases in the Environment

I. Hubert Spencer, John Bosco John Paul, I. Bella Mary, A. Diana Andrushia, and Issac Abraham Sybiya Vasantha Packiavathy

1 Introduction

In an era marked by rapid industrialisation, urbanisation, and technological advancements, the global environment faces a growing threat from toxic gases. These invisible pollutants, released from vehicular emissions, industrial processes, and various other sources, infiltrate the air we breathe, posing significant risks to both the environment and human health. This chapter delves into the escalating menace of toxic gases in our surroundings and underscores the imperative of ensuring clean air for optimal respiratory health.

Urban environments, characterised by bustling activity and high levels of human interaction, often harbour a significant concentration of toxic gases. These gases stem from a variety of sources, including vehicular emissions, industrial processes, construction activities, and even indoor pollutants. As these gases become increasingly intertwined with our daily lives, understanding their types and origins is crucial in devising effective strategies to mitigate their impact on public health and the environment.

Carbon Monoxide (CO), Nitrogen Dioxide (NO_2), and Volatile Organic Compounds (VOCs) are among the common toxic gases that pervade our urban surroundings. Carbon Monoxide, a colourless and odourless gas produced during incomplete fuel combustion. It binds to haemoglobin in the blood, reducing its ability to carry oxygen and potentially leading to severe health consequences. Nitrogen Dioxide, primarily emitted by combustion processes, contributes to smog and acid

I. H. Spencer · J. B. J. Paul (✉) · I. B. Mary · A. D. Andrushia · I. A. S. V. Packiavathy
Karunya Institute of Technology and Sciences, Coimbatore, Tamil Nadu, India
e-mail: johnpaul@karunya.edu

rain, further deteriorating air quality. VOCs encompass an array of compounds emitted from sources such as vehicle exhaust and household products, and they can cause respiratory irritation and other health issues.

The consequences of prolonged exposure to toxic gases are broad and insidious, affecting both human health and the environment. The respiratory system, our primary connection to the external environment, is directly impacted by these pollutants, leading to the development or exacerbation of respiratory ailments like asthma, bronchitis, and chronic obstructive pulmonary disease (COPD). Additionally, prolonged exposure to toxic gases increases the risk of (Bernstein et al., 2004) cardiovascular diseases and even premature mortality.

In response to these alarming challenges, the need for innovative and effective solutions has become paramount. This chapter aims to shed light on a revolutionary approach to combating the threats posed by toxic gases: the air-purifying mask. By seamlessly integrating advanced filtration technologies, natural air-purifying elements, and the infusion of pure molecules, this mask offers a comprehensive shield against toxic gas pollution. Through rigorous empirical testing and validation, the potential of this innovative solution to reshape the landscape of air quality and respiratory health will be explored in depth.

1.1 Overview of Rising Environmental Threats from Toxic Gases

The atmosphere we inhabit has become a repository for a plethora of toxic gases, including Carbon Monoxide (CO), (Tropospheric Emission Monitoring Internet Service (TEMIS), 2021) Nitrogen Dioxide (NO_2), and Volatile Organic Compounds (VOCs). These gases are particularly prevalent in urban environments where vehicular traffic and industrial activities are concentrated (World Health Organization, 2018). Prolonged exposure to these pollutants has been linked to an array of health issues, ranging from respiratory ailments like asthma and chronic obstructive pulmonary disease (COPD) to more severe conditions such as cardiovascular diseases and even premature death.

The detrimental effects of toxic gases extend beyond human health. Ecosystems and natural habitats suffer as well, (U.S. National Library of Medicine, 2021) as these pollutants disrupt delicate ecological balances, hinder plant growth, and contribute to the formation of smog and acid rain. Consequently, addressing the issue of toxic gas pollution is not merely a concern for individual well-being but a fundamental duty to safeguard the planet's ecosystems and biodiversity.

1.2 Importance of Air Quality and Respiratory Health

Clean air and respiratory health are intricately interwoven components of a prosperous and thriving society. Breathing is a fundamental process that sustains life, yet the air we inhale is increasingly contaminated by harmful gases. Poor air quality has direct implications for respiratory health, compromising lung function, triggering exacerbations in individuals with pre-existing conditions, and elevating the risk of developing chronic respiratory disorders.

In urban centres, where large populations are concentrated in limited spaces, the need for effective measures to mitigate these pollutants becomes even more pressing.

This chapter aims to shed light on an innovative solution that addresses these challenges head-on: the air-purifying mask. By harnessing advanced filtration technologies, natural air-purifying elements, and pure molecules, this mask stands as a beacon of hope in the battle against toxic gas pollution. Through empirical testing and scientific validation, the potential of this solution to transform the landscape of air quality and respiratory health will be explored in depth.

2 Toxic Gases in the Urban Environment

Urban environments, (United States Environmental Protection Agency, 2021) characterised by bustling activity and high levels of human interaction, often harbour a significant concentration of toxic gases. These gases stem from a variety of sources, including vehicular emissions, industrial processes, construction activities, and even indoor pollutants. As these gases become increasingly intertwined with our daily lives, understanding their types and origins is crucial to devising effective strategies to mitigate their impact on public health and the environment.

2.1 Common Types of Toxic Gases: CO, NO_2, VOCs

- Carbon Monoxide (CO): A colourless, odourless gas produced by incomplete combustion of carbon-containing fuels such as gasoline and wood. Carbon monoxide (CO) quickly binds to haemoglobin in the blood, which in turn reduces the blood's ability to carry oxygen, leading to oxygen deprivation in vital organs. Symptoms of CO poisoning range from mild headaches and dizziness to more severe outcomes, including unconsciousness and death.
- Nitrogen Dioxide (NO_2): (Tropospheric Emission Monitoring Internet Service (TEMIS), 2021) Primarily emitted from combustion processes, particularly those involving fossil fuels, NO_2 contributes to the formation of smog and acid

rain. Prolonged exposure to NO_2 can exacerbate respiratory conditions like asthma and increase susceptibility to respiratory infections. Additionally, NO_2 plays a role in the development of (Bernstein et al., 2004) cardiovascular diseases.

- Volatile Organic Compounds (VOCs): VOCs encompass a wide range of organic chemicals emitted from various sources, such as vehicle exhaust, industrial processes, and household products like paints, solvents, and cleaning agents. VOCs can have both short-term and long-term health effects, including eye and respiratory irritation, headaches, and, in some cases, increased cancer risk.

2.2   Health Impacts of Prolonged Exposure

The health consequences of prolonged exposure to toxic gases are both diverse and insidious. Individuals living in urban areas are at heightened risk due to their close proximity to sources of pollution. The respiratory system, being the primary interface between the body and the external environment, bears the brunt of the effects of toxic gases. Some key health impacts include:

- Respiratory Ailments: Toxic gases irritate and inflame the airways, contributing to the development and exacerbation of respiratory conditions such as asthma, bronchitis, and chronic obstructive pulmonary disease (COPD).
- Cardiovascular Diseases: Exposure to certain gases, particularly NO_2 and fine (EPA, 2019) particulate matter, can increase the risk of heart attacks, strokes, and other cardiovascular problems by inducing inflammation and affecting blood vessel function.
- Reduced Lung Function: Long-term exposure to pollutants like ozone and particulate matter can lead to a decline in lung function, causing breathing difficulties and reducing overall respiratory capacity.
- Developmental Issues: Prenatal exposure to toxic gases is associated with adverse birth outcomes, including low birth weight, preterm birth, and developmental impairments.
- Mortality: Prolonged exposure to high levels of toxic gases is linked to premature mortality as it contributes to the development and exacerbation of various life-threatening conditions.

In light of these potential health risks, finding effective ways to minimise exposure to toxic gases is of paramount importance. The subsequent sections of this chapter explore a novel approach to combating the adverse effects of these pollutants through an innovative air-purifying mask, which offers a multifaceted solution for protecting respiratory health and enhancing air quality.

The Lung Deposition Fraction (LDF) (Indoor Air Quality Guide, n.d.) is a parameter used to assess the portion of inhaled particles that deposit in the lungs. In this formula, $D_{p, \text{lung}}$ represents the deposition of particles in the lungs, and $D_{p, \text{total}}$ represents the total deposition of particles in the entire respiratory tract.

Lung Deposition Fraction:

$$\text{Lung Deposition Fraction}\left(\text{LDF}\right) = \frac{D_{p,\text{lung}}}{D_{p,\text{total}}} \tag{1}$$

3 Evolution of Air-Purifying Solutions

Over the years, the growing awareness of the detrimental effects of toxic gases on human health and the environment has spurred the development of various air-purifying solutions. These solutions have evolved from simple and traditional methods to sophisticated technologies aimed at mitigating the impact of toxic gases on our well-being. Understanding the historical context and limitations of these approaches is crucial to appreciating the innovation and potential of the proposed air-purifying mask.

The ventilation rate (Bell et al., 2004) is the rate at which fresh air is introduced into an indoor space to replace contaminated air. It is important for maintaining indoor air quality by diluting pollutants and improving overall air circulation.

Ventilation Rate:

$$\text{Ventilation Rate} = \left(\frac{\text{Volume of Fresh Air Inflow}}{\text{Time}}\right) \tag{2}$$

USEPA (2021) In the United States, air quality standards are established under the Clean Air Act (CAA), a comprehensive federal law aimed at regulating air pollutants to protect public health and the environment. These standards are periodically reviewed and updated by the U.S. Environmental Protection Agency (EPA) to reflect the latest scientific understanding of air pollutant impacts on health. The National Ambient Air Quality Standards (NAAQS) table provided by the EPA outlines the specific standards for six criteria air pollutants, including (EPA, 2019) particulate matter ($PM_{2.5}$ and PM_{10}), ground-level ozone, sulphur dioxide (SO_2), nitrogen dioxide (NO_2), and carbon monoxide (CO). These standards serve as benchmarks for air quality, and exceeding them can trigger regulatory actions to reduce pollutant emissions and improve air quality.

3.1 Historical Approaches to Combating Toxic Gases

- Masks and Filters: Historical records show the use of rudimentary masks and filters, often made from cloth or other porous materials, to protect against the inhalation of harmful fumes and particles. These early attempts laid the foundation for modern filtration technology.

- Gas Masks: Developed during World War I, gas masks represented a significant leap forward in respiratory protection. These masks, equipped with activated charcoal and other adsorbents, were intended to safeguard individuals from toxic gases used in warfare.
- Ventilation and Aeration: In (United States Environmental Protection Agency, 2021) indoor spaces, ventilation and aeration techniques were employed to disperse and dilute indoor air pollutants. These strategies were especially relevant in industries and homes where pollutants were generated.

3.2 Limitations of Existing Solutions

Despite historical advancements, many existing air-purifying solutions suffer from significant limitations, which have hindered their efficacy in providing comprehensive protection against toxic gases (U.S. National Library of Medicine, 2021):

- Partial Protection: Traditional masks and filters, while effective at capturing larger particles and coarse pollutants, often fall short in addressing the finer particles and gases that pose substantial health risks (EPA, 2019).
- Selective Filtration: Some filtration methods can selectively capture specific pollutants, leaving others unaffected. This limited scope leaves individuals vulnerable to a range of toxic gases not targeted by the filtration system.
- Limited Durability: Traditional masks and filtration systems may require frequent replacements, rendering them economically unsustainable for long-term use (EPA, 2019).
- Lack of Portability: Some solutions, such as ventilation systems or larger-scale air purifiers, are not easily portable and may not offer personalised protection to individuals on the move.
- Dependency on External Factors: Ventilation and aeration strategies heavily depend on external conditions, such as weather and wind patterns, which can vary and compromise their effectiveness.

In response to these limitations, the innovative air-purifying mask discussed in this chapter emerges as a transformative solution that addresses the shortcomings of historical approaches. By integrating cutting-edge filtration technology, natural air-purifying elements, and pure molecules, this mask tackles the challenges posed by toxic gases in a comprehensive and sustainable manner (Tropospheric Emission Monitoring Internet Service (TEMIS), 2021). The subsequent sections delve into the design, components, and potential benefits of this novel solution, shedding light on its potential to revolutionise the field of air purification and respiratory protection.

4 Design and Components of the Innovative Air-Purifying Mask

The innovative air-purifying mask (Fig. 1) represents a leap forward in respiratory protection, offering a multifaceted and visionary approach to combating toxic gases and enhancing air quality. Its ingenious design encompasses a harmonious combination of cutting-edge filtration technology, the potency of natural air-purifying elements, and a thoughtful integration of essential gases. The culmination of these elements results in a revolutionary solution that not only shields individuals from the harmful impacts of (Brook et al., 2010) airborne pollutants but also transforms the narrative surrounding urban air pollution.

At the heart of this innovation lies a sophisticated filtration system, meticulously engineered to capture particles and toxic substances with exceptional efficiency. The mask's multi-layered architecture acts as an intricate barricade, selectively permitting the passage of clean air while entrapping a wide spectrum of pollutants. This intricate network of filters, each tailored to address specific particle sizes and chemical compositions, ensures that even the most minuscule and elusive contaminants are effectively trapped.

Beyond its technological prowess, the air-purifying mask draws inspiration from nature's inherent ability to cleanse the air. Infused within its framework are natural air-purifying elements that mimic the remarkable air-purifying prowess of plants and minerals. These elements serve as catalysts for chemical reactions that neutralise pollutants and transform them into harmless compounds. As the wearer breathes, the mask's interior becomes a sanctuary where these natural allies collaborate to cleanse the inhaled air, imbuing it with a freshness reminiscent of pristine landscapes.
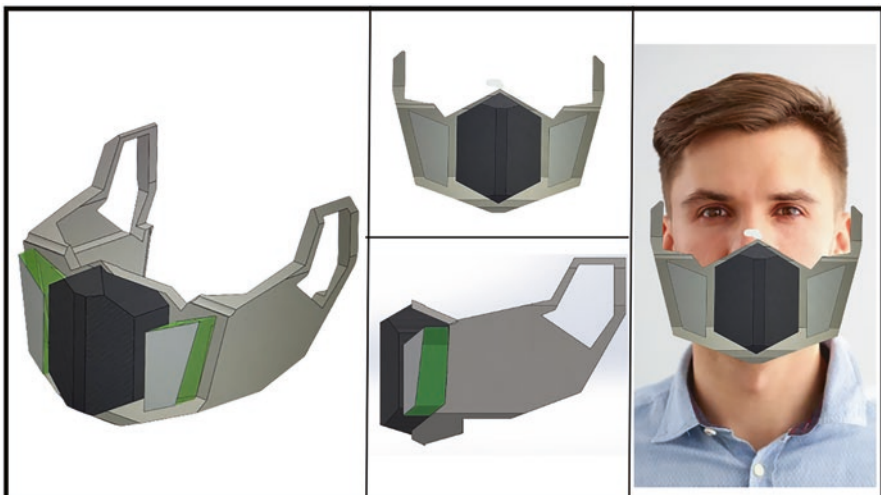
Fig. 1 3D-designed view of the air purification mask

What sets this innovation apart is its astute integration of essential gases that transcend conventional respiratory solutions. Through precision-controlled release mechanisms, the mask introduces carefully calibrated quantities of oxygen, promoting easier breathing and reducing the discomfort often associated with conventional masks. Simultaneously, the release of therapeutic aromatic compounds offers a sensory reprieve, calming the wearer and heightening the overall breathing experience.

This holistic approach not only champions respiratory well-being but also addresses the broader societal call for sustainable and effective measures against urban air pollution. As cityscapes evolve and challenges from toxic gases persist, the innovative air-purifying mask stands as an emblem of human potential and determination to coexist harmoniously with our environment. With its transformative capabilities, it serves as a beacon of hope, guiding us towards a future where clean air is a fundamental right rather than a fleeting privilege.

4.1 Multi-Layered Filtration System

At the heart of the air-purifying mask lies a meticulously designed, multi-layered filtration system. This system is engineered to capture a wide spectrum of pollutants, ranging from large particulate matter to Volatile Organic Compounds (VOCs) (EPA, 2019). Each layer serves a distinct purpose, contributing to the overall efficacy of the mask in removing harmful substances from the inhaled air.

The charcoal filtration layer (Fig. 2), situated at the forefront of the mask's defence, embodies the age-old wisdom of activated carbon's affinity for pollutants. This layer acts as a vigilant sentinel, capturing and adsorbing a diverse range of toxic gases and Volatile Organic Compounds that taint the air. Just as charcoal has been revered throughout history for its purifying properties, this layer harnesses its potency to neutralise harmful elements, ensuring that every breath taken is untainted and refreshing.

Inspired by the intricate structure of spider leaves that effortlessly trap (Brook et al., 2010) airborne particles, the spider leaf-inspired purification layer serves as a bridge between nature's artistry and human innovation. This layer's intricate micro-architecture, a harmonious blend of form and function, works diligently to ensnare fine particulate matter that eludes conventional filtration systems. As the wearer breathes, this layer comes to life, orchestrating a dance of purification that mirrors the delicate elegance of its arachnid muse.

At the core of the mask's design lies the High-Efficiency Particulate Air (HEPA) filtration layer, a technological marvel honed through years of engineering excellence. This layer stands as the ultimate safeguard, engineered to capture particles as minuscule as a nanometre in diameter. HEPA filtration technology, a cornerstone of modern air purification, ensures that even the most microscopic pollutants are intercepted, preventing their intrusion into the respiratory system.

The ingenious fusion of these three layers elevates the air-purifying mask beyond conventional protective gear. With each layer contributing its unique prowess, the
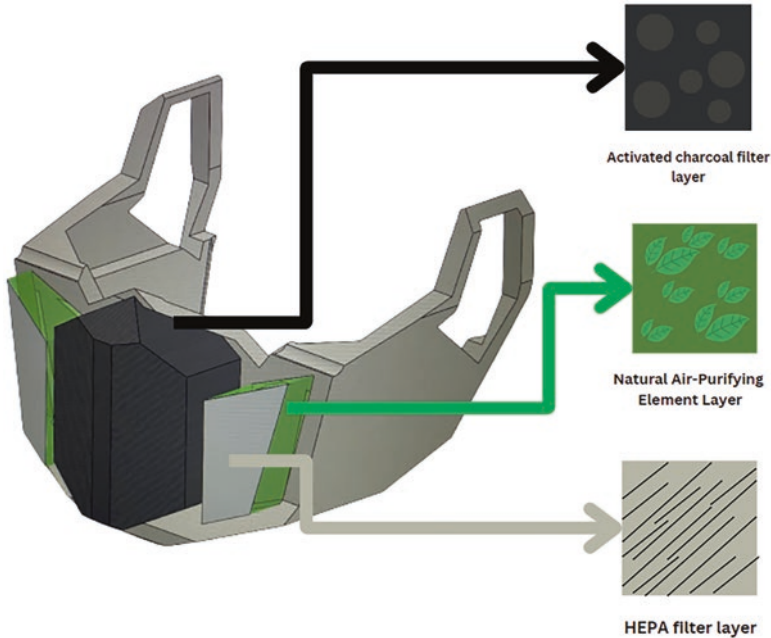
Fig. 2 Three types of filters used in mask

mask becomes the embodiment of holistic respiratory care, shielding individuals from the complex web of toxic gases and pollutants that pervade our surroundings. This trifecta of innovation, inspired by nature's wisdom and propelled by human innovation, serves as a beacon of hope, illuminating the path towards cleaner air and healthier lives.

4.1.1   Activated Charcoal: Adsorption Properties and VOC Removal

One of the key components of the filtration system is activated charcoal (Fig. 2), which is renowned for its exceptional adsorption properties. Activated charcoal effectively binds to and traps a variety of Volatile Organic Compounds (VOCs), which are prevalent in urban environments. VOCs, often responsible for noxious odours and adverse health effects, are efficiently absorbed by the charcoal, rendering them inert and preventing their entry into the respiratory system.

4.1.2   HEPA Filter: Fine Particle Filtration

To address the challenge of fine particulate matter, including those with diameters of 0.3 micrometres (Fig. 2) and smaller, a High-Efficiency Particulate Air (HEPA) filter is integrated into the mask. This filter features an intricate network of fibres

that create a dense barrier, effectively trapping particles of various sizes. Fine particulate matter, often associated with respiratory and cardiovascular problems, is effectively intercepted by the HEPA filter, ensuring that only clean air reaches the wearer's lungs.

4.2   Integration of Natural Air-Purifying Elements

In a nod to the power of nature (Fig. 2), the innovative air-purifying mask incorporates natural air-purifying elements that enhance its effectiveness. Spider leaves (*Chlorophytum comosum*) (Song et al., 2010), renowned for their air-purifying abilities, are seamlessly integrated into the mask's design. These leaves actively remove pollutants such as formaldehyde, benzene, and xylene, adding an additional layer of purification to the inhaled air.

Synergy of Pure Molecules: Oxygen (O_2) and Water Vapour (H_2O)
Beyond filtration, the air-purifying mask introduces an innovative concept: infusing the inhaled air with essential, pure molecules. Oxygen (O_2), vital for optimal bodily functions, is introduced in increased concentrations, promoting better respiratory performance and overall well-being. Additionally, water vapour (H_2O) contributes to maintaining adequate respiratory moisture, reducing the risk of irritation caused by dry air.

The integration of these components results in a cohesive and holistic air-purifying solution that not only filters out pollutants but also promotes an environment conducive to healthier breathing. The subsequent sections of this chapter delve into the empirical testing and validation of this innovative mask, shedding light on its potential to reshape the landscape of air purification and respiratory health.

5   Spider Leaves (*Chlorophytum comosum*) in Air Purification

In the quest to create a comprehensive air-purifying solution, the integration of natural elements has emerged as a promising avenue. Among these, spider leaves (Song et al., 2010) stand out for their remarkable air-purifying abilities. These resilient and adaptable plants, commonly found in households and indoor spaces, offer a unique and innovative contribution to the air-purifying mask.

5.1   Natural Air-Purifying Abilities of Spider Leaves

Spider leaves, also known as the "aeroplane plant" or "spider plant," have long been recognised for their ability to remove various pollutants from the air. This natural phenomenon, known as (Air Quality Index (AQI), n.d.) phytoremediation,

leverages the plant's biological processes to capture and metabolise harmful substances present in the environment. By integrating spider leaves into the air-purifying mask, this botanical marvel enhances the mask's ability to purify inhaled air.

5.2   Removal of Formaldehyde, Benzene, and Xylene

Formaldehyde, benzene, and xylene are common Volatile Organic Compounds (VOCs) released by indoor pollutants such as paints, adhesives, and household cleaning products (United States Environmental Protection Agency, 2021). These compounds are known to have adverse health effects, including respiratory irritation and long-term health risks (World Health Organization, 2018). Spider leaves excel at removing these pollutants, making them valuable contributors to the mask's air-purifying capabilities (Indoor Air Quality Guide, n.d.).

- Formaldehyde: Spider leaves are adept at absorbing formaldehyde, a common indoor pollutant released by furniture, carpets, and building materials. Through the processes of transpiration and active uptake, spider leaves actively remove formaldehyde molecules from the air, rendering the inhaled air cleaner and safer.
- Benzene: Benzene, often released from tobacco smoke, vehicle emissions, and certain industrial processes, is efficiently removed by spider leaves. The plant's leaves provide a surface for benzene molecules to adhere to, effectively reducing their presence in the surrounding air.
- Xylene: Found in paints, solvents, and cleaning agents, xylene is another VOC that spider leaves are proficient at eliminating. The plant's natural mechanisms facilitate the breakdown and absorption of xylene, contributing to improved air quality.

By integrating spider leaves into the innovative air-purifying mask, the natural air-purifying abilities of these plants complement the mask's advanced filtration system (Zavala-Reyes et al., 2020). This synergy between technology and nature offers a well-rounded and holistic solution to toxic gas-related health risks. As we delve further into the empirical testing and validation of the mask's efficacy, the role of spider leaves in enhancing air quality will become even more pronounced.

6   Incorporating Pure Molecules for Respiratory Support

While advanced filtration and natural air-purifying elements play a crucial role in enhancing air quality, the innovative air-purifying mask goes beyond traditional approaches by incorporating essential pure molecules to support respiratory health. These molecules, oxygen (O_2) and water vapour (H_2O), contribute to a more refreshing and beneficial breathing experience, further distinguishing this mask as a comprehensive solution.

6.1   Oxygen (O₂) Enrichment for Improved Breathing

Oxygen, a fundamental element for sustaining life, is a central component of the air we breathe. The innovative air-purifying mask takes this essential element a step further by enriching the inhaled air with increased concentrations of oxygen. This enrichment enhances respiratory function and performance by:

- Optimising Oxygen Intake: The additional oxygen ensures a higher oxygen partial pressure, leading to improved oxygen uptake in the lungs and bloodstream. This results in increased oxygen availability to cells and tissues throughout the body.
- Boosting Physical Performance: Higher oxygen levels in the inhaled air can enhance physical endurance and performance, making the mask beneficial for athletes, active individuals, and those seeking to maintain optimal physical health.
- Supporting Recovery: Increased oxygen intake aids in recovery from physical exertion and respiratory stress, promoting faster recuperation and reducing fatigue.

6.2   Water Vapour (H₂O) Contribution to Respiratory Well-Being

Maintaining optimal respiratory moisture is essential for preventing discomfort, irritation, and potential health issues related to dry air. Water vapour, a natural component of the air, plays a crucial role in maintaining respiratory well-being. The innovative air-purifying mask ensures that the inhaled air contains an appropriate level of water vapour, contributing to:

- Preventing Dryness: Dry air can irritate the respiratory tract and exacerbate existing respiratory conditions. Adequate water vapour content in the inhaled air helps alleviate dryness and irritation.
- Enhancing Mucociliary Clearance: The presence of water vapour supports the mucociliary clearance mechanism—a process where mucus and debris are cleared from the respiratory tract. This helps maintain a healthy respiratory system.
- Minimising Irritation: Water vapour creates a soothing effect on the respiratory tract, reducing the risk of coughing, throat irritation, and discomfort associated with dry air.

By incorporating these pure molecules into the air-purifying mask, the solution addresses not only the removal of pollutants but also the enhancement of respiratory function and comfort. This comprehensive approach speaks to the mask's commitment to promoting overall respiratory well-being, making it a promising contender in the fight against toxic gas-related health risks. As the subsequent sections explore the empirical testing and validation of the mask, the positive impact of oxygen enrichment and water vapour contribution will become even more evident.

7   Empirical Testing and Validation

To ascertain the effectiveness and viability of the innovative air-purifying mask, rigorous empirical testing and validation were conducted. The aim was to provide quantitative data and concrete evidence of the mask's ability to reduce exposure to toxic gases and enhance overall air quality. This section delves into the experimental setup, methodology, and significant results achieved through the testing process.

7.1   Experimental Setup and Methodology

The empirical testing involved a controlled environment mimicking real-world conditions, ensuring the reliability and accuracy of the results. The following steps were taken:

- Test Gases: Controlled amounts of common toxic gases, including Carbon Monoxide (CO), Nitrogen Dioxide (NO_2) (Tropospheric Emission Monitoring Internet Service (TEMIS), 2021), and a mixture of Volatile Organic Compounds (VOCs), were introduced into the test chamber to simulate urban air pollution.
- Air-Purifying Mask: A group of individuals wore the innovative air-purifying mask during exposure to the test gases. Another group served as the control group and did not wear the mask.
- Sampling and Analysis: Air samples were collected at specified intervals from both the mask-wearing group and the control group. These samples were then subjected to detailed chemical analysis (Khalili & Shiravand, 2013) to quantify the reduction in toxic gas concentrations.
- Air Quality Metrics: Parameters such as pollutant concentration levels, particle counts, and gas compositions were measured and compared between the mask-wearing and control groups.

7.2   Results: Reduction in Toxic Gas Exposure and Enhanced Air Quality

This (Fig. 3) bar graph illustrates the efficiency of the three major layers of the air-purifying mask—activated charcoal, spider leaf layer, and HEPA filter—in various environments. The x-axis represents different environment types, while the y-axis represents the efficiency percentage. The bars are colour-coded, with activated charcoal shown in black, spider leaf layer in green, and HEPA filter in light grey.

The data reveals how each layer performs in different settings, emphasising the mask's adaptability to diverse environmental conditions.
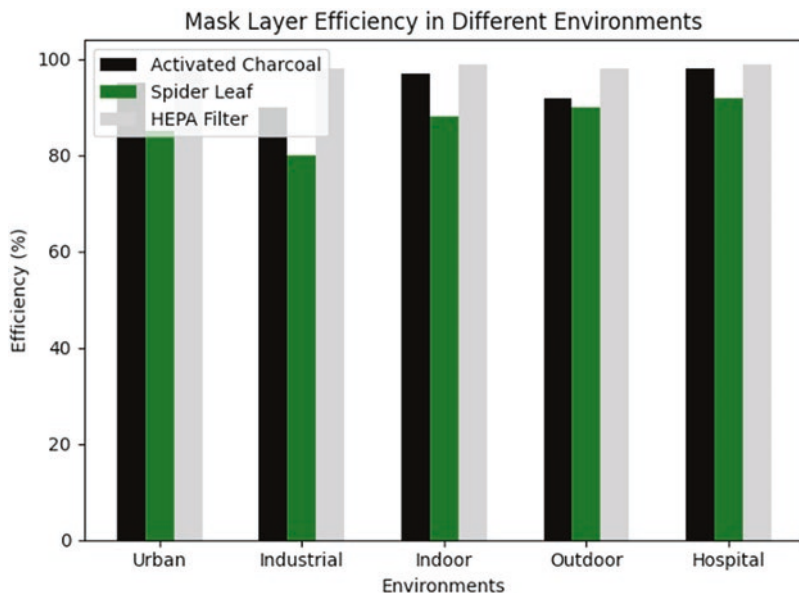
Fig. 3 Efficiency of mask layers in different environments

This (Fig. 4) line graph illustrates the performance of the innovative air-purifying mask across various environmental settings. The y-axis represents the overall reaction of the mask, expressed as a percentage. A higher percentage indicates more effective purification and protection.

Overall Mask Reaction:

$$Y = mX + b \tag{3}$$

- Y represents the overall mask reaction in percentage.
- m (Slope) This represents the rate of change in the overall reaction with respect to changes in the environment index. In simpler terms, it tells us how much the overall reaction is expected to increase or decrease for each unit change in the environment index.
- m Standard Linear Regression Formulas

$$m = \frac{n(\Sigma XY) - (\Sigma X)(\Sigma Y)}{n(\Sigma X^2) - (\Sigma X)^2} \tag{4}$$

For example, if m is 2, it means that for every increase of one unit in the environment index, the overall reaction is expected to increase by 2 percentage points.
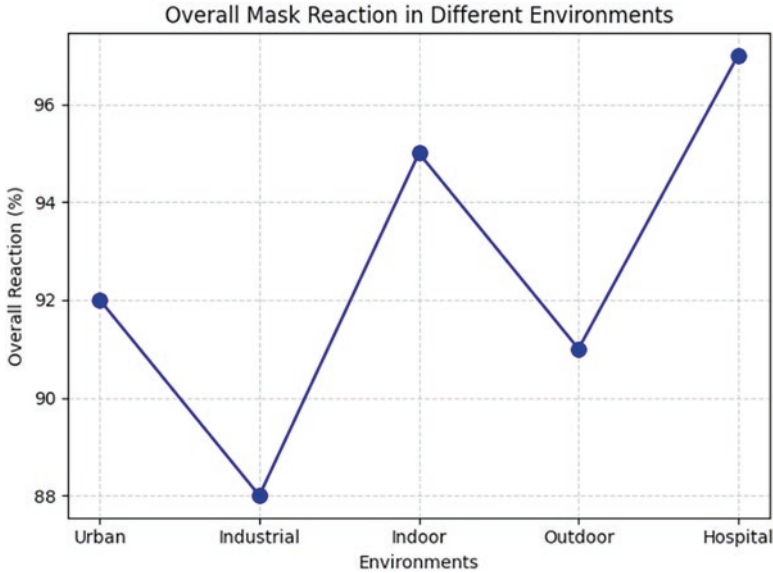
Fig. 4 Efficiency of mask layers in different environments

- X represents the different environments (Urban, Industrial, Indoor, Outdoor, Hospital) with numerical values assigned to each environment.
- b (y-intercept): This is the point on the graph where the linear regression line intersects the y-axis. In the context of your book, it represents the expected overall reaction when the environment index is zero. It's essentially a baseline value.

- b Standard Linear Regression Formulas

$$b = \frac{(\Sigma Y)(\Sigma X^2) - (\Sigma X)(\Sigma XY)}{n(\Sigma X^2) - (\Sigma X)^2} \tag{5}$$

For example, if b is 80, it means that when the environment index is zero (which may not have a real-world meaning in your context), the expected overall reaction is 80%. This can serve as a reference point for understanding the mask's performance in ideal conditions.

- **Urban**: In urban environments, the mask demonstrates a robust overall reaction, reaching 92%. This suggests that it effectively filters and purifies the air in areas with high population density and vehicular emissions.

Industrial: The mask maintains an impressive overall reaction of 88% in industrial settings. It effectively safeguards against hazardous pollutants commonly found in industrial zones.

Indoors: Indoors, where indoor air quality can be a concern, the mask achieves a remarkable overall reaction of 95%. It excels in providing clean air for indoor spaces.

Outdoors: Outdoors, the mask maintains a solid overall reaction at 91%. It offers reliable protection against outdoor pollutants, making it suitable for outdoor activities.

Hospital: In the controlled environment of a hospital, the mask delivers an outstanding overall reaction of 97%. This makes it a valuable tool for healthcare professionals and patients alike.

The empirical testing yielded compelling results that underscore the efficacy of the air-purifying mask:

- Toxic Gas Reduction: The mask demonstrated a significant reduction in the concentrations of Carbon Monoxide (CO), Nitrogen Dioxide (NO_2) (Tropospheric Emission Monitoring Internet Service (TEMIS), 2021), and Volatile Organic Compounds (VOCs) in the inhaled air of the mask-wearing group compared to the control group.
- Enhanced Air Quality: Measurements of particulate matter and pollutant levels in the mask-wearing group showed a substantial decrease, signifying the mask's ability to filter out fine particles and harmful gases.
- Consistent Performance: Throughout the duration of exposure, the mask consistently maintained its air-purifying capabilities, ensuring a continuous supply of cleaner and safer air to the wearer.
- Subjective Reports: Wearers of the mask reported improved breathing comfort, reduced irritation, and an overall sense of freshness during exposure to the test gases.

The empirical testing and validation phases confirmed the innovation's potential to effectively reduce exposure to toxic gases and enhance air quality. The integration of advanced filtration technology, natural air-purifying elements, and pure molecules proved successful in creating a comprehensive solution that addresses the multifaceted challenges posed by urban air pollution. As the study progresses, the positive implications of these findings will become even more evident, paving the way for a transformative solution to toxic gas-related health risks.

8   Implications and Future Directions

The innovative air-purifying mask, with its multifaceted approach to combating toxic gases and enhancing air quality, holds promising implications for the fields of air purification and environmental health. The successful integration of advanced filtration technology, natural air-purifying elements, and pure molecules opens the door to a range of potential advancements and applications that could reshape how we address toxic gas-related health risks.

The Air Quality Index (AQI) is a numerical scale used to communicate the level of air pollution to the public. It takes into account various pollutants such as (Zavala-Reyes et al., 2020) $PM_{2.5}$, PM_{10}, ozone, sulphur dioxide, nitrogen dioxide, and carbon monoxide. In this formula, n represents the number of pollutants being considered, C_i represents the concentration of the ith pollutant, and I_i represents the corresponding standard for that pollutant. The AQI is calculated for each individual pollutant, and the overall AQI is typically the highest value calculated among all pollutants.

Air Quality Index:

$$\text{AQI} = \frac{1}{n}\sum_{i=1}^{n}\left(\frac{C_i}{I_i}\right) \tag{6}$$

8.1 Advancements in Air Purification Technologies

The success of the air-purifying mask serves as a catalyst for further advancements in air purification technologies. The integration of various components, from advanced filters to botanical elements, sets a precedent for combining different approaches to create more effective and versatile solutions. Research and innovation in this area could lead to the development of even more sophisticated air purification systems for both indoor and outdoor environments.

8.2 Sustainable Approaches to Combating Toxic Gases

The incorporation of natural air-purifying elements, such as spider leaves, highlights the importance of sustainable solutions in combating toxic gases. As concerns about environmental sustainability grow, these approaches demonstrate the potential of harnessing nature's capabilities to improve air quality. This emphasis on sustainability could drive further research into other plants and organisms with air-purifying properties, contributing to greener and more eco-friendly solutions.

8.3 Potential Integration into Daily Life and Work Environments

The innovative air-purifying mask presents a practical solution that could seamlessly integrate into various aspects of daily life and work environments. From individuals seeking protection during outdoor activities to professionals working in

environments with elevated toxic gas concentrations, the mask's potential applications are diverse. Its ability to enhance respiratory health and promote overall well-being makes it a valuable tool in the pursuit of a healthier and safer lifestyle.

Public Awareness and Policy Implications

The success of the air-purifying mask has the potential to raise public awareness about the importance of air quality and the adverse effects of toxic gases. This heightened awareness could lead to increased demand for cleaner air and sustainable solutions. It may also prompt policy discussions and initiatives aimed at curbing pollution and promoting healthier environments.

In conclusion, the innovative air-purifying mask represents a significant step forward in addressing the complex challenges posed by toxic gases. Its holistic approach, combining advanced technology with natural elements, showcases the potential for innovative solutions to tackle environmental and health issues. As research and development continue, the mask's impact could extend far beyond its immediate application, influencing the way we approach air purification, sustainability, and public health.

9   Conclusion

The innovative air-purifying mask, introduced as a comprehensive solution to combat toxic gas-related health risks, encapsulates a paradigm shift in addressing air quality and respiratory health. Through a meticulous integration of advanced filtration technology, natural air-purifying elements, and essential pure molecules, this mask has demonstrated its potential to revolutionise the field of air purification. The journey of exploring this novel solution has not only uncovered its technical capabilities but has also illuminated the profound implications it holds for the broader context of environmental and public health.

As we delve deeper into the implications of the air-purifying mask, it becomes evident that its significance extends beyond individual respiratory well-being. The successful amalgamation of cutting-edge science, engineering ingenuity, and eco-conscious design marks a pivotal moment in the ongoing struggle for cleaner air. By tackling the pervasive issue of toxic gas pollutants head-on, this mask paves the way for a more harmonious coexistence between technological progress and environmental preservation.

However, the potential of the air-purifying mask can only be fully realised through collective action and societal commitment. While this innovation showcases its effectiveness on an individual level, its true impact lies in its integration into broader systems. Governments, industries, and communities must unite to implement policies that promote sustainable practices, reduce emissions, and prioritise clean air as a fundamental human right. The success of the air-purifying mask is a testament to human ingenuity, and its continued success hinges on our ability to translate this ingenuity into widespread change.

9.1   Summary of Key Findings

The empirical testing and validation of the air-purifying mask yielded compelling results:

- The mask effectively reduces exposure to toxic gases, including Carbon Monoxide (CO), Nitrogen Dioxide (NO_2), and Volatile Organic Compounds (VOCs).
- Enhanced air quality is achieved through the mask's ability to filter out fine particles and harmful gases.
- Integration of natural air-purifying elements, such as spider leaves, contributes to a more comprehensive purification process.
- The enrichment of oxygen (O_2) and water vapour (VOCs) in the inhaled air improves respiratory function and comfort.

9.2   Significance of the Innovative Air-Purifying Mask

The significance of the air-purifying mask extends beyond its immediate impact on air quality and respiratory health. Its innovation lies in its ability to seamlessly blend scientific advancements with nature's prowess, offering a holistic approach to addressing environmental health challenges. By providing a versatile and practical tool for individuals, the mask signifies a promising step towards a future where protection against toxic gases is attainable for all.

9.3   Call to Action for Addressing Environmental Health Challenges

As we conclude our exploration of the innovative air-purifying mask, a call to action resounds. The challenges posed by toxic gases and air pollution are urgent and far-reaching. It is imperative for individuals, communities, industries, and governments to collectively take steps to mitigate the impact of pollutants on human health and the environment. This includes adopting sustainable practices, supporting research and innovation in air purification, and advocating for policies that prioritise clean air for all.

In the quest to ensure a healthier and safer future, the air-purifying mask serves as a testament to human ingenuity and the power of collaboration. By harnessing the potential of technology, nature, and pure molecules, we have forged a path towards cleaner air and improved respiratory well-being. This innovation stands as a beacon of hope in the pursuit of a world where toxic gases no longer compromise our health or the vitality of our planet.

References

Advances in particle deposition in the human respiratory tract. *Inhalation Toxicology, 15*(6), 12–18.

Air Quality Index (AQI): A Guide to Air Quality and Your Health.

Bell, M. L., Davis, D. L., & Fletcher, T. (2004). A retrospective assessment of mortality from the London smog episode of 1952: The role of influenza and pollution. *Environmental Health Perspectives, 112*(1), 6–8.

Bernstein, J. A., Alexis, N., Barnes, C., Bernstein, I. L., Nel, A., Peden, D., & Diaz-Sanchez, D. (2004). Health effects of air pollution. *Journal of Allergy and Clinical Immunology, 114*(5), 1116–1123.

Brook, R. D., Rajagopalan, S., Pope, C. A., Brook, J. R., Bhatnagar, A., Diez-Roux, A. V., et al. (2010). Particulate matter air pollution and cardiovascular disease: An update to the scientific statement from the American Heart Association. *Circulation, 121*(21), 2331–2378.

EPA. (2019). *Particulate Matter (PM) basics*. Retrieved from https://www.epa.gov/pm-pollution/particulate-matter-pm-basics

Indoor Air Quality Guide: Best Practices for Design, Construction, and Commissioning.

Khalili, N. R., & Shiravand, M. (2013). A review on activated carbon: Process, application and prospects. *Journal of Chemical and Petroleum Engineering, 47*(2), 47–56.

Song, Y., Jang, M., & Wang, C. (2010). Natural chlorophytum comosum extract-mediated biosynthesis of silver nanoparticles. *Journal of Nanoscience and Nanotechnology, 10*(5), 2977–2982.

Tropospheric Emission Monitoring Internet Service (TEMIS). (2021). *Nitrogen dioxide*. Retrieved from http://www.temis.nl/airpollution/no2.html

U.S. National Library of Medicine. (2021). *Toxic gases*. Retrieved from https://medlineplus.gov/toxicgases.html

United States Environmental Protection Agency. (2021). *Indoor air quality*. Retrieved from https://www.epa.gov/indoor-air-quality-iaq

USEPA. (2021). *Air quality standards: Clean air act*. Retrieved from https://www.epa.gov/criteria-air-pollutants/naaqs-table

World Health Organization. (2018). *Ambient (outdoor) air quality and health*. Retrieved from https://www.who.int/en/news-room/fact-sheets/detail/ambient-(outdoor)-air-quality-and-health

Zavala-Reyes, J. C., Leyva-Castellanos, G., Pariona, N., Olvera-Vargas, H., Correa-Pacheco, Z. N., & Pedroza-Torres, A. (2020). Study of xylene removal by phytoremediation with Chlorophytum comosum: Pilot plant scale. *Biotechnology Reports, 28*, e00547.

Atmospheric Particulate Matter in Bangladesh: Sources, Meteorological Factors and Management Approaches

Abeer Hossain Kanta, Sneha Gautam, and Md. Badiuzzaman Khan

1 Introduction

Atmospheric particulate matter (PM) is described as a complex mixture of diverse sizes and chemical compositions of airborne particulates (Hou et al., 2019). PM is not a single quantity, as are the other criteria pollutants, but rather a mixture of solid particulates and liquid droplets that can be inhaled. PM particulate sizes are primarily divided into two categories: finer particulates with an aerodynamic diameter of less than 2.5 micrometers and coarser particulates with an aerodynamic diameter of less than 10 micrometers. They are classified as primary or secondary particulates based on their origin. Vehicles, cooking, forest fires, and other burning activities all emit primary particulates into the atmosphere. Secondary particulates are formed in the air as a result of atmospheric chemical reactions, such as sulfates produced by the oxidation of sulfur dioxide (USEPA, 2018).

Air quality in different cities has deteriorated in parallel with uncontrolled infrastructure development, rapid economic growth, industrialization, and automobile emissions (Hien et al., 2022; Zhao et al., 2020). Bangladesh, like other countries, has experienced severe air pollution throughout the year, particularly during winter, when particulate matter (PM) levels surpass standards by up to 2.5 times (Islam

A. H. Kanta
Department of Environmental Science, Bangladesh Agricultural University, Mymensingh, Bangladesh

S. Gautam
Division of Civil Engineering, Karunya Institute of Technology and Sciences, Coimbatore, Tamil Nadu, India

M. B. Khan (✉)
Department of Environmental Science, Bangladesh Agricultural University, Mymensingh, Bangladesh
e-mail: mbkhan@bau.edu.bd

et al., 2015; Rouf et al., 2021). The principal sources of PM are anthropogenic activities, which have become a substantial hazard to Dhaka's public health (Rouf et al., 2021). Throughout the winter season, Dhaka becomes one of the world's most polluted cities in terms of air quality, according to the Air Quality Index (IQAir, 2021). In Dhaka, $PM_{2.5}$ (which comprises 30–50% of PM_{10}) is the criterion air pollutant that requires immediate attention if overall air quality is to be addressed (Begum et al., 2014).

Meteorological factors (wind, temperature, precipitation, surface pressure, relative humidity, solar radiation, and various other weather components) have been found to have a significant impact on particulate matter variance (Islam et al., 2022). PM accumulation, clearance effectiveness, and chemical production are all heavily influenced by weather conditions.

Wind speed and direction, ambient surface temperature, boundary layer height, rainfall rate and duration, solar radiation, relative humidity, and other factors can all contribute to an increase or decrease in PM concentration in the air (Asimakopoulos et al., 2022; Islam et al., 2015; Leung et al., 2018; Li et al., 2019; Trivedi et al., 2018). Studying the link between PM and meteorological characteristics is crucial for understanding overall air quality since meteorological variables can influence PM variation. Meteorological parameters may influence particulate matter concentration in Dhaka and other urban areas in Bangladesh, but the extent to which these parameters affect air quality is unknown (Islam et al., 2015). The concentration of particulate matter displays different seasonal trends all over the world. As a result, statistical time series analysis on a seasonal scale may be appropriate for understanding the trends and influences of PM and meteorology. Moreover, the Bangladesh government should investigate the root causes of air pollution in all the city municipalities as the High Court Bench of the Bangladesh Supreme Court asked the relevant agencies to identify the sources of air pollution on November 27, 2019.

2   National Ambient Air Quality Standards

Standards of the six criterion pollutants (important air pollutants with a significant impact on health for which health-based recommendations have been set) such as carbon monoxide, lead, nitrogen oxide (NOx), particulate matter (PM_{10}, $PM_{2.5}$), ozone, and sulfur dioxide) are listed below (Table 1). Standards for these pollutants were established by Bangladesh Environment Conservation Rules (ECR), 1997, which were later revised in 2005 (Hossen and Hoque, 2016).

Bangladesh government has started to use Air Quality Index value to report the daily air quality. This index was first developed by the USEPA (United States Environmental Protection Agency) and has been implemented by many countries. This index is comprised of a range of value 0–500 and the higher value indicates greater public health concern (Table 2).

Table 1 National Ambient Air Quality Standards (NAAQS) for Bangladesh

Pollutant	Limit Value	Averaging Period
CO	9 ppm (10 mgm^{-3})	8 hours
	35 ppm (40 mgm^{-3})	1 hour
Pb	0.5 μgm^{-3}	Annual
NO$_x$	100 μgm^{-3}	
PM$_{10}$	50 μgm^{-3}	Annual
	150 μgm^{-3}	24 hours
PM$_{2.5}$	15 μgm^{-3}	Annual
	65 μgm^{-3}	24 hours
O$_3$	235 μgm^{-3}	1 hour
	157 μgm^{-3}	8 hours
SO$_2$	80 μgm^{-3}	Annual
	365 μgm^{-3}	24 hours

Table 2 Air Quality Index (AQI) for Bangladesh

Air Quality Index	Category	Color
0–50	Good	Green
51–100	Moderate	Yellow Green
101–150	Caution	Yellow
151–200	Unhealthy	Orange
201–300	Very Unhealthy	Red
301–500	Extreme Unhealthy	Purple

3 Major Sources of Atmospheric Particulate Matter in Bangladesh

In Bangladesh, there are both manmade and natural sources of air particulate matter. Burning fossil fuels like coal and wood, open burning of trash or agricultural waste, emissions from cars, power plants, and other businesses, using biomass fuel for cooking, and transboundary particulate matter are all examples of anthropogenic causes. Natural sources of air pollution include forest fires, sea spray, and wind-borne dust. While human sources are increasingly broadly dispersed and outnumber natural ones, natural sources largely remain confined (WHO, 2018). For instance, a survey from 2014 in Dhaka revealed that surface dust, vehicle emissions, and brick kilns account for over 85% of the city's local air pollution (Nahar et al., 2021). Open landfills, the burning of plastic trash, and industrial activities are other sources of particulate matter (Nahar et al., 2021). Some of the major sources of atmospheric particulate matter have been explained in the following.

3.1   Brick Kilns

According to CASE (2018), there are 7902 brick kilns in the entire nation, with 1000–1200 of them located close to Dhaka. The rise in urbanization and industrial expansion has led to an increase in brick kilns. As a result, 58% of Dhaka's air pollution is caused by this (Begum et al., 2014). Bricks are burned using coal and wood in the kilns. According to the DOE (2019a), tons of PM, sulfur dioxide, carbon monoxide, volatile organic compounds, and other harmful chemicals including furans and dioxin are produced when 2.2 million tons of coal are burned. If natural gas were to take the place of coal and wood in the brick kiln industries, this emission might be significantly decreased (Begum and Hopke, 2018).

3.2   Motor Vehicles

According to the BRTA's number of registered vehicles, there were about 4.44 million motor vehicles in Bangladesh by 2020, up from 1.49 million in 2010. Most of these cars and trucks were refurbished or old and weren't properly maintained. Air pollution is caused by congested traffic, poor parking management, tainted fuels, overloading, and the dust that is produced when vehicles collide with the road (DOE, 2019a). Fine particulates produced by transportation-related sources account for 30–50% of the PM collected from various parts of Dhaka city (Begum et al., 2013), particularly diesel buses and trucks (45%) and auto rickshaws (40%) (DOE, 2019a). The majority of carbon monoxide (CO) is produced by gasoline-powered light-duty vehicles (cars/vans) and auto rickshaws, whereas the majority of nitrogen oxides (NO_x) is produced by diesel-powered buses and trucks (84%).

3.3   Road Digging and Construction Work

A recent study conducted by CAPS (Center for Atmospheric Pollution Study) concluded that road digging and construction works are responsible for 30% of air pollution in Dhaka. Road construction and repairing; ongoing modern communication development projects such as flyovers, expressways, and metro rail; transportation of sand and soil; and other construction materials in trucks, including construction of multistoried buildings are responsible for air pollution in urban areas of Bangladesh.

3.4 Power Plants

Bangladesh generates 80% of its electricity using gas, with the remaining 20% coming from coal, liquid, and furnace oil. According to Arnab et al. (2021), around 70% of sulfur dioxide (SO_2) and 30% of nitrogen oxides (NO_x) are produced when coal is used in electrical utilities. The Barapukuria thermal power plant is one hydraulic power plant with SO_2, NO_x, and PM emissions under permissible limits. When it comes to air pollutants, notably PM, during the dry season, road dust and soil dust from various power plant-related projects play a significant role (DOE, 2019a).

3.5 Transboundary Air Pollution

Bangladesh is bordered by the heavily polluted nation of India on three sides (Fig. 1). Transboundary pollutants generally come from North-Western India, West Bengal, Nepal, and the surrounding regions, and they travel 200–500 kilometers to Bangladesh. 40% of the air pollution in Bangladesh is caused by transboundary PM from India's coal burning (Sakib, 2021; Rana et al., 2016), particularly between November and January. In addition, during October and November, burning agricultural fields in India produces smoke plumes that almost completely cover the Indo-Gangetic Plain (IGP) from West to East, including Bangladesh (Singh and Kaskaoutis, 2014), and can even travel through the Himalayan foothills (Bonasoni et al., 2020).

4 Link Between Meteorological Parameters and Atmospheric Particulate Matter

It is crucial to look at the properties of PM and their dependencies on other factors since several researches have shown that PM concentration is linked to negative health effects and a subsequent decline in air quality (Rahman et al., 2022). Numerous researches have mainly focused on the wind, temperature, and other meteorological factors for the change of PM levels since atmospheric dispersion is primarily responsible for the accumulation of PM in air. In the subsections that follow, we'll go through how particulate matter depends on meteorological characteristics and how those parameters affect particulate matter.
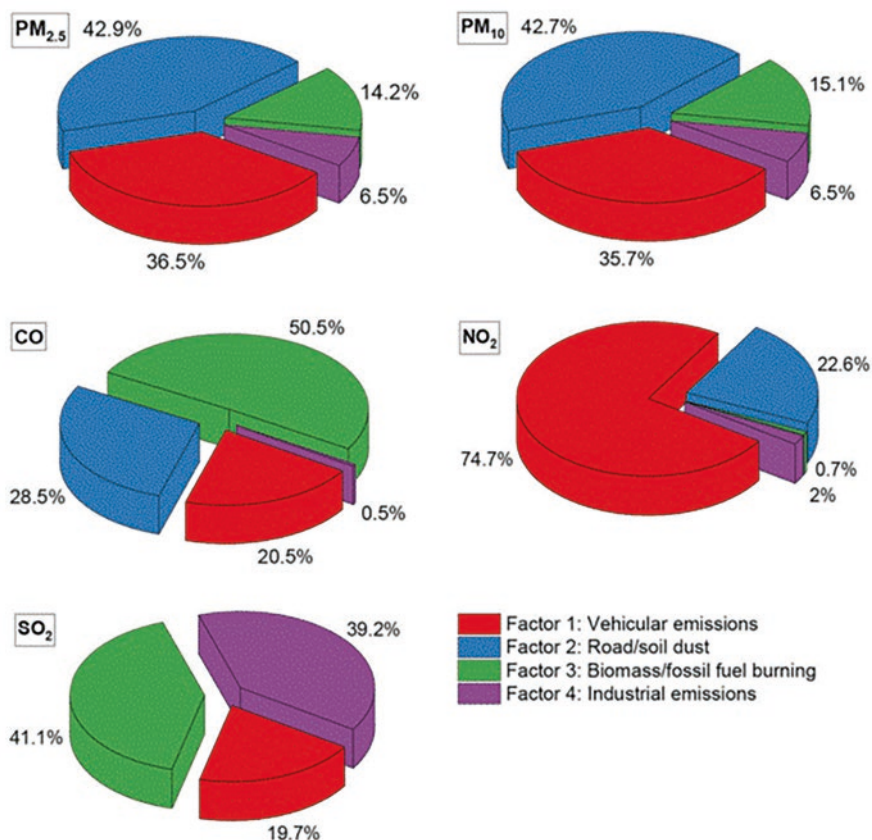
Fig. 1 Contribution of the major sources of air pollutants ($PM_{2.5}$, PM_{10}, CO, NO_2, and SO_2) in Bangladesh (Pavel et al., 2021)

4.1 Seasonal and Diurnal Variation

The seasonal and diurnal change of particulate matter in response to the variability of climatic conditions has been demonstrated by a good number of studies. Urban areas typically have the highest PM concentration in the winter and the lowest in the summer, whereas rural areas experience the highest PM concentration in the spring and the lowest in the winter. Peaks are caused by boundary layer height in urban areas during the winter and dust incidence in rural areas during the spring. Other research (Rahman et al., 2022; Kayes et al., 2019; Islam et al., 2022; Hoque et al., 2020; Hridoy et al., 2021) have found comparable seasonal variations in PM with greater concentrations in winter (December–March). Temporal trend of particulate matter in Dhaka city has been given in Fig. 2 which has been prepared based on six years of data (2013–2018). The lower PM concentrations in warmer months are
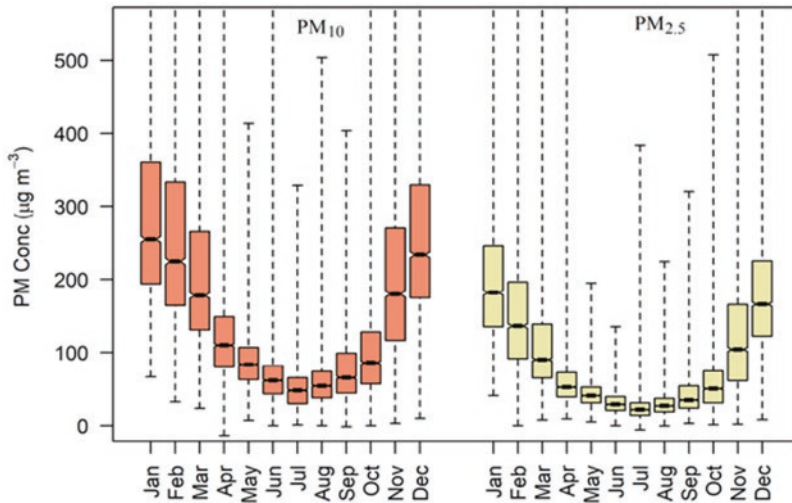
Fig. 2 Box-whisker plots of PM concentration in different months in Dhaka (Department of Environment, 2018)

linked to atmospheric dispersion due to increased wind speeds and wider mixing layer heights (Khan et al., 2016; Ferrero et al., 2010).

4.2 Temperature

Due to increased photochemical activity at higher temperatures, several studies found a positive relationship between temperature and particulate matter (Islam et al., 2022). According to several studies (Rahman et al., 2022; Hridoy et al., 2021; Hoque et al., 2020), the use of coal for space heating, increased household heating, and the production of stagnant air conditions in winter have all been linked to a negative association between PM and temperature. When the temperature regularly surpasses 29 °C and the humidity is high, high summer $PM_{2.5}$ levels are seen.

4.3 Rainfall

Precipitation reduces PM by scavenging (Kayes et al., 2019; Islam et al., 2022). It has been found to have a larger impact on PM_{10} than $PM_{2.5}$ (Islam et al., 2022). According to research, rainfall duration has a greater impact on PM concentration than rainfall volume (Rahman et al., 2022).

4.4 Wind Speed

Wind speed is the most important element in driving PM concentration, particularly at roadside locations (Hridoy et al., 2021; Hoque et al., 2020). Because of dilution, higher wind velocity lowers PM concentration. However, when a threshold value is exceeded, wind speed increases, showing that the diluting impact of wind speed is superseded at this point by the resuspension of road dust (Kayes et al., 2019; Islam et al., 2022). The buildup of $PM_{2.5}$ is shown to be positively influenced by low wind speed, but PM_{10} is influenced by high wind speed that exceeds a threshold due to long-distance transport (Hridoy et al., 2021). According to Cox and Chu (2016), calm winds are related to the highest $PM_{2.5}$ concentration.

4.5 Wind Direction

PM concentration is significantly influenced by both wind direction and speed. According to a number of studies (Begum et al., 2013, 2016; Islam et al., 2022) conducted in Bangladesh, the north-easterly wind in Bangladesh contributes to high PM concentration in the winter, which worsens the air quality.

4.6 Mixing Height

The majority of studies found bimodal diurnal fluctuation, with particulate matter concentration reaching its maximum peak in the morning. The morning's atmospheric stability circumstances (low wind speed and temperature inversion) produce a buildup of air particulates in the lower atmospheric layer that results in a foggy situation (Hridoy et al., 2021).

4.7 Relative Humidity

An indication of atmospheric moisture, such as relative humidity, should be considered when analyzing meteorological factors that impact particulate matter concentrations in atmosphere. According to the majority of research (Rahman et al., 2022; Hridoy et al., 2021), relative humidity continues to be positively linked with PM concentration (Table 3). High humidity levels have been linked to highest PM concentrations (Islam et al., 2022).

Table 3 Summarization of key meteorological factors that drive atmospheric particulate matter concentration and the rationality behind these mechanisms (Islam et al., 2022)

Parameters	Relation within particulate matter	Reasons behind such relation
Temperature	Positively related	High temperatures are conductive to chemical reactions in the atmosphere and cause the creation of SO_X at higher states.
	Negatively related	The creation of stagnant air conditions in the winter, increased space heating.
Rainfall	Negatively related	Moist deposition, scavenging effect.
Wind speed	Negatively related within $PM_{2.5}$	Ultrafine particulates are diluted by high wind speed, whereas ultrafine particulate formation is aided by low wind speed.
	Positively related with coarser particulate at wind speed >9 m/s	Road dust's resuspension imposes the dilution impact and long-range transport's contribution.
Boundary layer height	Negatively related	Greater dispersion is caused by higher mixing/ boundary layer heights.
Solar radiation	Positively related	Nitrate particulate generation, improved photochemical reaction, and secondary aerosol production.
Relative humidity	Positively related to sulfate and nitrate	High humidity speeds up the oxidation of SO_2 inside clouds and accelerates the creation of nitrates (ammonium).
	Inversely related to OC, EC	Reduced OC and EC production at high humidity, absorption of moisture, and subsequent particulate settling down.

5   Management Approaches to Mitigate Air Pollution

Two specific Sustainable Development Goals (SDG) 3 and SDG 11 must be addressed if we want to materialize the importance of air control management because both goals explicitly mention air pollution. These two SDGs are among the 17 Sustainable Development Goals (SDGs). In addition to mentioning the two SDGs, this problem also involves a number of drivers and associated sustainability consequences that link about 14 of the 17 SDGs of the UN (Khuda, 2020). These aims, targets, and indicators are linked to a number of causes, but the best way to ensure clean air is to use an integrated strategy to manage air quality. If not, the SDGs' vision would remain mostly unrealized and useless. The Bangladesh government and all municipal corporations might take into account the following approaches to lessen air pollution in Bangladesh.

- Since air pollution in Dhaka city often reaches dangerous levels between December and March and fluctuates depending on the season, an effective air control plan must be distinct from the government's other general management strategies.

- The key pollutants must be identified quickly for the development plan for air quality control. A solution for a certain region or place may be formed by identifying the pollutants and health risks brought on by poor air quality in that area or location.
- The rising amount of dust particulates, together with other air pollutants, is now posing a substantial health risk to the people living in Dhaka city, which is a major issue. For this reason, a cost-effective management system that incorporates control measures in light of lowering the sources of dust and waste points should be set up right away. Other significant source locations, such as building sites, brickfields, the whole Dhaka city transportation system, etc., should be taken into account in order to satisfy the SDG targets and indicators.
- The residents of a particular area can contribute significantly individually or collectively to the reduction of air pollution. By driving less and more carefully, utilizing fuel-efficient vehicles, public transportation, walking, cycling, and other methods, people may significantly reduce air pollution.
- However, the development of an integrated system is necessary to guarantee a better response in the control of municipal air quality. The Bangladesh government has some good policies and plans for managing air quality, but there aren't any good programs for implementation and monitoring. However, they are crucial not just for reducing air pollution but also for giving source point owners access to the data they want for continued system improvement and monitoring.
- Typically, Bangladeshi decision-makers operate the air control system in accordance with a traditional methodology. This system puts up a set of requirements for pollutants in the manufacturing sectors. This could be a success for the industrial sector alone, but the government can take it a step further by penalizing all polluters and offering incentives to stimulate the economy to reduce emissions.
- While there is now just a limited incentive system in place, it might be expanded to include a wide range of programs and activities, including tax incentives for reducing pollution, subsidies for waste treatment, rebate programs for trash disposal, etc.

6 The Role of the Government in Bangladesh Against Atmospheric Air Pollution

According to the government of Bangladesh's seventh five-year plan, urban $PM_{2.5}$ concentration was planned to reduce from 78 gm/m^3 in 2013 to 73 gm/m^3 in 2020 (Khandker et al., 2022). The government had put in place the Clean Air Program, Cleaner Fuel and Transport Standards, and Strict Brick Kiln Act 2013 enforcement to accomplish this aim.

6.1 Brick Kilns

The Brick Manufacturing and Kiln Construction (Control) Act 2013 changed conventional brick kilns into more energy-efficient ones in order to minimize air pollution, particularly particulate matter (PM), in urban air (DOE, 2019a). Improved Zigzag Kilns (IZKs) can replace Fixed Chimney Kilns (FCK) by burning less coal and emitting less particulate matter, and water scrubber systems can absorb particulate matter to cut emissions. The infrastructure Development Company Limited (IDCOL), the DOE, World Bank, Asian Development Bank (ADB), and other donor organizations have provided financial and technical assistance for this initiative. Additionally, it supports initiatives for solar energy, biogas, home energy, and rural electrification (ESMAP, 2019).

6.2 Motor Vehicles and Fuels

The 2011 motor vehicle legislation regulating car emissions regulations was published by the government of Bangladesh. At roadside checkpoints, vehicles are put through testing to reduce vehicle emissions (DOE, 2019b). In addition, the government decreased import taxes for modern automobiles and prohibited the entry of vehicles older than five years. In order to match the Euro 3 standard, the 1977 car emissions standard was improved in 2005 and again in 2014. The Chittagong oil refinery was updated to reduce the sulfur level in the oil to below 500 ppm, which is important for fuels. Compressed natural gas (CNG) was substituted for gasoline, lowering the amount of sulfur in the air (DOE, 2019b), which improved the air quality in Dhaka.

The government of Bangladesh has implemented "The Air Pollution Rules 2022 under section 20 of the Bangladesh Conservation Act, 1995 to improve the air quality status of Bangladesh."

6.3 Industry

Industries and projects are divided into four classifications for environmental clearance: Green, Amber-A, Amber-B, and Red. The government has exempted equipment and replacement parts for renewable energy projects, including energy audits, from 5% VAT and 5-year income tax. In an effort to lessen industrial pollution and boost electricity supply, Bangladesh Bank, the country's national bank, introduced the Bangladeshi Taka (BDT) 2 billion green banking refinancing program in August 2009 (UNEPA, 2021). As a result, Bangladesh is seeing an uptick in green financing (Rana & Siddique, 2019). According to Macgregor et al. (2016), the Bangladesh

government has contributed 7% of public spending toward green development initiatives.

6.4   Clean Cook Stoves

1.7 million improved cook stoves have been installed as part of the Bangladesh Improved Cook Stoves Program. People in a chosen coastal hamlet in Bangladesh get technical and financial assistance from the Bangladesh Environment and Development Society (BEDS). The villages now have solar lighting, solar panels, solar dwellings, solar generators, and fuel-efficient cooking stoves (BEDS, 2020).

From 2020, Dhaka routinely placed as the world's highest or the second-most polluted city, and Bangladesh rose to become the most polluted nation in the world (Khandker et al., 2022). In order to reduce air pollution, the government has enacted and revised rules, developed policies and strategic plans, and carried out a number of sector-specific programs and initiatives. The information produced by the Continuous Air Monitoring Stations (CAMS) is used to describe the types and levels of city pollution, to track national pollution trends, to build air models, and to support the Air Quality Index for the general public.

Besides, replacing brick with cement block for construction purpose is one of the best ways to reduce the concentrations of PM as brick kiln are the main sources of PM pollution in Bangladesh. Moreover, introduction of mass transport. especially train, metro, and tram within the metropolitan cities could reduce PM pollution. Running of high-speed trains from the surrounding and distant districts toward Dhaka will eventually reduce the number of vehicles especially buses and private cars, which will help to reduce PM pollution. Sweeping and watering of roads in the morning will help to settle down pollutants. Finally, regular monitoring and inspection, research activities, and public awareness will support to minimize particulate matter pollution.

References

Arnab, I. Z., Ali, T., Shidujaman, M., & Hossain, M. M. (2021). Consideration of environmental effect of power generation: Bangladesh perspective. *Energy and Power Engineering, 5*(04), 1521.

Asimakopoulos, D. N., Flocas, H. A., Maggos, T., & Vasilakos, C. (2022). The role of meteorology on different sized aerosol fractions (PM_{10}, $PM_{2.5}$, $PM_{2.5\text{-}10}$). *Science of the Total Environment, 419*, 124.

BEDS. (2020). *Echo Village Project in Bangladesh, 2015–2020*. Available from: https://www.bedsbd.org/projects/ongoing-projects/1. Accessed on 17.10.2021.

Begum, B. A., & Hopke, P. K. (2018). Ambient air quality in Dhaka Bangladesh over two decades: Impacts of policy on air quality. *Aerosol and Air Quality Research, 18*(7), 1910–1920. https://doi.org/10.4209/aaqr.2017.11.0465

Begum, B. A., Hopke, P. K., & Markwitz, A. (2013). Air pollution by fine particulate matter in Bangladesh. *Atmospheric Pollution Research, 4*(1), 75–86.

Begum, B. A., Saroar, G., Nasiruddin, M., & Biswas, S. K. (2014). Ground-level concentration of ozone in ambient air in Chittagong (Bangladesh) City. *Bangladesh Journal of Scientific and Industrial Research, 47*(1), 83–88.

Begum, B. A., Hopke, P. A., & Markwitz, A. (2016). An approach for quantitative estimation of long range transport of fine particulate matter entering Bangladesh. *Journal of Integrated Science and Technology, 2*, 34–38.

Bonasoni, P., Laj, P., Marinoni, A., Sprenger, M., Angelini, F., Arduini, J., et al. (2020). Atmospheric brown clouds in the Himalayas: First two years of continuous observations at the Nepal Climate Observatory-Pyramid (5079 m). *Atmospheric Chemistry and Physics, 10*(15), 7515–7531.

CASE. (2018). *Ambient air quality in Bangladesh. Clean air and sustainable environment project*. Department of Environment 2018, Agargaon, Dhaka. Available from: http://case.doe.gov.bd/index.php?option=com_content&view=article&id=5&Itemid=9. Accessed on 07.09.2021.

Cox, W. M., & Chu, S. H. (2016). Assessment of interannual ozone variation in urban areas from a climatological perspective. *Atmospheric Environment, 30*(14), 2615–2625.

Department of Environment. (2018). *Ambient air quality of Bangladesh. Clean air and sustainable environment project*. Ministry of Environment, Forest and Climate Change. Government of the Peoples' Republic of Bangladesh.

DOE. (2019a). *Sources of air pollution in Bangladesh*. Brick kiln & Vehicle emission Scenario. Department of Environment. Agargaon, Dhaka.

DOE. (2019b). *Air pollution reduction strategy for Bangladesh, final report, 2012*. Department of Environment. Available from: https://www.semanticscholar.org/paper/Air-Pollution-Reduction-Strategy-for-Bangladesh/a162734badbb64d530d55708226e4eacb4d12a39

ECR. (1997). *Environment Conservation Rules, 1997*. Ministry of Environment and Forest, Government of the People's Republic of Bangladesh.

ESMAP. (2019). *Bangladesh offers Successful Model of Clean Cooking Program: The Energy Sector Management Assistance Program (ESMAP): The World Bank: Issue −17*. Available from:https://documents1.worldbank.org/curated/en/571731573763114047/pdf/Bangladesh-Offers-Model-ofSuccessful-Clean-Cooking-Program.pdf. Accessed on 01.07.2021.

Ferrero, L., Perrone, M. G., Petraccone, S., Sangiorgi, G., Ferrini, B. S., Lo Porto, C., et al. (2010). Vertically resolved particle size distribution within and above the mixing layer over the Milan metropolitan area. *Atmospheric Chemistry and Physics, 10*, 3915–3932.

Hien, P. D., Bac, V. T., Tham, H. C., Nhan, D. D., & Vinh, L. D. (2022). Influence of meteorological conditions on PM2. 5 and PM2. 5− 10 concentrations during the monsoon season in Hanoi, Vietnam. *Atmospheric Environment, 36*(21), 3473–3484.

Hoque, M. M., Ashraf, Z., Kabir, H., Sarker, E., & Nasrin, S. (2020). Meteorological influences on seasonal variations of air pollutants (SO2, NO2, O3, CO, PM2. 5 and PM10) in the Dhaka megacity. *American Journal of Pure and Applied Biosciences, 2*(2), 15–23.

Hossen, M. A., & Hoque, A. (2016). Variation of ambient air quality scenario in Chittagong City: A case study of air pollution. *Journal of Civil Construction and Environmental Engineering, 3*(1), 10.

Hou, X., Zhu, B., Kumar, K. R., & Lu, W. (2019). Inter-annual variability in fine particulate matter pollution over China during 2013–2018: Role of meteorology. *Atmospheric Environment, 214*, 116842.

Hridoy, A. E. E., Mohiman, M. A., Tusher, S. M. S. H., Nowraj, S. Z. A., & Rahman, M. A. (2021). Impact of meteorological parameters on COVID-19 transmission in Bangladesh: A spatiotemporal approach. *Theoretical and Applied Climatology, 144*, 273–285.

IQAir. (2021). *Air quality in Dhaka*. Retrieved from https://www.iqair.com/bangladesh/dhaka. 29 May 2021.

Islam, M. M., Afrin, S., Ahmed, T., & Ali, M. A. (2015). Meteorological and seasonal influences in ambient air quality parameters of Dhaka city. *Journal of Civil Engineering, 43*(1), 67–77.

Islam, N., Toha, T. R., Islam, M. M., & Ahmed, T. (2022). The association between particulate matter concentration and meteorological parameters in Dhaka, Bangladesh. *Meteorology and Atmospheric Physics, 134*(4), 64.

Kayes, I., Shahriar, S. A., Hasan, K., Akhter, M., Kabir, M. M., & Salam, M. A. (2019). The relationships between meteorological parameters and air pollutants in an urban environment. *Global Journal of Environmental Science and Management, 5*(3), 265–278.

Khan, M. B., Masiol, M., Formenton, G., Di Gilio, A., de Gennaro, G., Agostinelli, C., & Pavoni, B. (2016). Carbonaceous $PM_{2.5}$ and secondary organic aerosols across the Vento region (NE Italy). *Science of the Total Environment, 52*, 172–181.

Khandker, S., Mohiuddin, A. S. M., Ahmad, S. A., McGushin, A., & Abelsohn, A. (2022). Air pollution in Bangladesh and its consequences.

Khuda, K. E. (2020). Causes of air pollution in Bangladesh's capital city and its impacts on public health. *Nature, Environment and Pollution Technology, 19*, 1483–1490.

Leung, D. M., Tai, A. P., Mickley, L. J., Moch, J. M., van Donkelaar, A., Shen, L., & Martin, R. V. (2018). Synoptic meteorological modes of variability for fine particulate matter (PM 2.5) air quality in major metropolitan regions of China. *Atmospheric Chemistry and Physics, 18*(9), 6733–6748.

Li, X., Song, H., Zhai, S., Lu, S., Kong, Y., Xia, H., & Zhao, H. (2019). Particulate matter pollution in Chinese cities: Areal-temporal variations and their relationships with meteorological conditions (2015–2017). *Environmental Pollution, 246*, 11–18.

Macgregor, J., Firoz, R., Uddin, N., Islam, S., & Sattar, M. A. (2016). Green growth diagnostic–Bangladesh. *Economic Dialogue on Green Growth*.

Nahar, N., Mahiuddin, S., & Hossain, Z. (2021). The severity of environmental pollution in the developing countries and its remedial measures. *Earth, 2*(1), 124–139.

Pavel, M. R. S., Zaman, S. U., Jeba, F., Islam, M. S., & Salam, A. (2021). Long-term (2003–2019) air quality, climate variables, and human health consequences in Dhaka, Bangladesh. *Frontiers in Sustainable Cities, 52*, 1–18.

Rahman, M. M., Shuo, W., Zhao, W., Xu, X., Zhang, W., & Arshad, A. (2022). Investigating the relationship between air pollutants and meteorological parameters using satellite data over Bangladesh. *Remote Sensing, 14*(12), 2757.

Rana, M., & Siddique, M. A. B. (2019). Green banking in Bangladesh: A descriptive analysis. *IOSR Journal of Business and Management, 21*(7), 57–67.

Rana, M. M., Mahmud, M., Khan, M. H., Sivertsen, B., & Sulaiman, N. (2016). Investigating incursion of transboundary pollution into the atmosphere of Dhaka, Bangladesh. *Advances in Meteorology, 2016*, 1.

Rouf, M. A., Nasiruddin, M., Hossain, A. M. S., & Islam, M. S. (2021). Trend of particulate matter PM 2.5 and PM 10 in Dhaka City. *Bangladesh*. *Journal of Scientific and Industrial Research, 46*(3), 389–398.

Sakib, S. N. (2021). Bangladesh: Air pollution engulfs lives, environment. *Experts attribute situation to transboundary air pollution, unplanned development and construction works*; Anadolu Agency: Dhaka, Bangladesh.

Singh, R. P., & Kaskaoutis, D. G. (2014). Crop residue burning: A threat to South Asian air quality. *Eos, Transactions American Geophysical Union, 95*(37), 333–334.

Trivedi, D. K., Ali, K., & Beig, G. (2018). Impact of meteorological parameters on the development of fine and coarse particulates over Delhi. *Science of the Total Environment, 478*, 175–183.

UNEPA: Air Quality Policy of Bangladesh. (2021). *The table is prepared based on research that UNEP conducted in 2015, in response to Resolution 7 of the UNEPA 1* https://wedocs.unep.org/bitstream/handle/20.500.11822/17093/Bangladesh.pdf?isAllowed=y&sequence=1. Accessed on 06.07.

USEPA. (2018). *United States Environmental Protection Agency*. Retrieved from https://www.epa.gov/pmcourse/what-particulate-pollution. 10 Oct 2020.

WHO. (2018). *Ambient (Outdoor) air pollution*. Retrieved from https://www.who.int/newsroom/fact-sheets/detail/ambient-(outdoor)-air-quality-and-health. 9 Oct 2020.

Zhao, X., Zhang, X., Xu, X., Xu, J., Meng, W., & Pu, W. (2020). Seasonal and diurnal variations of ambient PM2. 5 concentration in urban and rural environments in Beijing. *Atmospheric Environment, 43*(18), 2893–2900.

Review of the Role of Aerosols in the Spread of COVID-19

Nishi Srivastava

1 Introduction

In December 2019, Wuhan, China, received the first reports of coronavirus disease 2019 (COVID-19) because of SARS-CoV-2 (Severe Acute Respiratory Syndrome Coronavirus 2) and is known to spread from person-to-person via droplets, aerosols, and fomites (Chen et al., 2020; Gautam, 2020a, b; Wang & Du, 2020). COVID-19 was described as a highly contagious pandemic. The COVID-19 disease has been linked to millions of confirmed cases and lacs of death cases by May 2020 (WHO, 2020b). Fever, cough, myalgia, and weariness are prominent signs of a sickness that is brought on by the COVID-19 virus, which causes severe acute respiratory disease (Blessy et al., 2023; Huang et al., 2020; Judson & Munster, 2019; Nicas et al., 2005). Contrary to earlier recommendations (WHO, 2020b), there is mounting proof that SARS-CoV-2 is disseminated mainly through surface deposits (fomites), airborne particles, as well as through bigger droplets from coughing or sneezing (Morawska & Cao, 2020). Virus particles are generally disseminated whenever an infected person speaks, breathes, coughs, or sneezes. It is known that these viral particles are contained in drops of saliva, mucus, and water. The life of these drops in the environment relies on their size. Larger drops splash down nearby as droplets because they descend quicker than they evaporate (Grayson et al., 2016; Liu et al., 2016). Different paths exist for infectious pathogens to travel from their reservoir to a liable host. Classifications of the modes of transmission of various infectious agents have been documented in the literature. A taxonomy of virus transmission methods has been provided by Morawska (2006), encompassing human-to-human spread, aerosol transmission, endogenous infection, and community transport. Although droplet and aerosol transmission channels are thought to be the most important for spreading respiratory viruses, their importance in disease

N. Srivastava (✉)

Department of Physics, Birla Institute of Technology, Mesra, Ranchi, Jharkhand, India

© The Author(s), under exclusive license to Springer Nature Switzerland AG 2024
S. Gautam et al. (eds.), *Aerosol Optical Depth and Precipitation*,
https://doi.org/10.1007/978-3-031-55836-8_10

transmission is yet unknown (Morawska & Cao, 2020; Shiu et al., 2019). Based on the particle size, more especially the aerodynamic diameter, respiratory particles can frequently be separated as droplets or aerosols (Hinds, 1999). One can argue that, in contrast to bigger droplets, fine particles may present a more significant risk of the COVID-19 disease spreading amongst several sensitive animals distantly located. Aerosols of smaller drops disappear more quickly, hang about longer in the atmosphere, and travel further than drops. However, it has been demonstrated that viral illness epidemics transmitted by aerosols are less severe than anticipated due to the weakening and deactivation of viruses with a larger duration in the air (Shiu et al., 2019).

SARS-CoV-2's viability in aerosols and whether the infectious virus could spread from viral RNA was initially questioned (Anderson et al., 2020; Lewis, 2020). Aerosol transmission does not require coughing and can instead occur through regular breathing (Borak, 2020; Wei & Li, 2016), making it conceivable for asymptomatic people who are known to be COVID-19 carriers to spread the virus to others through this method (Asadi et al., 2020; Chen et al., 2020; Sugano et al., 2020). With a half-life of around an hour indoors, studies have demonstrated that the virus remains alive in aerosols (Ren et al., 2020; Schuit et al., 2020; Smither et al., 2020; Van Doremalen et al., 2020). However, the relative relevance of aerosol transmission compared to other pathways is still debatable (Buonanno et al., 2020; Jones, 2020; Vuorinen et al., 2020) and may vary depending on the environment. The precautionary principle requires that actions to obstruct this transmission path be taken with zeal (Morawska & Milton, 2020). The aerosol's physical properties differ in indoor and outdoor environments, and to quantify the behavior of bigger droplets, various extra containment techniques are required (Anderson et al., 2020; Jayaweera et al., 2020; Morawska et al., 2020). The accumulation of infectious aerosols in enclosed rooms with inadequate ventilation or excessive recirculation may also help to explain why asymptomatic people, including children, are a component of the transmission chain (Sugano et al., 2020), in addition to the significance of exposure time (Kumar et al., 2023; Vuorinen et al., 2020). The transmission of aerosols and big droplets can be slowed by social isolation (Halloran et al., 2012) and adequately fitting masks (Konda et al., 2020). However, further safety measures from aerosols are also required.

This chapter aims to investigate aerosols' possible role in the dispersal of COVID-19. The chapter is organized in the manner described below: The introduction to COVID-19, introduction to aerosols with emphasis on bioaerosols, various modes of transmission of COVID-19, the role of aerosol in its spread, and lastly, conclusions.

2 SARS-CoV-2 Virus: COVID-19

The highly contagious and infective Severe Acute Respiratory Syndrome Coronavirus 2 virus has caused an epidemic of severe respirational illness known as "coronavirus disease 2019", posing an extreme risk to public health and safety (Hu et al., 2021). The varied group of viruses known as coronaviruses can infect humans and cause respiratory diseases with varying severity in people. In Wuhan, China, at the end of 2019, a new coronavirus known as SARS-CoV-2 occurred, expanding an uncommon viral pneumonia epidemic. This recent coronavirus illness was highly contagious and has quickly spread worldwide (Hui et al., 2020; Wu et al., 2020). An exceptional threat to global public health has been posed by the ongoing COVID-19 outbreak (Deng & Peng, 2020; Han et al., 2020). Several hospitals in Wuhan reported groups of patients with pneumonia of unknown origin in late December 2019. The majority of the first few recorded hospitalized patients had epidemiological ties to Huanan Seafood Wholesale Market, a wet market in the heart of Wuhan that sells living animals along with seafood, including poultry and wildlife (Deng & Peng, 2020; Jiang et al., 2020). A retrospective examination indicates that the first case appeared on December 8, 2019 (Wu & McGoogan, 2020). The World Health Organization (WHO) and the Wuhan Municipal Health Commission both received notice of a pneumonia outbreak on December 31. Soon, this new coronavirus pneumonia affected other cities in Hubei province and other regions of China. The WHO announced this coronavirus as a public health crisis of global concern in January 2020. The coronavirus was designated "SARS-CoV-2" by the International Committee on Taxonomy of Viruses and "COVID-19" by the WHO (Coronaviridae Study Group, 2020). The rapid global spread of COVID-19 was made possible by the immediate transmission efficacy of SARS-CoV-2 and the prevalence of international travel. The WHO formally categorized the global COVID-19 epidemic as a pandemic in March 2020 (WHO, 2020a).

3 Aerosols

The SARS-CoV-2 in inhaled aerosols has a significant role in the propagation of COVID-19. Aerosols are suspended solid or liquid particles in the air and are produced by natural or man-made activities (Judson & Munster, 2019; Tellier, 2009). The different aerosols in the atmosphere come from various sources and paths and are made of different materials. Dust, sea salt, carbonaceous aerosols, sulfate and nitrate aerosols, non-sea salt aerosols, and biogenic aerosols are prime aerosols present in the environment. All the aerosols suspended in the air can act as carriers for the coronavirus, and coronaviruses can also be suspended in the air. The suspended living organisms in the air are called bioaerosols or biological aerosols. Bioaerosol plays an essential role in the spread of contagious diseases. We have briefly discussed bioaerosols in the following paragraphs.

Biogenic aerosols are particles from plants and animals released into the atmosphere. These aerosols include bacteria, algae, viruses, protozoa, and fungi, which have diameters of less than 1 μm, as well as pollen, spores, bronchoscopes, and pieces of animals and plants that range in size from 1 μm to 250 μm. Regarding health-related problems, bioaerosols pose a more significant threat than aerosols' problems with radiative forcing.

Indoor air quality significantly impacts the transmission of infectious diseases among people. There are both direct and indirect paths used by bioaerosols, which are the cause of pandemic transmission. Infectious aerosols can bend around obstacles and travel great distances indoors, according to simulations by Kudryashova et al. (2021). Infected droplets are released into the environment via respiratory processes like breathing, sneezing, talking, or coughing, albeit the specific infected bioaerosols released during these processes can differ. Although extensive study is lacking for COVID-19, recent analysis demonstrates that bioaerosols are crucial for SARS-CoV-2 transmission. Although this work was conducted on animals, preliminary research (Bao et al., 2020) revealed that SARS-CoV-2 spreads readily through bioaerosols. Bioaerosol transmission is an important method of virus transmission for SARS-CoV-2.

Given that bioaerosols are a crucial means of transmission for COVID-19, the WHO emphasizes the need for ventilation in combating the illness. Droplets fall swiftly on the surface under gravity and are unaffected by ventilation in the case of transmission through the droplet. Aerosol concentrations are significantly affected by ventilation, and there is strong evidence that this disease is spread via aerosols.

4   Mode of Transmission and Origin

The present section discusses the various possible modes of transmission of the COVID-19 virus. Multiple ways of transmission may contribute to the spread of COVID-19, which involves physical contact, fecal–oral, through blood transmission, fomite transmission, to babies from mother during pregnancy, airborne materials, and animal to human. Different paths exist for infectious pathogens to travel from their original reservoir to a vulnerable host. In the literature, numerous infectious agents have been categorized according to their transmission routes. Morawska (2006) proposed a taxonomy of virus transmission techniques that included person-to-person, airborne, fomites, endogenic infection, and shared vehicles. Although droplet and aerosol transmission pathways are crucial for transmitting respiratory viruses, research on their role in spread of disease is continuing (Morawska & Cao, 2020; Shiu et al., 2019).

Although the primary source of aerosols and droplets is direct transmission from an infected person(s). Other situations, such as medical procedures, surgeries, infected water, and fecal–oral transmission, also produce aerosols, contaminated with infectious pathogens (Morawska, 2006). Influenza viruses, rhinoviruses, coronaviruses, respiratory syncytial viruses, and parainfluenza viruses are documented

as the most typical. Several viruses, such as influenza, rhino, corona, respiratory syncytial, and parainfluenza viruses, cause respiratory infection through aerosol transmission (Morawska, 2006). Three possible ways for the influenza virus to spread are suggested by Tellier (2009): aerosol transmission, droplet transmission, and from infected hands. Judson and Munster (2019) offer a different classification, sometimes called airborne transmission to define the illness disseminated by aerosols and tiny droplets, and the term droplet transmission to characterize contamination by bigger droplets. The definition of "airborne transmission" provided by Morawska (2006) and the one made by Judson and Munster (2019) are very similar. Potential infection paths include direct touch and fomite transfer caused by aerosol-generating medical procedures (Judson & Munster, 2019). When an infected patient sneezes, talks, or coughs, huge droplets are directly sprayed into a vulnerable host's conjunctiva or mucous membranes, causing droplet transmission (Boone & Gerba, 2007; Nicas et al., 2005). Meanwhile, contact transmission can occur through direct contact between a contaminated source and a vulnerable host, and through indirect means (Brankston et al., 2007; Tellier, 2006). Detailed discussion regarding the prime mode of transmission of COVID-19 is given in this section.

4.1 Contact Transmission

Infection can be caused by saliva, respiratory secretions, or respiratory droplets emitted when a contaminated person coughs, sneezes, or talks. Infected secretions may contain SARS-CoV-2, which is contagious directly or indirectly through contact with an infected person. When a person is close to an infected person who exhibits respiratory symptoms or when conversing, respiratory droplets containing the virus may enter a vulnerable person's mouth, nose, or eyes and cause infection. Transmission via indirect contact, in which a susceptible host comes into contact with a contaminated object or surface, is also conceivable.

4.2 Surface Transmission

It is believed that COVID-19 viruses travel directly from one person to another through the air, usually during extended close contact, but it is also possible that fomites may be involved. Fomites are environmental items that can support infectious virions and serve as a means of transmitting diseases from one person to another. For fomite transmission to occur, an adequate amount of contagious virus must be released into the environment, and it must remain ex vivo at sufficiently high titers to cause an infection when exposed to a susceptible person's mucosal surfaces.

Ambient temperature, humidity, and surface type govern the viable SARS-CoV-2 virus and RNA that can be found on some surfaces for hours to days. This is

especially true in high concentrations in COVID-19 healthcare facilities. Fomites gather SARS-CoV-2-contaminated droplets; if a vulnerable host touches one of these surfaces, they will become infected. However, some droplets expelled from an infected person change into aerosols and end up in the atmosphere (Morawska, 2006). Such virus-filled aerosol particles can potentially propagate the disease by infecting those who breathe them in.

4.3 Aerosol/Airborne Transmission

Additionally, there have been several transport events where bigger droplets evaporate and shrink into smaller particles known as droplet nuclei. Thus, the terms "aerosol," "bioaerosol," and "droplet nuclei" are used interchangeably in this research to refer to aerosol particles that have viruses encapsulated in them. The mechanism for the generation of droplets and the conversion of droplets into aerosols needs extensive research to understand the mechanisms involved. The term "airborne transmission" refers to the propagation of droplet nuclei or aerosols that retain their contagious properties after being suspended in the air for a lengthy time period and over great distances (WHO, 2014). Aerosols produced during medical treatments can spread SARS-CoV-2 (WHO, 2020c). Without aerosol-generating techniques, WHO and the scientific community have been actively debating and assessing whether SARS-CoV-2 may also be transmitted by aerosols, particularly in indoor environments with inadequate ventilation. According to various research, airborne transmission is the primary method by which viral infections, such as COVID-19, propagate across the community (Asadi et al., 2020; Bai et al., 2020; Morawska, 2006; Nicas et al., 2005; Prather et al., 2020; Weber & Stilianakis, 2008).

The typical particle size of droplets and aerosols has been the subject of various disputes (Shiu et al., 2019). According to the WHO, particles larger than 5 µm are droplets, and those smaller than 5 µm are aerosols or droplet nuclei. However, fine particles, i.e., particles with a diameter below 5 µm (Newman, 2009), can successfully penetrate the lower regions of the respiratory system, i.e., the tiny bronchi and pulmonary alveoli. Inhalable aerosols must comprise particles or liquid droplets smaller than 20 µm. The particles smaller than 5 µm are referred to as "droplet nuclei," and particles larger than 20 µm as "droplets" in the airborne transmission of diseases by liquid aerosol particles (Killingley & Nguyen-Van-Tam, 2013).

According to other hypotheses, particles smaller than 20 µm are considered aerosols (Gralton et al., 2011; Nicas et al., 2005; Tellier, 2009). Large droplets are confined in the upper airways, while small aerosols are more likely to be inhaled deeply into the lung, infecting the alveolar tissues of the lower respiratory tract (Thomas, 2013).

Many people have felt that droplets are more effective in spreading the disease than aerosols; thus, over time, research efforts have been concentrated on droplet transmission mechanism (Morawska & Cao, 2020; Wang & Du, 2020). But recently, data have been presented to disprove the prior theory and predict that aerosols also

play a crucial role in virus transport (Morawska & Cao, 2020; Wang & Du, 2020). As a result, many experts, including the WHO (Morawska & Cao, 2020), appear to be guessing and perplexed about the SARS-CoV-2 virus's transmission mechanisms. This is an unresolved contradiction since no clear research has been done to distinguish between droplet and aerosol transmission of viruses.

Evaporation, contact with other particles, transport, and removal from the air through deposition on solid surfaces are the physicochemical processes determining airborne aerosols' fate (Morawska, 2006). According to Baron and Willeke (2001), airborne particles are frequently affected by Brownian motion, gravity, electrostatic forces, thermal gradients, electromagnetic radiation, turbulent diffusion, and inertial forces. One of these methods, diffusion, is crucial for transmitting viruses when combined with other aerosol particles and particles with a lower submicrometer range (Baron & Willeke, 2001). Gravity overrides Brownian motion and governs the trajectory of large droplet movements (Cox, 1995). Smaller droplets frequently evaporate before touching the ground when the atmospheric conditions are normal, and the evaporated droplet remnants remain in the air for a very long time (Morawska, 2006). With the evaporation of liquid content, droplets usually convert into bioaerosols and remain suspended in the environment (Morawska, 2006). However, the amount of time a virus can survive in the atmosphere varies depending on the type of bioaerosol.

According to McCluskey et al. (1996), airborne droplets below 20 μm remain suspended in the air causing respiratory tract infection. However, droplets don't appear to stay in the air for very long before evaporating and becoming bioaerosol residues, which can linger in the atmosphere for a long time. The SARS-CoV-2 virus can survive in aerosols for 3 hours, but virus droplets are more stable and can survive for variable hours on plastic, stainless steel, copper, cardboard, and glass (van Doremalen et al., 2020).

2-m is recognized as the safe distance to prevent droplet transmission to a susceptible host; though thorough investigations are required to support this (Jayaweera et al., 2020). Recent studies conducted after the COVID-19 outbreak by Bourouiba (2020) and Loh et al. (2020) were consistent with Xie et al.'s (2007) findings that infected droplets can travel for more than 2 m during coughs and sneezes.

5 Effects of Environmental Conditions on Droplet and Aerosol's Behavior

Temperature, humidity, solar radiation, and ventilation are the most significant environmental elements that potentially affect the survivability of airborne microorganisms (Marthi, 1994). According to Kumar and Morawska's (2019) studies, various viruses are less than 100 nanometers in size. Environmental stressors may change the severity of bioaerosols before reaching a vulnerable host. The composition of the bioaerosols carrying the virus and their payload, as well as the physical

properties of the surrounding environment, all affect how well the virus-laden aerosols tolerate the environment (Schuit et al., 2020).

It is essential to investigate the impact of environmental conditions on the transmission of coronavirus because they significantly influence the extent of viral load in different geographical outdoor and indoor environments. As mentioned before, the other aerosols can also contribute significantly to the spread of COVID-19 by acting as host for the virus (Zhu et al., 2020). Such viral loads in an indoor setting are primarily propelled by local ventilation patterns' advective pressures to become airborne, and they disperse further by diffusion and dispersion mechanisms. The correlations between viral payloads resulting from various transmission pathways and environmental characteristics vary.

6   Protections Against the Spread of Aerosols and Drops

The transfer of droplets and aerosols severely affects healthcare professionals and caregivers handling COVID-19-infected patients; hence, it is crucial to protect them adequately. Facemasks are essential to avoiding the spread of the disease via droplets and aerosols from a source to a host. Facemasks are widely used to control and prevent virus transmission (Long et al., 2020). Various types of masks and respirators with varying degrees of efficacy are used globally to prevent COVID-19 virus infection.

Maintaining a minimal distance between an infected individual and a host is debatable. It is established based on scientific proof that even social separation would be promising in the fight against COVID-19. The use of masks can have two purposes: to prevent infectious droplets from an infected individual from entering the breathing system of a vulnerable host and prevent the escape of contagious substances from a patient. Mask use may be beneficial in preventing the spread of covid. However, this is debatable and not entirely feasible. The efficiency of various commercial masks in preventing the spread of infectious agents varies, as is well documented.

7   Conclusions

Airborne transmission is a significant pathway to spreading the SARS-CoV-2 pandemic along with the fomites and large droplet transmissions, though which way is most dominant is a matter of detailed research. The most crucial factor for getting infected is exposure to the infected surface or air. The viral load in the space with inadequate ventilation or insignificant recirculation can significantly increase the asymptomatic individuals or children in the transmission chain. Social isolation and correctly fitting masks both reduce the transmission of aerosols and large droplets, but additional safety precautions specific to aerosols are also necessary.

References

Anderson, E. L., Turnham, P., Griffin, J. R., & Clarke, C. C. (2020). Consideration of the aerosol transmission for COVID-19 and public health. *Risk Analysis, 40*, 902–907. https://doi.org/10.1111/risa.13500

Asadi, S., Bouvier, N., Wexler, A. S., & Ristenpart, W. D. (2020). The coronavirus pandemic and aerosols: Does COVID-19 transmit via expiratory particles? *Aerosol Science and Technology, 54*, 635–638.

Bai, Y., Yao, L., Wei, T., et al. (2020). Presumed asymptomatic carrier transmission of COVID-19. *Journal of the American Medical Association, 323*, 1406–1407.

Bao, L., Gao, H., Deng, W., Lv, Q., Yu, H., Liu, M., et al. (2020). Transmission of SARS-CoV-2 via close contact and respiratory droplets among hACE2 mice. *The Journal of Infectious Diseases, 222*, 551–555. https://doi.org/10.1093/infdis/jiaa281

Baron, P. A., & Willeke, K. (2001). *Aerosol measurement principles, techniques and applications* (2nd ed.). Wiley.

Blessy, A., John Paul, J., Gautam, S., et al. (2023). IoT-based air quality monitoring in hair salons: Screening of hazardous air pollutants based on personal exposure and health risk assessment. *Water, Air, and Soil Pollution, 234*, 336. https://doi.org/10.1007/s11270-023-06350-4

Boone, S. A., & Gerba, C. P. (2007). Significance of fomites in the spread of respiratory and enteric viral disease. *Applied and Environmental Microbiology, 73*(6), 1687–1696. https://doi.org/10.1128/AEM.02051-06. Epub 2007 Jan 12. PMID: 17220247; PMCID: PMC1828811.

Borak, J. (2020). Airborne transmission of COVID-19. *Occupational Medicine, 370*, 303–304. https://doi.org/10.1093/occmed/kqaa080

Bourouiba, L. (2020). Turbulent gas clouds and respiratory pathogen emissions: Potential implications for reducing transmission of COVID-19. *Journal of the American Medical Association*. https://doi.org/10.1001/jama.2020.4756

Brankston, G., Gitterman, L., Hirji, Z., Lemieux, C., & Gardam, M. (2007). Transmission of influenza A in human beings. *The Lancet Infectious Diseases, 7*, 257–265. https://doi.org/10.1016/S14733099(07)70029-4

Buonanno, G., Stabile, L., & Morawska, L. (2020). Estimation of airborne viral emission: Quanta emission rate of SARS-CoV-2 for infection risk assessment. *Environment International, 141*, 105794. https://doi.org/10.1016/j.envint.2020.105794

Chen, W., Zhang, N., Wei, J., Yen, H. L., & Li, Y. (2020). Short-range airborne route dominates exposure of respiratory infection during close contact. *Building and Environment, 176*, 106850. https://doi.org/10.1016/j.buildenv.2020.106859

Coronaviridae Study Group. (2020). Coronaviridae Study Group of the International Committee on Taxonomy of Viruses. The species severe acute respiratory syndrome- related coronavirus: Classifying 2019-nCoV and naming it SARS-CoV-2. *Nature Microbiology, 5*, 536–544.

Cox, C. S. (1995). Physical aspects of bioaerosols particles. In C. S. Cox & C. M. Wathes (Eds.), *Bioaerosols handbook* (pp. 15–25). Lewis Publishers.

Deng, S. Q., & Peng, H. J. (2020). Characteristics of and public health responses to the coronavirus disease 2019 outbreak in China. *Journal of Clinical Medicine, 9*, 575.

Gautam, S. (2020a). COVID-19: Air pollution remains low as people stay at home. *Air Quality, Atmosphere and Health, 13*, 853–857. https://doi.org/10.1007/s11869-020-00842-6

Gautam, S. (2020b). The influence of COVID-19 on air quality in India: A boon or inutile. *Bulletin of Environmental Contamination and Toxicology, 104*, 724–726. https://doi.org/10.1007/s00128-020-02877-y

Gralton, J., Tovey, E., McLaws, M. L., & Rawlinson, W. D. (2011). The role of particle size in aerosolised pathogen transmission: A review. *The Journal of Infection, 62*, 1–13.

Grayson, S. A., Griffiths, P. S., Perez, M. K., & Piedimonte, G. (2016). Detection of airborne respiratory syncytial virus in a pediatric acute care clinic. *Pediatric Pulmonology, 52*, 684–688. https://doi.org/10.1016/j.jinf.2010.11.010

Halloran, S. K., Wexler, A. S., & Ristenpart, W. D. (2012). A comprehensive breath plume model for disease transmission via expiratory aerosols. *PLoS One, 7*, e0037088. https://doi.org/10.1371/journal.pone.0037088

Han, Q., Lin, Q., Jin, S., & You, L. (2020). Coronavirus 2019-nCoV: A brief perspective from the front line. *The Journal of Infection, 80*, 373–377.

Hinds, W. C. (1999). *Aerosol technology: Properties, behavior, and measurement of AirBorne particles* (2nd ed.). Wiley.

Hu, B., Guo, H., Zhou, P., et al. (2021). Characteristics of SARS-CoV-2 and COVID-19. *Nature Reviews. Microbiology, 19*, 141–154. https://doi.org/10.1038/s41579-020-00459-7

Huang, Y., Yang, C., Xu, X. F., Xu, W., & Liu, S. W. (2020). Structural and functional properties of SARS-CoV-2 spike protein: Potential antivirus drug development for COVID-19. *Acta Pharmacologica Sinica, 41*, 1141–1149.

Hui, D. S., et al. (2020). The continuing 2019-nCoV epidemic threat of novel coronaviruses to global health—The latest 2019 novel coronavirus outbreak in Wuhan, China. *International Journal of Infectious Diseases, 91*, 264–266.

Jayaweera, M., Perera, H., Gunawardana, B., & Manatunge, J. (2020). Transmission of COVID-19 virus by droplets and aerosols: A critical review on the unresolved dichotomy. *Environmental Research, 188*, 109819. https://doi.org/10.1016/j.envres.2020.109819

Jiang, S., Du, L., & Shi, Z. (2020). An emerging coronavirus causing pneumonia outbreak in Wuhan, China: Calling for developing therapeutic and prophylactic strategies. *Emerging Microbes & Infections, 9*, 275–277.

Jones, R. M. (2020). Relative contributions of transmission routes for COVID-19 among healthcare personnel providing patient care. *Journal of Occupational and Environmental Hygiene, 17*, 408–415. https://doi.org/10.1080/15459624.2020.1784427

Judson, S. D., & Munster, V. J. (2019). Nosocomial transmission of emerging viruses via aerosol-generating medical procedures. *Viruses, 11*, 940. https://doi.org/10.3390/v11100940

Killingley, B., & Nguyen-Van-Tam, J. (2013). Routes of influenza transmission. *Influenza and Other Respiratory Viruses, 7*, 42–51.

Konda, A., Prakash, A., Moss, G. A., Schmoldt, M., Grant, G. D., & Guha, S. (2020). Aerosol filtration efficiency of common fabrics used in respiratory cloth masks. *ACS Nano, 14*, 6339–6347. https://doi.org/10.1021/acsnano.0c03252

Kudryashova, O. B., Muravlev, E. V., Antonnikova, A. A., & Titov, S. S. (2021). Propagation of viral bioaerosols indoors. *PLoS One, 16*(1), e0244983. https://doi.org/10.1371/journal.pone.0244983. PMID: 33400714; PMCID: PMC7785217.

Kumar, P., & Morawska, L. (2019). Could fighting airborne transmission be the next line of defence against COVID-19 spread? *City and Environment Interactions, 4*, 100033. https://doi.org/10.1016/j.cacint.2020.100033

Kumar, R. P., Perumpully, S. J., Samuel, C., et al. (2023). Exposure and health: A progress update by evaluation and scientometric analysis. *Stochastic Environmental Research and Risk Assessment, 37*, 453–465. https://doi.org/10.1007/s00477-022-02313-z

Lewis, D. (2020). Is the coronavirus airborne? Experts can't agree. *Nature, 580*, 175. https://doi.org/10.1038/d41586-020-00974-w

Liu, L., Wei, J., Li, Y., & Ooi, A. (2016). Evaporation and dispersion of respiratory droplets from coughing. *Indoor Air, 27*, 179–190. https://doi.org/10.1111/ina.12297

Loh, N. H. W., Tan, Y., Taculod, J., Gorospe, B., Teope, A. S., Somani, J., & Tan, A. Y. H. (2020). The impact of high-flow nasal cannula (HFNC) on coughing distance: Implications on its use during the novel coronavirus disease outbreak. *Canadian Journal of Anesthesia*, 1–2. https://doi.org/10.1007/s12630-020-01634-3

Long, Y., Hu, T., Liu, L., Chen, R., Guo, Q., Yang, L., Cheng, Y., Huang, J., & Du, L. (2020). Effectiveness of N95 respirators versus surgical masks against influenza: A systematic review and meta-analysis. *Journal of Evidence-Based Medicine*. https://doi.org/10.1111/jebm.12381

Marthi, B. (1994). Resuscitation of microbial bioaerosols. In B. Lighthart & A. J. Mohr (Eds.), *Atmospheric microbial aerosols* (pp. 192–225). Springer. https://doi.org/10.1007/978-1-4684-6438-2_7

McCluskey, R., Sandin, R., & Greene, J. (1996). Detection of airborne cytomegalovirus in hospital rooms of immuno-compromised patients. *Journal of Virological Methods, 56*, 115–118. https://doi.org/10.1016/0166-0934(95)01955-3

Morawska, L. (2006). Droplet fate in indoor environments, or can we prevent the spread of infection. *Indoor Air, 16*, 335–347.

Morawska, L., & Cao, J. (2020). Airborne transmission of SARS-CoV-2: The world should face the reality. *Environment International, 139*, 105730. https://doi.org/10.1016/j.envint.2020.105730

Morawska, L., & Milton, D. K. (2020). It is time to address airborne transmission of coronavirus disease 2019 (COVID-19). *Clinical Infectious Diseases, 71*(9), 2311–2313. https://doi.org/10.1093/cid/ciaa939

Morawska, L., Tang, J. W., Bahnfleth, W., Bluyssen, P. M., Boerstra, A., Buonanno, G., et al. (2020). How can airborne transmission of COVID-19 indoors be minimised? *Environment International, 142*, 105832. https://doi.org/10.1016/j.envint.2020.105832

Newman, S. (2009). *Respiratory drug delivery. Essential theory and practice*. RDD Online-VCU.

Nicas, M., Nazaroff, W. W., & Hubbard, A. (2005). Towards understanding the risk of secondary airborne infection: Emission of respirable pathogens. *Journal of Occupational and Environmental Hygiene, 2*, 143–154.

Prather, K. A., Marr, L. C., Schooley, R. T., McDiarmid, M. A., Wilson, M. E., & Milton, D. K. (2020). Airborne transmission of SARS-CoV-2. *Science, 370*, 303–304.

Ren, S. Y., Wang, W. B., Hao, Y. G., Zhang, H. R., Wang, Z. C., Chen, Y. L., et al. (2020). Stability and infectivity of coronaviruses in inanimate environments. *World Journal of Clinical Cases, 8*, 1391–1399. https://doi.org/10.12998/wjcc.v8.i8.1391

Schuit, M., Ratnesar-S, S., Yolitz, J., Williams, G., Weaver, W., Green, B., et al. (2020). Airborne SARS-CoV-2 is rapidly inactivated by simulated sunlight. *The Journal of Infectious Diseases, 222*, 564–571. https://doi.org/10.1093/infdis/jiaa334

Shiu, E. Y. C., Leung, N. H. L., & Cowling, B. J. (2019). Controversy around airborne versus droplet transmission of respiratory viruses: Implication for infection prevention. *Current Opinion in Infectious Diseases, 32*, 372–379. https://doi.org/10.1097/QCO.0000000000000563

Smither, S. J., Eastaugh, L. S., Findlay, J. S., & Lever, M. S. (2020). Experimental aerosol survival of SARS-CoV-2 in artificial saliva and tssue culture media at medium and high humidity. *Emerging Microbes & Infections, 9*, 1415–1417. https://doi.org/10.1080/22221751.2020.1777906

Sugano, N., Ando, W., & Fukushima, W. (2020). Cluster of SARS-CoV-2 infections linked to music clubs in Osaka, Japan: Asymptomatically infected persons can transmit the virus as soon as 2 days after infection. *The Journal of Infectious Diseases, 222*, 1635–1640. https://doi.org/10.1093/infdis/jiaa542

Tellier, R. (2006). Review of aerosol transmission of influenza A virus. *Emerging Infectious Diseases, 12*, 1657–1662. https://doi.org/10.3201/eid1211.060426

Tellier, R. (2009). Aerosol transmission of influenza A virus: A review of new studies. *Journal of The Royal Society Interface, 6*, S783–S790. https://doi.org/10.1098/rsif.2009.0302.focus

Thomas, R. J. (2013). Particle size and pathogenicity in the respiratory tract. *Virulence, 4*, 847–858. https://doi.org/10.4161/viru.27172

Van Doremalen, N., Bushmaker, T., Morris, D. H., Holbrook, M. G., Gamble, A., Williamson, B. N., et al. (2020). Aerosol and surface stability of SARS-CoV-2 as compared with SARS-CoV-1. *The New England Journal of Medicine, 382*, 1564–1567.

Vuorinen, V., Aarnio, M., Alava, M., Alopaeus, V., Atanasova, N., Auvinen, M., et al. (2020). Modelling aerosol transport and virus exposure with numerical simulations in relation to SARS-CoV-2 transmission by inhalation indoors. *Safety Science, 130*, 104866. https://doi.org/10.1016/j.ssci.2020.104866

Wang, J., & Du, G. (2020). COVID-19 may transmit through aerosol. *Irish Journal of Medical Science*, 1–2. https://doi.org/10.1007/s11845-020-02218-2

Weber, T. P., & Stilianakis, N. I. (2008). Inactivation of influenza A viruses in the environment and modes of transmission: A critical review. *The Journal of Infection, 57*, 361–373.

Wei, J. J., & Li, Y. G. (2016). Airborne spread of infectious agents in the indoor environment. *American Journal of Infection Control, 44*, S102–S108. https://doi.org/10.1016/j.ajic.2016.06.003

WHO. (2014). *Infection prevention and control of epidemic-and pandemic-prone acute respiratory infections in health care*. https://www.who.int/publications/i/item/infection-prevention-and-control-of-epidemic-and-pandemic-prone-acute-respiratory-infections-in-health-care. Accessed 6 Sept 2023.

WHO. (2020a). *Coronavirus disease 2019 (COVID-19)* (Situation report – 51). World Health Organization. https://www.who.int/docs/default-source/coronaviruse/situation-reports/20200311-sitrep-51-covid-19.pdf?sfvrsn=1ba62e57_10

WHO. (2020b). *Modes of transmission of virus causing COVID-19: Implications for infection prevention and control (IPC) precaution recommendations and includes new scientific evidence available on transmission of SARS-CoV-2, the virus that causes COVID-19*. Scientific Brief.

WHO. (2020c). *Advice on the use of masks in the context of COVID-19. Interim guidance*. World Health Organization. Available at https://www.who.int/publications/i/item/advice-on-the-use-of-masks-in-the-community-during-home-care-and-in-healthcare-settings-in-the-context-of-the-novel-coronavirus-(2019-ncov)-outbreak

Wu, Z., & McGoogan, J. M. (2020). Characteristics of and important lessons from the coronavirus disease 2019 (COVID-19) outbreak in China: Summary of a report of 72314 cases from the Chinese Center for Disease Control and Prevention. *The Journal of the American Medical Association, 323*, 1239–1242.

Wu, J. T., Leung, K., & Leung, G. M. (2020). Nowcasting and forecasting the potential domestic and international spread of the 2019-nCoV outbreak originating in Wuhan, China: A modelling study. *Lancet, 395*, 689–697.

Xie, X., Li, Y., Chwang, A. T., Ho, P. L., & Seto, W. H. (2007). How far droplets can move in indoor environments–revisiting the Wells evaporation-falling curve. *Indoor Air, 17*, 211–225. https://doi.org/10.1111/j.1600-0668.2007.00469.x

Zhu, Y., Xie, J., Huang, F., & Cao, L. (2020). Association between short-term exposure to air pollution and COVID-19 infection: Evidence from China. *Science of the Total Environment, 727*, 138704. https://doi.org/10.1016/j.scitotenv.2020.138704

Aerosol-Social-Health Nexus: Unveiling the Reciprocity with Aerosol Optical Depth

Sneha Mahalingam and Ramsundram Narayanan

1 Introduction

Aerosol optical depth (AOD) is universally acknowledged as a pivotal parameter for comprehending atmospheric physics and assessing local air quality due to its inherent capacity to quantify the presence of aerosols within the atmosphere (Meng et al., 2021). The primary method for assessing aerosol loading on a broad scale has evolved into the retrieval of AOD through observations from space-borne sensors. Aerosols typically comprise both liquid and solid particles suspended within the atmosphere, originating from a combination of natural sources and human-driven actions (Ezhilkumar et al., 2021). Naturally occurring aerosols stem from phenomena such as dust, fog, forest emissions, and geyser emissions, while anthropogenic activities, such as industrial processes, transportation, and wildfires, predominantly generate haze, particulate air pollutants, and smoke (Sneha et al., 2022). These aerosols possess the capacity to induce several significant impacts on the atmosphere. They can modify cloud characteristics and durations, perturb the radiative processes within the atmosphere, exert influence over atmospheric circulation patterns, and exert an impact on ambient air temperatures (Chuang et al., 2020). The quantification of AOD assumes a pivotal role in the evaluation of air quality and the prevailing environmental circumstances, bearing significant consequences for the welfare of children under 5 years old. By delving more profoundly into the intricate interplay

S. Mahalingam
Department of Civil Engineering, Kumaraguru College of Technology,
Coimbatore, Tamil Nadu, India

Anna University, Chennai, Tamil Nadu, India

R. Narayanan (✉)
Department of Civil Engineering, Kumaraguru College of Technology,
Coimbatore, Tamil Nadu, India
e-mail: ramsundram.civil@kct.ac.in

between AOD and nutritional aspects, we can formulate more comprehensive strategies to address malnutrition and its associated intricacies. This collaborative endeavor strives to ameliorate the holistic well-being of underprivileged communities inhabiting regions profoundly impacted by aerosol pollution.

Malnutrition contributes significantly to child mortality, accounting for approximately one-third to half of deaths among children below the age of five. While there has been a gradual and steady decline in undernutrition rates, it is expected to accelerate due to improvements in socioeconomic conditions (Petrikova, 2022). Nevertheless, the intergenerational impact of undernutrition implies that achieving comprehensive change may span several decades. Approximately one-third of infants, equivalent to 7.8 million annually, are born with a low birth weight, defined as less than 2500 grams (Du et al., 2022). This alarming statistic represents a substantial 26% of the global burden, the highest burden among all countries. Notably, 60% of these low birth weight infants are born at full term following fetal growth restriction. The initial 2 years of life, especially the early months, represent a critical window for addressing undernutrition stemming from a combination of factors, including low birth weight, suboptimal feeding practices, and susceptibility to infections such as diarrhea. Early undernutrition carries the risk of causing irreversible effects on various life aspects, including educational attainment, adult stature, income levels, and the birth weight of subsequent generations.

The National Family Health Survey (NFHS) is a comprehensive and extensive survey initiative that has been carried out in multiple phases since 1992 across a representative selection of households throughout India. This survey is administered under the guidance of the Ministry of Health and Family Welfare, Government of India, with the International Institute for Population Sciences (IIPS) in Mumbai serving as the central coordinating agency. As of now, four rounds of the NFHS have been conducted, namely NFHS-1 (1992–1993), NFHS-2 (1998–1999), NFHS-3 (2005–2006), NFHS-4 (2015–2016), NFHS-5 (2019–2021). Notably, the most recent NFHS-5 has introduced a noteworthy enhancement by providing district-level estimates for a comprehensive range of indicators, marking the first time such extensive data has been made available for all 640 districts in India.

In recent years, there has been a growing recognition of the significant role that environmental factors play in shaping human health and well-being. One such factor, AOD, which measures the opacity and concentration of atmospheric aerosols, has gained considerable attention due to its potential impact on public health. While previous studies have examined the association between AOD and various health outcomes, our study seeks to explore an uncharted area—the relationship between AOD and child nutrition. By investigating how changes in aerosol optical depth may affect the nutritional status of children, we hope to contribute valuable insights into this often-overlooked aspect of public health research at the intersection of environmental science and healthcare. Our research offers a unique perspective that delves into the intricate interactions between atmospheric conditions and the well-being of our most vulnerable population—young children who are <5 years old.

Therefore, this study was conducted in the districts of Chennai, Coimbatore, and Salem, situated in Tamil Nadu, India. Nutritional status data were sourced from the

Demographic Health Survey. Our objective is to comprehensively investigate these associations, with the overarching goal of advancing scientific comprehension and providing valuable insights to inform evidence-based policy decisions aimed at safeguarding health and securing a prosperous future for future generations.

2 Methodology

2.1 Study Area Description

Chennai   Chennai, the capital city of Tamil Nadu, encompasses a strategic location along the Coromandel Coast on the southeastern coast of India. With geographical coordinates approximately between 13.04° N latitude and 80.27° E longitude, Chennai enjoys an advantageous position in terms of trade and connectivity. As India's fourth-largest city covering an area spanning about 426 square kilometers, it stands as a bustling metropolis with immense economic potential. The tropical wet and dry climate adds to its charm by exhibiting distinctive seasons throughout the year. Influenced by the Bay of Bengal, Chennai experiences monsoon rains from October to December known as the northeast monsoon season alongside occasional cyclones which shape this coastal region's weather patterns. Renowned for its rich history, diverse population mix, and flourishing industries like automotive manufacturing, information technology services, and healthcare provision, Chennai merits recognition as not only an industrial center but also as a cultural hub. The study area within Chennai comprises both urban and peri-urban regions that exemplify how these zones synergistically blend featuring residential areas interspersed amidst commercial spaces surrounded by thriving industrial sectors.

Coimbatore   Coimbatore, often hailed as the "Manchester of South India," is a prominent and thriving city situated in the western part of Tamil Nadu. With its geographical coordinates at approximately 10.59° N latitude and 76.22° E longitude, Coimbatore expands across an expansive area spanning around 246 square kilometers (Mahalingam & Narayanan, 2023). The city experiences a tropical wet and dry climate with distinct monsoon seasons, owing to its location nestled against the foothills of the majestic Western Ghats—an influential factor that contributes to its delightful weather. Known for its rich industrial landscape encompassing textiles, manufacturing, agriculture, and education sectors amongst others; Coimbatore boasts not only extensive economic diversity but also serves as a significant hub for trade and commerce within the region it resides in. When conducting research or observation studies within this dynamic city setting one must consider both urbanized areas alongside suburban regions alike—truly capturing Coimbatore's multifaceted identity characterized by flourishing industries along with residential developments that shape this extraordinary metropolis.

Salem Salem, a city located in the western part of Tamil Nadu, is situated at approximately 11.67° N latitude and 78.16° E longitude. Spanning an area of about 100 square kilometers, Salem boasts a tropical wet and dry climate that is influenced by its proximity to both the Eastern Ghats and the Bay of Bengal. One notable aspect of Salem's identity lies in its thriving agricultural sector, which focuses predominantly on mangoes and sugarcane cultivation. Furthermore, this bustling city's economy thrives on not just agriculture but also mining activities as well as various industries like textiles and steel manufacturing. As such, it serves as a crucial hub for trade involving agricultural commodities. The study area within Salem encompasses both urbanized regions and rural landscapes since they are representative of the diverse industrial features alongside agrarian practices found throughout the city.

The study areas of Chennai, Coimbatore, and Salem in Tamil Nadu as shown in Fig. 1 offer a rich diversity that serves as valuable research opportunities. These regions boast unique geographical landscapes, varying climatic conditions, and distinct economic characteristics. It is crucial for researchers to have a deep understanding of these attributes in order to conduct thorough and comprehensive studies within these localities because these are Tier I, Tier II, and Tier III cities.
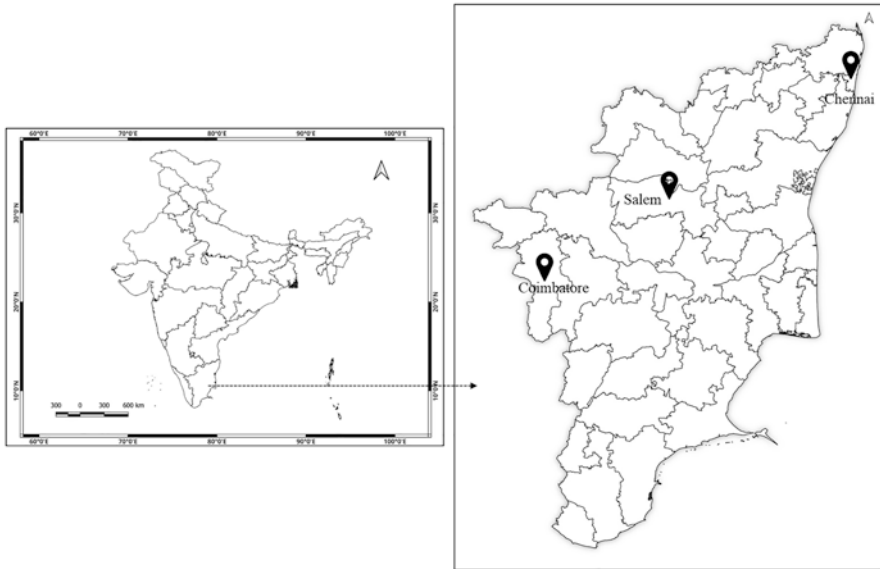
Fig. 1 Geographical locations of the districts considered for the study

3   Data Acquired

3.1   VIIRS

The study utilized aerosol optical depth data sourced from the Visible Infrared Imaging Radiometer Suite sensor (VIIRS) aboard the Suomi National Polar-orbiting Partnership satellite. VIIRS, a highly esteemed technology known for its fine spatial resolution and ability to track atmospheric parameters, provided crucial insights for our research. Specifically, we focused on three major cities in Tamil Nadu, India—Chennai, Coimbatore, and Salem—due to their strategic locations and varied environmental conditions. These cities were carefully selected to facilitate an extensive analysis of AOD trends with respect to their urban characteristics.

The VIIRS Level-2 AOD data was obtained from the NASA Earth data archive, a reputable source. These measurements specifically focus on the 550 nm wavelength range, providing valuable insights into atmospheric aerosol content (Muruganandam et al., 2023). The study period encompassed years between 2015 and 2021, allowing for a comprehensive assessment of aerosol levels and their temporal variations over this extended period. To narrow down our analysis to specific locations relevant to our research—Chennai (13.04° N, 80.27° E), Coimbatore (10.59° N, 76.22° E), and Salem (11.67° N, 78.16° E)—we subsetted the VIIRS data using their corresponding geographical coordinates. Before conducting any in-depth analyses on these retrieved VIIRS AOD datasets, they underwent an elaborate preprocessing phase for quality control purposes. What this entailed was the removal of missing or erroneous data points along with correction measures accounting for different atmospheric conditions (Deshmukh et al., 2013). Furthermore, data were also calibrated against established references to ensure utmost accuracy, repeatability, and consistency throughout. For better temporal comparisons, the aggregated yearly average values of AOD were computed. This allowed us to examine annual trends as well as long-term variations present within these datasets.

3.2   NFHS Data

The anthropometric measurements of height and weight obtained during the 2015–16 and 2019–21 National Family Health Survey (NFHS) enable the assessment and analysis of the nutritional well-being of young children in India. This assessment aids in the identification of specific segments within the child population that face an elevated risk of growth deficiencies, illnesses, compromised cognitive development, and mortality.

Stunting (evaluated through height-for-age): Height-for-age serves as an indicator of linear growth retardation and the cumulative effects of growth deficits. Wasting (evaluated through weight-for-height): The weight-for-height index

assesses the relationship between body mass and body height or length, reflecting the current nutritional status of an individual. Underweight (evaluated through weight-for-age): Weight-for-age represents a composite measure that accounts for both acute and chronic undernutrition. It considers the child's weight in relation to both their height-for-age and weight-for-height. Hence, these parameters were considered for this study to understand the relationship between AOD and nutritional status of the children.

3.3 Data Verification

A crucial step in ensuring the reliability of the remote sensing data for subsequent analyses involved validating the accuracy of retrieved AOD data by comparing it with ground-based measurements from monitoring stations located within the study cities. This scrutiny helped establish confidence in the reliability and trustworthiness of our datasets.

4 Results and Discussion

4.1 Temporal Variation of AOD

The atmospheric optical depth measurements in Chennai have shown a gradual upward trend from 2015 to 2019, reaching the highest recorded value of 0.1579 in that year. However, subsequent data for both 2020 and 2021 indicate a slight decrease in AOD levels, hovering around approximately 0.1534 and 0.1541 respectively as shown in Fig. 2. These fluctuations may suggest possible shifts in local atmospheric conditions or alterations in aerosol sources present within the region. Coimbatore exhibited a remarkable level of stability in terms of AOD values throughout the duration of the study. The recorded AOD for 2015 stood at 0.1630, which remained fairly consistent from 2016 to 2019. However, there was a slight incremental shift observed in both 2020 and 2021 where the AOD increased to reach a value of approximately 0.1554. This particular trend may indicate localized fluctuations in aerosol loading within the region. Salem exhibited a comparable pattern to that of Coimbatore. The levels of AOD remained relatively consistent from 2015 to 2019, followed by a slight decline in 2020 and a subsequent rise in 2021, both converging toward the value of 0.1551. These subtle variations can be ascribed to various factors including meteorological influences and human activities on the environment.

The analysis revealed substantial oscillations in the maximum AOD values across all three cities and over the study period. Chennai, in particular, exhibited a noteworthy pattern. In 2015, Chennai registered its highest recorded AOD value at
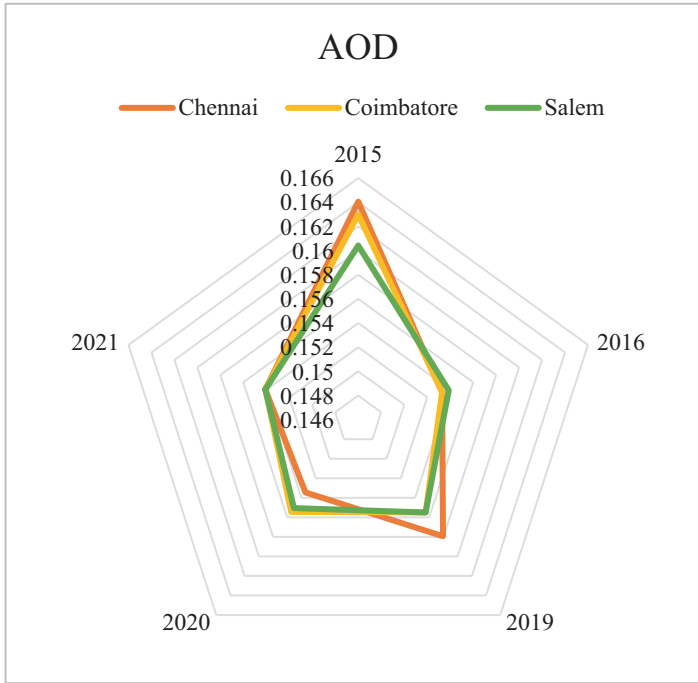
Fig. 2 Spatiotemporal variation of AOD at Chennai, Coimbatore, Salem

2.7020, only to undergo a considerable reduction to reach its nadir of 2.5192 in 2021. Coimbatore, mirroring this trend, showcased a peak AOD value of 2.7044 in 2015, which steadily declined to its lowest recorded measurement of 2.5192 in the year 2021. Salem, too, displayed analogous variability, with the zenith of its maximum AOD occurring in 2015, boasting an impressive value of 2.7502, followed by a subsequent diminishment to reveal its most minimal reading, approaching 2.5192.

Notably, Chennai presents a compelling case study of reduced AOD variability. In 2015, the standard deviation stood at 0.1244, while by 2021, it had discernibly diminished to 0.1165. This decline provides convincing evidence of decreased fluctuations in aerosol concentrations within Chennai over the years. Coimbatore exhibits a comparable trend in AOD variability. In 2015, the standard deviation was recorded at 0.1282, and by 2021, it had receded to 0.1170. This diminishing standard deviation underscores the potential reduction in AOD variability within the city. In contrast to Chennai and Coimbatore, Salem consistently maintained a relatively stable standard deviation throughout the study period.

The interannual variability observed across all three locations indicates that there are occasional fluctuations in the AOD values. However, it is noteworthy that these variations generally fall within a relatively tight range. This trend suggests a level of consistent aerosol levels over time, with any deviations likely to be associated with specific local factors like weather patterns and pollution sources. Upon analyzing

the AOD values of the three cities, it becomes evident that Chennai consistently showcases slightly higher levels compared to Coimbatore and Salem. This variation in AOD could potentially stem from a range of factors such as disparities in urbanization patterns, industrial activities, and even differences in topography (Macêdo & Ramos, 2020). These unique elements ultimately contribute to diverse aerosol concentrations within each city's environment.

4.2   AOD and Nutritional Association

A compelling observation emerges when examining the comparison of AOD trends and child nutritional status across these cities. Chennai and Salem, both witnessing either increasing or consistent AOD levels, experienced significant deteriorations in child nutrition indicators. In contrast, Coimbatore, despite a decrease in AOD levels, managed to maintain relatively stable child nutrition indicators. These findings prompt thought-provoking questions about the potential connections between elevated AOD levels and declining child nutritional status in Chennai and Salem. However, it is important to emphasize that this correlation does not establish causation since various socioeconomic factors, healthcare conditions, and environmental influences may also contribute to these trends.

The data in Table 1 reveals the number of children affected by stunting, wasting, and underweight in three districts: Chennai, Coimbatore, and Salem. Meanwhile, Fig. 3 illustrates the percentage contribution of these conditions among children. Interestingly, all three factors—stunting, wasting, and underweight—have nearly equal percentages of contribution across the districts. However, it is noteworthy that Chennai has a slightly higher proportion at approximately 22%. Intriguingly enough though when examining the correlation between AOD and malnutrition rates specifically with regards to stunting (0.33%), wasting (0.32%), as well as underweight (0.34%) respectively—some compelling insights emerge from this analysis. Although the contributions appear minute individually, they hold significant implications on a broader scale.

Table 1 Nutritional status of children

Districts	Height-for-Age (Stunting)	Weight-for-Height (Wasting)	Weight-for-Age (Underweight)
Chennai 2015–2016	130	128	134
Chennai 2019–2021	235	224	245
Coimbatore 2015–2016	128	126	132
Coimbatore 2019–2021	221	223	227
Salem 2015–2016	122	119	125
Salem 2019–2021	223	218	229
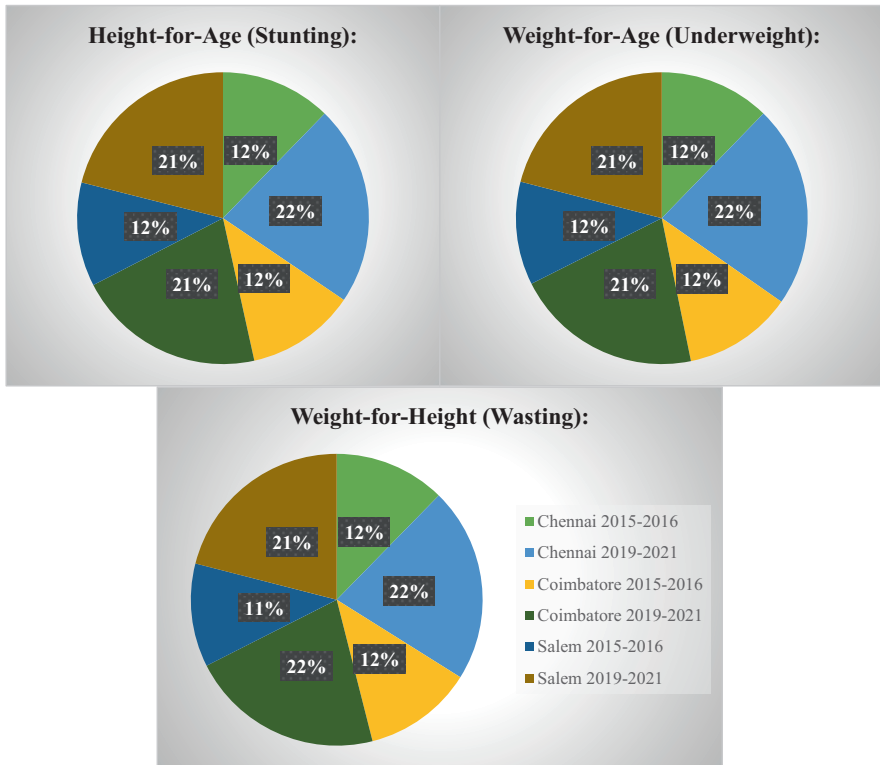
Fig. 3 Percentage contribution of Stunting, Underweight and wasting for each district

5   Conclusion

Coimbatore and Salem have yielded valuable insights into the spatiotemporal dynamics of aerosol loading. Chennai exhibited an upward AOD trend from 2015 to 2019, followed by a slight decline in 2020 and 2021. This suggests shifts in local atmospheric conditions or aerosol sources. Remarkably, Chennai showed reduced AOD variability over the years, with a decreasing standard deviation from 0.1244 (2015) to 0.1165 (2021), indicating increased stability. Coimbatore displayed a stable AOD pattern from 2016 to 2019, with slight increases in 2020 and 2021, hinting at localized fluctuations. A declining standard deviation from 0.1282 (2015) to 0.1170 (2021) suggests potential AOD reduction. Salem mirrored Coimbatore, maintaining stability from 2015 to 2019, with slight 2020 decline and 2021 rise. Standard deviation remained consistent, indicating minor AOD variability. Substantial oscillations in maximum AOD values underscore aerosol loading's dynamic nature. Chennai experienced a significant decrease from 2.7020 (2015) to 2.5192 (2021). Coimbatore and Salem exhibited analogous variability. In conclusion, our analysis of AOD trends and child nutrition in Chennai, Coimbatore, and

Salem reveals intriguing connections. Chennai and Salem, with increasing or steady AOD levels, saw declining child nutrition. Coimbatore, despite lower AOD, maintained stable nutrition indicators. This raises questions about AOD's role, though causation isn't proven, considering socioeconomic, healthcare, and environmental factors. Notably, these factors contribute almost equally across districts, with Chennai at about 22%. While AOD's individual impact appears small (0.33% for stunting, 0.32% for wasting, and 0.34% for underweight), their combined effect is significant. In summary, our study comprehensively assesses aerosol optical depth dynamics, illuminating the intricate link between atmospheric conditions and aerosol concentrations. These findings hold implications for air quality and environmental understanding, vital for public health and urban planning.

References

Chuang, K. J., Lin, L. Y., Ho, K. F., & Su, C. T. (2020). Traffic-related PM2.5 exposure and its cardiovascular effects among healthy commuters in Taipei, Taiwan. *Atmospheric Environment: X, 7*, 100084. https://doi.org/10.1016/j.aeaoa.2020.100084

Deshmukh, D. K., Deb, M. K., & Mkoma, S. L. (2013). Size distribution and seasonal variation of size-segregated particulate matter in the ambient air of Raipur city, India. *Air Quality, Atmosphere and Health, 6*, 259–276. https://doi.org/10.1007/s11869-011-0169-9

Du, H., Sun, Y., Zhang, Y., et al. (2022). Interaction of PM2.5 and pre-pregnancy body mass index on birth weight: A nationwide prospective cohort study. *Frontiers in Endocrinology (Lausanne), 13*, 1–11. https://doi.org/10.3389/fendo.2022.963827

Ezhilkumar, M. R., Karthikeyan, S., Aswini, A. R., & Hegde, P. (2021). Seasonal and vertical characteristics of particulate and elemental concentrations along diverse street canyons in South India. *Environmental Science and Pollution Research, 29*, 85883. https://doi.org/10.1007/s11356-021-15272-9

Macêdo, M. F. M., & Ramos, A. L. D. (2020). Vehicle atmospheric pollution evaluation using AERMOD model at avenue in a Brazilian capital city. *Air Quality, Atmosphere and Health, 13*, 309–320. https://doi.org/10.1007/s11869-020-00792-z

Mahalingam, S., & Narayanan, R. (2023). Covid-19 influence on mixed urban cluster air quality: A case study from India. *Asian Pacific Journal of Environment and Cancer, 6*, 3–14. https://doi.org/10.31557/APJEC.2023.6.1.3

Meng, X., Liu, C., Zhang, L., et al. (2021). Estimating PM2.5 concentrations in Northeastern China with full spatiotemporal coverage, 2005–2016. *Remote Sensing of Environment, 253*, 112203. https://doi.org/10.1016/j.rse.2020.112203

Muruganandam, N., Narayanan, R., & Kabilan, V. (2023). Ephemeral prediction of aerosol optical depth associated with precipitation: A data-driven approach. *Geological Journal*, 1–24. https://doi.org/10.1002/gj.4831

Petrikova, I. (2022). The role of complementary feeding in India's high child malnutrition rates: Findings from a comprehensive analysis of NFHS IV (2015–2016) data. *Food Security, 14*, 39–66. https://doi.org/10.1007/s12571-021-01202-7

Sneha, M., Alshetty, D., Ramsundram, N., & Shiva Nagendra, S. M. (2022). Particulate matter exposure analysis in 12 critical urban zones of Chennai, India. *Environmental Monitoring and Assessment, 194*, 667. https://doi.org/10.1007/s10661-022-10321-3

Aerosol Optical Depth vs. PM$_{2.5}$: Adaptation of Hybrid Optimization Algorithms for Temporal Prediction

Niveditha Muruganandam and Ramsundram Narayanan

1 Introduction

Particulate matter, an atmospheric aerosol, can impact Earth's climate system by either directly or indirectly altering incoming solar energy and outgoing long-wave radiation (Huang et al., 2014). The absorption and scattering of short- and long-wave radiation by aerosols is often referred to as a direct effect of aerosols on radiation, as are aerosol-induced changes in cloud macro- and microphysical properties that contribute to cloud condensation. The indirect consequences are cores or ice cores (Liu et al., 2012; Zhao & Garrett, 2015). Harmful radiation from aerosols is relatively strong in East Asia due to increasing pollutant emissions. (Liu et al., 2012). Aerosol can also influence precipitation amounts and patterns by affecting the microphysical properties of the cloud (Gautam et al., 2023).

In addition, aerosol caused by human-made environmental pollution can have serious consequences on the atmosphere and human health by transporting harmful elements (Samoli et al., 2008; Xu et al., 2013). Therefore, reliable information on aerosol parameters namely aerosol optical depth (AOD) and particles with a size of no more than 2.5 m aerodynamic diameter (PM$_{2.5}$) is crucial. Images from satellites, ground remote sensing, and in vivo land and aircraft observations are often used to measure aerosol properties.

N. Muruganandam
Department of Civil Engineering, Kumaraguru College of Technology,
Coimbatore, Tamil Nadu, India

Anna University, Chennai, Tamil Nadu, India

R. Narayanan (✉)
Department of Civil Engineering, Kumaraguru College of Technology,
Coimbatore, Tamil Nadu, India
e-mail: ramsundram.civil@kct.ac.in

Remote sensing observations often provide optical aerosol metrics such as AOD and aerosol extinction coefficient, but not aerosol mass or number concentration. Aerosol concentrations and $PM_{2.5}$, on the other hand, can be measured in real time. However, the few samples for aircraft observations and limited areas for ground-based in situ measurements make it difficult to obtain data at multiple locations, especially spatial dispersion. Recent studies have provided methods for estimating ground $PM_{2.5}$ levels using AOD readings from satellites (Wang et al., 2010; Xin et al., 2016).

Despite the fact that $PM_{2.5}$ via AOD has low temporal precision and is not accessible when the sky is clouded or very polluted, these techniques provide a global and regional overview of $PM_{2.5}$ (Wang et al., 2010; Xin et al., 2016). Many studies have been carried out in order to develop statistical regression models for estimating surface $PM_{2.5}$ using AOD. For example, (Guo et al., 2009) used long-term combined MODIS AOD and hourly $PM_{2.5}$ readings from the government's China Meteorological China Atmosphere Watch Network (CAWNET) to establish for the first time a correlation between MODIS AOD and ground-based $PM_{2.5}$ over eastern China. They also investigated the effects of planetary boundary layer height (PBLH) and relative humidity (RH) on the $PM_{2.5}$-AOD relationship.

A worldwide chemical transport model (CTM) was used to determine the universal $PM_{2.5}$ concentration spread from the AOD derived from satellite (Van Donkelaar et al., 2010). The 2012–13 Atmospheric Aerosol Research China network campaign determined the correlation between AOD and $PM_{2.5}$ (Xin et al., 2016). There are substantial differences in the relationship between $PM_{2.5}$ and AOD for various locations (Guo et al., 2009; Ma et al., 2014). In the sequence of numerous studies meteorological studies along with the types of aerosols may influence the association between AOD and PM (Ma et al., 2014).

Existing studies have relied on MODIS for data consideration and understanding of the association existing between AOD and $PM_{2.5}$. This is the first study where Visible Infrared Imaging Radiometer Suite (VIIRS) satellite data is used for $PM_{2.5}$ prediction and to determine the relationship that exists between AOD and $PM_{2.5}$. The results were incorporated to check the reliability of machine learning algorithms such as artificial neural network (ANN), support vector machine (SVM) along with hybrid algorithm ANN-BAT for the location Chennai precisely to Manali.

The aim of the study was to predict daily $PM_{2.5}$ levels using AOD data where there are few ground monitoring stations. The study conducted covered the period 2016–2020 for the Manali, Chennai location with a total of 1509 daily records. The study was inspired by a hybrid algorithm, so the study helped to diverge the results of machine learning algorithm, namely artificial neural network, and a hybrid algorithm, namely artificial neural network—BAT algorithm.

2   Methodology

2.1   Site Description

Chennai is the fifth biggest metropolitan area in India and the administrative center of the state of Tamil Nadu, situated at (13.0827°N, 80.2707°E) on the Bay of Bengal's southeast coast. Chennai has a land size of 426 square kilometers and a population of approximately 10.435 million people. Anthropogenic sources of air pollution have had an impact on Chennai in recent decades. The specific site location chosen in Chennai is Manali whose latitude and longitude are 13.1779°N, 80.2701°E.

The entire study was conducted on 1509 data sets. Data collected for AOD was from VIIRS, NASA and PM$_{2.5}$ was collected from CPCB. Due to the enormous data length, we found that better results were achieved in 98% and 99% of training and in 2% and 1% of testing. The 98% of data is 1478 data for training and 31 data for testing, which is 2%. Likewise, it turned out that 99% of the data, which contained 1493 data and 16 data for testing, was 1%. The study included two machine learning algorithms, namely artificial neural network (ANN) and support vector machine (SVM), including polykernel function, normalized polykernel function, PUK and RBF function, and a hybrid algorithm ANN-BAT. The flowchart in Fig. 1 represents the methodology incorporated in our study to establish the relationship between AOD and PM2.5. A similar kind of methodology for precipitation has been marked in the study (Muruganandam et al., 2023).
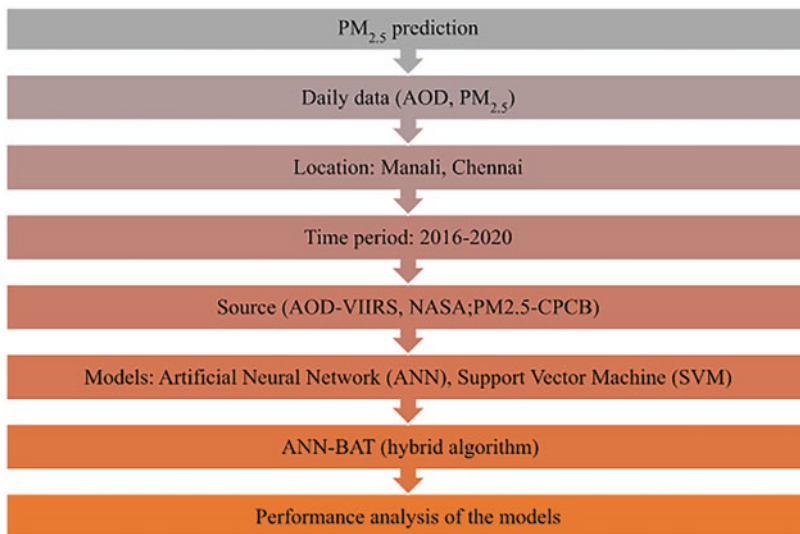
Fig. 1 The methodology of the study

2.2 Artificial Neural Network

Artificial neural networks (ANNs) are biologically inspired computer programs that mimic how the human brain processes information. ANNs learn (or are taught) by discovering correlations and patterns in data, and they form (or are trained) through experience, not programming. An ANN consists of hundreds of discrete units, so-called artificial neurons or processing components, which are coupled to the neural structure via coefficients (weights) and organized into layers. The brain's ability to calculate depends on the interaction of the neurons in a chain of neurons. A transfer function, weighted inputs, and an output are all part of each processing component. The behavior of a neural network is influenced by the transmission of the properties of its neurons, which is called learning (Agatonovic-Kustrin & Beresford, 2000; Muruganandam et al., 2023).

2.3 Support Vector Machine

Support Vector Machine is a traditional machine learning technique that can still be used to handle huge data categorization challenges. It is especially useful for multi-domain applications that operate in an environment with large amounts of data (Suthaharan, 2016). This study covered the performance of four various functions of SVM sets including normalized polykernel, polykernel, RBF, and PUK.

2.4 Hybrid Algorithm

ANN-BAT is a natural and animal-inspired metaheuristic algorithm. Optimization techniques and random investigations are unique approaches for discovering optimal or nearly optimal solutions. Because these algorithms are random, it is not limited to finding the local best approach to a restricted number of answers. The ability to identify the properties of a little bat in seeking prey inspired Bat's optimized algorithm. In order for the little bat to track its prey in the dark, it sends and receives sounds (Mostafaeipour et al., 2018). The algorithm is built using the following three laws:

All bats use echolocation to determine distances and distinguish between food and obstacles. As hunting bait, bats fly randomly at a speed of vi, a fixed frequency of f min at location xi, different wavelengths, and a volume of A0. Due to the proximity of the prey, they can additionally configure distributed waves and automatically send pulse frequencies (r[0,1]) (Yang & He, 2013).

3   Results and Discussion

The results sections show the relationship that exists between AOD and PM$_{2.5}$ for different training and test sets. The results showed various predicted and actual results for machine learning techniques ANN, SVM, and a hybrid optimization algorithm ANN-BAT. Fig. 2a, b show the AOD and PM$_{2.5}$ for 98% of training and 2% of testing for ANN. Figure 3a, b show 99% of the training sets.

Figure 4a, c, e, g show the training set, while Fig. 4b, d, f, h show the testing of four show various features of SVM, namely polykernel, PUK, RBF, and normalized polykernel features for 98% of training and results of 2% of tests. Similarly, Fig. 5a, c, e, g show the training, and Fig. 5b, d, f, h show the results of 99% of training and 1% of testing for the four different functions of SVM in the order of polykernel function, PUK function, RBF and normalized polykernel function.

The performance of the models was verified using performance indicators namely relative mean square error (RMSE). The correlation coefficient (R^2) of PM$_{2.5}$ and AOD is 0.58. Statistical analysis shows that the mean and standard deviation of AOD and PM$_{2.5}$ are 55.53 ± 42.11 and 2.89 ± 1.45, respectively, along with their skewness of 3.477 and 0.289, respectively, followed by a kurtosis of AOD and PM$_{2.5}$ at 328 0.97 and 17.06, respectively. The results showed that 98% and 99% of training and 2% and 1% of ANN tests had better results with RMSE of 21.09 μg/m^3, 22.05 μg/m^3 during training, and 17.95 μg/m^3 and 12.54 μg/m^3 provided for testing. For SVM, out of four functions, the normalized polykernel function was found to be better with an RMSE of 21.79 μg/m^3 in training and 19.7 μg/m^3 in testing for 98% of training and 2% of tests. Simultaneous SVM normalized polykernel with 99% training and 1% testing RMSE of 21.86 μg/m^3 is achieved during training and 13.19 μg/m^3 during testing. Similarly, the results from ANN-BAT show that 98%
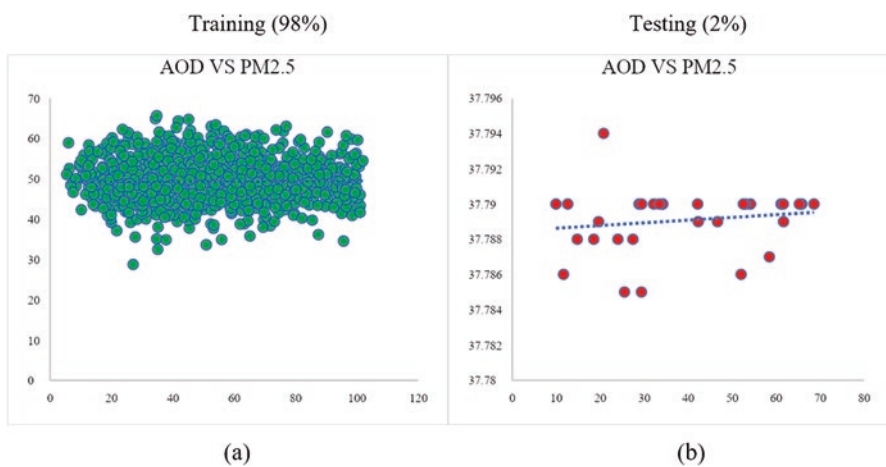
Fig. 2 (**a**, **b**) show the AOD and PM$_{2.5}$ for 98% of training and 2% of testing for ANN
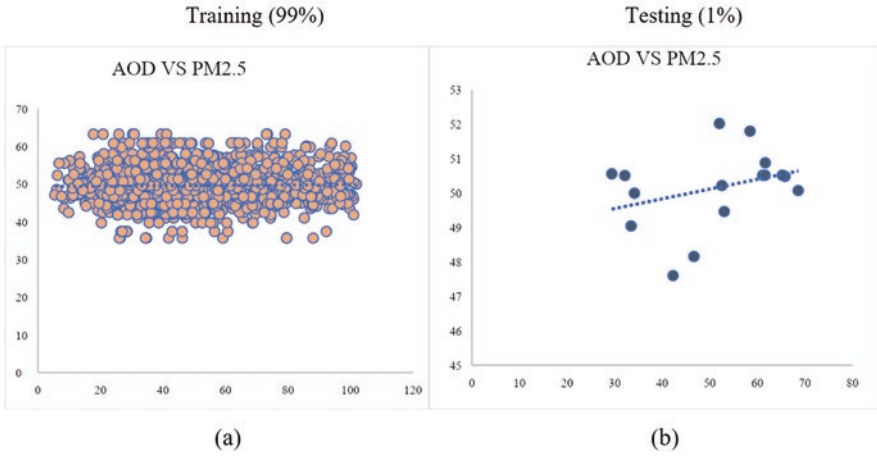
Fig. 3 (a, b) show the AOD and PM$_{2.5}$ for 99% of training and 1% of testing for ANN
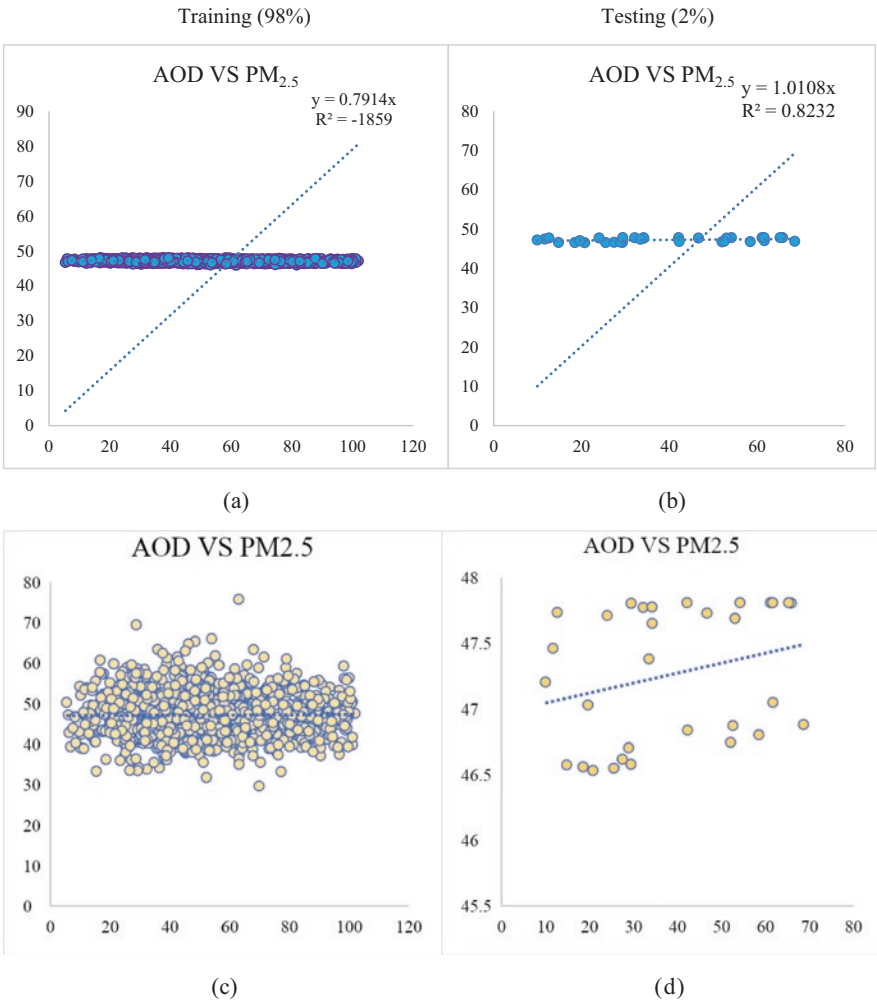
Fig. 4 Shows the AOD and PM$_{2.5}$ for 98% of training and 2% of testing for various functions of SVM including polykernel, normalized Polykernel, PUK, and RBF

AOD VS PM$_{2.5}$

y = 0.7917x
R² = 0.8443

AOD VS PM$_{2.5}$

y = 1.0099x
R² = 0.8233

(e)

(f)

AOD VS PM2.5

AOD VS PM2.5

(g)

(h)
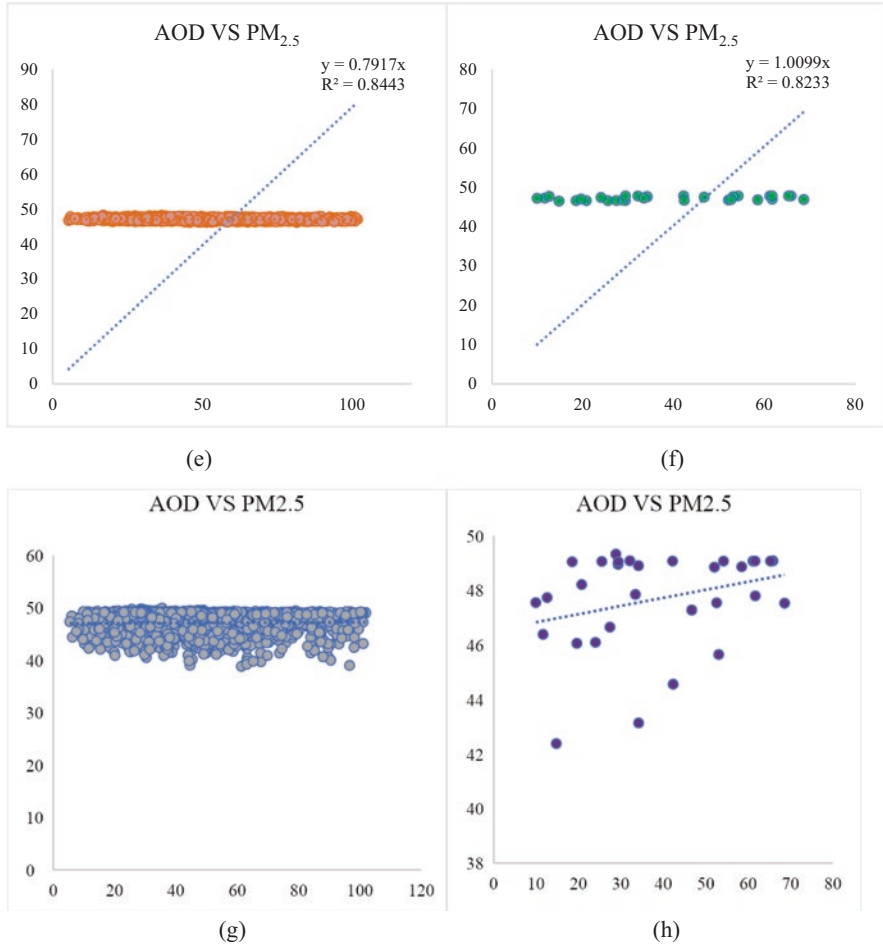
Fig. 4 (continued)

and 99% of training and 2% and 1% of testing with better RMSE of 14.09 μg/m³, 11.36 μg/m³, and during testing it obtained an RMSE of 10.15 μg/m³ and 7.43 μg/m³.

The results show that ANN performs better than SVM even though several features of SVM were tried. The RMSE values of ANN are found to be lower than that of SVM for both training and test sets at 98%, 99%, 2%, 1%. The R2 value of SVM for 99% training and 1% testing was found to be higher than that of ANN and ANN-BAT, represented in Figs. 6a, b and 7a, b. This means that in the 15 days of prediction, the SVM model performs better than the ANN according to (Muruganandam et al., 2023) with an R2 of 0.8 for training and 0.9 for testing. The ANN-BAT has better RMSE and R2 values compared to ANN in both 98%, 99% of training and 2.1% of testing. This helps us understand that hybrid algorithms give better results. The ANN-BAT produced better results for four hidden layers along with 10 bats after 20 iterations for both 98%, 99% of training and 2%, 1% of testing. Table 1 shows the RMSE results of SVM during training and testing.

4   Limitations

This chapter has some constraints, most notably the concentration on the coastline region, which is limited to a certain section in Tamil Nadu's capital. The VIIRS data are used due to the fact that unlike MODIS AQUA and TERRA, it provides a single value. The verification sites in southern India should be extended as well without any orbital gap. The key rationale for using VIIRS instead of MODIS is that there are no orbital gaps. Because the data in this study are thought to be normally distributed, the performance indicator is based on the distribution. The wavelength for
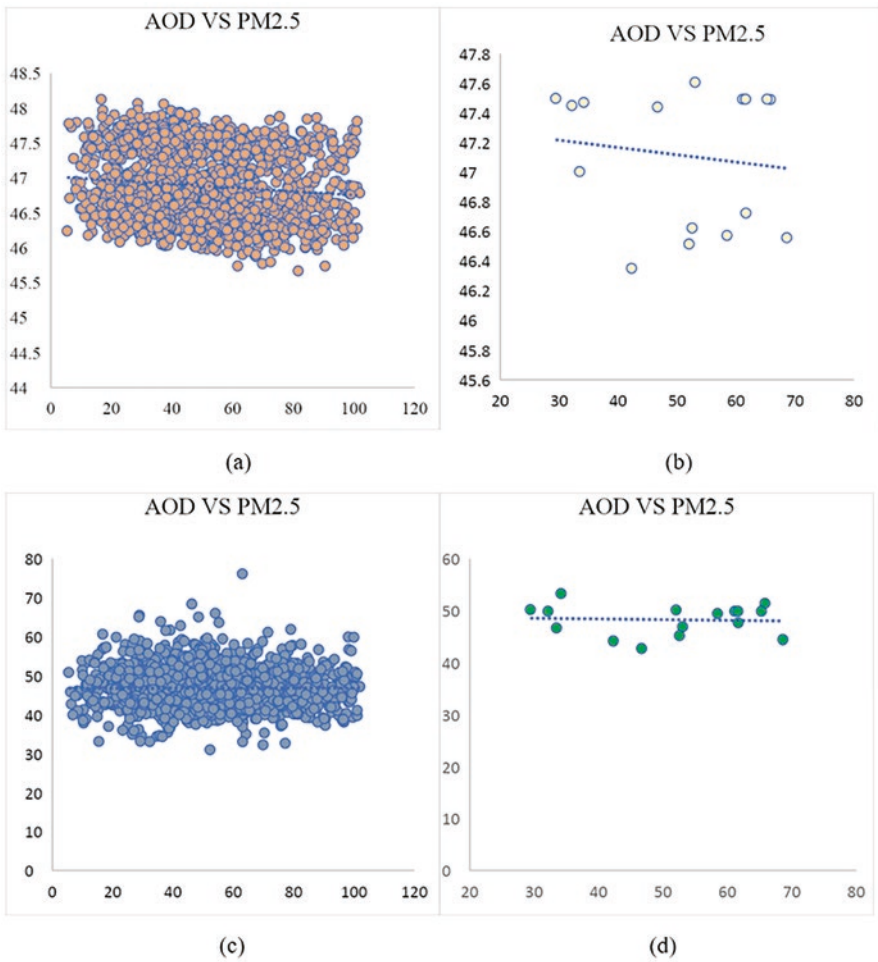
Fig. 5 Shows the AOD and PM$_{2.5}$ for 99% of training and 1% of testing for various functions of SVM, including polykernel, normalized polykernel, PUK, and RBF

(e)   (f)

(g)   (h)
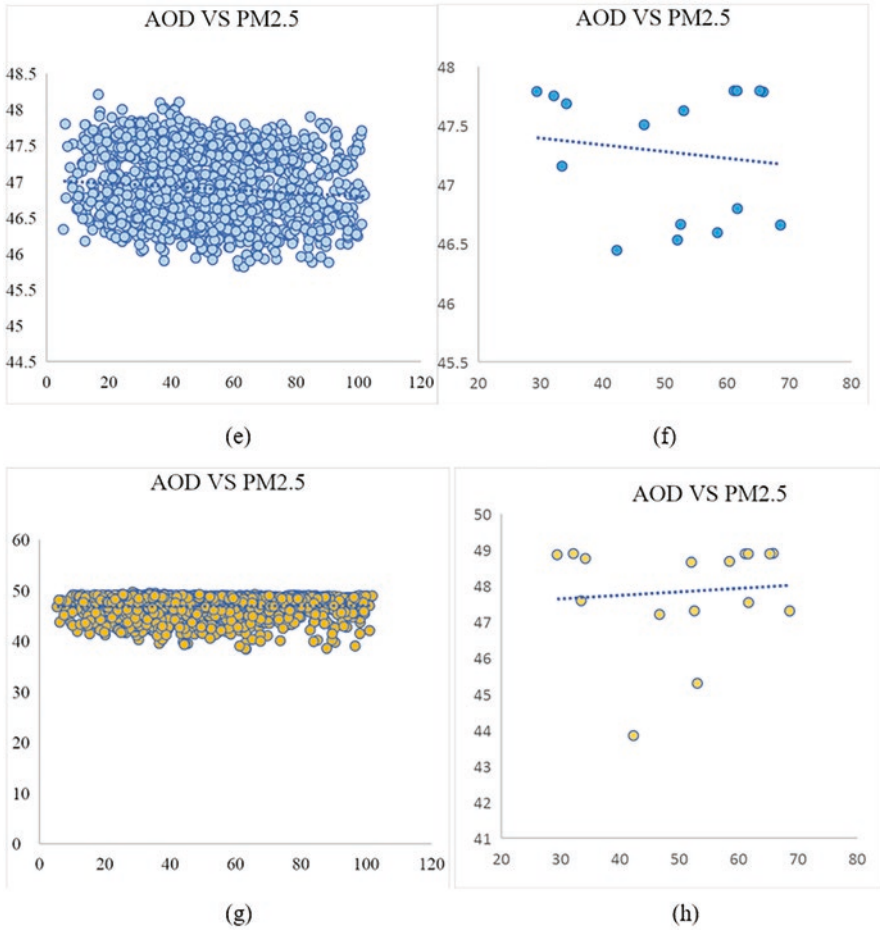
Fig. 5 (continued)

Table 1 contains the RMSE values of training and testing for SVM for four different functions at two different percentages

Training and testing percentages	Functions of SVM	Training RMSE (µg/m³)	Testing RMSE (µg/m³)
Training – 98% Testing – 2%	Normalized Polykernel	21.79	19.78
	Polykernel	21.81	19.88
	PUK	22.27	21.07
	RBF	21.80	19.84
Training – 99% Testing – 1%	Normalized Polykernel	21.86	13.19
	Polykernel	21.88	13.51
	PUK	22.38	13.62
	RBF	21.86	13.475
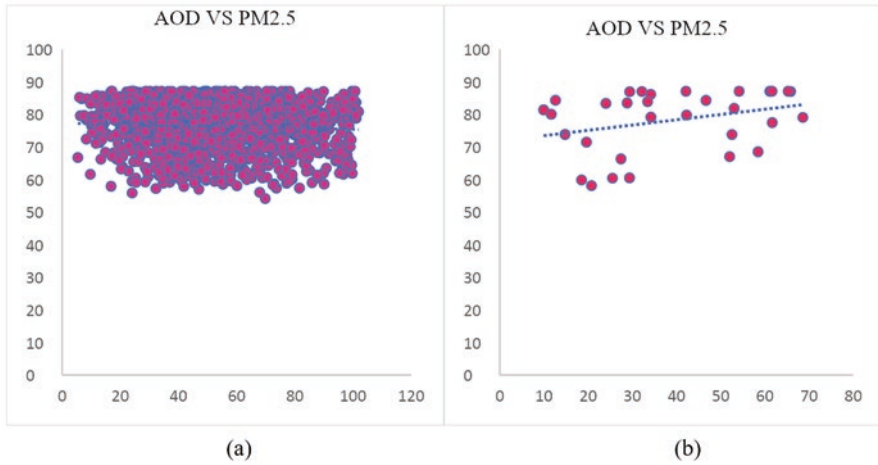
Fig. 6 (**a**, **b**) show the AOD and $PM_{2.5}$ for 98% of training and 2% of testing for ANN-BAT for 20 iterations
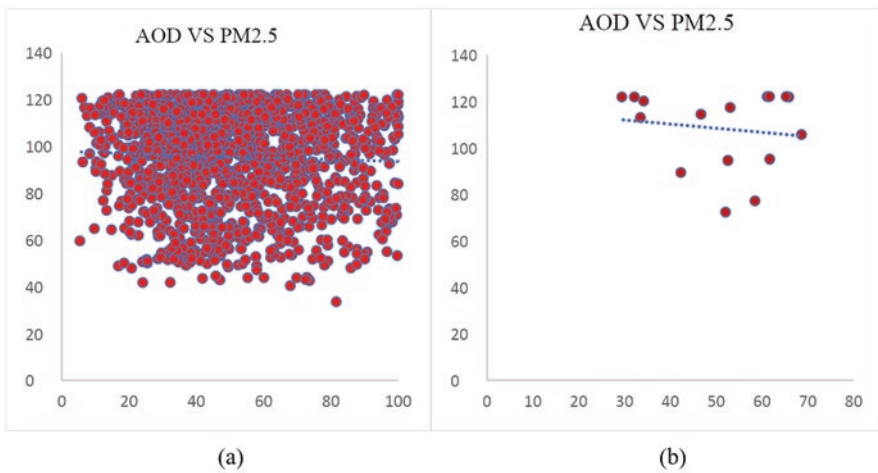
Fig. 7 (**a**, **b**) show the AOD and $PM_{2.5}$ for 99% of training and 1% of testing for ANN-BAT for 20 iterations

AOD was determined using AERDB L2 VIIRS SNPP at a resolution accuracy of 6 km × 6 km. These weaknesses should be addressed in future research. The study aims to bring the betterment of ANN with ANN-BAT and hence it proves it with the results of RMSE.

5 Conclusion

The prediction efficiency shows that from hybrid algorithm and machine learning algorithm, the hybrid algorithm performed better. The study concludes that the hybrid algorithm model proves AOD's ability to make near-term future PM$_{2.5}$ predictions. The best fit was obtained for 20 iterations of ANN-BAT for 98%, 99% of training and 2%, 1% of testing. Overall, the BAT along with ANN performed better than other models in pattern recognition. According to Nguyen et al., 2020, the application of VIIRS may be limited due to the accuracy of the results when compared to MODIS, even though VIIRS is the latest launch to be associated with all modifications rectified by MODIS. Land surveying devices can be utilized in a focused manner for greater comprehension of whether further inquiry is required. The outcomes and data analysis performed revealed superior predictions 15 days ahead. All these forecasts could be helpful in future prediction of PM$_{2.5}$ without costly ground monitoring from PM$_{2.5}$ stations and help authorities in strategic planning, which could help in making environmental policies and regulations when the PM$_{2.5}$ value exceeds the limit. The optimization algorithms help ensure the maximum adaptation to the maximum constraints. The development of nature-inspired optimization algorithms thus leads to an improvement in the environment without much manual effort. One such algorithm used here is ANN-BAT. This study projects the possibility of utilizing the AOD for PM2.5 prediction/pattern mapping, the studies have to be focused toward improving the data mapping capability of the algorithms.

References

Agatonovic-Kustrin, S., & Beresford, R. (2000). Basic concepts of artificial neural network (ANN) modeling and its application in pharmaceutical research. *Journal of Pharmaceutical and Biomedical Analysis, 22*, 717–727. https://doi.org/10.1016/S0731-7085(99)00272-1

Gautam, S., Hens, L., Gautam, A. S., & Shao, L. (2023). Introduction to the special issue 'aerosol optical depth, aerosols, and precipitation'. *Geological Journal, 58*, 4299.

Guo, J.-P., Zhang, X.-Y., Che, H.-Z., Gong, S.-L., An, X., Cao, C.-X., Guang, J., Zhang, H., Wang, Y.-Q., & Zhang, X.-C. (2009). Correlation between PM concentrations and aerosol optical depth in eastern China. *Atmospheric Environment, 43*, 5876–5886.

Huang, J., Wang, T., Wang, W., Li, Z., & Yan, H. (2014). Climate effects of dust aerosols over East Asian arid and semiarid regions. *Journal of Geophysical Research—Atmospheres, 119*, 11–398.

Liu, X., Shi, X., Zhang, K., Jensen, E. J., Gettelman, A., Barahona, D., Nenes, A., & Lawson, P. (2012). Sensitivity studies of dust ice nuclei effect on cirrus clouds with the Community Atmosphere Model CAM5. *Atmospheric Chemistry and Physics, 12*, 12061–12079.

Ma, Z., Hu, X., Huang, L., Bi, J., & Liu, Y. (2014). Estimating ground-level PM2. 5 in China using satellite remote sensing. *Environmental Science & Technology, 48*, 7436–7444.

Mostafaeipour, A., Goli, A., & Qolipour, M. (2018). Prediction of air travel demand using a hybrid artificial neural network (ANN) with Bat and Firefly algorithms: A case study. *The Journal of Supercomputing, 74*, 5461–5484. https://doi.org/10.1007/s11227-018-2452-0

Muruganandam, N., Narayanan, R., & Kabilan, V. (2023). Ephemeral prediction of aerosol optical depth associated with precipitation: A data-driven approach. *Geological Journal, 58*, 4379. https://doi.org/10.1002/gj.4831

Samoli, E., Peng, R., Ramsay, T., Pipikou, M., Touloumi, G., Dominici, F., Burnett, R., Cohen, A., Krewski, D., & Samet, J. (2008). Acute effects of ambient particulate matter on mortality in Europe and North America: Results from the APHENA study. *Environmental Health Perspectives, 116*, 1480–1486.

Suthaharan, S. (2016). Support vector machine. In S. Suthaharan (Ed.), *Machine learning models and algorithms for big data classification: Thinking with examples for effective learning* (pp. 207–235). Springer US. https://doi.org/10.1007/978-1-4899-7641-3_9

Van Donkelaar, A., Martin, R. V., Brauer, M., Kahn, R., Levy, R., Verduzco, C., & Villeneuve, P. J. (2010). Global estimates of ambient fine particulate matter concentrations from satellite-based aerosol optical depth: Development and application. *Environmental Health Perspectives, 118*, 847–855.

Wang, J., Xu, X., Spurr, R., Wang, Y., & Drury, E. (2010). Improved algorithm for MODIS satellite retrievals of aerosol optical thickness over land in dusty atmosphere: Implications for air quality monitoring in China. *Remote Sensing of Environment, 114*, 2575–2583.

Xin, J., Gong, C., Liu, Z., Cong, Z., Gao, W., Song, T., Pan, Y., Sun, Y., Ji, D., & Wang, L. (2016). The observation-based relationships between PM2. 5 and AOD over China. *Journal of Geophysical Research—Atmospheres, 121*, 10–701.

Xu, P., Chen, Y., & Ye, X. (2013). Haze, air pollution, and health in China. *Lancet, 382*, 2067.

Yang, X.-S., & He, X. (2013). Bat algorithm: Literature review and applications. *International Journal of Bio-Inspired Computation, 5*, 141–149.

Zhao, C., & Garrett, T. J. (2015). Effects of Arctic haze on surface cloud radiative forcing. *Geophysical Research Letters, 42*, 557–564.

Monsoon Shifts and Their Impact on Air Quality and Weather: A Case Study of the Amaravathi River Basin, India

Roshini Praveen Kumar, J. Brema, Sneha Gautam, and G. Catherina

1 Introduction

Climate change is a major factor contributing to changes in monsoon variability, the Intergovernmental Panel on Climate Change (IPCC) has noted that "it is virtually certain that there will be changes in the frequency, intensity, and duration of some extreme weather and climate events" due to climate change (IPCC, 2014). Rising temperatures caused by global warming have been linked to changes in the timing and intensity of monsoon rainfall. A study by Wang et al. (2017) found that increasing temperatures in the Tibetan Plateau were associated with a reduction in monsoon rainfall. Similarly, a study by Li et al. (2017) found that the warming of the Indian Ocean was causing a delay in the onset of the Indian monsoon season. Land use change is another factor that may be contributing to changes in monsoon variability. As people clear forests and other natural habitats for agriculture and development, it can alter the surface properties of the land and affect the local climate. For example, deforestation can reduce the amount of moisture that is released into the atmosphere, which can impact rainfall patterns. A study by Findell et al. (2017) found that land use changes in South Asia, including deforestation and urbanization, were contributing to a decline in monsoon rainfall. The study suggested that changes in land use can affect the surface temperature and moisture content of the land,

R. P. Kumar · J. Brema · G. Catherina
Division of Civil Engineering, Karunya Institute of Technology and Sciences, Coimbatore, Tamil Nadu, India

S. Gautam (✉)
Division of Civil Engineering, Karunya Institute of Technology and Sciences, Coimbatore, Tamil Nadu, India

Water Institute, A Centre of Excellence, Karunya Institute of Technology and Sciences, Coimbatore, Tamil Nadu, India
e-mail: snehagautam@karunya.edu

211

which can in turn impact the atmospheric circulation patterns that drive the monsoon. There is also an involvement of atmospheric aerosols and it can have both warming and cooling effects on the Earth's climate, depending on their composition and location in the atmosphere. One way that aerosols can impact monsoon rainfall is by altering the amount of incoming solar radiation that reaches the Earth's surface. Aerosols can reflect and scatter sunlight back into space, reducing the amount of energy that reaches the surface and leading to cooler temperatures. Aerosols can also impact cloud formation and precipitation processes, which can affect the timing and intensity of monsoon rainfall. For example, aerosols can act as cloud condensation nuclei, providing a surface on which water vapor can condense and form clouds. This can increase the number of clouds and the amount of precipitation, potentially leading to heavier rainfall during the monsoon season.

1.1   Aerosol Loading and Monsoon Variability

The factor that can impact the amount of aerosols in the atmosphere is human activity, including the burning of fossil fuels and biomass, industrial processes, and land use changes. These activities can release large amounts of aerosols into the atmosphere, leading to increased atmospheric loading. Several studies have investigated the relationship between aerosol loading and monsoon variability. For example, a study by Li et al. (2017) found that increased aerosol loading in the atmosphere was associated with a delay in the onset of the Indian monsoon season. The study suggests that aerosols can alter the atmospheric circulation patterns that drive the monsoon, leading to changes in the timing and intensity of rainfall. Another study by Lau et al. (2006) found that increased aerosol loading in Southeast Asia was associated with a reduction in monsoon rainfall. The study suggests that the aerosols were absorbing incoming solar radiation, leading to a decrease in the amount of energy available to drive the monsoon. Aerosol loading is one of the factors that can contribute to changes in monsoon variability, including shifts in the timing of monsoon months. Certain studies (Chen et al., 2022, 2019; Engelstaedter et al., 2006; Choobari et al., 2014) also convey that dust emission influences the hydrological cycles, industries, nuclear powerplants followed by firing kilns impact the aerosol loading usually after mild rainfall events (Williams 1990). The study by Feng et al. (2016) found that suspended PM had major repercussions on human health and weather condition, where as the secondary aerosols also impact the seasonal patterns (Mentel et al., 2013), these research provide insights that natural sources of aerosol load have an evident influence to effect the weather conditions and hydrological cycles. Few studies have investigated the AOD loading during monsoon months for the South Indian climate. For example, a study by Gogoi et al. (2016) found that AOD values during the monsoon season over a tropical coastal site in the Bay of Bengal region of South India were higher than those during the pre-monsoon season. The study suggested that the increased AOD loading during monsoon months may be due to the transport of aerosols from the ocean and land surfaces.

Another study by Babu et al. (2013) examined the seasonal variation in AOD over the Indian Ocean during the monsoon season. The study found that AOD values were higher during the monsoon season compared to the pre-monsoon and post-monsoon seasons. The study also suggests that the increased AOD loading during the monsoon season is likely due to the transport of aerosols from the Indian sub-continent. In a more recent study, Raju et al. (2021) investigated the AOD loading and its impact on monsoon precipitation over the Indian region. The study found that the AOD loading during the monsoon season was higher over the Indian sub-continent compared to other regions and that the increased AOD loading was associated with a decrease in monsoon precipitation. These studies suggest that AOD loading during monsoon months in the South Indian climate is influenced by various factors such as transport from land and ocean surfaces, and has a significant impact on monsoon precipitation. Therefore the correlation between AOD values and monsoon months of all four districts for the years 2000, 2010, and 2022 is studied to understand the probable reason for the shift of rainfall during the monsoon for the four districts of Amaravathi River basin.

2   Material and Methods

The study focuses on the Amaravthi river basin to investigate the relationship between Aerosol Optical Depth (AOD), rainfall patterns, for south-west monsoon between 2000, 2010 and 2022, and their impact on four major industrial districts: Coimbatore, Erode, Karur, and Dindigul. These districts, known for their industries, tanneries, and significant waste disposal, have severely polluted the river. Additionally, rapid urbanization in the area has led to declining air quality, influencing the local climate (Moench, 1999).

The Amaravathi river basin is geographically located between 10°06′51″ N and 11°02′10″ N latitude and 77°03′24″E and 78°13′06″ E longitude, as illustrated in Fig. 1. It is a major tributary of the Cauvery River, characterized by its fan-shaped drainage basin (TNIAMWARAM, n.d.). Recent climate changes in Coimbatore and Karur are believed to be attributed to increased pollution levels. Data for the analysis spans 23 years, and rainfall data, temperature, and humidity from 2000 to 2022, are taken from NASA Power Data Access Viewer, The AOD dataset, crucial to the study, was acquired from the SDS AOD 550 mm Dark Target and Deep via Terra Modis data (NASA Earth Observations (NEO), n.d.) in spatial resolution 1° for daily data for the years 2000, 2010, and 2022. It specifically covers the months of June through September, offering monthly averaged data. Furthermore, anthropogenic emissions data for various pollutants such as Black Carbon (BC), Carbon Monoxide (CO), Nitrogen Dioxide (NO_2), Ozone (O_3), Particulate Matter with a diameter of 2.5 micrometers or less (PM2.5), and Sulfur Dioxide (SO_2) were collected from NASA's Giovanni website. This comprehensive dataset contributes to a thorough analysis of the Amaravathi River basin's climate and pollution trends.
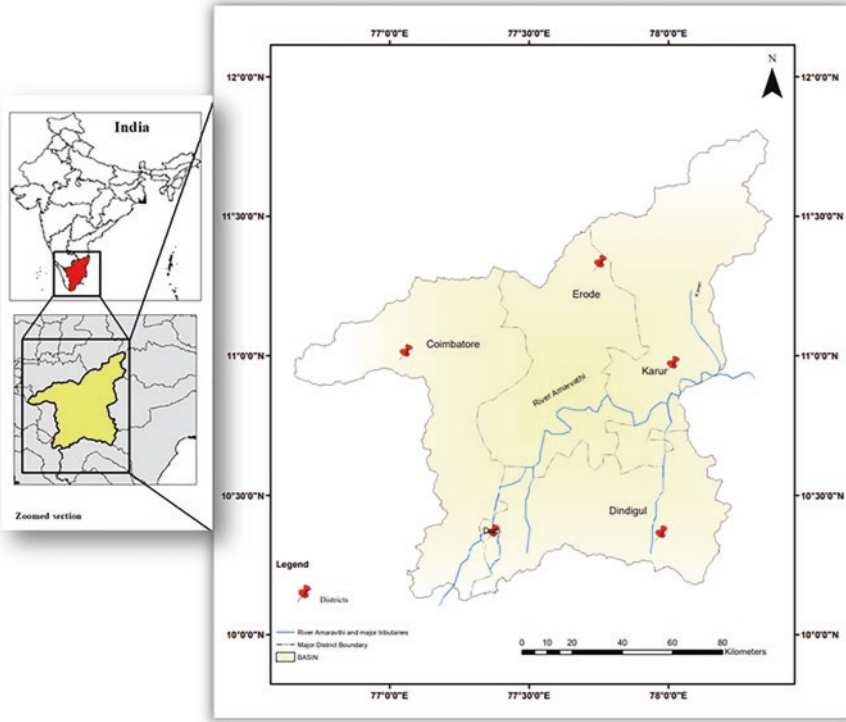
Fig. 1 Study area comprising major districts of Amaravthi River basin and the river's tributaries

2.1 Statistical Approach

Standard deviation (SD), Mean (M), and Linear trend

The values of the mean rainfall for the years 2000–2022 are measured in terms of the dispersion of the points from the mean (the data of rainfall is divided into the overall rainfall values for the given period) which is also known as the root of the variance. In terms of rainfall, Bofu Yu (2005) state the wet day in terms of maximum rainfall shows increased SD values, these analyses are needed in order to find shifts in temporal variations (Soumya et al., 2011). Singh (1998) state, that linear relationships are a better fit than logarithmic relationships for huge datasets, it also reveals the variations found in mean seasonal rainfalls (Jia et al., 2019). The equation is in the form of $y = mx + b$ (linear trend equation) where y represents the influencing factor, m signifies the regression coefficient, x represents the influenced factor and b denotes the y-intercepts (Wang et al., 2020). The value of R2 determines the slope's best fit for the linear regression, which can be seen in the value ranging from 0–1, where the perfect fit exists only when the value is 1. The detailed list is provided in Table 1.

Table 1 Represents the linear trend of the Southwest monsoon and the rainfall variability observed from 2000 to 2022

2000–2022	SD	Mean	CV(%)	Linear Trend	R^2	Range of CV^a
						Rainfall variability
Coimbatore	174.89	604.85	28.91	$y = 12.235x + 458.03$	0.2	Moderately variable (20% < CV < 30%)
Dindigul	172.26	322.78	53.37	$y = 7.6288x + 203.81$	0.2	High variation (30% < CV < 40%)
Erode	110.63	312.69	35.38	$y = 14.558x + 148.09$	0.3	Very high variation (CV > 40%)
Karur	111.67	295.35	37.81	$y = 5.6065x + 245.42$	0.1	

[a]Source: Hare (2003)

2.2 Pearson Correlation

Pearson correlation is a linear correlation technique that establishes the correlation between two variables that favors providing the strength and direction of the linear relationship (e.g. indicating the positive or negative correlation between rainfall and temperature). The Pearson correlation coefficient (r) is determined by using the formula below.

$$r = \left[\Sigma\left(x - \bar{x}\right)\left(y - \bar{y}\right) \right] / \left[\sqrt{\left\{ \Sigma\left(x - \bar{x}\right)2 \right\}} * \sqrt{\left\{ \Sigma\left(y - \bar{y}\right)2 \right\}} \right]$$

where x and y are the examined variables, $\bar{x}$, and $\bar{y}$ are their arithmetic means, and Σ represents the sum of the values for each variable (Pearson, 1896). The Pearson correlation coefficient (r) is a normalized parameter to obtain a sequential relationship between two variables, with its values always ranging between -1 and 1.

3 Results and Discussion

We calculated rainfall data to determine its variation by analyzing the standard deviation and mean. We also used a statistical measure called the coefficient of variation (CV) to assess how spread out the rainfall data is around its average value during a specific time period (Ananthakrishnan & Soman, 1989). The results indicate that the south-west monsoon season in Coimbatore has moderate variability in rainfall, whereas in Karur, it shows a high level of variability. The trend equations for the data analyzed in this study, the rainfall that occurred during the south-west monsoon from 2000 to 2022 indicated a positive trend for the four districts, the values are listed in Table 1. Coimbatore and Dindigul seem to have rainfall variability around the mean. The r square values of Erode have 30% of the variability in the rainfall data. Dindigul has a very high variation and Coimbatore shows moderate variability. These results emphasize the distinct rainfall patterns and levels of variability across these districts.

3.1 Pearson's Correlation for AOD vs. Monsoon

Relationship between AOD and Monsoons experienced between 2000, 2010, and 2022.

The monthly average data of Aerosol Optical Depth (AOD) and rainfall for the districts of Coimbatore, Dindigul, Erode, and Karur have been evaluated for the monsoon months (June, July, August, and September) of 2000, 2010, and 2022. A study by Kumar et al. (2009) states that the presence of AOD levels becomes weaker during the monsoon and higher during drought seasons all over India. Our study

area, the Amaravati Basin, may have variability concerning rainfall in association with AOD. Our findings show that the AOD values increased in June for all four districts during the study years. Additionally, rainfall for 2000 in June increased for Erode, Dindigul, and Karur, while Coimbatore showed variability. July experienced a decrease in the AOD levels for the period 2000–2010 when compared to 2010–2022.

Districts like Karur, Erode, and Coimbatore have a continuously increasing pattern of rainfall, whereas Dindigul experienced variation in its rainfall duration. August observed a variability shift in the AOD levels for all four districts. The rainfall for August continuously increased for Dindigul, Erode, and Karur. The AOD level of Coimbatore ceaselessly decreased in the month of September, whereas the districts of Dindigul, Erode, and Karur showed varying AOD values. Rainfall has been continuously increasing in Coimbatore when compared to the rest. Please refer to Fig. 2, 3 and 4 for further details.

During the lockdown, India's overall AOD reduced to 9% (0.18) (Rani & Kumar, 2022). Coimbatore experienced 0.29 in June 2020 and 0.28 in July, which was the highest when compared to other districts. In August, Erode had the highest value of 0.3 in the Amaravati Basin, while Karur had the highest value of 0.24 in September. These values for the year 2020 clearly indicate the impact of AOD caused by anthropogenic activities and natural pollutants. Correlation analysis between rainfall and AOD for the years 2000, 2010, and 2022 (June–September) indicates a positive correlation ($0 < r < 1$) between rainfall and AOD for the four districts in the year 2000. The study verifies the behavior of AOD < 0.5 when rainfall increases; AOD also increases (Sun et al., 2022).

Coimbatore showed a negative correlation ($r = -0.76$) in the year 2010, while all the other districts showed positive correlation values. For the year 2022, Erode
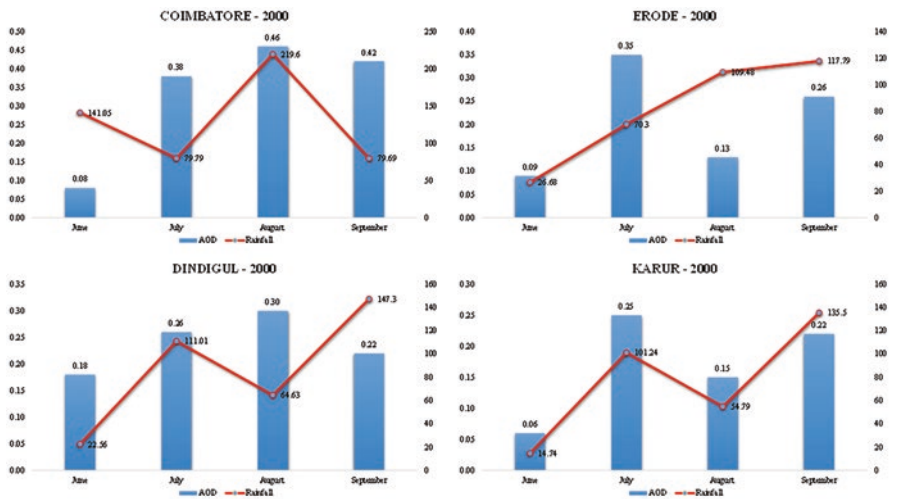
Fig. 2 Represents the AOD vs. rainfall graphs for 2000
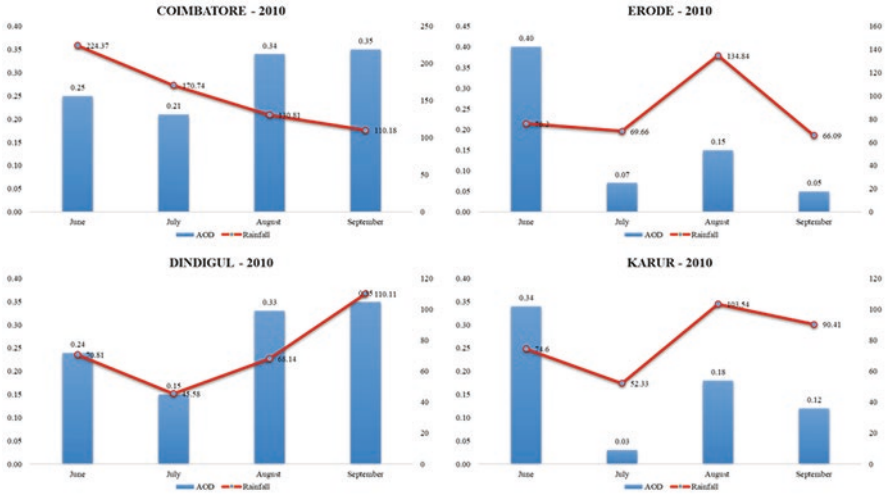
Fig. 3 Represents the AOD vs. rainfall graphs for 2010
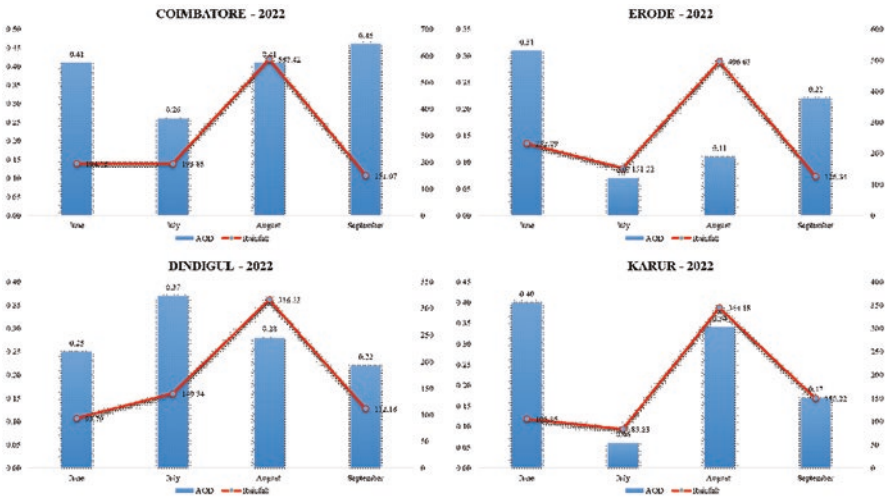
Fig. 4 Represents the AOD vs. rainfall graphs for 2022

showed a negative correlation ($r = -0.25$), while the other districts showed a positive correlation. Furthermore, excessive aerosol loading may cause a decrease in rainfall (Sun et al., 2022). Hence, the correlation between AOD and rainfall seems to be dependent on parameters such as temperature, humidity, and other physiological characteristics, and yet the relationship between them is not definite. Refer to Figs. 5, 6, 7 and 8 for the correlation between monsoon rains and AOD for the years 2000, 2010, and 2022.
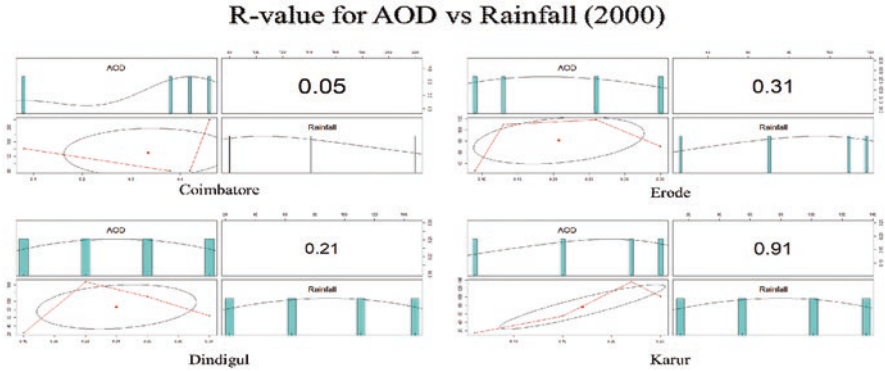
Fig. 5 Represents the correlation between rainfall and AOD for 2000
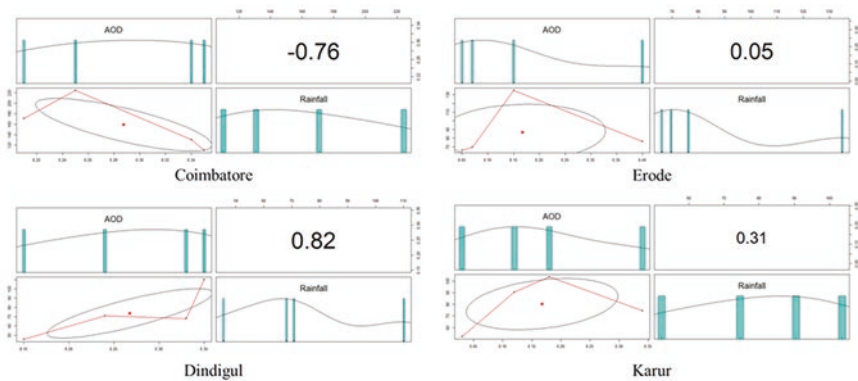
Fig. 6 Represents the correlation between rainfall and AOD for 2010

The alterations in atmospheric circulation can lead to a more vigorous hydrological cycle and a heightened capacity for atmospheric moisture retention while escalating global surface temperatures are expected to bring about precipitation and moisture changes (Tan et al., 2015). These shifts in rainfall patterns impact temperature levels, agricultural practices, and groundwater reserves. The distribution of aerosols in the lower part of the troposphere can have a significant influence on rainfall patterns during the monsoon season (Barik et al., 2020). A study by Lau et al. (2006) suggests that the elevated heat pump (EHP) theory, pre-monsoon dust, and Black Carbon-absorbing aerosol load may influence rainfall over the Indian region during the pre-monsoon and summer monsoon seasons (Barik et al., 2020). Our study area has revealed a direct correlation between rainfall and AOD in the initial years of 2000–2010, but this relationship appears to be fluctuating in the years 2010–2022. The Amaravati River basin may have some pollution, but the AOD levels remain under 0.5, which is not a significant concern for the climate. However, Coimbatore, Dindigul, and Erode are exhibiting AOD values above 0.5
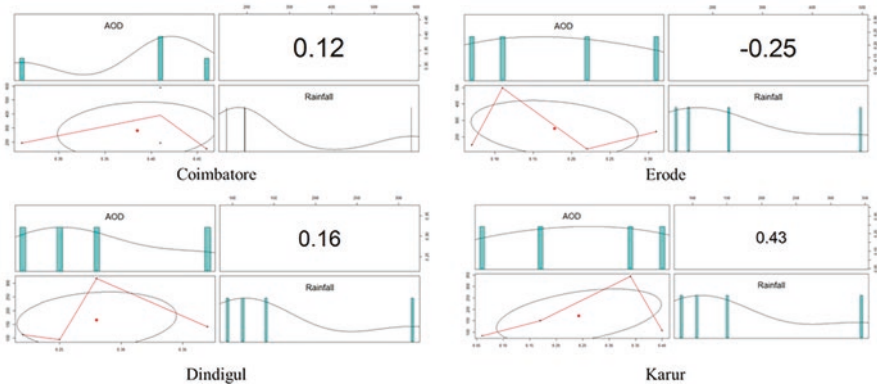
Fig. 7 Represents the correlation between rainfall and AOD for 2022

toward the end of the 2022 monsoon season, suggesting that pollutants may exert an influence on the climate in the near future.

Coimbatore has an elevation of approximately 411 meters above sea level and studies have explored the impact of elevation on Aerosol Optical Depth (AOD) loading and monsoon rainfall in this city. For example, a study by Ramachandran et al. (2015) examined the relationship between AOD and rainfall in the Western Ghats mountain range of South India, which includes Coimbatore. The study found that higher AOD values were associated with decreased rainfall and that the impact of AOD on rainfall was more significant at higher elevations in the mountain range. Another study by Babu et al. (2013) investigated the impact of elevation on AOD over the Indian Ocean which is adjacent to the Tamil Nadu coast.

The study found that AOD values were generally higher at higher elevations, with the maximum values observed at elevations greater than 2 km. The study also suggests that the impact of elevation on AOD may be due to the transport of aerosols from the land and ocean surfaces to higher elevations. While there is no specific study on the impact of elevation on AOD loading for rainfall in Coimbatore, Karur Erode, and Dindigul, the general findings from these studies suggest that elevation may play a role in the distribution of AOD and pollutants emerging by anthropogenic factors that is impacting the monsoon rainfall. Further research is necessary to better understand the mechanisms underlying these relationships in the region.

The air quality index (AQI) of Coimbatore, Erode, Dindigul, and Karur, India revealed that the major pollutants in these areas are PM2.5, SO_2, CO, O_3, and NO_2. To understand the correlation between these pollutants and the weather conditions, including rainfall, humidity, and temperature, the researchers plotted a single multi-variable correlation plot using data ranging from 2000 to 2022 these are shown in Figs. 8, 9, 10 and 11. The monthly average values for each parameter were considered. The results showed that Coimbatore had a positive correlation between rainfall and relative humidity, as well as BC and SO_2. However, the r value for PM2.5 and CO was 0, indicating no correlation between them. The other parameters showed a
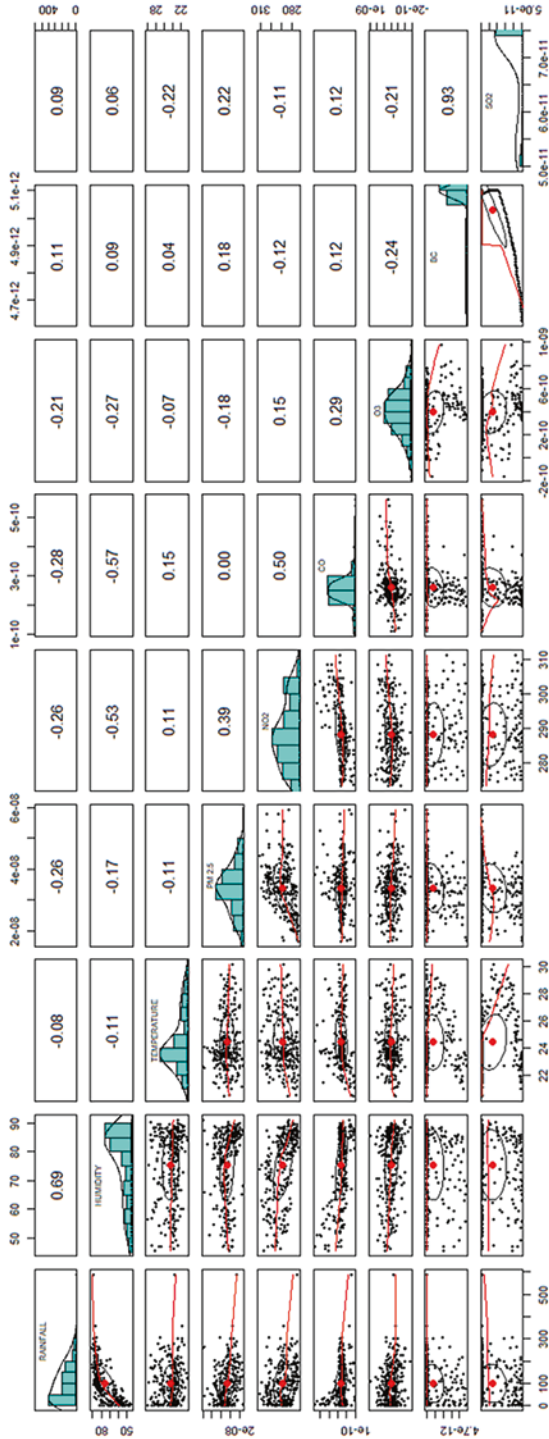
Fig. 8 Represents the Pearson multivariable correlation for Coimbatore
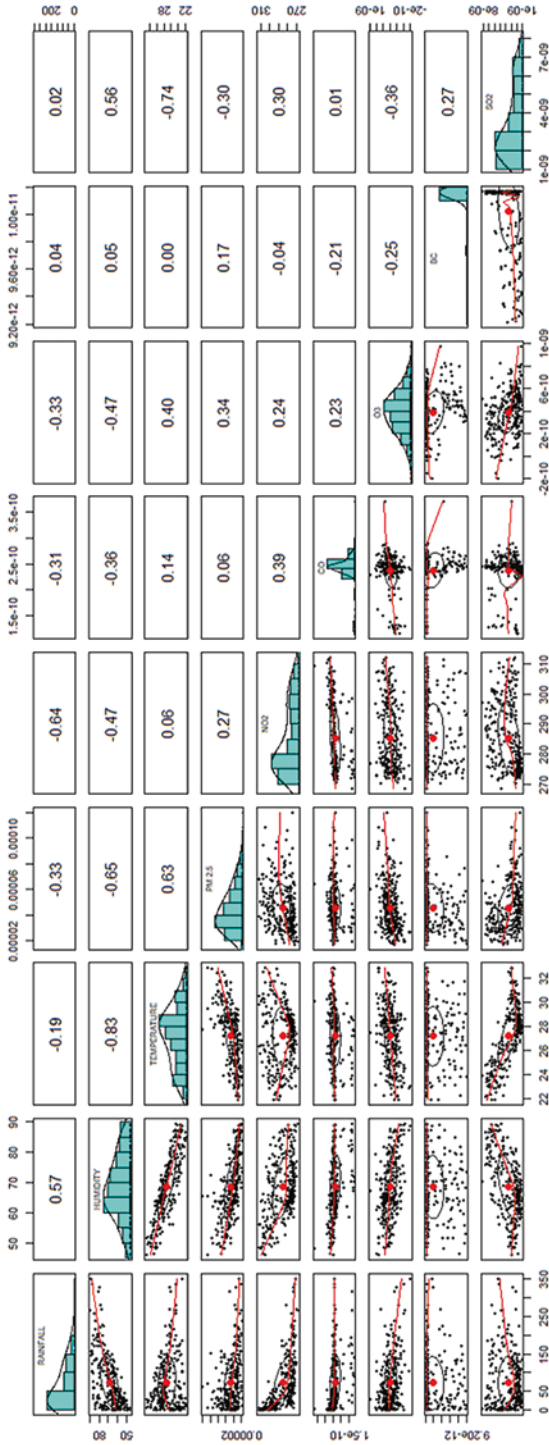
Fig. 9 Represents the Pearson multivariable correlation for Dindigul
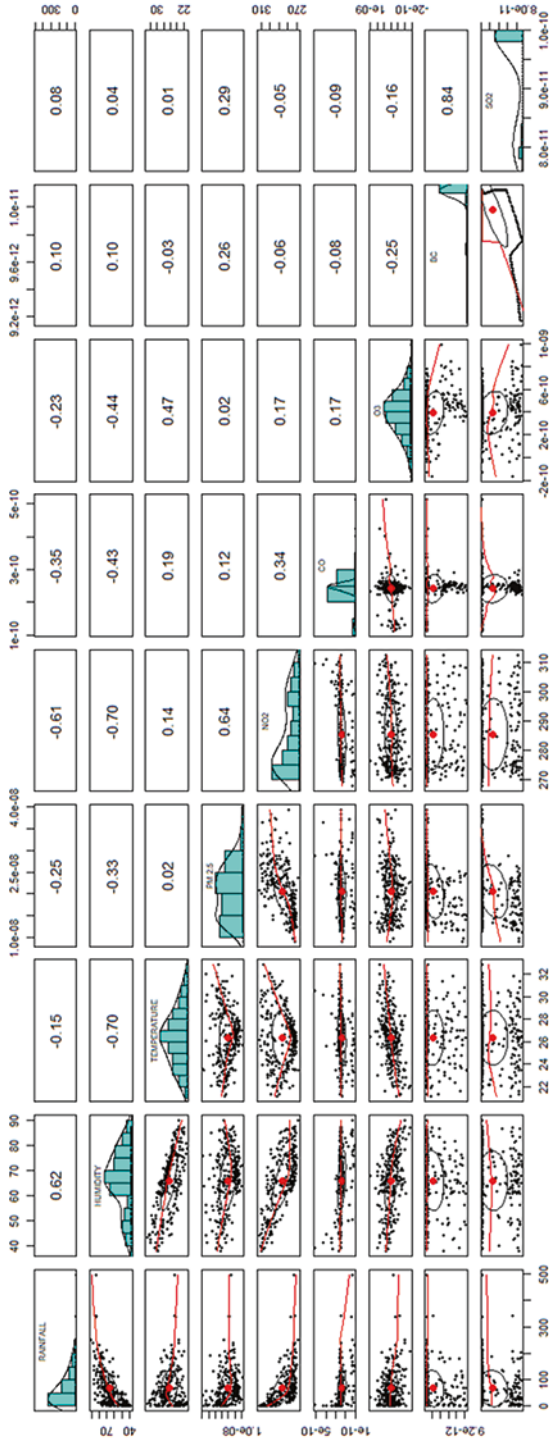
Fig. 10 Represents the Pearson multivariable correlation for Erode
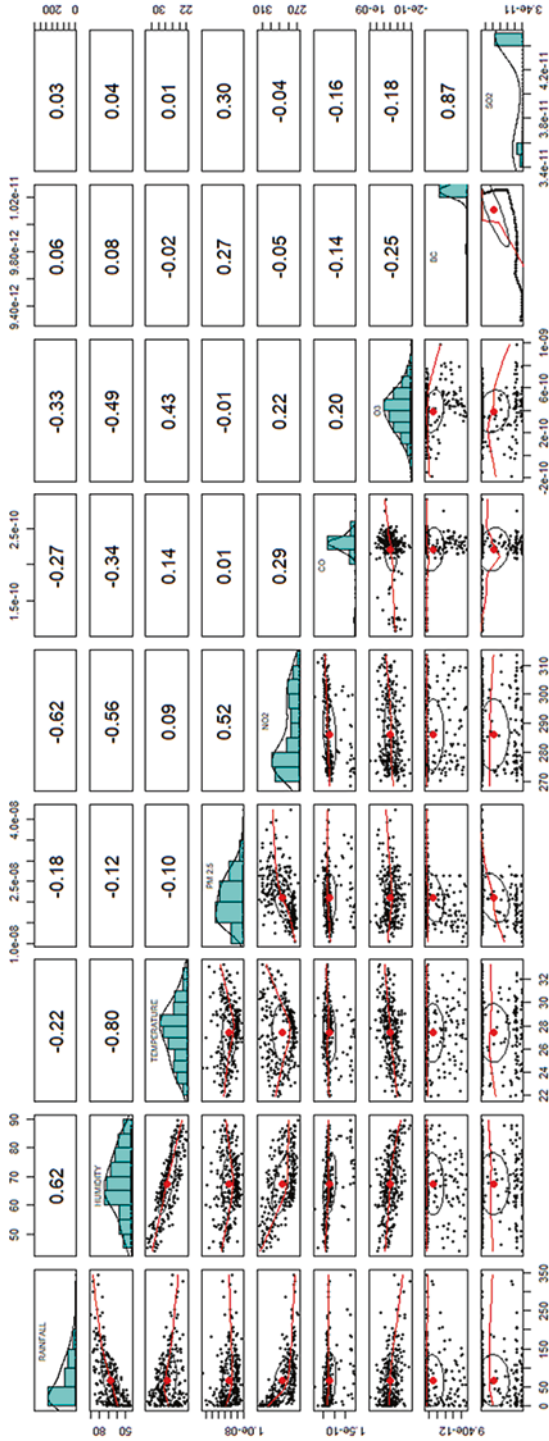
Fig. 11 Represents the Pearson multivariable correlation for Karur The overall analysis brings out five areas addressed mentioned in Fig. 12

Fig. 12 Five insights of analysis in the study addressed

negative correlation. Among the positive correlations, BC and SO_2 had the highest r value (0.93), while relative humidity and SO_2 had the lowest r value (0.06). For Dindigul, the monthly mean for the 23 years showed that BC had no significant correlation with temperature, while the other parameters had a negative correlation. Positive correlations were observed for rainfall and PM2.5, with the highest r value (0.63), while CO and SO_2 had the lowest r value (0.01). In Erode, there was a positive correlation between rainfall and relative humidity, BC, and SO_2. The temperature also had a positive correlation with PM2.5, NO_2, CO, O_3, and SO_2. The positive correlations observed between BC and SO_2 had the highest r value (0.84), while temperature and SO_2 had the lowest r value (0.01). In Karur, a positive correlation was observed between rainfall and relative humidity, BC, and SO_2, while relative humidity had a positive correlation between BC and SO_2. The temperature had a positive correlation with NO_2, CO, O_3, and SO_2, while PM2.5 had a positive correlation with NO_2, CO, BC, and SO_2. Positive correlations were also observed between BC and SO_2, with the highest r value (0.87), while temperature, SO_2, PM2.5, and CO had the lowest r value (0.01). Das and Chatterjee (2020) observed that rainfall and humidity are particularly sensitive to NO_2, PM2.5, and CO. Similarly, Amanatidis (1992) noted that high rainfall in an area can lead to the occurrence of sulfur components from long-range transport, resulting in a positive relationship between rainfall and SO_2. Since all four districts are highly industrialized, the positive correlation between temperature and NO_2 emissions is a concern as it can cause major respiratory issues through the potential decomposition of Nitrous acid (HONO) (Miyama et al., 2020). Ji et al. (2022) found that PM2.5 and NO_2 have a significant association with ill health, particularly in parts of China with higher concentrations of these pollutants, leading to increased mortality rates. Temperature also has a significant relationship with pollutants like BC, NO_2, and CO. While these pollutants have remained within their limits over the 23-year study period, it is important to address the leading sources of pollution to avoid adverse effects in the future. Black Carbon (BC), which is a constituent of PM2.5 and a tracer for combustion-related air pollution, has certain adverse health effects compared to PM 2.5 (Bell et al., 2009; McLinden & Van Der Gon, 2007; Spira-Cohen et al., 2011). The correlation between rainfall, humidity, and temperature with pollutants highlights the influence of major pollutants that can affect rainfall. However, since the pollutants have not reached extreme limits, no conclusions can be drawn yet on the major effects of pollutants on rainfall patterns in these districts. Further research is necessary to understand the mechanisms underlying the observed AOD loading patterns and their implications for the South Indian climate.

• Monsoon Shifts and Variability: Our analysis reveals a consistent positive trend in monsoon rainfall across the four districts of Coimbatore, Erode, Dindigul, and

Karur during the selected years. However, it is crucial to note that the extent of variability in monsoon patterns varies among these districts, reflecting the localized influence of factors such as industrial activities and pollution levels on regional climate.

- Aerosol Optical Depth (AOD) and Monsoons: AOD, a vital indicator of air quality, exhibits intriguing patterns, especially during the monsoon months. Notably, AOD levels increased in June across all districts during our study years, indicating a potential association between industrial emissions, air quality, and monsoon behavior. This link underscores the significance of monitoring and addressing pollution sources as they may influence the timing and intensity of the monsoon.

- Air Quality and Weather Conditions: Our correlation analyses between air quality pollutants (PM2.5, SO_2, CO, O_3, and NO_2) and weather conditions during the monsoon months offer valuable insights. We observed positive correlations between rainfall and relative humidity, BC, and SO_2 in some districts, while other parameters displayed negative correlations. These findings highlight the complex relationships between weather conditions and pollutant concentrations, which can impact monsoon.

- Health Concerns: Potential health concerns emerged, particularly in highly industrialized districts. The positive correlation between temperature and NO_2 emissions during the monsoon season raises apprehensions about respiratory issues due to the potential decomposition of Nitrous acid (HONO). Additionally, we emphasize the adverse health effects of Black Carbon (BC) found in PM2.5.

- Future Implications and Ongoing Research: Despite pollution levels remaining within acceptable limits over the selected study years, our study underscores the importance of proactive measures to address pollution sources. This forward-looking approach is imperative to mitigate potential adverse effects on monsoon patterns, regional climate, and public health in the future.

4   Conclusions

In this comprehensive study conducted in the Amaravathi River Basin of India, we have delved into the critical aspects of monsoon shifts and their intricate relationship with environmental factors, with a specific focus on the years 2000, 2010, and 2022. Our investigation has unearthed essential insights into the of monsoon patterns and their interactions with industrialization, pollution, and climate conditions within the region. It sheds light on the intricate interactions between these shifts and various environmental factors, including industrialization, pollution, and climate conditions. The findings underscore the necessity of adopting holistic environmental management strategies and maintaining ongoing research to comprehend and adapt to the evolving challenges posed by shifting monsoon, climate change, and pollution in this unique and industrially significant area.

References

Amanatidis, G. (1992). ulfate, sulfur dioxide and rainfall relationships in the Athens basin, Greece. *Fresenius Environmental Bulletin, 1*, 462–467.

Ananthakrishnan, R., & Soman, M. (1989). Statistical distribution of daily rainfall and its association with the coefficient of variation of rainfall series. *International Journal of Climatology, 9*, 485–500. https://doi.org/10.1002/JOC.3370090504

Babu, S. S., et al. (2013). Seasonal variation of aerosol optical depth over the Indian Ocean: A study based on satellite data and model simulations. *Atmospheric Environment, 80*, 369–377.

Barik, G., Acharya, P., Maiti, A., Gayen, B. K., Bar, S., & Sarkar, A. (2020). A synergy of the linear model and wavelet analysis towards space-time characterization of aerosol optical depth (AOD) during pre-monsoon season (2007–2016) over the Indian subcontinent. *Journal of Atmospheric and Solar-Terrestrial Physics, 211*, 105478.

Bell, M. L., Ebisu, K., Peng, R. D., Samet, J. M., & Dominici, F. (2009). Hospital admissions and chemical composition of fine particle air pollution. *American Journal of Respiratory and Critical Care Medicine, 179*(12), 1115–1120. https://doi.org/10.1164/rccm.200808-1240oc

Chen, S., Jiang, N., Huang, J., Zang, Z., Guan, X., Ma, X., Luo, Y., Li, J., Zhang, X., & Zhang, Y. (2019). Estimations of indirect and direct anthropogenic dust emission at the global scale. *Atmospheric Environment*. https://doi.org/10.1016/J.ATMOSENV.2018.11.063

Chen, W., Meng, H., Song, H., & Zheng, H. (2022). Progress in dust modelling, global dust budgets, and soil organic carbon dynamics. *Land*. https://doi.org/10.3390/land11020176

Choobari, O., Zawar-Reza, P., & Sturman, A. (2014). The global distribution of mineral dust and its impacts on the climate system: A review. *Atmospheric Research, 138*, 152–165. https://doi.org/10.1016/J.ATMOSRES.2013.11.007

Das, K., & Chatterjee, N. D. (2020). Examine the impact of weather and ambient air pollutant parameters on daily case of COVID-19 in India. *medRxiv*. https://doi.org/10.1101/2020.06.08.20125401

Engelstaedter, S., Tegen, I., & Washington, R. (2006). North African dust emissions and transport. *Earth-Science Reviews, 79*, 73–100. https://doi.org/10.1016/J.EARSCIREV.2006.06.004

Feng, S., Gao, D., Liao, F., Zhou, F., & Wang, X. (2016). The health effects of ambient PM2.5 and potential mechanisms. *Ecotoxicology and Environmental Safety, 128*, 67–74. https://doi.org/10.1016/j.ecoenv.2016.01.030

Findell, K. L., et al. (2017). Impact of anthropogenic land use change on the South Asian monsoon. *Journal of Climate, 30*(7), 2373–2387.

Gogoi, M. M., et al. (2016). Variability of aerosol properties over Bay of Bengal during the passage of two consecutive tropical cyclones. *Environmental Science and Pollution Research, 23*(16), 16635–16649.

Hare, W. (2003). *Assessment of knowledge on impacts of climate change, contribution to the specification of art. 2 of the UNFCCC*. WBGU.

Intergovernmental Panel on Climate Change. (2014). Climate change 2014: Synthesis report. Contribution of working groups I, II and III to the fifth assessment report of the intergovernmental panel on climate change. In R. K. Pachauri & L. A. Meyer (Eds.), (151 pp). IPCC.

Ji, J. S., Liu, L., Zhang, J., et al. (2022). NO2 and PM2.5 air pollution co-exposure and temperature effect modification on pre-mature mortality in advanced age: A longitudinal cohort study in China. *Environmental Health, 21*, 97. https://doi.org/10.1186/s12940-022-00901-8

Jia, G., Tang, Q., & Xu, X. (2019). Evaluating the performances of satellite-based rainfall data for global rainfall-induced landslide warnings. *Landslides, 17*, 283–299. https://doi.org/10.1007/s10346-019-01277-6

Kumar, K., Narasimhulu, K., Reddy, R., Gopal, K., Reddy, L., Balakrishnaiah, G., Moorthy, K., & Babu, S. (2009). Temporal and spectral characteristics of aerosol optical depths in a semiarid region of southern India. *The Science of the total environment, 407*(8), 2673–88. https://doi.org/10.1016/j.scitotenv.2008.10.028

Lau, W. K., et al. (2006). The aerosol-environmental impacts on clouds and precipitation in tropical Asia: An overview. *Atmospheric Environment, 40*(30), 5043–5062.

Li, Y., et al. (2017). Delayed Indian monsoon onset due to warming of the Indian Ocean. *Nature Climate Change, 7*(11), 1–7.

McLinden, C. A., & Van Der Gon, H. D. (2007). On the variability of Black Smoke and carbonaceous aerosols in The Netherlands. *Atmospheric Environment, 41*(28), 5908–5920.

Mentel, T., Kleist, E., Andres, S., Maso, M., Hohaus, T., Kiendler-Scharr, A., Rudich, Y., Springer, M., Tillmann, R., Uerlings, R., Wahner, A., & Wildt, J. (2013). Secondary aerosol formation from stress-induced biogenic emissions and possible climate feedbacks. *Atmospheric Chemistry and Physics, 13*, 8755–8770. https://doi.org/10.5194/ACP-13-8755-2013

Miyama, T., Matsui, H., Azuma, K., Minejima, C., Itano, Y., Takenaka, N., & Ohyama, M. (2020). Time series analysis of climate and air pollution factors associated with atmospheric nitrogen dioxide concentration in Japan. *International Journal of Environmental Research and Public Health, 17*(24), 9507. https://doi.org/10.3390/ijerph17249507

Moench, M. (1999). Chapter 1: Rethinking the mosaic: Investigations into local water management, addressing constraints in complex systems. In *Meeting the water management needs of South Asia in the 21st century* (pp. 145–146). Nepal Water Conservation Foundation, Kathmandu, and the Institute for Social and Environmental Transition, Boulder, Colorado, U.S.A.

NASA Earth Observations (NEO). (n.d.). *Aerosol optical thickness* (1 month – Terra/MODIS). NASA Earth Observations (NEO).

Pearson, K. (1896). Mathematical contributions to the theory of evolution. VII. On the correlation of characters not quantitatively measurable. *Philosophical Transactions of the Royal Society A, 187*, 253–318. https://doi.org/10.1098/rsta.1896.0007

Raju, M. P., et al. (2021). Aerosol impact on Indian summer monsoon: A review. *Theoretical and Applied Climatology, 143*(1–2), 1–21.

Ramachandran, S., et al. (2015). Aerosol optical depth–rainfall correlation over the Western Ghats. *Atmospheric Environment, 122*, 584–591.

Rani, S., & Kumar, R. (2022). Spatial distribution of aerosol optical depth over India during COVID-19 lockdown phase-1. *Spatial Information Research, 30*(3), 417–426. https://doi.org/10.1007/s41324-022-00442-9

Singh, C. (1998). Relationships between rainy days, mean daily intensity and seasonal rainfall in normal, flood and drought years over India. *Advances in Atmospheric Sciences, 15*, 424–432. https://doi.org/10.1007/S00376-998-0012-X

Soumya, B., Sekhar, M., Riotte, J., Audry, S., Lagane, C., & Braun, J. (2011). Inverse models to analyze the spatiotemporal variations of chemical weathering fluxes in a granito-gneissic watershed: Mule Hole, South India. *Geoderma, 165*, 12–24. https://doi.org/10.1016/J.GEODERMA.2011.06.015

Spira-Cohen, A., Chen, L. C., Kendall, M., Lall, R., & Thurston, G. D. (2011). Personal exposures to traffic-related air pollution and acute respiratory health among Bronx schoolchildren with asthma. *Environmental Health Perspectives, 119*, 559–565.

Sun, N., Fu, Y., Zhong, L., et al. (2022). Aerosol effects on the vertical structure of precipitation in East China. *npj Climate and Atmospheric Science, 5*, 60.

Tamil Nadu Irrigated Agriculture Modernization and Waterbodies Restoration Management (TNIAMWARM). (n.d.). *Amaravathi sub basin*. Retrieved September 9, 2023, from https://www.tniamwarmtnau.org/sub-basins/area/amaravathi

Tan, J., Jakob, C., Rossow, W., & Tselioudis, G. (2015). Increases in tropical rainfall driven by changes in frequency of organized deep convection. Nature, 519, 451–454. https://doi.org/10.1038/nature14339

Wang, Y., et al. (2017). The contribution of local cooling to the suppression of precipitation by aerosols over the Tibetan Plateau. *Atmospheric Chemistry and Physics, 17*(10), 6327–6344.

Wang, Y., Xu, Y., Tabari, H., Wang, J., Wang, Q., Song, S., & Hu, Z. (2020). Innovative trend analysis of annual and seasonal rainfall in the Yangtze River Delta, eastern China. *Atmospheric Research, 231*, 104673. https://doi.org/10.1016/j.atmosres.2019.104673

Williams, M. (1990). Nuclear aerosol behavior during reactor accidents. *Progress in Nuclear Energy, 23*, 101–108. https://doi.org/10.1016/0149-1970(90)90007-R

Yu, B. (2005). Adjustment of CLIGEN parameters to generate precipitation change scenarios in southeastern Australia. *Catena, 61*, 196–209. https://doi.org/10.1016/J.CATENA.2005.03.004

Evaluation and Scientometric Analysis of Aerosols and Associated Implications

Steffi Joseph Perumpully and Sneha Gautam

1 Introduction

A variety of study areas require an understanding of the global atmospheric aerosol. The radiation balance of the earth-atmosphere cycle is directly influenced by aerosols since they capture and deflect solar radiation (Feingold et al., 2003). Aerosols can be either anthropogenic or natural, based on where they come from. Urban and industrial areas are the primary sources of anthropogenic particulate matter in the atmosphere. Here, we can include traffic, various industrial processes, construction, and residential emissions. The condition of asthma, stroke, coronary artery disease, and pregnancy difficulties can all be brought on by poor air quality, according to the World Health Organization (WHO) (Bove et al., 2019; Kelly & Fussell, 2015; Mannuccci et al., 2017). Aerosols can additionally have a supplementary impact on weather patterns. The spectral aerosol optical depth (AOD), directional dependence of scattering (also known as the phase matrix), spectral single scattering albedo (SSA), and vertical profile are the important aerosol properties. Satellite measurements can significantly advance studies in these fields because of the considerable spatiotemporal variability of aerosol loading (Ramanathan et al., 2001). Several studies additionally indicate that black carbon (BC) and soot aerosols, which can take in solar radiation and radiate thermal energy outside, might affect clouds. Three

S. J. Perumpully (✉)
Division of Civil Engineering, Karunya Institute of Technology and Sciences, Coimbatore, Tamil Nadu, India

S. Gautam
Division of Civil Engineering, Karunya Institute of Technology and Sciences, Coimbatore, Tamil Nadu, India

Water Institute, A Centre of Excellence, Karunya Institute of Technology and Sciences, Coimbatore, Tamil Nadu, India

million premature deaths occurred in 2013 due to ambient fine particulate matter (PM2.5) concentrations, which considerably increased the extent of disease world-wide (Forouzanfar et al., 2015). Long-term regionally distributed aerosol optical depth values can be obtained by the ground-based AERONET the sun's photometer network, which sheds light on the relative proficiency of different retrieval systems (Holben et al., 1998). The new atmospheric reanalysis for the new age satellite era (1980 forward) produced by the NASA Global Modeling and Assimilation Office is called Modern-Era Retrospective Analysis for Research and Applications, version 2 (MERRA-2) (Giordano, 2015). Enormous attempts have been undertaken to significantly expand both space- and ground-based studies of aerosols in the past few years to further comprehend the importance of aerosols in the climate system and their effects on the quality of the air. Due to cloud damage, unpredictability of aerosol retrievals, sensor-specific data gaps, and satellite measurements cover a limited area and range for a short period. For a more accurate assessment and prevention of aerosol impacts on human health, it is necessary to clarify the role of diverse particulate matter elements in affecting wellness and mortality through combined studies across several spatiotemporal levels. Furthermore, this has been previously shown that aerosols that enter the breathing system interact and affect both blood and brain units (Liu et al., 2015; Sah et al., 2018).

2 Material and Methods

This study includes bibliographic analysis and converts the texts into organized structures to find novel data about aerosol (Ranjbari et al., 2021, 2022). Based on the shared characteristics among the references provided, the articles come together to form various clusters. By removing the nouns that the authors and researchers have used, the obtained datasets are mined. All the data are gathered from the Web of Sciences for the years 2013–2023. The findings would show how crucial it is to pay attention to this area because aerosols are a growing problem that has to be handled, especially in the current environment. Table 1 represents the steps involved in the data collection process.

A well-organized arrangement of the desired literature of pertinent research is needed for a systematic review (Chaudhary et al., 2021). During the field mining, the keywords "aerosol," "aerosol optical depth," "precipitation," "temperature," "relative humidity," "exposure," "anthropogenic sources," "threats," and "human health" were used. The main aim of this research work is to study the area of aerosols and the various parameters associated with aerosols. The information was gathered for the past 10 years, and 24 plain text files containing 8697 documents were obtained. The datasets are analyzed using credible conditions, research articles, editorial comments, and other information.

Table 1 Steps involved in gathering data

Search string	"Aerosol-precipitation-aerosol optical depth temperature-relative humidity-exposure-human health" OR "Aerosol-aerosol optical depth-exposure-anthropogenic sources" OR "Aerosol-aerosol optical depth-exposure-threats" OR "Aerosol-aerosol optical depth-exposure-human health" OR "Aerosol-aerosol optical depth-precipitation-temperature-Relative Humidity" OR "Aerosol-aerosol optical depth -Exposure" OR "Aersosol-aerosol optical depth-anthropogenic sources" OR "Aerosol-Human health-Threats" OR "Aerosol-aerosol optical depth"
Fields mined	Article titles and abstract, author keywords
Database	Web of Science (WoS)
Final sample	8697 articles
Search date	25 July 2023
Inclusion	Journals and review articles

Scientometric Analysis

A statistical method known as "bibliometric analysis" establishes the quantitative analysis of research papers that are focused on a specific topic. By connecting articles, journals, authors, and keywords with co-citations and co-occurrence networks, it produces a variety of interpretations (Feng et al., 2017). The software used for performing this analysis is VOSviewer (1.616) was adopted by (Van Eck & Waltman, 2010). This study illustrates the network's geographic spread, productivity of the authors and influences, journals, articles, and clusters indicating topics pertinent to this field. Data cleaning is performed to remove recurring words, nouns, shortened forms, etc.

3 Results and Discussion

3.1 Regional Distribution of Publications

The set of data is distributed regionally physically, and it lists the main countries that have contributed to aerosol, aerosol optical depth, precipitation, temperature, relative humidity, exposure, source, threats, and human health. Out of the 127 nations that have published publications on this topic, 79 of them have participated in the co-authorship network. Figure 1 shows the Geographical distribution of co-authorship countries on aerosol, aerosol optical depth, precipitation, temperature, relative humidity, exposure, source, threats, and human health. Table 2 describes the top 10 nations in terms of both the total number of articles published and the countries with the most co-authors. Table 3 illustrates the top 10 nations in terms of total citations and overall co-authorship. China ranks one in terms of a number of articles published with 2630 articles and ranks second in the number of citations with
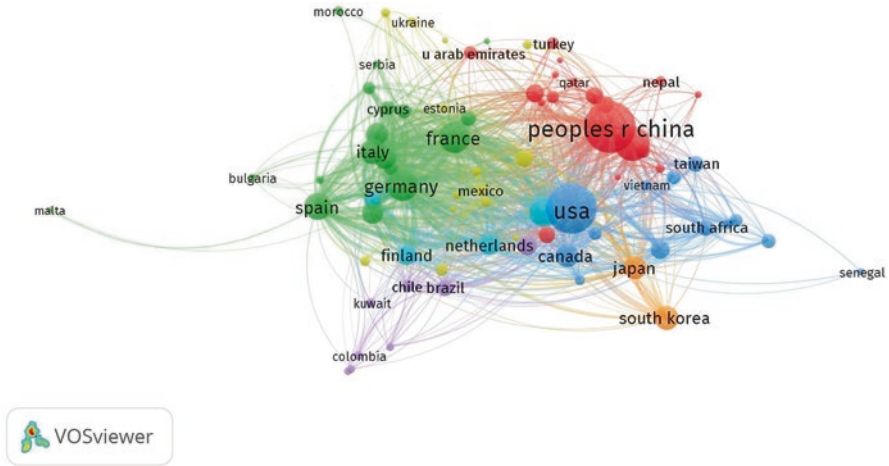
Fig. 1 Geographical distribution of co-authorship countries on aerosol, aerosol optical depth, precipitation, temperature, relative humidity, exposure, source, threats, and human health

Table 2 Top 10 countries in terms of overall published articles and the number of co-author countries

Rank	Articles published (Number of articles)	Number of co-author countries (Number of countries)
1	People's Republic of China (2630)	USA (74)
2	USA (2543)	People's Republic of China (67)
3	India (867)	Germany (66)
4	Germany (584)	England (66)
5	France (569)	France (63)
6	England (521)	Italy (60)
7	Spain (386)	Spain (57)
8	Italy (323)	Netherlands (56)
9	Canada (243)	Canada (55)
10	Netherlands (205)	India (54)

51,687 citations. The USA comes first in the number of co-authored countries with 74 countries and is highest in the number of citations with 73,456 citations. USA and India rank second and third in the number of articles published in the field of aerosol, aerosol optical depth, precipitation, temperature,relative humidity, exposure, source, threats, and human health followed by other countries such as Germany, France and England. Germany and France rank third and fourth in total co-authorship and citations. Countries such as Spain, Netherlands, Canada, and Italy comes in the top 10 in these categories according to Tables 2 and 3.

Table 3 Top 10 countries in terms of overall co-authorship and citation number

Rank	Total co-authorship (Number of co-authorship)	Citation (Number of citations)
1	USA(2975)	USA (73456)
2	People's Republic of China (1732)	People's Republic of China (51687)
3	Germany (1389)	Germany (14937)
4	England (1312)	England (14479)
5	France (1286)	France (13745)
6	Italy (842)	India (12439)
7	Spain (793)	Canada (9292)
8	Netherlands (646)	Netherlands (7440)
9	Canada (568)	Spain (7375)
10	India (558)	Italy (6851)
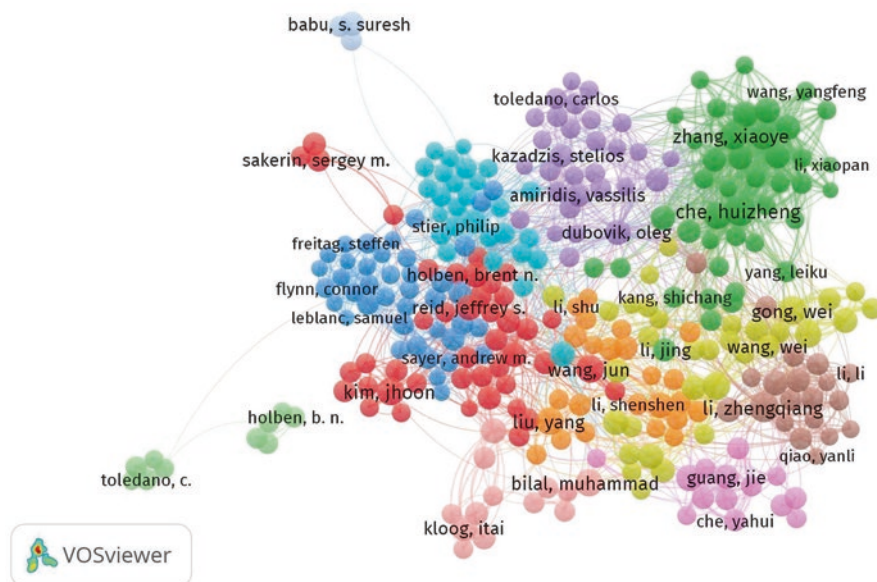
Fig. 2 Network visualization of most influential authors

3.2 Authors' Productivity and Influence

In all areas of research, authors play a significant role. A total of 22,019 authors are known to have worked on aerosols, and 1625 authors have contributed at least five articles to the area of research. In our analysis of data, the authors who have produced the most papers are regarded as the most productive authors. Similarly to this, the authors who have had the most articles cited are regarded as the most influential authors. Figure 2 represents the network visualization of the most influential authors and their geographic distribution according to the number of citations and

co-authorships. Tables 4 and 5 discuss the most productive and influential authors who have contributed to this field of study**.** The most productive author in this field of study of aerosols in terms of articles published is Dr. Huizheng Che (114 articles and 2834 citations) followed by Dr. Yeng Liu and Dr. Alexei Lyapustin with 74 and 52 articles published. Dr. Alexei Lyapustin ranks first as the most influential author with 5092 citations and 274 total co-authorship. The fourth highest most productive and influential author is Dr.ItaiKloog with 46 published articles and 3070 citations.

Table 4 Most productive author in the area of aerosol, aerosol optical depth, precipitation, temperature, relative humidity, exposure, source, threats, and human health

Author name according to VOS viewer	Author	Articles	Citation	Total co-authorship	Co-author
che, huizheng	Dr. Huizheng Che	114	2834	816	174
liu, yang	Dr. Yeng Liu	74	4570	258	86
lyapustin, alexei	Dr. Alexei Lyapustin	52	5092	274	124
kloog, itai	Dr. Itai Kloog	46	3070	155	24
schwartz, joel	Dr. Joel Schwartz	34	2552	130	32
wang, yujie	Dr. Yujie Wang	28	2508	125	58
van donkelaar, aaron	Dr. Aaron van Donkelaar	23	3242	102	40
martin, randall v.	Dr. Randall V. Martin	21	3029	75	38
hsu, n. c.	Dr. Nai-Yung Christina Hsu	14	2453	37	10
brauer, michael	Dr. Michael Brauer	12	2371	70	31

Table 5 The most influential author in the area of aerosol, aerosol optical depth, precipitation, temperature, relative humidity, exposure, source, threats, and human health

Author name according to VOS Viewer	Author	Citation	Articles	Total co-authorship	Co-author
lyapustin, alexei	Dr. Alexei Lyapustin	5092	52	274	124
liu, yang	Dr. Yeng Liu	4570	74	258	86
van donkelaar, aaron	Dr. Aaron Van Donkelaar	3242	23	102	40
kloog, itai	Dr. Itai Kloog	3070	46	155	24
martin, randall v.	Dr. Randall V. Martin	3029	21	75	38
che, huizheng	Dr. Huizheng Che	2834	114	816	174
schwartz, joel	Dr. Joel Schwartz	2552	34	130	32
wang, yujie	Dr. Yujie Wang	2508	28	125	58
hsu, n. c.	Dr. Nai-Yung Christina Hsu	2453	14	37	10
brauer, michael	Dr. Michael Brauer	2371	12	70	31

Dr.Michael Brauer (2371 citations, 12 articles) ranks tenth in the most influential and productive authors involved in this study area.

Most Productive Author

Most Influential Author

3.3 Core Journals

The most productive journals based on the number of articles published have been illustrated in Fig. 3. The journal *Atmospheric Chemistry and Physics* has the highest number of articles published (668 articles) making it the most productive journal in this study area followed by the journals *Remote Sensing* and *Atmospheric Environment* with 521 and 498 published articles. In terms of articles published, other productive journals are *Journal Of Geophysical Research Atmospheres*, *Atmospheric Environmental Measurement Techniques,* and *Atmospheric Research*.

3.4 Articles

Influential Articles

Figure 4 emphasizes the most influential journals based on the number of citations. In the context of the research field, the articles that are frequently cited are consequently regarded as influential articles. The journal *Atmospheric Chemistry and*
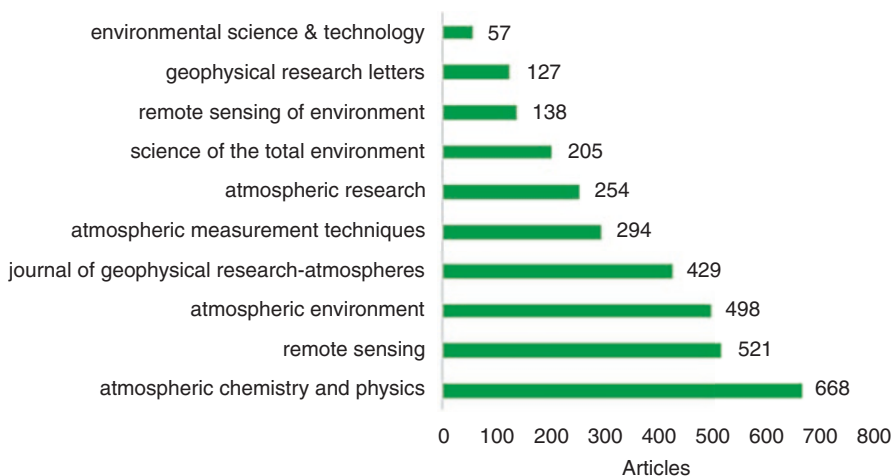
Fig. 3 Top productive journals in terms of published articles
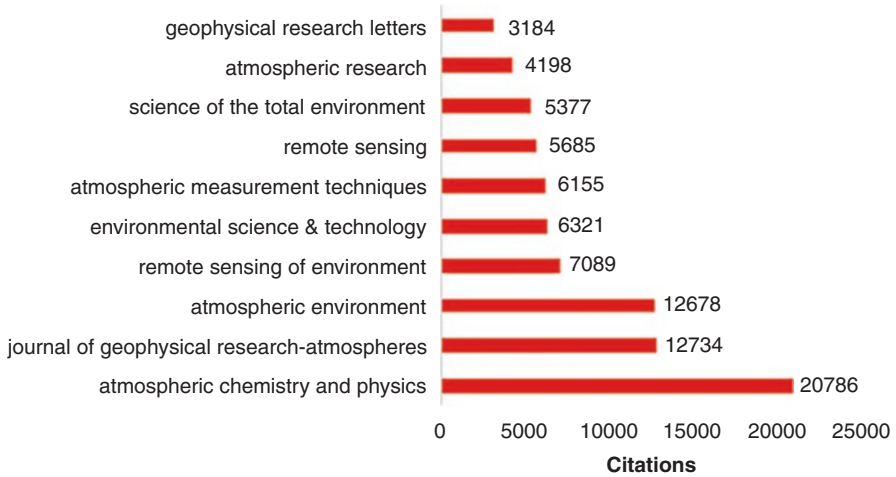
Fig. 4 Top influential journals in terms of citations

Physics is the most influential journal based on the number of citations (20,786 citations). The second highest influential journal is the *Journal Of Geophysical Research Atmospheres* followed by *Atmospheric Environment* and *Remote Sensing Of Environment*.

Table 6 represents the highly cited articles along with the citation number. The article by Van Donkelaar et al. (2016) ranks first with 723 citations focuses on combining data from simulations, monitors, and satellites, to predict worldwide fine particulate matter (PM2.5) concentrations, and has been published in *Environmental Science and Technology*. This article demonstrates that adding sporadic ground-based measurements to continuous worldwide sources of PM 2.5 data can result in significant improvements to PM 2.5 characterization on a worldwide level. The article by Hsu et al. (2013) ranks second with 706 citations describes using the Moderate Resolution Imaging Spectroradiometer (MODIS) collection 5.1 deep blue method, aerosol products were recovered that had useful data regarding the characteristics of aerosols over brightly reflecting terrain surfaces. Randles et al. (2017) describe the MERRA-2 aerosol data assimilation system and give preliminary validation of the processed aerosol optical depth fields. The work by Lyapustin et al. (2018) explains the recent version of the algorithm MAIAC that was implemented to process the MODIS Collection 6 data record. The article also discusses MCD19 data products, assurance of quality flags, MAIAC cloud identification, aerosol retrievals, and atmospheric correction. Bellouin et al. (2020) expressed their views on aerosol absorption and the reasons for changes in surface radiative fluxes limiting the forcing resulting from aerosol-radiation interactions and the article has been published in *Reviews Of Geophysics* with 301 citations.

Table 6 Top 10 highly cited articles in the field of aerosol, aerosol optical depth, precipitation, temperature, relative humidity, exposure, source, threats, and human health

Rank	Author	Title	Journal	Citation
1	Van Donkelaar et al. (2016)	Global estimates of fine particulate matter using a combined geophysical statistical method with information from satellites, models, and monitors	Environmental Science and Technology	723
2	Hsu et al. (2013)	Enhanced deep blue aerosol retrieval algorithm: The second generation	Journal of Geophysical Research - Atmospheres	706
3	Randles et al. (2017)	The MERRA-2 aerosol reanalysis, 1980 onward, part I: System description and data assimilation evaluation	Journal of Climate	593
4	Giles et al. (2019)	Advancements in the aerosol robotic network (AERONET) version 3 database automated near-real-time quality control algorithm with improved cloud screening for sun photometer aerosol optical depth (AOD) measurements	Atmospheric Measurements Techniques	500
5	Sayer (2014)	MODIS collection 6 aerosol products: Comparison between aqua's e-deep blue, dark target, merged data sets, and usage recommendations	Journal of Geophysical Research - Atmospheres	459
6	Buchard et al. (2017)	The MERRA-2 aerosol reanalysis, 1980 onward, part II: Evaluation and case studies	Journal of Climate	384
7	Lyapustin et al. (2018)	MODIS collection 6 MAIAC algorithm	Atmospheric Measurement Techniques	377
8	Inness et al. (2019)	The CAMS reanalysis of atmospheric composition	Atmospheric Chemistry and Physics	344
9	Van Donkelaar et al. (2019)	Regional estimates of chemical composition of fine particulate matter using a combined geoscience-statistical method with information from satellites, models, and monitors	Environmental Science and Technology	319
10	Bellouin et al. (2020)	Bounding global aerosol radiative forcing of climate change	Reviews of Geophysics	301

3.5 Bibliographic Coupling

To identify appropriate categories and major themes, bibliographic coupling of articles is done. Figure 5 represents three major domains in this study area. Tables 7, 8, and 9 show the top three articles in each cluster. The red cluster highlights the estimation of fine particulate matter and aerosol retrieval algorithms. The blue cluster discusses the reanalysis techniques of atmospheric composition. Articles related to aerosol optical properties are analyzed in green cluster.
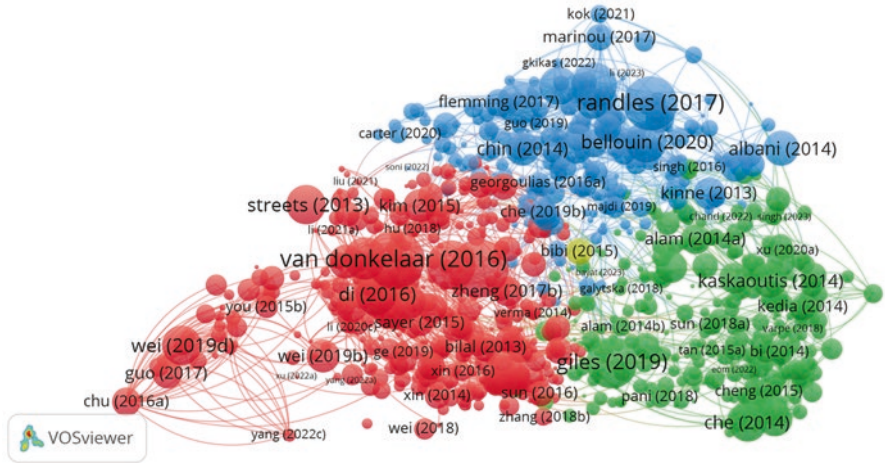
Fig. 5 Bibliographic coupling of articles within the study area of aerosol, aerosol optical depth, precipitation, temperature, relative humidity, exposure, source, threats, and human health

Table 7 Top three highly cited articles related to estimation of fine particulate matter and aerosol retrieval algorithms

Cluster A(Red): Estimation of fine particulate matter and aerosol retrieval algorithms	
References	Article citation
Van Donkelaar et al. (2016)	723
Hsu et al. (2013)	706
Sayer (2014)	459

Table 8 Top three highly cited articles based on reanalysis techniques of atmospheric composition

Cluster B(Blue): Reanalysis techniques of atmospheric composition	
References	Article citation
Randles et al. (2017)	593
Buchard et al. (2017)	384
Inness et al. (2019)	344

Table 9 Top three highly cited articles based on aerosol optical properties

Cluster C(Green): Aerosol optical properties	
References	Article citation
Giles et al. (2019)	500
Che et al. (2014)	244
Kaskaoutis et al. (2014)	197

The red cluster in the bibliographic coupling discusses the various aerosol retrieval algorithms and fine particulate matter estimation from various sources such as models, monitors, and satellites. By relative ambiguity, which was computed using ground-based sun photometer (AERONET) measurements during 1998–2014, aerosol optical depth from several satellite products was integrated with simulation (GEOS–Chem). Due to emissions in the Asian and African countries, the yearly average PM2.5 concentrations were three times higher than the WHO recommendation of 10 g/m³ (Van Donkelaar et al., 2016). Three techniques are used in the Moderate Resolution Imaging Spectroradiometer (MODIS) to obtain aerosol optical depth which includes Enhanced Deep Blue (DB), and dark target (DT) over water and land (Hsu et al., 2013).

The blue cluster discusses various reanalysis techniques such as The Modern-Era Retrospective Analysis version 2 (MERRA-2) and Copernicus Atmosphere Monitoring Service (CAMS). Aerosol optical depth (AOD) synthesis from multiple ground- and space-based remote sensing systems has been incorporated in MERRA-2. The MERRA-2 aerosol integration is described, together with the GEOS-5 coupled to GOCART aerosol modules, aerosol emission levels, quality control, and air-climate interactions by studying the clear-sky aerosol direct radiative effect (Randles et al., 2017). The article by Buchard et al. (2017) focuses on the assessment and verification of the existing MERRA −2 aerosol properties which have no direct impact on the AOD assimilation. Inness et al. (2019) describe the CAMS reanalysis which is utilized to create climatologies, research patterns, assess models, compare them to other reanalyzes, or act as boundary criteria for local models.

The green cluster discusses about AERONET for measuring the aerosol optical depth measurements and AERONET stations have multiplied dramatically over the past 25 years, millions of readings must now be manually checked for consistency (Giles et al., 2019). Kaskaoutis et al. (2014) This research uses a combination of ground-based measurements and observations from satellites to look at the way burning paddy crop residue across northern India throughout the post-monsoon (October–November) season of 2012 affected aerosol properties, long-range propagation of smoke plumes, and altitude features.

3.6   Keyword Analysis

An outline of the study domain and the structure of the gathered articles can be provided by keyword analysis. In general, there were 10,273 keywords in our data collection. The keywords were evaluated based on five minimum occurrences, and 723 met the required frequency. Figure 6 illustrates the main hotspots in this stud area. The most frequently used keywords are shown in Table 10. The keyword aerosol optical depth ranks first in the most frequently used keyword with a frequency of 940. The keywords MODIS and aerosol rank second and third with 603 and 512 frequency, respectively. The keywords air pollution and air quality rank eighth and

Fig. 6 The main hotspots of the keywords

Table 10 Top 15 frequently used author keywords in the domain of aerosol, aerosol optical depth, precipitation, temperature, relative humidity, exposure, source, threats, and human health

Rank	Keywords	Frequency
1	Aerosol optical depth	940
2	Modis	603
3	Aerosol	512
4	Aod	506
5	Aeronet	370
6	Remote sensing	354
7	PM 2.5	325
8	Air pollution	247
9	Air quality	166
10	Particulate matter	156
11	Lidar	131
12	Biomass burning	130
13	Radiative forcing	128
14	Dust	127
15	Black carbon	125

ninth in the top fifteen frequently used keywords. Other keywords used in this domain are AERONET, radiative force, black carbon, particulate matter, dust, biomass burning, and many others.

4 Conclusions

The current study makes an effort to comprehend current developments in the domain of aerosol by bibliography analysis. The analysis' findings led to some outstanding research studies in the area of aerosol. Much research has been done in this study domain over the last 10 years. The most significant study areas identified in the field are the estimation of fine particulate matter and aerosol retrieval algorithms, reanalysis techniques of atmospheric composition, and aerosol optical properties. Many countries and authors have contributed to this field of study and have published papers in various journals. The evaluation attempted to highlight the main areas that require attention, investigation, and study. For scientists, researchers, and inventors, this assessment might be regarded as an initial investigation. Evaluating and conducting a scientometric analysis of aerosols and their associated implications is an important area of research, especially considering their impact on air quality, climate change, and human health. While substantial progress has been made in this field, there are still several areas that require further exploration and improvement. Certain areas that require specific improvement include the development of more techniques for characterizing the chemical and physical properties of aerosols, advancement in modeling and simulation, and analyzing the regional and global climate impacts of aerosols, including their role in extreme weather events. I suggest more studies on emerging technologies, such as sensors and remote sensing techniques, for improving aerosol monitoring and analysis. Machine learning and AI techniques could be incorporated for more accurate modeling. More research has to be conducted on the health effects of different types of aerosols, including fine particulate matter (PM2.5) along with their chemical constituents and long-term health implications beyond respiratory diseases, such as cardiovascular and neurological effects. A fundamental study on aerosol is emerging, and in the past 10 years, 8697 articles have been published on this topic. The study has certain limitations because the datasets were only obtained via the Web of Science, and there is a risk that some outstanding works in this subject may have been missed.

References

Bellouin, N., Quaas, J., Gryspeerdt, E., Kinne, S., Stier, P., Watson-Parris, D., et al. (2020). Bounding global aerosol radiative forcing of climate change. *Reviews of Geophysics, 58*, e2019RG000660.

Bove, H., Bongaerts, E., Slenders, E., Bijnens, E. M., Saenen, N. D., Gyselaers, W., Van Eyken, P., Plusquin, M., Roeffaers, M. B. J., Ameloot, M., et al. (2019). Ambient black carbon particles reach the fetal side of human placenta. *Nature Communications, 10*, 3866.

Buchard, V., Randles, C. A., Da Silva, A. M., Darmenov, A., Colarco, P. R., et al. (2017). The MERRA-2 aerosol reanalysis, 1980 onward. Part II: Evaluation and case studies. *Journal of Climate, 30*, 6851–6872.

Chaudhary, S., Dhir, A., Ferraris, A., & Bertoldi, B. (2021). Trust and reputation in family businesses: A systematic literature review of past achievements and future promises. *Journal of Business Research, 137*, 143–161.

Che, H., Xia, X., Zhu, J., Li, Z., Dubovik, O., Holben, B., et al. (2014). Column aerosol optical properties and aerosol radiative forcing during a serious haze-fog month over North China Plain in 2013 based on ground-based sun photometer measurements. *Atmos Chem Phys., 14*, 2125–2138.

Feingold, G., Eberhard, W. L., Veron, E., & Previdi, M. (2003). First measurements of the Twomey indirect effect using ground-based remote sensors. *Geophysical Research Letters, 30*(6), 1287–1291.

Feng, Y., Zhu, Q., & Lai, K. H. (2017). Corporate social responsibility for supply chain management: A literature review and bibliometric analysis. *Journal of Cleaner Production, 158*, 296–307.

Forouzanfar, M. H., Alexander, L., Anderson, H. R., Bachman, V. F., Biryukov, S., et al. (2015). Global, regional, and national comparative risk assessment of 79 behavioural, environmental and occupational, and metabolic risks or clusters of risks in 188 countries, 1990–2013: A systematic analysis for the Global Burden of Disease Study 2013. *The Lancet, 86*(10010), 2287–2323.

Giles, D. M., Sinyuk, A., Sorokin, M. G., Schafer, J. S., et al. (2019). Advancements in the Aerosol Robotic Network (AERONET) Version~3 database – Automated near-real-time quality control algorithm with improved cloud screening for Sun photometer aerosol optical depth (AOD) measurements. *Atmospheric Measurement Techniques, 12*, 169–209.

Giordano, L. (2015). Assessment of the MACC reanalysis and its influence as chemical boundary conditions for regional air quality modeling in AQMEII-2. *Atmospheric Environment, 115*, 371–388.

Holben, B. N., Eck, T. F., Slutsker, I., Tanre, D., Buis, J. P., et al. (1998). AERONET – A federated instrument network and data archive for aerosol characterization. *Remote Sensing of Environment, 66*(1), 1–16.

Hsu, N. C., Jeong, M.-J., Bettenhausen, C., Sayer, A. M., Hansell, R., Seftor, C. S., et al. (2013). Enhanced deep blue aerosol retrieval algorithm: The second generation. *Journal of Geophysical Research—Atmospheres, 118*, 9296–9315.

Inness, A., Ades, M., Agust-Panareda, A., & Barr, J. (2019). The CAMS reanalysis of atmospheric composition. *Atmospheric Chemistry and Physics, 19*, 3515–3556.

Kaskaoutis, D. G., Kumar, S., Sharma, D., Singh, R P., Kharol, S. K., Sharma, M., Singh, A. K., et al. (2014). Effects of crop residue burning on aerosol properties, plume characteristics, and long-range transport over northern India. *Journal of Geophysical Research: Atmospheres, 119*, 5424–5444.

Kelly, F. J., & Fussell, J. C. (2015). Air pollution and public health: Emerging hazards and improved understanding of risk. *Environmental Geochemistry and Health, 37*, 631–649.

Liu, F., Huang, Y., Zhang, F., Chen, Q., Wu, B., Rui, W., Zheng, J. C., & Ding, W. (2015). Macrophages treated with particulate matter $PM_{2.5}$ induce selective neurotoxicity through glutaminase-mediated glutamate generation. *Journal of Neurochemistry, 134*, 315–326.

Lyapustin, A., Wang, Y., Korkin, S., & Huang, D. (2018). MODIS collection 6 MAIAC algorithm. *Atmospheric Measurement Techniques, 11*, 5741–5765.

Mannucci, P. M., & Franchini M Health. (2017). Effects of ambient air pollution in developing countries. *International Journal of Environmental Research and Public Health, 14*, 1048.

Ramanathan, V., Crutzen, P. J., Kiehl, J. T., & Rosenfeld, D. (2001). Aerosols, climate, and the hydrological cycle. *Science (New York, NY), 294*(5549), 2119–2124.

Randles, C. A., Da Silva, A. M., Buchard, V., Colarco, P. R., et al. (2017). The MERRA-2 aerosol reanalysis, 1980 onward. Part I: System description and data. Assimilation evaluation. *Journal of Climate, 30*, 6823–6850.

Ranjbari, M., Saidani, M., Shams Esfandabadi, Z., et al. (2021). Two decades of research on waste management in the circular economy: Insights from bibliometric, text mining, and content analyses. *Journal of Cleaner Production, 314*, 128009.

Ranjbari, M., Shams Esfandabadi, Z., Ferraris, A., Quatraro, F., Rehan, M., et al. (2022). Biofuel supply chain management in the circular economy transition: An inclusive knowledge map of the field. *Journal of Chemosphere, 296*, 0045–6535.

Sah, D., Verma, P. K., Kandikonda, M. K., & Lakhani, A. (2018). Pollution characteristics, human health risk through multiple exposure pathways, and source apportionment of heavy metals in PM_{10} at Indo-Gangetic site. *Urban Climate, 27*, 149–162.

Sayer, A. M., Munchak, L. A., Hsu, N. C., Levy, R. C., Bettenhausen, C., & Jeong, M.-J. (2014). MODIS collection 6 aerosol products: Comparison between Aqua's e-deep blue, dark target, and "merged" data sets, and usage recommendations. *Journal of Geophysical Research— Atmospheres, 119*, 13,965–13,989.

Van Donkelaar, A., Martin, R. V., Brauer, M., Hsu, N. C., et al. (2016). Global estimates of fine particulate matter using a combined geophysical-statistical method with information from satellites, models, and monitors. *Environmental Science & Technology, 50*(7), 3762–3772.

Van Donkelaar, A., Martin, R. V., Li, C., & Burnett, R. T. (2019). Regional estimates of chemical composition of fine particulate matter using a combined geoscience-statistical method with information from satellites, models, and monitors. *Environmental Science & Technology, 5*, 2595–2611.

Van Eck, N. J., & Waltman, L. (2010). Software survey: VOSviewer, a computer program for bibliometric mapping. *Scientometrics, 84*(2), 523–538.

Anthropogenic Influence on Aerosol Optical Depth

S. Najma Nikkath and S. Tamil Selvi

1 Introduction

Climate is a dynamic system characterized by long-term averages of weather conditions, encompassing variations in factors such as wind patterns, temperature, and precipitation. Recent years have witnessed an increase in the frequency and intensity of weather-related events, raising significant concerns about their causes and impacts. Anthropogenic activities, driven by factors like urbanization and population growth, have led to increased energy consumption. While greenhouse gases are often the focus of discussions, it is now recognized that human-induced activities also release aerosols, originating from both natural and anthropogenic sources. These aerosols play a role in altering rainfall patterns, leading to shifts in drought occurrence, and influencing the frequency and severity of extreme weather events.

Aerosols serve as crucial components within clouds, alongside water vapor, temperature, and relative humidity, acting as nucleating agents for water vapor condensation. Both natural and human-induced sources contribute to aerosol levels, but there has been a notable exponential increase in recent decades. This surge has led to a significant upswing in aerosol research, particularly within climate studies. One key impact attributed to aerosols is the intensification of rainfall events, resulting in more pronounced downpours and an elevated risk of flooding in certain regions (Dong et al., 2021).

The increase in heavy rainfall events and flash floods poses significant challenges to human lives and property. Conversely, aerosols can also exacerbate droughts by impeding rainfall. Regions experiencing reduced precipitation or prolonged dry

S. N. Nikkath (✉)
Department of Physics, Bhaktavasalam Memorial College for Women,
Chennai, Tamil Nadu, India

S. T. Selvi
Department of Physics, KCG College of Technology, Chennai, Tamil Nadu, India

spells may face water scarcity, diminished agricultural yields, and ecological strain. It is essential to acknowledge that the impact of anthropogenic activities on rainfall and drought varies across regions. Local factors such as topography, changes in land use, and natural climate fluctuations interact with global climate shifts, yielding diverse outcomes. Ongoing scientific research continues to shed light on the effects of anthropogenic activities on rainfall and drought.

In this chapter, we delve into various types of aerosols and their mechanisms for insulating radiation. We examine pivotal aspects of aerosol studies, such as aerosol optical depth (AOD), and review its historical contributions to either heightening or diminishing precipitation. Insights into precipitation mechanisms specific to India, with a focus on urban precipitation, are also provided. Additionally, diverse strategies to mitigate the impacts of anthropogenic effects are discussed. The debate over whether AOD leads to increased or decreased precipitation persists, varying in temporal and spatial scales and contingent upon regional contributions. The influence of aerosols, coupled with meteorological parameters, is highly complex due to their diverse size, composition, and origin, necessitating further exploration and study in this field.

1.1 What Are Aerosols?

Aerosols are suspended liquid or solid particles with diameters spanning four orders of magnitude, ranging from approximately 3 nanometers to a few hundredths of millimeters. These particles are generally smaller than cloud droplets and exhibit a wide dynamic range of composition and shape, influenced by their sources and atmospheric processes (Aitken, 1980; Wilson, 1987). It is widely recognized that aerosols play a crucial role in the environment (Fig. 1).

Aerosol particles of anthropogenic origin both reflect and absorb solar energy as the solar beam penetrates the atmosphere. Consequently, these particles can diminish the amount of energy reaching the Earth's surface as heat. Scientists estimate that human-produced particles have contributed to a net loss of solar energy (heat) at the ground, particularly evident in densely populated areas, with reductions of up to 8 percent observed over the past few decades.

Anthropogenic activities are the primary source of aerosols (Tsai et al., 2012). Research indicates that the majority of ultrafine aerosols originate from combustion processes, particularly emissions from vehicle exhausts (Kittelson, 1998).

1.2 Classification of Aerosols

Aerosols pose hazards to both human health and the environment. It is estimated that globally, 10–20% of aerosols can be attributed to anthropogenic sources (Andreae, 1995). Anthropogenic aerosols such as dust, smoke, haze, and urban

Fig. 1 Aerosols covered urban city view

smog are prevalent in and downwind of urban environments, while volcanic eruptions emit large quantities of primary aerosols into the atmosphere, acting as natural aerosols. The lifetimes of aerosols typically range from a few days to a week, depending on their properties and meteorological conditions (Raes et al., 2000). Aerosols are removed from the atmosphere through dry or wet deposition, including rainfall. The transport velocity of aerosols is approximately 5 m/s, with a transport distance of up to 3000 km. Consequently, the amount and nature of aerosols can vary substantially at any given location due to variability in atmospheric transport and aerosol formation processes, largely influenced by meteorological factors.

Atmospheric aerosols comprise a diverse range of particle types with varying compositions, sizes, shapes, and optical properties. The loading of aerosols in the atmosphere is typically quantified by mass concentration or by an optical measure known as aerosol optical depth (AOD).

1.2.1 Based on Source

Primary particles are directly emitted as liquids or solids from various sources, including biomass burning, incomplete combustion of fossil fuels, volcanic eruptions, as well as wind-driven or traffic-related biological materials such as plant fragments, microorganisms, and pollen (Fig. 2). Additionally, gas-to-particle conversion processes in the atmosphere, such as nucleation and condensation of gaseous precursors, contribute to the formation of secondary particles.
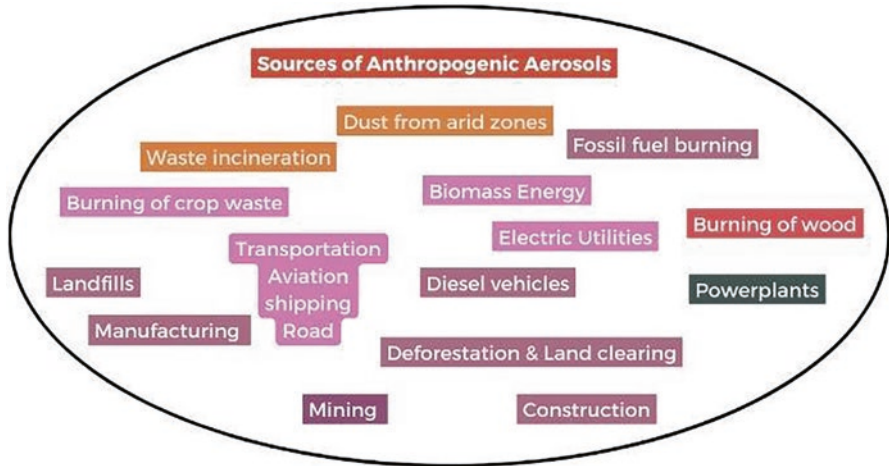
Fig. 2 Anthropogenic aerosols
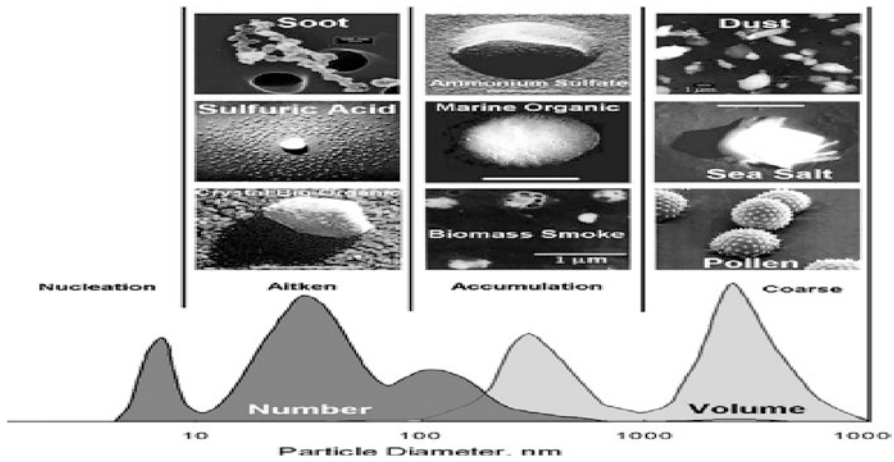
Fig. 3 Size of Aerosols

1.2.2 Based on Size

Pruppacher and Klett (1997) classified aerosols based on their size into three categories: ultrafine/nucleation mode (size range: 0.001—0.1 μm, Fig. 3), accumulation mode (size range: 0.1–1 μm), and coarse mode (size greater than 1 μm radius). The terms "nucleation" and "accumulation" refer to the mechanical and chemical processes by which aerosol particles in these size ranges are formed.

Nucleation mode particles are smaller in size and constitute only a few percent of the aerosols in the atmosphere. Coarse mode particles are formed due to mechanical processes such as windblown dust and sea-salt aerosols produced by the

breaking of sea waters. The chemical nature of aerosols depends on their source, while their size distribution depends on the underlying mechanisms. In oceanic regions, giant salt particles play a significant role in cloud development (Chin et al., 2002).

1.2.3 Based on Composition

Aerosols are classified based on their composition into various categories, including sulfates, nitrates, sea salt, mineral dust, and carbonaceous components such as black carbon (BC, often referred to as soot) and organic carbon (OC) (Fig. 4). Each aerosol particle is composed of different chemical constituents, as noted by Prospero et al. (1983).

1.2.3.1 Sea-Salt Aerosols

Sea-salt particles are primarily produced over the sea through processes associated with the bursting of bubbles (Hoppel et al., 1990; Satheesh & Moorthy, 2005) (Fig. 5). During periods of very strong winds exceeding 10 m/s, direct sea-spray production occurs as wave crests break. At moderate wind speeds of approximately 3–5 m/s, white capping occurs when ocean surface waves overturn, generating bubbles. The bursting of these bubbles produces a fine mist of extremely small particles known as film droplets, which subsequently evaporate to maintain relative humidity. Depending on the relative humidity, the particles can exist either as solution droplets or crystalline matter. Literature suggests that the production rate of sea-salt

Fig. 4 Types of aerosols
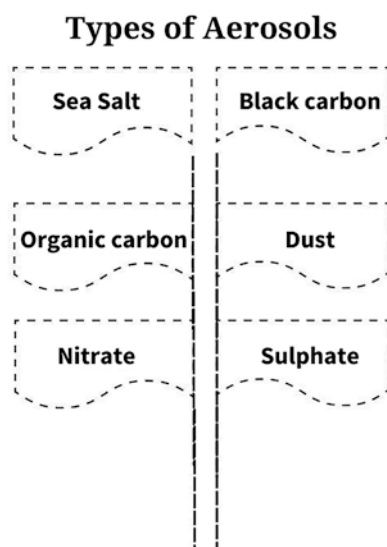
Fig. 5 Tearing of wave crusts leading to sea-salt production

particles depends not only on sea surface wind speed but also on sea surface temperature (O'Dowd & de Leeuw, 2007).

1.2.3.2 Sulfate and Nitrate Aerosols

Sulfate and nitrate aerosols are primarily produced due to anthropogenic activities (Prospero et al., 1983). Sulfate formation occurs through aqueous phase reactions within cloud droplets and oxidation of sulfur dioxide (SO_2) via gaseous phase reactions with hydroxyl radicals (OH), as well as by condensational growth onto pre-existing particles (Penner et al., 2001). The majority (72%) of SO_2 emissions into the atmosphere stem from fossil fuel burning, with a smaller contribution (2%) from biomass burning. Sulfur compounds in the atmosphere include sulfur dioxide, hydrogen sulfide, carbon disulfide, carbonyl sulfide, and dimethyl sulfide. Naturally, sulfate aerosols are produced over oceans by emissions from oceanic phytoplankton (Clarke et al., 1987; Russell & Heintzenberg, 2000). Dimethyl sulfide (DMS), emitted by oceanic phytoplankton (of biogenic origin), undergoes conversion to sulfate aerosols over oceans. DMS-derived aerosols constitute approximately 19% of total sulfate aerosols in the atmosphere. Additionally, volcanic eruptions emit sulfate aerosols (~7%) into the atmosphere (refer to Fig. 6). These aerosols scatter solar radiation and increase planetary albedo. They are hygroscopic in nature, acting as cloud condensation nuclei. On a global scale, sulfate aerosols are believed to cool the planet and partly offset heating due to greenhouse gases (Gautam et al., 2009).

Atmospheric nitrates arise from the oxidation of nitrogen dioxide to nitric acid, which forms particles through reactions with ammonia or sodium chloride (Harrison et al., 1996). The most common pure nitrate particulate matter is ammonium nitrate (NH4NO3). Precursor gases of particulate nitrate include nitrogen oxides, volatile nitrogen-bearing acids, and gaseous nitrates (Harrison & McCatrney, 1979).

Fig. 6 A volcanic eruption emitting massive amount of gases and ash

Fig. 7 Transport of mineral aerosols during a dust storm

1.2.3.3   Mineral Dust Aerosols

Winds generate mineral dust aerosols over arid and semiarid regions (D'Almeida et al., 1991) (Fig. 7). The chemical composition of mineral dust aerosols is influenced by the production and characteristics of the soil region serving as their source (Miller & Tegen, 1998). The long-range transport of mineral dust is facilitated by the combined action of convection currents and general circulation systems, making these particles significant constituents even at locations far from their sources. As

these particles are generated at the Earth's surface, they are predominantly confined within the troposphere.

1.2.3.4 Carbonaceous Aerosols

The primary sources of carbonaceous aerosols include fossil fuel and bio-fuel combustion, biomass burning, and the oxidation of biogenic and anthropogenic volatile organic compounds (Fig. 8). These aerosols are broadly classified into two categories: Black Carbon (BC) and Organic Carbon (OC) (Cachier et al., 1989).

Black carbon aerosols, often referred to as BC, are primarily produced by fossil fuel or biomass burning at low temperatures and are predominantly absorbed in nature (Schwartz et al., 1995). The absorption properties of BC depend on the amount of graphitic carbon present, which varies based on the completeness of combustion. BC is relatively inert and finite in size, capable of being transported over long distances with a residence time of a few weeks (Horvath, 1993). It contributes to atmospheric heating due to its absorption properties (Babu et al., 2002), with some studies suggesting that BC warming may be second only to CO_2, thereby complementing global warming (Jacobson, 2001; Jacobson, 2002). Another type of carbon, known as brown carbon, results from biomass burning and has gained global attention due to its significantly different absorption properties compared to BC (D'Almeida et al., 1991). Brown carbon absorbs strongly in the blue and ultraviolet regions with minimal absorption in the mid-visible spectrum. Globally, approximately 20% of BC is emitted from burning biofuels, 40% from fossil fuels, and 40% from open biomass burning (Miller & Tegen, 1998). Despite the differences in their lifetimes (weeks for BC compared to approximately 100 years for

Fig. 8 Biomass burning and ejecting organic aerosols into the atmosphere

CO_2), the impact of BC is significant on a global scale. The radiative effects of BC are most significant at visible wavelengths rather than at infrared wavelengths.

Organic carbon (OC), the other type of carbonaceous aerosol, is one of the largest single components of biomass-burning aerosols, thereby dominating carbonaceous aerosol emissions. It has both natural and anthropogenic sources and behaves more like sulfate, primarily scattering radiation. Unlike BC, OC encompasses a wide range of individual compounds, each with varying radiative effects. Hundreds of different atmospheric organic compounds have been detected, contributing to the complex nature of organic aerosols (Tyson et al., 1996; Uematsu et al., 1983). Organic aerosols are emitted as primary aerosol particles and are also formed as secondary aerosol particles through the condensation of organic gases (Satheesh & Srinivasan, 2002).

1.3 Radiative Effects of Aerosol

The effect on Earth's radiation and climate is possible both directly and indirectly by the aerosols. The effects of aerosols have been widely studied.

1.3.1 Direct Effect

Aerosols are highly reflective, they increase the albedo of the Earth, thereby cooling the surface and effectively offsetting greenhouse gas warming by about 25–50% (Rueckerl et al., 2011).

1.3.2 Indirect Effect

Aerosols in the low atmosphere act as sites at which water vapor can accumulate during cloud droplet formation, serving as cloud condensation nuclei (CCN). Aerosols also increase in cloud brightness, a reduction in precipitation (Twomey, 1974), and an increase in cloud lifetime (enhancing the cloud reflectance (short albedo).

1.3.3 Semidirect Effect

Aerosols often contain black carbon particles that strongly absorb incoming sunlight (Fig. 9). The effects of this type of aerosol are twofold: warming the atmosphere and cooling the surface below; reducing the atmosphere's vertical temperature gradient and therefore contributing to the reduction of formation of convective cloud.
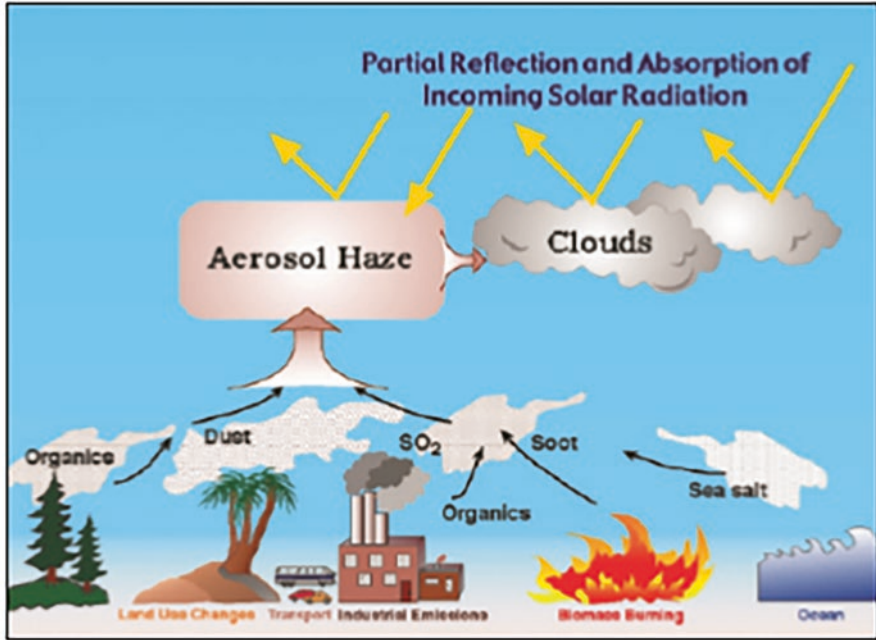
Fig. 9 Radiative effects of aerosols

1.4 Aerosol Optical Depth

One of the most common and important aerosol optical properties is aerosol optical depth (AOD) which has been used by several researchers as an aerosol loading indicator to elucidate the high pollution levels over a region. All the solid particles and liquid droplets suspended in the ambient air are collectively known as atmospheric aerosols (Lippmann, 2000). Aerosols are vital trace materials in the atmosphere. As a basic optical parameter, aerosol optical depth (AOD) is a measure of the extinction effect of atmospheric aerosols and is widely used as a key parameter for assessing the degree of air pollution. The estimation of aerosol optical depth (AOD) at various suitable wavelengths is one of the essential, easier, and suitable parameters for the characterization of aerosols. AOD has a direct relation with processes such as scattering and absorption of radiation in the atmosphere (Ranjan et al., 2007) and is being frequently used for analyzing the atmospheric processes as well as for understanding the climate variability of different regions (Kaufman et al., 2002).

1.5 AOD and Precipitation

Increase in air pollution and other particulate matter in the atmosphere can strongly affect cloud development in ways that reduce precipitation (Fig. 10). Aerosol optical depth (AOD) and precipitation are both crucial factors influencing Earth's climate and weather patterns. AOD represents the amount of light absorbed or scattered by tiny aerosol particles suspended in the atmosphere within a specific column of air. The impact of aerosols on precipitation patterns depends on the type of aerosols and atmospheric conditions. The relationship between AOD and precipitation varies across regions. Different aerosol types and concentrations, along with diverse meteorological conditions, can lead to distinct outcomes regarding precipitation. Aerosols can indirectly influence precipitation by affecting atmospheric circulation patterns. Changes in aerosol concentrations can alter the thermal properties of the atmosphere, leading to shifts in atmospheric stability and circulation, which, in turn, can impact precipitation. Changes in precipitation patterns can also influence aerosol concentrations.

Aerosol particles, a necessary ingredient for cloud droplet formation, are not the primary driver for clouds. Rather, they can modify cloud microphysics in sometimes subtle ways to generate feedback that may amplify or dampen their influence.

1.5.1 Plausible Reasons for the Change in Precipitation Patterns

Let's discuss findings and insights from some relevant research studies on AOD and precipitation relationship. Here are few key points;
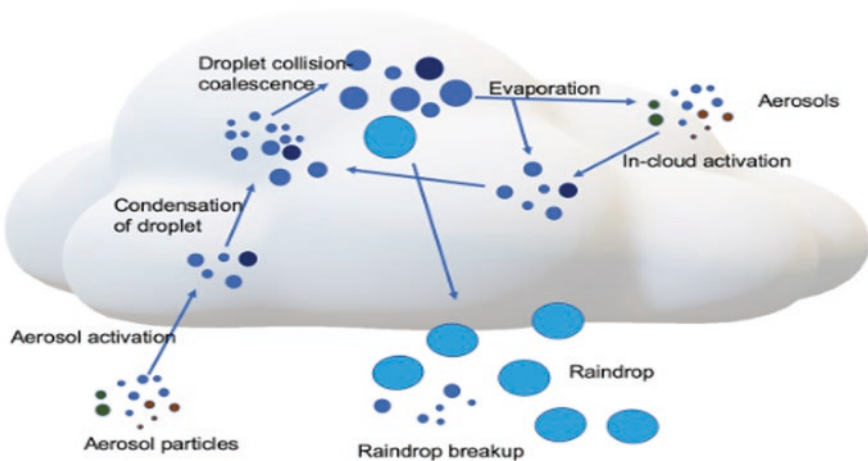
Fig. 10 Formation of raindrop

1.5.1.1 Inverse Relationship

An inverse relationship is seen in regions with high levels of air pollution implying that increased aerosol concentration can lead to decrease in precipitation. Aerosols act as cloud condensing nuclei CCN thus altering the microphysics of precipitation (Vijayakumar et al., 2012).

1.5.1.2 Regional Variability

The AOD and precipitation relationship can significantly vary based on geographical location and meteorological condition. Positive AOD and rainfall relationship indicate invigoration effect, which possibly enhanced the precipitation during the dissipating phase in the presence of aerosol based on study while else it may suppress precipitation (Sunny et al., 2021).

1.5.1.3 Monsoon Regions

Research in monsoonal regions, such as South Asia, has shown complex interactions between AOD and monsoon precipitation patterns. High AOD levels can affect the timing and intensity of monsoon rains, with potential implications for agriculture and water resources. A strong land-ocean asymmetry in solar heating due to aerosols over South Asia has significantly affected atmospheric circulation and meteorological variables are the fundamental causes for the observed trends in meteorological variables (Bollasina et al., 2011; Ganguly et al., 2012; Lau et al., 2006; Ramanathan et al., 2005). This has serious implications for agriculture sector.

1.5.1.4 Extreme Weather Events

Regional external forcings, including land use changes and emissions of anthropogenic aerosols, play an important role in the changes of temperature extremes in some regions (high confidence). Irrigation and crop expansion have attenuated increases in summer hot extremes in some regions. Urbanization has likely exacerbated changes in temperature extremes in cities, in particular for nighttime extremes. Human-induced climate change has likely contributed to the observed intensification of heavy precipitation at the continental scale in North America, Europe, and Asia. Evidence of a human influence on heavy precipitation has emerged in some regions.

1.5.1.5 Modeling and Predictability

Numerical models have been used to simulate the AOD –AOD-precipitation relationship. This has aided in the improved modeling technique and contributed to the better prediction of weather and climate impacts associated with aerosol concentration. The significant relation between aerosol–cloud and rainfall features appears to be substantial, based on stimulating and modeling indications of the microphysical influence of aerosol over the region. (Prashantha Kumar & Busnur Rachotappa, 2023).

1.6 Rainfall Mechanism for the Indian Subcontinent

The mechanism as given for the Indian subcontinent by Lau et al. (2008) is as follows.

1.6.1 Surface Dimming Effect

As proposed by Ramanathan et al., 2005 namely the surface dimming effect is due to the aerosol loading from South Asia over the Indian Ocean affects the monsoon pattern. It has also been shown by Satheesh and Ramanathan (2000) that aerosols cause solar insolation. This mechanism suggests the weakening of monsoon circulation and reduction of monsoon rainfall The solar insolation at the ocean surface causes reduction of sunlight and cuts the evaporation rates which further suppresses convection from the ocean surface leading to suppression of rain during the peak monsoon season.

1.6.2 Elevated Heat Pump (EHP) Hypothesis

As proposed by Lau et al. (2006) the elevated heat pump mechanism is due to the aerosol loading over northern India, primarily the IGP (Indo-Gangetic Plain) and over the foothills of the Himalayas. The aerosols are exposed to elevated altitudes causing significant warming in the middle and upper troposphere which sets up a temperature anomaly and draws in more moisture from the Indian Ocean. This mechanism supports the advancement and intensification of the early summer monsoon. Aerosols can also affect cloud properties such as cloud albedo, effective radius, liquid water path, and so on (Kaufman & Fraser, 1997; Rosenfeld et al., 2001). Needless to mention a lot of research in the Indian subcontinent is done on the aerosols which are hygroscopic that enhance precipitation, like sulfate, when served as CCN and hydrophobic aerosols like soot and dust which suppress rainfall when served as CCN.

1.6.3   Urban Precipitation

Before the 1960s, the probability of a heavy rainfall event over a rural area was almost twice as large as that over an urban area of similar size. However, due to the increasing trend over the urban region, these probabilities appear to be equal in recent times. The urbanization impact alters the regional rainfall patterns through (Urban Heat Island) UHIs, mesoscale convergences, and urban aerosol interactions. The convectively unstable environment of monsoon is still an active area of research.

There is increasing evidence that urbanization and changes in urban–rural boundaries can have significant feedback on the spatiotemporal patterns of precipitation (Shepherd et al., 2002). Common theories of urban precipitation impacts identify four areas where cities influence the process, these are 1. The effect of increases in water vapor 2. Surface roughness 3. Surface temperature and 4 Hygroscopic nuclei. The surface temperature and hygroscopic nuclei together with the Urban Heat Island (UHI), can increase convection and mixing in the atmosphere over the urban area, leading to a greater possibility of cloud formation and therefore precipitation.

Urban areas have been found to influence many attributes of urban precipitation. Both increases and decreases in precipitation have been observed, as well as variations in the location of influence (Huff & Changnon, 1973). Lowry (1977) reviewed previous research and the current understanding of urban precipitation. Kratzer (1956) shows thermal energy released by cities is heavier and frequent precipitation takes place. This contradicts to findings of Rosenfeld (2000), who suggested that there may be urban effects on the clouds (smaller droplet size) over the city and downwind, indicating that precipitation is diminished. The study of urban climate of Sydney reveals an increase in rainfall amount and the number of rain days per year besides there have been a strong correlations between population and rain days supports the proposition that there has been some impact of urbanization of rainfall in Sydney. Urbanization may also influence precipitation through associated enhancement in aerosol concentration (Zhong et al., 2017). The UHI-rainfall relationship may change regionally, both, qualitatively and quantitatively, the Gangetic Basin (GB) in North India is one of a kind. Recent years have witnessed devastating flash floods over various major cities of North India during the monsoon season, causing loss of properties and human life (Gupta & Nair, 2011).

1.6.4   Urban Precipitation—India

Some of the urban locations in India are subjected to extreme events in weather and climate (De & Dandekar, 2001). The variation is attributed to dynamical and anthropogenic causes. Biomass and fossil fuel combustion are thought to be major anthropogenic sources of carbonaceous aerosols causing atmospheric smog and haze (Novakov et al., 2000), while industrial emissions and agricultural soils are also potential sources of anthropogenic aerosols. This also is further studied by Rao et al. (2005) on extreme events in India and concluded that coastal stations are showing an increasing trend. Pavuluri et al. (2010) reported highly elevated aerosols

over South Indian metro-city Chennai, which they interpret in terms of sources from local animal excreta and bio-fuel/biomass burning. Mitra et al. (2012) showed that urbanization in the last 50 years has led to a tenfold increase in rainfall over Kolkata, a large metropolitan located in the eastern Gangetic Basin. In addition, Kishtawal et al. (2010) reported the observational signatures of urban-induced rainfall anomaly during the Indian summer monsoon. Using numerical simulations, Lei et al. (2008) showed that localized convection and heavy rainfall over Mumbai, a large metropolitan in western India, may be due to convergence associated with urban circulation. Similar positive associations between urban land use and rainfall have also been reported over Chennai.

2 Mitigation

Precipitation patterns evolving with temperature rise have impacted in altering the monsoon and these would be manifold if temperatures continue to rise. Climate change is an everyday issue and failing to act on it would cause to human kind and life on Earth. Extreme weather events have become normal to surplus. In this regard, countries can follow in restricting carbon footprint by restricting the increase of global temperature rise to 1.5 °C. Steps involved in net zero emissions are mitigating greenhouse gas emissions, stringent measures to curb air pollution, mitigating forest fire and sustainable cities and communities and use of renewable energy in a circular economy. Transition to net zero emissions would also require systematic changes in key sectors such as energy food and health. Increasing city temperature mean their trees are becoming more important than ever. The magic is as they act as umbrellas as the water rises from the root to the leaves and evaporates from the leaves acting as natural air conditioners.

Trees can also be flood-proofing tool. Trees can lower daytime temperature by up to 4–5 °C. Planting trees to create shade is an obvious response to hot weather as they give a big cooling effect on the cities. They not only add beauty but character to our streets. Canopy cover is crucial for keeping the areas livable and shading our streets to help us cope with hot weather and to counter powerful Urban Heat Island effect. Medelin in Columbia has reduced Urban Heat Island effect by 2 °C by green corridors, Cool street model in Vienna Australia is done by traffic calmed spaces with light-colored road surface, fog showers that activate on hot days, water features shade trees, and drinking fountain. Urban green space can also intercept in absorbing stormwater like the Basin Ang Mo Kio Park in Singapore where the utilitarian concrete channel was tremendously transformed into a naturalized river landscape. Paris residents have a focus on reducing car use, encouraging travel on foot and public transport. Ruling out laws to have mandatory green buildings, provides natural habitats for birds like in Seattle and Brisbane. Many Indian cities are among the most polluted cities. The government is promoting the use of clean alternative fuels such as biodiesel and hydrogen fuel cells to tackle the worsening air pollution in the country.

Some simple steps to curb air pollution can be using public transport, maintaining and using fuel-efficient vehicles, limit burning of wood, and switch to renewable energy sources. Avoid incineration by proper disposal of waste as it releases pollutants, plant trees, and implement clean energy policies cities must be willing to invest in new green spaces and in subsidies to encourage greening by private party owners. The challenge is to move from a handful of trials to large-scale systematic rollout of infrastructure to adapt our cities to climate change.

3   Conclusion

The role of aerosols in precipitation is multifaceted. While aerosols are integral components of precipitation, they are also removed from the atmosphere through precipitation events. The relationship between Aerosol Optical Depth (AOD) and precipitation can be positive, negative, or mixed. Anthropogenic sources such as urbanization, industrialization, biomass burning, and incomplete combustion from vehicles significantly influence the concentration, size, and composition of aerosols, which in turn affect precipitation patterns.

Aerosols have been shown to alter precipitation patterns. Hygroscopic aerosols can enhance precipitation, whereas hydrophobic black carbon resulting from the incomplete combustion of fossil fuels has been found to suppress precipitation. Distinguishing between natural and anthropogenic aerosols in measurements is challenging, and the presence of mixed aerosols—natural aerosols coated with anthropogenic components—further complicates the issue.

The spatial and temporal variations of aerosols are influenced by meteorological conditions, and understanding their residence time in the atmosphere is an area of ongoing research. Increasing the study of simultaneous measurements of aerosols through ground-based and space-based measurements can provide more comprehensive insights into their behavior.

Rising temperatures and precipitation levels are exponentially impacting the economy of urban regions, highlighting the urgent need for mitigation strategies. Precise planning by policymakers, along with subsidized mitigation plans, can help address the intricate interplay between aerosols and meteorology in the atmosphere, ultimately mitigating their adverse effects.

References

Aitken, J. (1980). On dust, fogs, and clouds. *Proceedings. Royal Society of Edinburgh, 9*, 14–18.
Andreae, M. (1995). Climatic effects of changing atmospheric aerosol levels. In A. Henderson-Sellers (Ed.), *World survey of climatology* (Future climates of the world) (Vol. 16, pp. 341–392). Elsevier.
Ashworth, J. R. (1929). The influence of smoke and hot gases from factory chimneys on rainfall. *Quarterly Journal of the Royal Meteorological Society, 55*, 341–350.

Babu, S. S., Satheesh, S. K., & Moorthy, K. K. (2002). Aerosol radiative forcing due to enhanced black carbon at an urban site in India. *Geophysical Research Letters, 29*(18), 1880–1883.

Bollasina, M. A., Ming, Y., & Ramaswamy, V. (2011). Anthropogenic aerosols and the weakening of the South Asian summer monsoon. *Science, 334*, 502–505.

Cachier, H., Bbremond, M. P., & Buatmenard, P. (1989). Carbonaceous aerosols from different tropical biomass burning sources. *Nature, 340*, 371–373.

Chin, M., Ginoux, P., Kinne, S., Torres, O., Holben, B. N., Duncan, B. N., Martin, V., Logan, J. A., Higurashi, A., & Nakajima, T. (2002). *Journal of the Atmospheric Sciences, 59*, 461–483.

Clarke, A. D., Ahlquist, N. C., & Covert, D. S. (1987). The Pacific marine aerosols: Evidence for natural acid sulphates. *Journal of Geophysical Research, 92*, 4179–4190.

D'Almeida, G. A., Koepke, P., & Shettle, E. P. (1991). *Atmospheric aerosols—Global climatology and radiative characteristics* (p. 561). A. Deepak, Hampton, VA.

De, U. S., & Dandekar, M. M. (2001). Natural disasters in urban areas. *Deccan Geographer, 39*, 1–12.

Dong, Z., Wang, L., Xu, P., Pimonsree, S., Limsakul, A., & Singhruck, P. (2021). Interdecadal variation of the wintertime precipitation in Southeast Asia and its possible causes. *Journal of Climate, 34*, 3503–3521. https://doi.org/10.1175/JCLI-D-20-0480.1

Ganguly, D., Rasch, P. J., Wang, H., & Yoon, J.-H. (2012). Climate response of the South Asian monsoon system to anthropogenic aerosols. *Journal of Geophysical Research, 117*, D13209.

Gautam, R., Hsu, N., Lau, K.-M., & Kafatos, M. (2009). Aerosol and rainfall variability over the Indian monsoon region: Distributions, trends and coupling. *Annales Geophysicae, 27*, 3691–3703.

Gupta, A. K., & Nair, S. S. (2011). Urban floods in Bangalore and Chennai: Risk management challenges and lessons for sustainable urban ecology. *Current Science, 100*(11), 1638–1645.

Harrison, R. M., & McCatrney, H. A. (1979). Some measurements of ambient air-pollution arising from the manufacturing of nitric acid and ammonium nitrate fertilizer. *Atmospheric Environment, 13*(8), 1105–1120.

Harrison, R. M., Peak, J. D., & Msibi, M. I. (1996). Measurements of airborne particulate and gaseous Sulphur and nitrogen species in the area of the Azores, Atlantic Ocean. *Atmospheric Environment, 30*(1), 133–143.

Hoppel, W. A., Fitzgerald, J. W., Frick, G. M., & Larson, R. F. (1990). Aerosol size distribution and optical properties found in the marine boundary layer over the Atlantic Ocean. *Journal of Geophysical Research, 95*, 3659–3686.

Horvath, H. (1993). Atmospheric light absorption: A review. *Atmospheric Environment, 27*, 293–317.

Huff, F. A., & Changnon, S. A. (1973). precipitation modification by major urban areas. *Bulletin of the American Meteorological Society, 54*(12), 1220–1232. http://www.jstor.org/stable/26255213

Jacobson, M. Z. (2001). Strong radiative heating due to the mixing state of black carbon in atmospheric aerosols. *Nature, 409*, 695–697.

Jacobson, M. Z. (2002). Control of fossil-fuel particulate black carbon and organic matter, possibly the most effective method of slowing global warming. *Journal of Geophysical Research, D. 107*, D4410(1–12).

Kaufman, Y. J., & Fraser, R. S. (1997). The effect of smoke particles onclouds and climate forcing. *Science, 277*, 1636–1639.

Kaufman, Y. J., Tanre, D., & Boucher, O. (2002). A satellite view of aerosols in the climate system. *Nature, 419*(6903), 215.

Kishtawal, C. M., Niyogi, D., Tewari, M., Pielke, R. A., & Shepherd, J. M. (2010). Urbanization signature in the observed heavy rainfall climatology over India. *International Journal of Climatology, 30*(13), 1908–1916.

Kittelson, D. B. (1998). Engines and nanoparticles: A review. *Journal of Aerosol Science, 29*(5), 575–588. https://doi.org/10.1016/S0021-8502(97)10037-4

Kratzer, P. A. (1956). *The climate of cities* (AMS Translation) Bedfrd, Mass, A. F. Cambridge Research Laboratories Wexler (AFCRL -62- 837) (p. 215).

Lau, K. M., Kim, M. K., & Kim, K. M. (2006). Asian monsoon anomalies induced by aerosol direct effects. *Climate Dynamics, 26*, 855–864.

Lau, K. M., Ramanathan, V., Wu, G.-X., Li, Z., Tsay, S. C., Hsu, C., Siika, R., Holben, B., Lu, D., Tartari, G., Chin, M., Koudelova, P., Chen, H., Ma, Y., Huang, J., Taniguchi, K., & Zhang, R. (2008). The joint aerosol-monsoon experiment: A new challenge in monsoon climate research. *Bulletin of the American Meteorological Society, 89*, 369–383.

Lei, M., Niyogi, D., Kishtawal, C., PielkeSr, R. A., Beltrn-Przekurat, A., Nobis, T., & Vaidya, S. (2008). Effect of explicit urban land surface representation on the simulation of the 26 July 2005 heavy rain event over Mumbai, India. *Atmospheric Chemistry and Physics, 8*(20), 5975–5995.

Lippmann, M. (Ed.). (2000). *Environmental toxicants: Human exposure and their health effects*. Wiley.

Lowry, W. P. (1977). Empirical estimation of urban effects on climate: A problem analysis. *Journal of Applied Meteorology, 16*(2), 129–135.

Miller, R. L., & Tegen, I. (1998). Climate response of soil dust aerosols. *Journal of Climate, 11*, 3247–3267.

Mitra, C., Shepherd, J. M., & Jordan, T. (2012). On the relationship between the premonsoonal rainfall climatology and urban land cover dynamics in Kolkata city, India. *International Journal of Climatology, 32*(9), 1443–1454.

Novakov, T., Andreae, M. O., Gabriel, R., Kirchstetter, T. W., Mayol-Bracero, O. L., & Ramnathan, V. (2000). Origin of carbonaceous aerosols over tropical Indian Ocean: Biomass burning or fossil fuel? *Geophysical Research Letters, 27*, 4061–4063.

O'Dowd, C., & de Leeuw, G. (2007). Marine aerosol production: A review of the current knowledge. *Philosophical Transactions of the Royal Society of London. Series A, 365*, 1753–1774.

Pavuluri, C. M., Kawamura, K., Tachibana, E., & Swaminathan, T. (2010). Elevated nitrogen isotope ratios of tropical Indian aerosols from Chennai: Implication for the origins of aerosol nitrogen in South and Southeast Asia. *Atmospheric Environment, 44*, 3597. https://doi.org/10.1016/j.atmosenv.2010.05.039

Penner, J. E., et al. (2001). Aerosols, their direct and indirect effects. In *Climate change 2001, Intergovernmental Panel on Climate Change (IPCC) Third Assessment Report (TAR)* (pp. 291–348). Cambridge University Press.

Prashantha Kumar, K., & Busnur Rachotappa, M. (2023). Impacts of aerosol orographic precipitation interaction associated with Western disturbances over India using satellite observations. *Water, 15*(16), 2901.

Prospero, J. M., et al. (1983). The atmospheric aerosol system – An overview. *Reviews of Geophysics and Space Physics, 21*, 1607–1629.

Pruppacher, H. R., & Klett, J. D. (1997). *Microphysics of clouds and precipitation* (Vol. 954, p. 1997). Reidel.

Raes, F., Bates, T., McGovern, F., & Van Liedekerke, M. (2000). The 2nd aerosol characterization experiment (ACE-2): General overview and main results. *Tellus B, 52*(2), 111–125.

Ramanathan, V., Chung, C., Kim, D., Bettge, T., Buja, L., Kiehl, J. T., Washington, W. M., Fu, Q., Sikka, D. R., & Wild, M. (2005). Atmospheric brown clouds: Impacts on South Asian climate and hydrological cycle. *Proceedings of the National Academy of Sciences of the United States of America, 102*, 5326–5333.

Ranjan, R. R., Joshi, H. P., & Iyer, K. N. (2007). Spectral variation of total column aerosol optical depth over Rajkot: A tropical semi-arid Indian station. *Aerosol Air Quality Research, 7*(1), 33–45.

Rao, G. S. P., Murty, M. K., & Joshi, U. R. (2005). Climate change over India as revealed by critical extreme temperature analysis. *Mausam, 56*, 601–608.

Rosenfeld, D. (2000). Suppression of rain and snow by urban and industrial air pollution. *Science, 287*(5459), 1793–1796.

Rosenfeld, D., Rudich, Y., & Lahav, R. (2001). Desert dust suppressing precipitation: A possible desertification feedback loop. *Proceedings of the National Academy of Sciences of the United States of America, 98*, 5975–5980.

Rueckerl, R., Schneider, A., Breitner, S., Cyrys, J., & Peters, A. (2011). *Inhalation Toxicology, 23*, 555–592.

Russell, P. B., & Heintzenberg, J. (2000). An overview of the ACE-2 clear sky column closure experiment (CLEARCOLUMN). *Tellus B, 52*, 463–483.

Satheesh, S. K., & Moorthy, K. K. (2005). Radiative effects of natural aerosols: A review. *Atmospheric Environment, 39*(11), 2089–2110.

Satheesh, S. K., & Ramanathan, V. (2000). Large differences in tropical aerosol forcing at the top of the atmosphere and Earth's surface. *Nature, 405*, 60–63.

Satheesh, S. K., & Srinivasan, J. (2002). Enhanced aerosol loading over Arabian Sea during pre-monsoon season: Natural or anthropogenic? *Geophysical Research Letters, 29*(18), 1–4.

Schwartz, S. E., et al. (1995). Group report: Connections between aerosol properties and forcing of climate. In R. J. Charlson & J. Heintzenberg (Eds.), *Aerosol forcing of climate* (pp. 251–280). Wiley.

Shepherd, J. M., Pierce, H. F., & Negri, A. J. (2002). Rainfall modification by major urban areas: Observations from spaceborne rain radar on the TRMM satellite. *Journal of Applied Meteorology, 41*, 689–701.

Sunny, K., Panda, J., Rao, P., Sarangi, C., & Ghude, S. D. (2021). Study of aerosol-cloud-precipitation-meteorology interaction during a distinct weather event over the Indian region using WRF-Chem. *Atmospheric Research, 247*, 105–144.

Tsai, J. H., Huang, K. L., Lin, N. H., Chen, S. J., Lin, T. C., Chen, S. C., Lin, C. C., Hsu, S. C., & Lin, W. Y. (2012). Influence of an Asian dust storm and southeast Asian biomass burning on the characteristics of seashore atmospheric aerosols in southern Taiwan. *Aerosol and Air Quality Research, 12*, 1105–1115.

Twomey, S. (1974). Pollution and the planetary albedo. *Atmospheric Environment, 8*, 1251–1256.

Tyson, P. D., Garstang, M., Swap, R., Kallberg, P., & Edwards, N. (1996). An air transport climatology for subtropical southern Africa. *International Journal of Climatology, 16*, 256–291.

Uematsu, M., Duce, R. A., Prospero, J. M., Chen, L., Merill, J. T., & McDonald, R. L. (1983). Transport of mineral aerosol from Asia over the North Pacific Ocean. *Journal of Geophysical Research, 88*, 5343–5352.

Vijayakumar, K., Devara, P., & Simha, C. (2012). Aerosol features during drought and Normal monsoon years: A study undertaken with multi-platform measurements over a tropical urban site. *Aerosol and Air Quality Research, 12*, 1444–1458.

Wilson, C. T. R. (1987). Condensation of water vapour in the presence of dust-free air and other gases. *Philosophical Transactions of the Royal Society of London A, 189*, 265–307.

Zhong, S., Qian, Y., Zhao, C., Leung, R., Wang, H., Yang, B., Fan, J., et al. (2017). Urbanization-induced urban heat Island and aerosol effects on climate extremes in the Yangtze River Delta Region of China. *Atmospheric Chemistry and Physics, 17*(8), 5439–5457.

The Effect of Additives on Particulate Matter Emissions from Biomass Combustion

Zuhal Akyürek

1 Introduction

The rising energy demand, rapid population growth, industrialization, urbanization, and economic development have led to serious global problems such as air pollution and global warming in the last decades. Worldwide energy-related CO_2 emissions have been continuously increasing since 1900s and have reached 36.8 $GtCO_2$ in the year 2022 (Fig. 1) (International Energy Agency, 2022).

The depletion of fossil fuel reserves and strict environmental regulations, along with increasing demand for energy have accelerated the search for alternative fuels. To reduce the adverse environmental impact of fossil fuels, renewable energy sources are promising options to reduce the carbon dioxide emissions from heat and power sector (Johansson et al., 2021). Renewable energy technologies had 14.1% share in the primary energy supply in 2019 (World Bioenergy Association, 2021). Figure 2 shows the growing share of energy from renewable sources in gross electricity consumption between 2005 and 2020 (Eurostat, 2023a). Solid biomass has the largest share among the other renewables representing 41% of all the renewable energy supply in Europe followed by wind, hydropower, liquid biofuels, and biogas (European Environment Agency, 2021; Eurostat, 2023b).

The growing global demand for renewable energy and abundancy and high availability of the biomass sources promote the interest in pellet fuel industry, processing a variety of the bio-sources such as forest residues, woody biomass, bark, cereals, herbaceous materials, energy crops and agricultural residues. Biomass can be converted into energy through thermochemical, and biochemical technologies. The thermochemical processes include combustion, pyrolysis and gasification and

Z. Akyürek (✉)
Energy Systems Engineering Department, Faculty of Engineering and Architecture, Burdur Mehmet Akif Ersoy University, Burdur, Turkey
e-mail: zuhalakyurek@mehmetakif.edu.tr
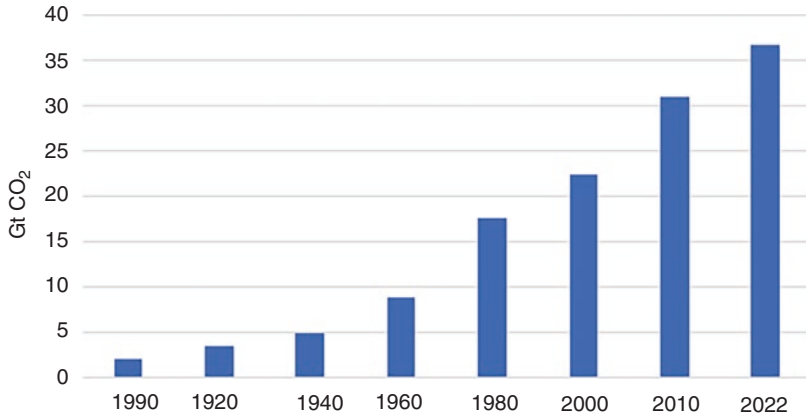
Fig. 1 Global energy-related CO_2 emissions. (International Energy Agency, 2022)
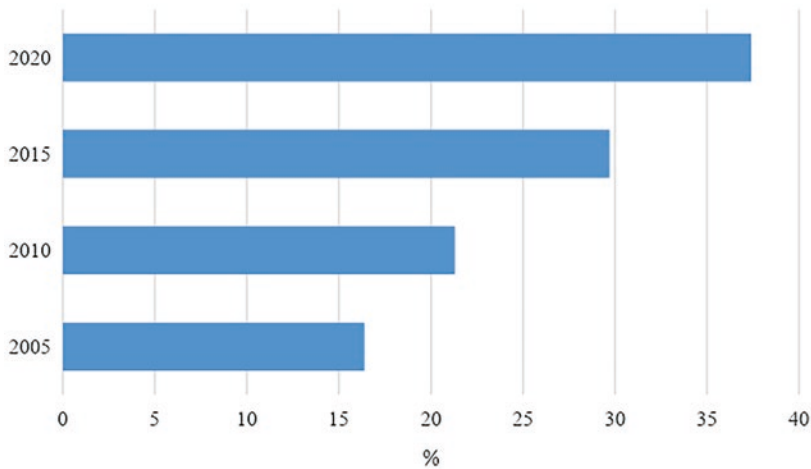
Fig. 2 Share of energy from renewable sources (% of gross final energy consumption). (Eurostat, 2023a)

biochemical conversion technologies include anaerobic digestion, fermentation, etc. where the main product is energy in the form of thermal, steam, electricity, etc. (Pant and Mohanty, 2014). Heat and chemical reactions are used to convert biomass into energy in the thermochemical processes while in the biological processes enzymes and microorganisms are used (Nanda et al., 2014). Among the thermochemical conversion technologies (combustion, gasification, and pyrolysis), combustion is the most mature technology for heat and power production from solid fuels. Biomass and biomass derived biofuels could be used as fossil fuel substitute in existing combustion systems to reduce net carbon dioxide emissions (Okolie et al., 2020).

Biofuels are characterized by their high moisture content, low bulk density, low calorific value, and low melting point ash. Combustion of biomass is a complex process due to various heterogeneous and homogeneous reactions taking place consecutively (Nussbaumer, 2003). The combustion process starts with the drying of the fuel and continues with devolatilization, gasification, char combustion, and oxidation in the gas phase. The moisture content of biomass is one of the most important parameters for biomass combustion. Moisture content less than 50% is regarded as feasible for combustion (McKendry, 2002). Particle size and chemical composition of biomass, boiler temperature, and other operating conditions determine the reaction time required for each step.

Although biofuels have a positive influence on the environment; energy generation from biofuels still has challenges regarding their sustainable utilization due to their severe fuel characteristics which harden logistics and handling and limit the scale of the combustion process (Míguez et al., 2021; Yang et al., 2021). Solid fuel combustion generates atmospheric pollutant emissions such as SO_2, NOx, CO, and particulate matter (PM) (Du et al., 2020; Kwon et al., 2020). Air pollutant aerosols/particulate matter contain toxic materials that are harmful to human health and also have a significant influence on the earth's energy balance through many direct and indirect routes. Thus, emission mitigation methods are critical to control and reduce PM emissions.

2 Particulate Matter (PM) Emission

PM represents all the particles present in the atmosphere in both liquid and solid form with a broad range of particle sizes and various physical and chemical characteristics (Zhu et al., 2021). PM emissions have both natural and anthropogenic sources. The source of natural emissions are forest fires, wildfires, heathland fires, etc. Anthropogenic PM emissions are formed during combustion of biomass fuels, agricultural biomass/waste burning, domestic and industrial emissions from heating and cooking applications, etc. (Johnston et al., 2019). Particle size and chemical composition of the solid fuel have a strong influence on PM emissions. According to the particle size, PM can be classified into three groups as coarse particles (PM10), fine particles (PM2.5), and ultrafine (PM0.1) with aerodynamic diameters of less than 0.1 μm, 2.5 μm and 10 μm, respectively (Yang et al., 2021; Wu et al., 2020).

PM emission is the main reason for air pollution in most urban areas having developed industrial sectors (Zhang et al., 2019). Pollutant emissions from biomass combustion have become a threat to the ecological environment in recent years. Atmospheric pollution has raised global concern about PM emissions due to their detrimental effect on human health. Despite the amount of ultrafine and fine particles emitted during solid fuel combustion is relatively lower than the amount of emitted coarse particles, fine particles have higher surface areas which adsorb huge amounts of toxic elements (Wei et al., 2019). They are more dangerous due to their

longer residence time in the atmosphere, longer transport distance, and higher toxicity capacity (Kim et al., 2015; Liaw et al., 2016; Shang et al., 2019). Especially, fine and ultrafine particulate matter emissions pose much higher health risks than coarse particles as they act as a transport vector for pathogens, such as SARS-CoV-2–COVID-19 (Amoatey et al., 2020; Setti et al., 2020), which trigger multiple organ damage in human body (Forman & Finch, 2018). Ultrafine particles can enter the blood circulation system and can cause many diseases such as lung cancer, heart disease, asthma, etc. (Kumar et al., 2015). The toxicity level of PM generally depends on the physicochemical properties such as composition, shape, size, and surface area (Johnston et al., 2019).

The influence of PM is only limited to human health. Particulate matter especially PM2.5 and PM10 have a damaging impact on the environment, air quality, and human health (Pipal & Satsangi, 2015). Emitted PM has a high potential to absorb and scatter sunlight and modify the cloud properties. Anthropogenic PM emissions stem from industrialization and urbanization promote the aerosol particle loading. These anthropogenic aerosols are mainly consisting of elemental carbon, organic carbon, dust, sulfates, nitrates, and fly ash (Ramanathan et al., 2005). These particulates have direct and indirect impacts on climate change. They directly promote the absorption and scattering of solar radiation and indirectly enhance the accumulation of cloud condensation nuclei that increases the cloud albedo and hence contribute to global warming (Cattani et al., 2006; Tiwari et al., 2014; Amaral et al., 2016).

PM emissions from energy generation, industrial applications, and traffic-related sources are essentially limited by legislation. The limitations for PM emissions in EU Directives from small-scale biomass combustion systems (<1 MWth) to medium-scale combustion systems (1–50 MWth input) and large-scale combustion systems (>50 MWth input) are illustrated in Fig. 3.

PM emissions play a significant role in sustainability of ecological environment. It is essential to take appropriate measures to control anthropogenic pollutants to
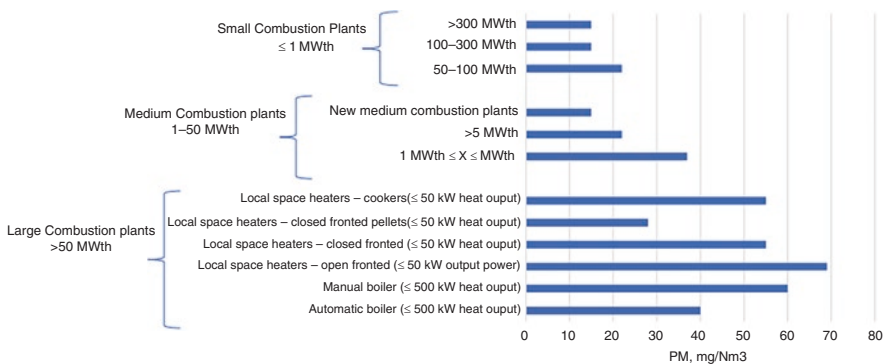
Fig. 3 PM emissions limits for technologies for different scales of combustion. (Commission Regulation (EU), 2015/1185; Directive (EU), 2015/2193; Directive (EU), 2010/75

protect the environment and public health. PM emissions that originate from incomplete combustion of biomass can be avoided by optimizing the operating conditions such as combustion temperature, residence time, and oxygen content in the boilers. However, partially volatilized inorganic ash elements in biomass boost the inorganic PM emissions, which require other control methods such as using additives (Gollmer et al., 2019).

3   Additives for PM Emission Control

Biomass fuels are generally characterized by their low heating value and low ash melting temperatures that limit their utilization in power generation industry. The operational problems in biomass combustion are associated with the ash composition of biomass having elevated amounts of sodium (Na), potassium (K) and chlorine (Cl) which reduce the ash fusion temperatures (AFT) (Vassilev et al., 2013, Hariana et al., 2023). Particulate matter emitted from combustion of biomass is generally higher due to the high alkali content of biomass ash. The problematic elements (K, P, Ca, Mg, S, Cl, Si, Na, Fe, Mn, Al, Ti) naturally present in biomass ash lead to high PM emission. Fig. 4 shows the ash composition of some selected agricultural and woody biomass.

There are different methods have proposed to avoid operational problems and PM emissions in biomass combustion systems, such as (i) using fuel blends (Zeng et al., 2016), (ii) biomass leaching (Schmidt et al., 2018), and (iii) using additives (Matus et al., 2018; Carroll & Finnan, 2015; Backman et al., 2013). Among them, the use of additives in the fuel mixture is considered to be one of the most beneficial methods that change the ash structure of the solid fuel, increase the ash melting
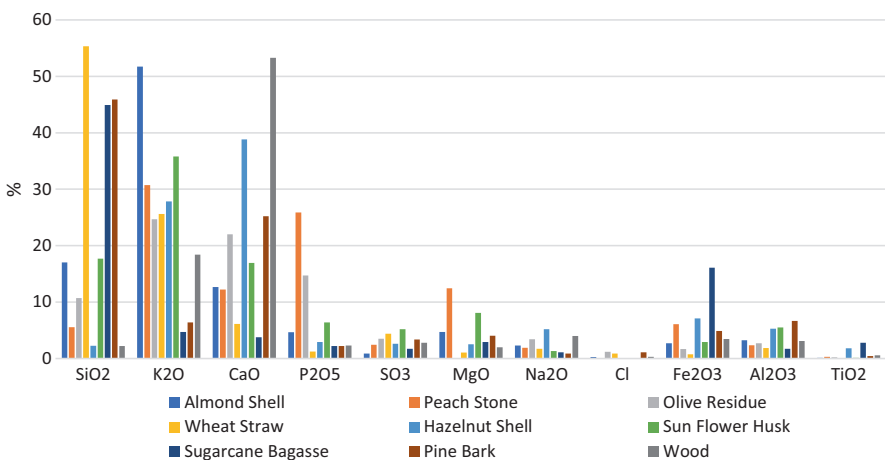
Fig. 4 Ash composition of various biomass

temperature, and reduce the release of particulate matter of inorganic origin (Clery et al., 2018; Gollmer et al., 2019).

Based on reactive components contained additives are classified as: (Höfer & Kaltschmitt, 2017; Wang et al., 2012; Miquez et al., 2021)

- Alumino-silicate-based additives
- Calcium-based additives
- Phosphorus-based additives
- Other types of additives (sulfur-based, etc.)

Kaolin is the most widely used alumina-silicate-based additives. Kaolin ($Al_2Si_2O_5(OH)_4$) interacts with the potassium in the biomass to form potassium alumina-silicate compounds Kalsilite ($KAlSiO_4$) and Leucite ($KAlSi_2O_6$)) with ash melting temperatures of 1600 °C and 1500 °C, respectively (Steenari et al., 2009; Wang et al. 2012). The key reactions involved between kaolin and potassium-containing species can be listed as:

$$2KOH + Al_2Si_2O_5(OH)_4 \rightarrow 2KAlSiO_4 + 3H_2O \tag{1}$$

$$2KCl + Al_2Si_2O_5(OH)_4 \rightarrow 2KAlSiO_4 + 2HCl + H_2O \tag{2}$$

$$K_2SO_4 + Al_2Si_2O_5(OH)_4 \rightarrow 2KAlSiO_4 + SO_3 + 2H_2O \tag{3}$$

$$2KOH + Al_2Si_2O_5(OH)_4 + 2SiO_2 \rightarrow 2KAlSiO_6 + 3H_2O \tag{4}$$

$$K_2SO_4 + Al_2Si_2O_5(OH)_4 + 2SiO_2 \rightarrow 2KAlSiO_6 + SO_3 + 2H_2O \tag{5}$$

$$2KCl + Al_2Si_2O_5(OH)_4 + 2SiO_2 \rightarrow 2KAlSiO_4 + 2HCl + H_2O \tag{6}$$
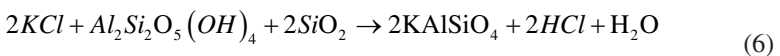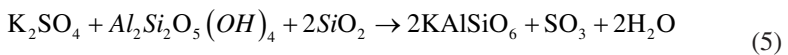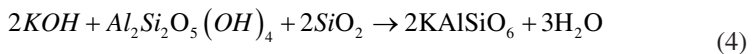
Previous research has demonstrated that using additives and blending biomass can be used to reduce PM emissions. There are studies on the kaolin application as additive in pellet burning systems where woody biomass are used alone or together with straw. In the study of Schmitt and Kaltschmitt (2013), the effect of additives containing 1 wt. % and 2 wt. % $Ca(OH)_2$ and kaolin on the combustion of wood and straw mixture pellets was analyzed by thermogravimetric analysis (TGA). The ashes analysis has shown that the slagging of both additives decreased. It has also been stated that kaolin addition has led to lower particulate matter emission than $Ca(OH)_2$. Gehrig and Wöhler (2018) carried out combustion experiments with of pelletized spruce (Picea abies), short-rotation-coppice (SRC) willow (Salix spec.; Clone Tordis) and kaolin in a residential biomass boiler (12 kW). Fuel blends were prepared according to EN 14961-2 standard. Addition of kaolin reduced emitted PM even in low concentrations (0.2 wt.%) Kaolin addition also reduced the K concentration in the collected particles with an increased share of Zn.

Gollmer et al. (2019) investigated the reduction rate of particulate matter emission and potassium retention during combustion of beech wood sawdust pellet in

five different additive media (Kaolin, anorthite, calcium silicate, titanium dioxide, aluminum hydroxide) and at five different temperatures (550 °C, 700 °C, 900 °C, 1000 °C, 1100 °C). Highest potassium retention rate was observed with kaolin (76.7%), anorthite (73.4%) and calcium silicate (51%) during the release of inorganic particulate matter at 1100 °C. Gollmer et al. (2021), produced high thermal resistant ashes from combustion of four different types of wood chips with two types of kaolin in laboratory scale combustor. The ash recovery rate and PM forming element K have assessed with respect to the wood chips combusted with additives. The additive contents between 1.49 wt% a.r. and 3.53 wt% a.r. were determined as suitable for wood chips with the kaolin additive based on aluminum-silicate.

Clery et al. (2018) conducted combustion experiments with three types of biomasses (wheat straw, olive cake, wood pellets in the presence of kaolin additive. Wheat straw and olive cake have both greater ash and Cl contents with respect to wood pellets. Combustion test revealed that 70–100% of K is retained in the ash by using additive in wood combustion; K retention rate was in the range of 60–80% and 70–100% for straw and olive pellets, respectively.

4   Predicting PM Emissions

Several studies have been conducted on measurement and characterization of particulate emissions from biomass burning energy systems to obtain the amount of PM formation and air pollutants (Johansson et al., 2003; Wierzbicka et al., 2005; Ghafghazi et al., 2011; Höfer et al., 2021).

Emission factor defined in Eq. 1 is a representative data to relate the amount of the pollutant released to the atmosphere to fuel consumption. The unit of the emission factor (EFx) is g kg − 1 (grams of species X per kg of dried biomass).

$$EF_x = \frac{V_{\text{Stack gas}}}{m_{\text{biomass, dry basis}}} \times \frac{x \times M_x}{V_x}$$

(1)

where:

$V_{\text{Stack gas}}$ is the total volume of gas flow through (m^3).
x is the molar fraction of species x.
M_X is the species X molecular weight (g mol − 1); m(fuel(dry basis)).
V_X is the molar volume of gas under standard conditions (m^3) (STP) (=0.0224 m^3).

Emission factors make it possible to estimate emissions from various sources of air pollution (Amaral et al., 2016). The results obtained from previous studies have showed that the estimated EF values for CO_2 and $PM_{2.5}$ values are in good agreement with the experimental data (França et al., 2012). Combustion of biomass in pellets/briquettes form results in lower emission factors compared to their natural form. $PM_{2.5}$ emission factors tended to be higher in forest biomass combustion
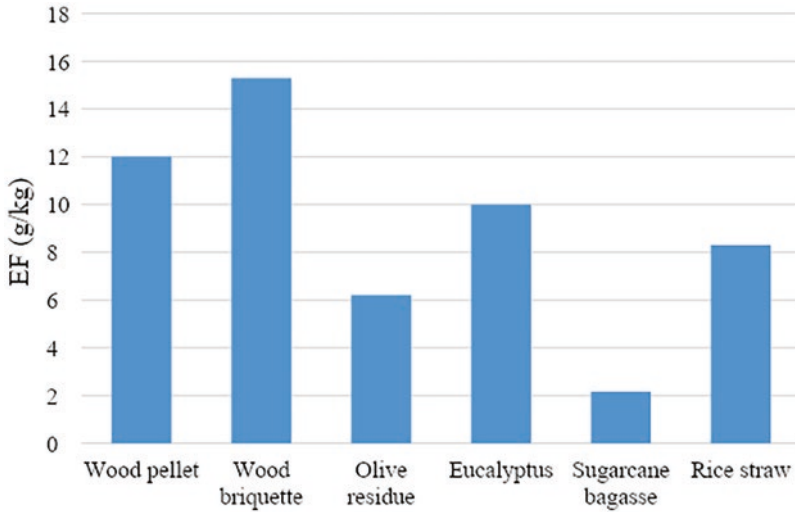
Fig. 5 EF values (PM$_{2.5}$) from residential burning of biomass. (Gonçalves et al., 2012; Alves et al. 2011; Oanh et al., 2011)
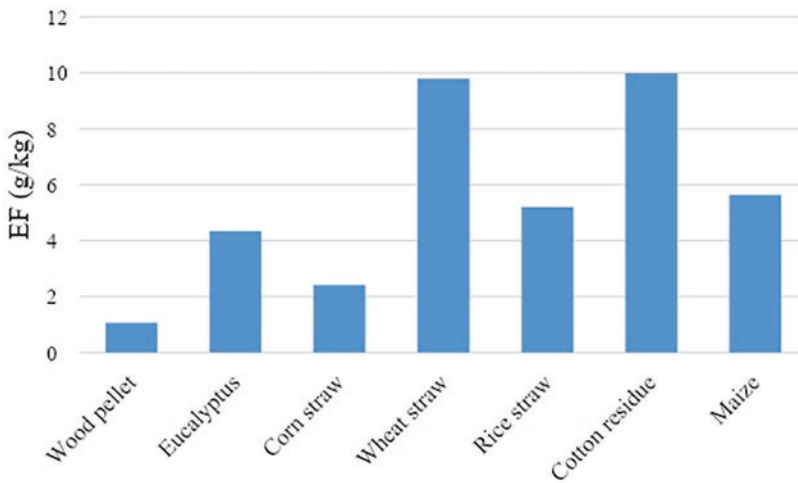
Fig. 6 EF values (TSP) from residential burning of biomass. (Ozgen et al., 2014; Shen et al. 2012; Wei et al., 2014; Saud et al., 2013)

(Fig. 5) whereas PM$_{10}$ and total suspended particles (TSP) prevails in agricultural biomass combustion (Fig. 6) (Amaral et al., 2016).

There are also some indices based on the ash-forming elements for predicting the formation of aerosols and particles during biomass combustion. For instance, for aerosol formation the sum of (K + Na + Pb + Zn) (mg/kg, on dry basis) can be used

as an indicator (Zeng et al., 2016; Höfer et al., 2021). The aerosol index less than 1000 mg/kg refers to low PM formation (Sommersacher et al., 2012).

The Na, K, S, Cl, Si and Al contents have high influence on PM10 emissions. The molar ratio of $(Na_2O + K_2O)/(SiO_2 + Al_2O_3)$ can be used to estimate ultrafine particle emissions especially PM0.3. As the ratio decreases, the proportion of PM0.3 in PM10 emissions from biomass combustion decreases (Yang et al., 2021). Alumina-silicate-based additives have been proven to reduce PM emission by altering the ratio of $(Na_2O + K_2O)/(SiO_2 + Al_2O_3)$ in the fuel.

The amount of K released from the fuel also affects the aerosol formation (Höfer et al., 2021). The higher molar ratio of Si/K in biomass enhances stable potassium silicates deposition in bottom ash and hence reduce the rate of K released in the gaseous stream. The Si/K molar ratio higher than 15 favors for K deposition in bottom ash (Sommersacher et al., 2012). The amount of P influences the release of K in gas stream as P binds K to form potassium phosphates in the bottom ash. S and Cl contents in biomass turn into alkaline sulfates and alkaline chlorides that have also impact on PM and deposit formation on heat exchange surfaces. The molar ratio of 2S/Cl lower than 2 in the fuel implies higher Cl content in aerosol emissions having corrosion risk in the boiler (Sommersacher et al., 2012).

5 Conclusions

Combustion is one of the most reliable thermo-chemical conversion methods that generates energy from solid fuels (coal, biomass, waste). Replacement of fossil fuels with biomass in combustion process is a useful route to mitigate carbon emissions to the atmosphere and hence to contribute to climate change combat. However, ash constituents of biomass can lead to increase in gaseous and PM emissions and operational problems. Ultrafine size PM emission is one of the major contributors of air pollution that can pose detrimental effect on human health. Therefore, measures have to be taken in order to control PM emissions during biomass combustion. One of the promising control strategies to mitigate operational problems associated with biomass ash and to reduce PM emissions is using additives by modifying chemical composition of biomass ash. Alumino-silicate based additives, calcium-based additives, phosphorus-based additives other types of additives (sulfur based, etc.) can be applied during combustion of biomass. For efficient control of PM emissions, it is needed to develop further understanding on the effect of different additive types on pathways of ash transformation according to heterogeneous biomass composition and operating conditions.

References

Alves, C., Gonçalves, C., Fernandes, A. P., Tarelho, L., & Pio, C. (2011). Fireplace and woodstove fine particle emissions from combustion of western Mediterranean wood types. *Atmospheric Research, 101*, 692–700. https://doi.org/10.1016/j.atmosres.2011.04.015

Amaral, S. S., Andrade de Carvalho, J., Jr., Costa, M. A. M., & Pinheiro, C. (2016). Particulate matter emission factors for biomass combustion. *Atmosphere, 7*(11), 141. https://doi.org/10.3390/atmos7110141

Amoatey, P., Omidvarborna, H., Baawain, M. S., & Al-Mamun, A. (2020). Impact of building ventilation systems and habitual indoor incense burning on SARS-CoV-2 virus transmissions in Middle Eastern countries. *Science of the Total Environment, 733*, 139356. https://doi.org/10.1016/j.scitotenv.2020.139356

Backman, R., Khalil, R. A., Todorovic, D., Skreiberg, Ø., Becidan, M., Goile, F., Skreiberg, A., & Sørum, L. (2013). The effect of peat ash addition to demolition wood on the formation of alkali, lead and zinc compounds at staged combustion conditions. *Fuel Process Technology, 105*, 20–27. https://doi.org/10.1016/j.fuproc.2011.04.035

Carroll, J., & Finnan, J. (2015). The use of additives and fuel blending to reduce emissions from the combustion of agricultural fuels in small scale boilers. *Biosystems Engineering, 129*, 127–133. https://doi.org/10.1016/j.biosystemseng.2014.10.001

Cattani, E., Costa, M. J., Torricella, F., Levizzani, V., & Silva, A. M. (2006). Influence of aerosol particles from biomass burning on cloud microphysical properties and radiative forcing. *Atmospheric Research, 82*, 310–327. https://doi.org/10.1016/J.ATMOSRES.2005.10.010

Clery, D. S., Masona, P. E., Rayner, C. M., & Jones, J. M. (2018). The effects of an additive on the release of potassium in biomass combustion. *Fuel, 214*, 647–655. https://doi.org/10.1016/j.fuel.2017.11.040

Commission Regulation (EU) 2015/1185 of 24 April 2015 implementing Directive 2009/125/EC of the European Parliament and of the Council with regard to ecodesign requirements for solid fuel local space heaters. https://eur-lex.europa.eu/legal-content/EN/TXT/?uri=uriserv%3AOJ.L_.2015.193.01.0001.01.ENG

Directive (EU) 2015/2193 of the European Parliament and of the Council of 25 November 2015 on the limitation of emissions of certain pollutants into the air from medium combustion plants (2015). https://eur-lex.europa.eu/legal-content/EN/TXT/?uri=CELEX%3A32015L2193

Directive 2010/75/EU of the European Parliament and of the Council of 24 November 2010 on industrial emissions (integrated pollution prevention and control) (2010). https://eur-lex.europa.eu/legal-content/EN/TXT/?uri=celex%3A32010L007

Du, X., Jin, X., Zucker, N., Kennedy, R., & Urpelainen, J. (2020). Transboundary air pollution from coal fired power generation. *Journal of Environmental Management, 270*, 110862. https://doi.org/10.1016/j.jenvman.2020.110862

European Environment Agency. (2021). *Share of energy consumption from renewable sources in Europe* (8th EAP). https://www.eea.europa.eu/ims/share-of-energy-consumption-from#:~:text=Among%20renewable%20energy%20sources%2C%20the,%25)%20and%20biogas%20(6%25).

Eurostat. (2023a). *Renewable energy statistics*. https://ec.europa.eu/eurostat/statistics-explained/index.php?title=Renewable_energy_statistics

Eurostat. (2023b). *Shedding light on energy – 2023 edition*. https://ec.europa.eu/eurostat/web/interactive-publications/energy-2023

Forman, H. J., & Finch, C. E. (2018). A critical review of assays for hazardous components of air pollution. *Free Radical Biology and Medicine, 117*, 202–217. https://doi.org/10.1016/j.freeradbiomed.2018.01.030

Gehrig, M., & Wöhler, M. (2018). Kaolin as additive in wood pellet combustion with several mixtures of spruce and short-rotation-coppice willow and its influence on emissions and ashes. *Fuel, 235*(2), 610–616. https://doi.org/10.1016/j.fuel.2018.08.028

Ghafghazi, S., Sowlati, T., Sokhansanj, S., Bi, X., & Melin, S. (2011). Particulate matter emissions from combustion of wood in district heating applications. *Renewable and Sustainable Energy Reviews, 15*, 3019–3028. https://doi.org/10.1016/j.rser.2011.04.001

Gollmer, C., Höfer, I., & Kaltschmitt, M. (2019). Additives as a fuel-oriented measure to mitigate inorganic particulate matter (PM) emissions during small-scale combustion of solid biofuels. *Biomass Conversion and Biorefinery, 9*, 3–20. https://doi.org/10.1007/s13399-018-0352-4

Gollmer, C., Höfer, I., & Kaltschmitt, M. (2021). Laboratory-scale additive content assessment for aluminum-silicate-based wood chip additivation. *Renewable Energy, 164*, 1471–1484. https://doi.org/10.1016/j.renene.2020.10.135

Gonçalves, C., Alves, C., & Pio, C. (2012). Inventory of fine particulate organic compound emissions from residential wood combustion in Portugal. *Atmospheric Environment, 50*, 297–306. https://doi.org/10.1016/j.atmosenv.2011.12.013

Hariana, H., Ghazidin, H., Darmawan, A., Hilmawan, E., & Prabowo, A. M. (2023). Effect of additives in increasing ash fusion temperature during co-firing of coal and palm oil waste biomass. *Bioresource Technology Reports, 23*, 101531. https://doi.org/10.1016/j.biteb.2023.101531

Höfer, I., & Kaltschmitt, M. (2017). Effect of additives on particulate matter formation of solid biofuel blends from wood and straw. *Biomass Conversion and Biorefinery, 7*(1), 101–116. https://doi.org/10.1007/s13399-016-0217-7

Höfer, I., Gollmer, C., & Kaltschmitt, M. (2021). Inorganic PM and K emissions during ashing of solid biofuels and Kaolinite – Data measurement in laboratory scale. *Fuel, 296*, 120704. https://doi.org/10.1016/j.fuel.2021.120704

International Energy Agency. (2022). *CO_2 Emissions in 2022*. https://iea.blob.core.windows.net/assets/3c8fa115-35c4-4474-b237-1b00424c8844/CO2Emissionsin2022.pdf

Johansson, L. S., Tullin, C., & Leckner, S. P. (2003). Particle emissions from biomass combustion in small combustors. *Biomass & Bioenergy, 25*, 435–446. https://doi.org/10.1016/10.1016/S0961-9534(03)00036-9

Johansson, A. C., Molinder, R., Vikström, T., & Wiinikka, H. (2021). Particle formation during suspension combustion of different biomass powders and their fast pyrolysis bio-oils and biochars. *Fuel Processing Technology, 218*, 106868. https://doi.org/10.1016/j.fuproc.2021.106868

Johnston, H., Mueller, W., Steinle, S., Vardoulakis, S., Tantrakarnapa, K., Loh, M., & Cherrie, J. W. (2019). How harmful is particulate matter emitted from biomass burning? A Thailand perspective. *Current Pollution Reports, 5*, 353–377. https://doi.org/10.1007/s40726-019-00125-4

Kim, K. H., Kabir, E., & Kabir, S. (2015). A review on the human health impact of airborne particulate matter. *Environment International, 74*, 136–143. https://doi.org/10.1016/j.envint.2014.10.005

Kumar, M., Singh, R. S., & Banerjee, T. (2015). Associating airborne particulates and human health: Exploring possibilities. *Environment International, 84*, 201–202. https://doi.org/10.1016/j.envint.2015.06.002

Kwon, H. S., Ryu, M. H., & Carlsten, C. (2020). Ultrafine particles: Unique physicochemical properties relevant to health and disease. *Experimental & Molecular Medicine, 52*, 318–328. https://doi.org/10.1038/s12276-020-0405-1

Liaw, S. B., Rahim, M. U., & Wu, H. (2016). Trace elements release and particulate matter emission during the combustion of char and volatiles from in situ biosolid fast pyrolysis. *Energy & Fuels, 30*, 5766–5771. https://doi.org/10.1021/acs.energyfuels.6b00776

Matúš, M., Križan, P., Šooš, L., & Beniak, J. (2018). The effect of papermaking sludge as an additive to biomass pellets on the final quality of the fuel. *Fuel, 219*, 196–204. https://doi.org/10.1016/j.fuel.2018.01.089

McKendry, P. (2002). Energy production from biomass (Part 2): Conversion technologies. *Bioresource Technology, 83*, 47–54. https://doi.org/10.1016/S0960-8524(01)00119-5

Míguez, J. L., Porteiro, J., Behrendt, F., Blanco, D., Patino, D., & Dieguez-Alonso, A. (2021). Review of the use of additives to mitigate operational problems associated with the combustion of biomass with high content in ash-forming species. *Renewable and Sustainable Energy Reviews, 141*, 110502. https://doi.org/10.1016/j.rser.2020.110502

Nanda, S., Mohammad, J., Reddy, S. N., Kozinski, J. A., & Dalai, A. K. (2014). Pathways of lignocellulosic biomass conversion to renewable fuels. *Biomass Conversion and Biorefinery, 4*, 157–191. https://doi.org/10.1007/s13399-013-0097-z

Nussbaumer, T. (2003). Combustion and co-combustion of biomass: Fundamentals, technologies, and primary measures for emission reduction. *Energy & Fuels, 17*, 1510–1521. https://doi.org/10.1021/ef030031q

Oanh, N. T. K., Bich, T. L., Tipayarom, D., Manadhar, B. R., Prapat, P., Simpson, C. D., & Liu, L.-J. S. (2011). Characterization of particulate matter emission from open burning of rice straw. *Atmospheric Environment, 45*, 493–502. https://doi.org/10.1016/j.atmosenv.2010.09.023

Okolie, J. A., Nanda, S., Dalai, A. K., Berruti, F., & Kozinski, J. A. (2020). A review on subcritical and supercritical water gasification of biogenic, polymeric and petroleum wastes to hydrogen-rich synthesis gas. *Renewable and Sustainable Energy Reviews, 119*, 109546. https://doi.org/10.1016/j.rser.2019.109546

Ozgen, S., Caserini, S., Galante, S., Giugliano, M., Angelino, E., Marongiu, A., Hugony, F., Migliavacca, G., & Morreale, C. (2014). Emission factors from small scale appliances burning wood and pellets. *Atmospheric Environment, 94*, 144–153. https://doi.org/10.1016/j.atmosenv.2014.05.032

Pant, K. K., & Mohanty, P. (2014). Biomass, conversion routes and products – An overview. *Transformation of Biomass*, 1–30. https://doi.org/10.1016/10.1002/9781118693643.ch1

Pipal, A. S., & Satsangi, P. G. (2015). Study of carbonaceous species, morphology and sources of fine (PM2.5) and coarse (PM10) particles along with their climatic nature in India. *Atmospheric Research, 154*, 103–115. https://doi.org/10.1016/j.atmosres.2014.11.007

Ramanathan, V., Chung, C., Kim, D., Bettge, T., Buja, L., Kiehl, J. T., Washington, W. M., Fu, Q., Sikka, D. R., & Wild, M. (2005). Atmospheric brown clouds: Impacts on South Asian climate and hydrological cycle. *Proceedings of the National Academy of Sciences of the United States of America, 102*, 5326–5333. https://doi.org/10.1073/pnas.0500656102

Saud, T., Saxena, M., Singh, D. P., Dahiya, M., Sharma, S. K., Datta, A., Gadi, R., & Mandal, T. K. (2013). Spatial variation of chemical constituents from the burning of commonly used biomass fuels in rural areas of the Indo-Gangetic Plain (IGP), India. *Atmospheric Environment, 71*, 158–169. https://doi.org/10.1016/j.atmosenv.2013.01.053

Schmidt, G., Trouvé, G., Leyssens, G., Schönnenbeck, C., Genevray, P., & Cazier, F. (2018). Wood washing: Influence on gaseous and particulate emissions during wood combustion in a domestic pellet stove. *Fuel Processing Technology, 174*, 104–117. https://doi.org/10.1016/j.fuproc.2018.02.020

Schmitt, V. E. M., & Kaltschmitt, M. (2013). Effect of straw proportion and Ca- and Al-containing additives on ash composition and sintering of wood–straw pellets. *Fuel, 109*, 551–558. https://doi.org/10.1016/j.fuel.2013.02.064

Setti, L., Passarini, F., De Gennaro, G., Barbieri, P., Perrone, M. G., Borelli, M., Palmisani, J., Di Gilio, A., Torboli, V., Fontana, F., & Clemente, L. (2020). SARS-Cov2RNA found on particulate matter of Bergamo in northern Italy: First evidence. *Environmental Research, 188*, 109754. https://doi.org/10.1016/j.envres.2020.109754

Shang, Y., Wu, M., Zhou, J., Zhang, X., Zhong, Y., An, J., & Qian, G. (2019). Cytotoxicity comparison between fine particles emitted from the combustion of municipal solid waste and biomass. *Journal of Hazardous Materials, 367*, 316–324. https://doi.org/10.1016/j.jhazmat.2018.12.065

Shen, G., Tao, S., Wei, S., & Zhang, Y. (2012). Reductions in emissions of carbonaceous particulate matter and polycyclic aromatic hydrocarbons from combustion of biomass pellets in comparison with raw fuel. *Environmental Science & Technology, 46*, 6409–6416. https://doi.org/10.1021/es300369d

Sommersacher, P., Brunner, T., & Obernberger, I. (2012). Fuel indexes: A novel method for the evaluation of relevant combustion properties of new biomass fuels. *Energy & Fuels, 26*, 380–390. https://doi.org/10.1021/ef201282y

Steenari, B. M., Lundberg, A., Pettersson, H., Wilewska-Bien, M., & Andersson, D. (2009). Investigation of ash sintering during combustion of agricultural residues and the effect of additives. *Energy & Fuels, 23*(11), 5655–5662. https://doi.org/10.1021/ef900471u

Tiwari, S., Bisht, D. S., Srivastava, A. K., Pipal, A. S., Taneja, V., Srivastava, M. K., & Attri, S. D. (2014). Variability in atmospheric particulates and meteorological effects on their mass concentrations over Delhi, India. *Atmospheric Research, 145–146*, 45–56. https://doi.org/10.1016/j.atmosres.2014.03.027

Vassilev, S. V., Baxter, D., Andersen, L. K., & Vassileva, C. G. (2013). An overview of the composition and application of biomass ash.: Part 2. Potential utilisation, technological and ecological advantages and challenges. *Fuel, 105*, 19–39. https://doi.org/10.1016/j.fuel.2012.10.001

Wang, L., Hustad, J. E., Skreiberg, Ø., Skjevrak, G., & Grønli, M. (2012). A critical review on additives to reduce ash related operation problems in biomass combustion applications. *Energy Procedia, 20*, 20–29. https://doi.org/10.1016/j.egypro.2012.03.004

Wei, S., Shen, G., Zhang, Y., Xue, M., Xie, H., Lin, P., Chen, Y., Wang, X., & Tao, S. (2014). Field measurement on the emissions of PM, OC, EC and PAHs from indoor crop straw burning in rural China. *Environmental Pollution, 184*, 18–24. https://doi.org/10.1016/j.envpol.2013.07.036

Wei, X. Y., Liu, M., Yang, J., Du, W. N., Sun, X., Huang, Y. P., Zhang, X., Khalil, S. K., Luo, D. M., & Zhou, Y. D. (2019). Characterization of PM2.5-bound PAHs and carbonaceous aerosols during three-month severe haze episode in Shanghai, China: Chemical composition, source apportionment and long-range transportation. *Atmospheric Environment, 203*, 1–9. https://doi.org/10.1016/j.atmosenv.2019.01.046

Wierzbicka, A., Lillieblad, L., Pagels, J., Strand, M., Gudmundsson, A., & Gharibi, A. (2005). Particle emissions from district heating units operating on three commonly used biofuels. *Atmospheric Environment, 39*, 139–150. https://doi.org/10.1016/j.atmosenv.2004.09.027

World Energy Association. (2021). *Global bioenergy statistics*. https://www.worldbioenergy.org/uploads/211214%20WBA%20GBS%202021.pdf

Wu, B., Tian, H., Hao, Y., Liu, S., Sun, Y., Bai, X., Liu, W., Lin, S., Zhu, C., Hao, J., Luo, L., Zhao, S., & Guo, Z. (2020). Refined assessment of size-fractioned particulate matter (PM2.5/PM10/PMtotal) emissions from coal-fired power plants in China. *Science of the Total Environment, 706*, 135735. https://doi.org/10.1016/j.scitotenv.2019.135735

Yang, W., Pudasainee, D., Gupta, R., Li, W., Wang, B., & Sun, L. (2021). An overview of inorganic particulate matter emission from coal/biomass/MSW combustion: Sampling and measurement, formation, distribution, inorganic composition and influencing factors. *Fuel Process Technology, 213*, 106657. https://doi.org/10.1016/j.fuproc.2020.106657

Zhang, F., Chen, Y., Cui, M. Feng, Y., Yang, X., Chen, J., Zhang, Y., Gao, H., Tian, C., Matthias, V., & Liu, H. (2019). Emission factors and environmental implication of organic pollutants in PM emitted from various vessels in China. *Atmospheric Environment, 200*, 302–311. https://doi.org/10.1016/j.atmosenv.2018.12.006

Zeng, T., Weller, N., Pollex, A., & Lenz, V. (2016). Blended biomass pellets as fuel for small scale combustion appliances: Influence on gaseous and total particulate matter emissions and applicability of fuel indices. *Fuel, 184*, 689–700. https://doi.org/10.1016/j.fuel.2016.07.047

Zhu, C., Maharajan, K., Liu, K., & Zhang, Y. (2021). Role of atmospheric particulate matter exposure in COVID-19 and other health risks in human: A review. *Environmental Research, 198*, 111281. https://doi.org/10.1016/j.envres.2021.111281

Index